INL/MIS-13-30314 Rev. 2

September 2015

Assessment of BISON: A Nuclear Fuel Performance Analysis Code

BISON Release 1.2

D. M. Perez
R. W. Williamson
S. R. Novascone
R. J. Gardner
K. A. Gamble
A. T. Rice
G. Pastore
J. D. Hales
B. W. Spencer

INL/MIS-13-30314 Rev. 2

Assessment of BISON: A Nuclear Fuel Performance Code

D. M. Perez
R. W. Williamson
S. R. Novascone
R. J. Gardner
K. A. Gamble
A. T. Rice
G. Pastore
J. D. Hales
B. W. Spencer

September 2015

Idaho National Laboratory
Fuel Modeling and Simulation Department
Idaho Falls, Idaho 83415

Prepared for the
U.S. Department of Energy
Office of Nuclear Energy
Under U.S. Department of Energy-Idaho Operations Office
Contract DE-AC07-99ID13727

Assessment of BISON: A Nuclear Fuel Performance Analysis Code Rev.2

D. M. Perez, R. L. Williamson, S. R. Novascone,
R. J. Garder, K. A. Gamble, A. T. Rice, G. Pastore, J. D. Hales, B. W. Spencer

Fuels Modeling & Simulation Department
Idaho National Laboratory
Idaho Falls, ID

Abstract

A high-level summary of an effort to assess the predictive capability of BISON, a nuclear fuel performance code, is presented. This assessment was focused mainly on LWR fuel, and to a lesser degree, TRISO particle fuel. A comparison of BISON simulation results to a variety of experimental measurements of instrumented LWR fuel rods are shown. The source of LWR experimental data is primarily from the IAEA's FUMEX program. Benchmark simulation results of TRISO-coated particles are compared to BISON simulations. The TRISO benchmark simulations originate from the IAEA Coordinated Research Program. A brief discussion of material models and modeling approaches is also presented. There was a concerted effort to avoid model tuning to a particular set of experimental measurements. The material models and approaches were reviewed by the BISON team, and a subset of these were used for all the BISON simulations. As such, the BISON results shown in this assessment document are best-estimate as of fall 2015.

Overall, BISON simulations compare quite well with LWR experimental measurements and benchmark TRISO simulations. Discussion of future development and assessment efforts are also presented. More detailed versions of each assessment case are documented and can be found at the INL BISON repository.

Contents

1. Introduction

BISON is a modern finite-element based nuclear fuel performance code that has been under development at the Idaho National Laboratory since 2009 [1]. The code is applicable to both steady and transient fuel behavior and can be used to analyze either 1D spherical, 2D axisymmetric or 3D geometries. BISON has been applied to a variety of fuel forms including Light Water Reactor (LWR) fuel rods [1], TRISO-coated particle fuel [2], and metallic fuel in both rod [3] and plate geometries.

From the beginning, the development of BISON and related software has been accompanied by the creation of numerous verification tests in which specific features of the code are tested to see if they compute the correct analytical or known solution. There are currently over 800 of these regression tests for the MOOSE/BISON code hierarchy. During code development, the tests are run frequently (typically several times a day) and the solutions checked on a variety of computer platforms.

In addition, efforts have begun to assess BISON's ability to predict fuel behavior by comparison to data from a variety of instrumented LWR fuel rods and by code comparison for a series of TRISO-coated particle fuel benchmark cases. This assessment effort has been invaluable, leading to the discovery of development oversights not apparent from the simpler regression tests. Additionally it has led to improved confidence in BISON's ability to predict nuclear fuel behavior.

To date, 58 integral LWR fuel rod assessment cases have been completed. These cases were selected to assess the code's ability to simulate a variety of physical behaviors including thermal response both early in life and during power ramping, fission gas release, and mechanical behavior including both cladding elongation and pellet clad mechanical interaction (PCMI). Many of these assessment cases grew out of participation in the International Atomic Energy Agency (IAEA) sponsored FUMEX-III Coordinated Research Project [4] and are priority cases from either FUMEX-II [5] or FUMEX-III. Other cases were chosen based on recommendations from nuclear fuel experts.

For TRISO-coated particle fuel, a set of 13 benchmark cases have been considered which compare BISON results to those from other fuel performance codes, under normal operation and operational transients. These cases originated as part of an IAEA Coordinated Research Program (CRP-6) on High Temperature Gas Reactor (HTGR) fuel [6].

Chapters 2 and 3 summarize the LWR and TRISO cases, respectively. Each LWR assessment case is discussed in further detail in the attached appendices. Each result reported here-in is based on BISON 1.2 and ran on a MacPro workstation. All cases can also be run, and do run nightly, on the INL high performance computer FISSION.

2. Light Water Reactor Fuel

2.1. Assessment Cases

As summarized in Table 2.1, 58 integral fuel rod LWR assessment cases have been simulated. Indicated in the table are the measured quantities for comparison, namely fuel centerline temperature (FCT) at beginnng of life (BOL), throughout life (TL), and during power ramps (Ramps), fission gas release (FGR), cladding elongation (Clad-Elong), and cladding outer diameter following pellet clad mechanical interaction (PCMI).

Table 2.1.: Summary table of BISON LWR assessment cases.

Experiment	Rod	FCT BOL	FCT TL	FCT Ramps	FGR	Clad-Elong	Clad-Dia (PCMI)
IFA-431	1,2,3	X					
IFA-432	1,2,3	X					
IFA-515.10	A1	X	X				
US PWR 16x16	TSQ002,TSQ022		X		X		X
IFA-519	DH,DK						
IFA-534	18,19				X		
IFA-535.5/6	809,810				X	X	
IFA-597.3	7,8			X	X	X	
IFA-562	15,16,17		X		X		
IFA-636						X	X
Risø-3	AN2				X		X
Risø-3	AN3			X	X		
Risø-3	AN4			X	X		
AREVA Idealized Case					X		
HBEP	BK363,BK365,BK370				X		
R.E. Ginna	2,4				X		
FUMEX-II	27(1)				X		
FUMEX-II	27(2a)				X		
FUMEX-II	27(2b)				X		
FUMEX-II	27(2c)				X		
FUMEX-II	27(2d)				X		
Risø-2	GEm				X		X
Risø-3	II3				X		X
Risø-3	II5				X		X
Risø-3	GE7				X		X
OSIRIS	J12						X
OSIRIS	H09						X
REGATE					X		X
TRIBULATION	BN1/3,BN1/4,BN3/15				X	X	X
Calvert Cliffs	13 rods				X	X	X

2.2. Material and Behavioral Models

This section briefly reviews the BISON material and behavior models used in analyzing the LWR assessment cases. Theoretical details may be found in the BISON Theory Manual [7], and descriptions of the input options for the models are in the BISON User's Manual [8].

Burnup Evolution of burnup is typically driven by a table of rod averaged linear power at given times in the analysis. Axial variations are described in a similar manner. The radial power profile is modeled according to [9]. Given the local power, the local fission rate may be computed, and the fission rate is directly related to the evolving burnup. (See [7, Power, Burnup, and Related Models][8, Burnup].)

Contact Mechanical contact is enforced using node/face constraints. The penalty algorithm is commonly used. The interaction is enforced with a frictionless model. (See [7, Mechanical Contact][8, Mechanical Contact].)

Elastic An elastic material law is used for the fuel. A creep model is available but was not chosen due to the fact that it predicts excessive creep as a result of excessively high stresses in the absence of a cracking model. Typical parameters are 2×10^{11} N/m^2 for Young's modulus and 0.345 for Poisson's ratio. The coefficient of thermal expansion is 10×10^{-6} m/m/K. (See [8, Solid Mechanics Models].)

GrainRadiusAux When a polycrystalline material is subject to high temperatures, larger grains tend to grow at the expense of the smaller ones. As a consequence, the latter gradually disappear, thus reducing the total number of grains per unit volume and increasing the average grain size. The granular structure of the fuel affects physical processes such as fission gas behavior (Section 2.4). A simple empirical model [10] is implemented in BISON for calculating grain growth in UO_2 fuel. (See [7, Grain Growth][8, Other AuxKernels].)

HeatConductionMaterial The general HeatConductionMaterial is used to set the thermal conductivity and specific heat for the clad. Thermal conductivity is set at 16 W/m/K, and specific heat is 330 J/kg/K. (See [8, Thermal Models].)

MechZry The MechZry model is capable of tracking primary, thermal, and irradiation-induced creep in clad. Typical parameters are 7.5×10^{10} N/m^2 for Young's modulus and 0.3 for Poisson's ratio. The coefficient of thermal expansion is 5×10^{-6} m/m/K.The Franklin irradiation growth model is also incorporated into this material model. (See [7, Thermal and Irradiation Creep; Limbäck Creep Model][8, Solid Mechanics Models].)

RelocationUO2 RelocationUO2 accounts for cracking and relocation of fuel pellet fragments in the radial direction. This model is necessary for accurate modeling of LWR fuel. (See [7, Relocation][8, Solid Mechanics Models].)

Sifgrs The Simple Integrated Fission Gas Release and Swelling (Sifgrs) model is intended for consistently evaluating the kinetics of both fission gas swelling and release in UO_2. (See [7, Fission Gas Behavior][8, Fission Gas Models].)

ThermalContact The transfer of heat from the fuel to the cladding is accomplished via the ThermalContact model. The model is based on [11]. This model includes a computation of the conductivity of the gas using the MATPRO model [12], increased conductance due to mechanical contact [11], and radiant heat transfer. Temperature jump distance is computed [13]. Typical roughness values are 1 μm for the clad and 2 μm for the fuel, with a roughness coefficient of 3.2. (See [7, Gap Heat Transfer][8, Thermal Contact].)

ThermalFuel The ThermalFuel model incorporates several empirical fits for thermal conductivity of UO_2. The assessment cases were run with the NFIR correlation [14]. The NFIR model contains a temperature dependent thermal recovery function that accounts for self-annealing of defects in the fuel as it heats up. The ultimate effect of the self-annealing is a slight increase of the thermal conductivity over a range of temperatures up to ∼1200 K. (See [7, Thermal Properties][8, Thermal Models].)

2.3. Thermal Behavior

The ability to accurately predict fuel rod thermal behavior is essential for fuel performance analysis. Temperatures drive many other important physical phenomena, such as fission gas release and clad thermal creep. Peak fuel temperatures are of primary importance in determining fuel rod performance and lifetime.

2.3.1. Beginning of Life

Seven of the rods simulated to date considered only the first rise to power, also referred to as beginning of life (BOL). Temperature comparisons during the first rise to power are significant as they isolate several important aspects of fuel rod behavior before complexities associated with higher burnups are encountered. Proper prediction of BOL centerline temperatures requires accurate models for the fuel and clad thermal conductivity, gap heat transfer, thermal expansion of both the fuel and the clad materials (to predict an accurate gap width), and fuel relocation. Figure 2.1 summarizes the BOL fuel centerline temperature comparisons for all cases considered. Plotted is the measured versus predicted temperature as the rod power is increased during power-up. The solid line indicates a perfect comparison, and the dashed lines indicate ±10 percent error. For all BOL cases considered to date, BISON does a good job of predicting the fuel centerline temperature.

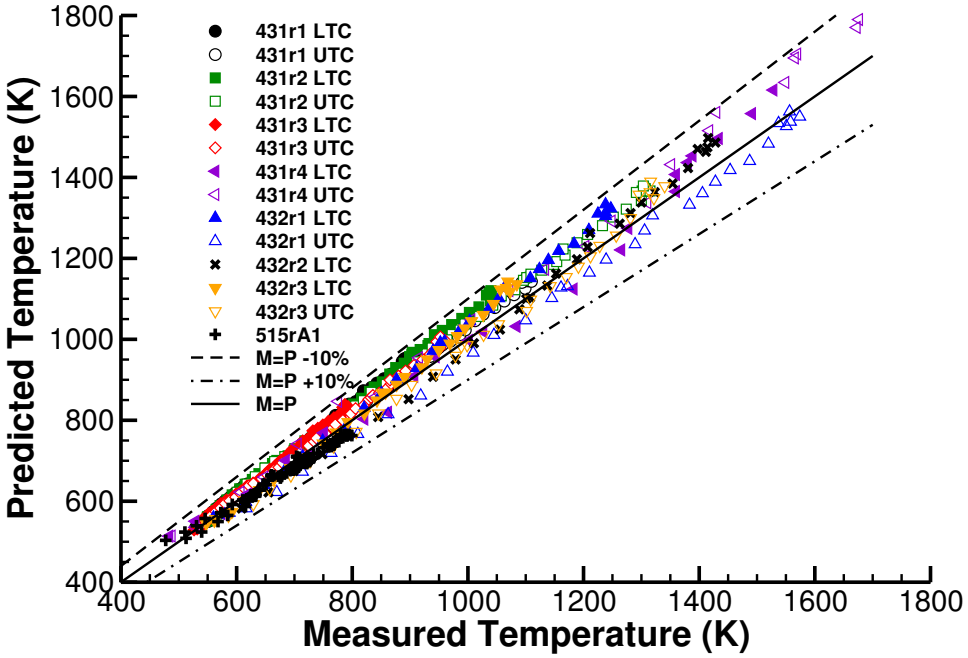

Figure 2.1.: BOL measured vs. predicted fuel centerline temperature for rods 1, 2, and 3 in IFA-431, IFA-432, and IFA-515.10 Rod A1. LTC and UTC stand for lower and upper thermocouple measurements, respectively.

2.3.2. Through Life

Four experimental cases in Table 2.1 contained through life temperature data, IFA-515.10 Rod A1 and IFA-562 Rods 15, 16 and 17 [15, 16] . The four cases were composed of annular UO_2 fuel pellets enclosed in a Zircaloy-2 cladding. The through life temperature measurements were obtained using centerline expansion thermometers (ET) that were placed inside the inner diameter of the fuel stack. These ETs spanned the entire length of the fuel stack and therefore provided average fuel centerline measurements. The temperature is derived from the expansion of the ET that is measured by a LVDT. These rods were irradiated to high burnups (75.5 MWd/kgUO_2 for IFA-515.10 Rod A1 and an average of 49.4 MWd/kgUO_2 for the IFA-562.2 rods) to assess temperature evolution as a function of burnup. To more accurately assess BISON's capabilities of predicting temperature through life, measured vs. predicted plots are given for four different burnup increments: $0 \leq Bu < 20$, $20 \leq Bu < 40$, $40 \leq Bu < 60$, and $Bu \geq 60$ MWd/kgUO_2 as shown in Figure C.5.

Considering IFA-515.10 Rod A1 it is observed the temperature predictions show similar behavior for all burnup ranges illustrated in Figures C.5(a), C.5(b), C.5(c), and 2.2(d) as illustrated by the blue circles. At low temperatures BISON matches the experiment quite well with the majority of points falling close to the M=P line. At higher temperatures BISON primarily under predicts the centerline temperature with a few points falling outside the $\pm 10\%$ range. Even in the high burnup region shown in Figure 2.2(d) almost all data points fall within the $\pm 10\%$ range indicating that the thermal conductivity degradation as a function of burnup is accurately captured. Overall BISON predicts the centerline temperature quite well through life for IFA-515.10 Rod A1 considering the complexities associated fuel and cladding evolution over such long irradiation times.

Contrarily to the the IFA-515.10 irradiation, the rods analyzed from the IFA-562.2 experiment illustrate that BISON primarily over predicts the temperature with less scatter in the points for all burnup ranges. As expected all the IFA-562.2 rods have very similar predicted temperatures since the power histories were similar. The reason for including two simulations of Rod 17 with two different assumed fuel roughnesses, denoted by R_f, is to highlight the changes in predictions based solely on the interpretation of the experiment. The documentation for the IFA-562.2 rods did not provide an as-fabricated fuel roughness and therefore the roughness was assumed to be the BISON default value of 2 μm. This default value is used for any validation case for which a fuel roughness is not provided. The chosen value of 0.2 μm was the reported value for the IFA-515.10 experiment [15]. Comparing the two data sets for Rod 17 in Figure C.5 it is observed that the simulation with the lower surface roughnesses predicts lower fuel centerline temperatures. The deviation between the two simulations becomes larger as irradiation progresses. This is because at higher burnups the fuel has come into contact with the cladding and the fuel roughness plays a crucial role in the solid-solid conductance term of the heat transfer coefficient between the fuel and cladding. What this simple study illustrates is that the interpretation of the experimental documentation can have a significant impact on predictions of the fuel performance code. The purpose of a mechanistic fuel performance code is to provide predictions without any tuning of parameters. In order to do this experiments should provide all of the details associated with the experiment including uncertainties such that model predictions can be assessed against the uncertainty within the experimental measurements.

2.3.3. Ramp Tests

Similar to Figs. 2.1 and C.5, Fig. 2.3 compares measured and predicted fuel centerline temperatures for the five ramp test experiments. Comparisons are reasonable, with some points falling outside the $\pm 10\%$ error bands. Note that focusing only on data from the Risø-3 experiments indicates a tendency to over predict temperature at low power and under predict temperature at high power. However, the single Halden experiment (IFA-597.3 rod 8) shows no such trend. Additional ramp test comparisons are needed (and in progress) to better understand this observation.

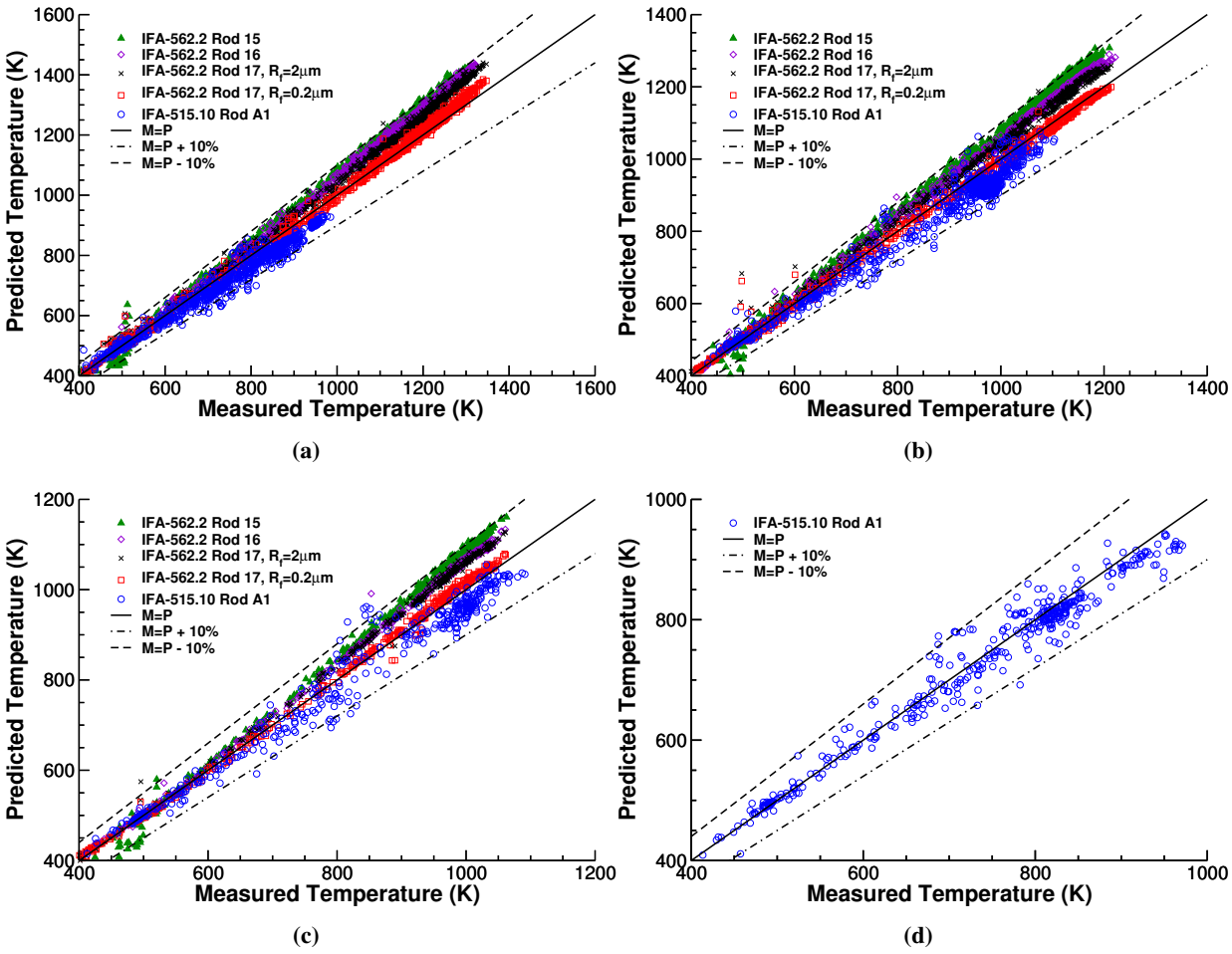

Figure 2.2.: Comparison of the measured vs. predicted fuel centerline temperature for through life rods for four different burnup ranges: (a) $0 \leq Bu < 20$, (b) $20 \leq Bu < 40$, (c) $40 \leq Bu < 60$, and (d) $Bu \geq 60$ MWd/kgUO$_2$. The R$_f$ parameter in the IFA-562.2 Rod 17 series labels indicate the fuel roughness used in the simulation.

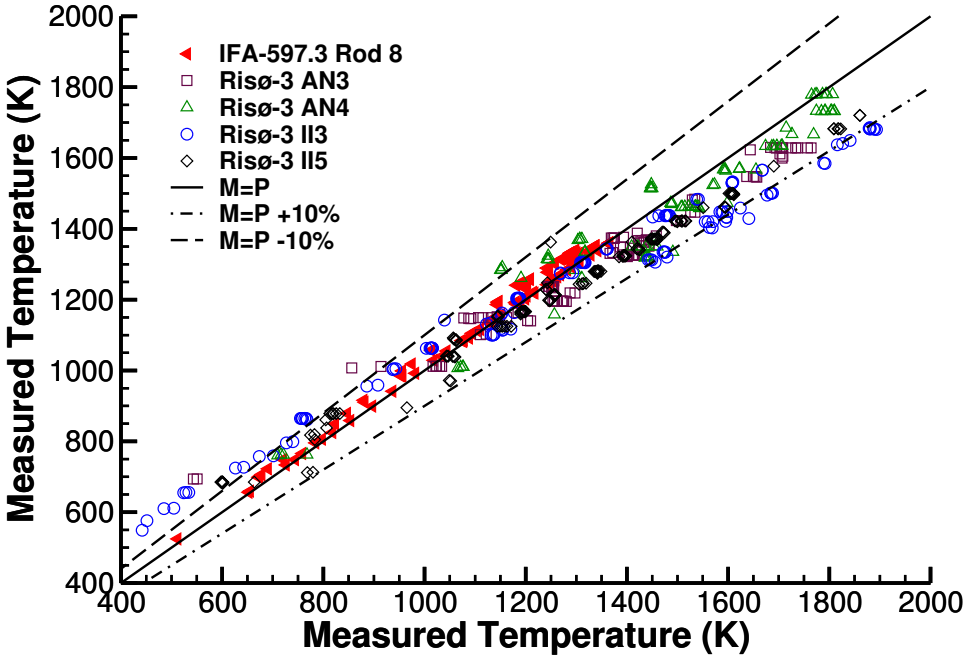

Figure 2.3.: Comparison of the measured vs. predicted fuel centerline temperature for fuel rods that experienced power ramps.

2.3.4. Thermal Behavior Summary

BOL, through-life, and ramp temperature measurements of LWR experiments were compared to BISON simulation results in order to evaluate the models used in BISON. The comparisons show the BISON calculations are reasonably close to experimental measurements. This is significant because fuel temperatures strongly affect important physical processes such as fission gas release and clad creep and directly determine fuel rod life.

2.4. Fission Gas Behavior

The processes induced by the generation of the fission gases xenon and krypton in nuclear fuel have a strong impact on the thermo-mechanical performance of the fuel rods. On the one hand, the fission gases tend to precipitate into bubbles resulting in fuel swelling, which promotes pellet-cladding gap closure and the ensuing pellet-cladding mechanical interaction (PCMI). On the other hand, fission gas release (FGR) to the fuel rod free volume causes pressure build-up and thermal conductivity degradation of the rod filling gas.

A Simple Integrated Fission Gas Release and Swelling (Sifgrs) model is available in BISON for the coupled fission gas swelling and release in UO_2. The model is founded on a physics-based description of the relevant processes, while retaining a level of complexity consistent with the application to engineering-scale nuclear fuel analysis. The Sifgrs model draws on and extends the approach described in [17].

The mutual dependence between fission gas behavior and grain growth is taken into account in Sifgrs through coupling with the grain growth model (Section 2.2).

As a first step, the model was implemented and tested in BISON for the analysis of FGR only [17]. More recently, the calculation of the fission gas swelling as coupled with the FGR has been introduced and matched with the mechanical analysis in BISON. Testing of the full Sifgrs fission gas release and swelling model is underway. First results are presented in this report, including comparisons with the empirical fission swelling model from MATPRO [12], also available in BISON.

The Vitanza Criterion was simulated to determine the burnup dependent threshold temperature at which more than 1% FGR can be expected. BISON falls within the ranges of other well-known fuel performance codes as shown in Figure 2.4.

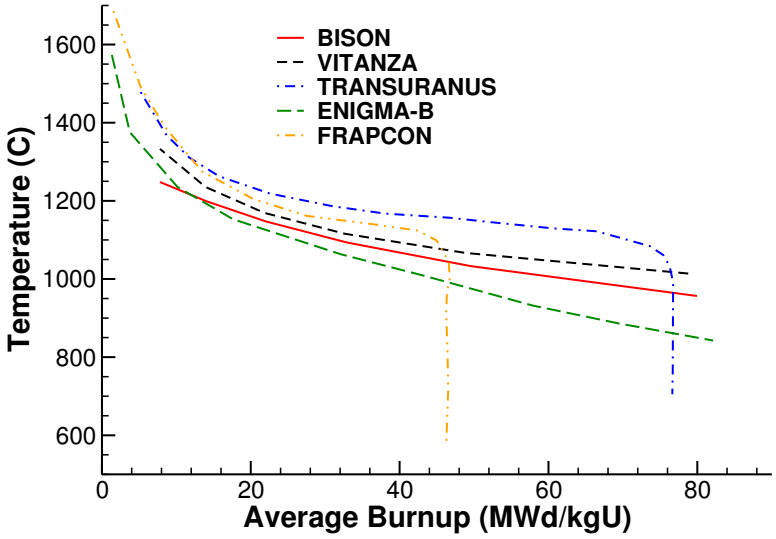

Figure 2.4.: 27(1) BISON and other code results compared to Vitanza criteria [18].

FGR comparisons were performed with multiple assessment cases (see Table 2.1). To best summarize

a majority of these comparisons, a measured versus predicted plot of the end of life total fission gas release is shown in Figure 2.5.

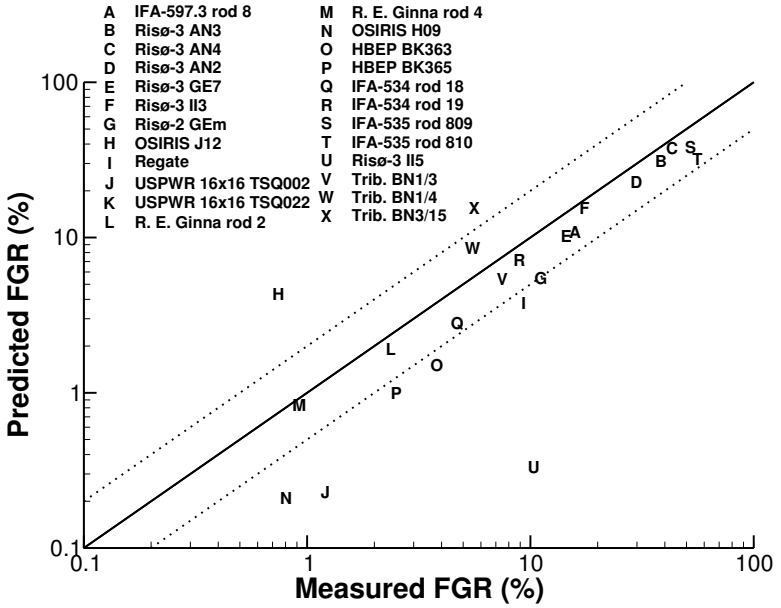

Figure 2.5.: Measured vs. predicted end of life total fission gas release comparisons.

2.4.1. Fission Gas Behavior Summary

BISON predicts the total FGR well at low burnup, however, at high burnup, BISON under predicts the total FGR. To date, the Sifgrs model provides a basis for integrating increasingly accurate descriptions of the fission gas swelling and release mechanisms. Development of the more advanced description of the intra-granular gas behavior, including consideration of the fuel swelling contribution due to intra-granular gas bubbles is currently underway.

2.5. Mechanical Behavior

Accurately representing the mechanical behavior of the fuel and clad is also essential when simulating fully-coupled thermomechanics problems like LWR fuel pins. Together with the thermal solution, the mechanical models determine the fuel-clad gap size, which may be the single most important characteristic to quantify in LWR simulations. Simulating realistic mechanical behavior is also critical when attempting to make predictions about clad structural integrity during pellet clad mechanical interaction (PCMI).

The following sections summarize BISON simulations of experiments where the fuel pellets have come into contact with the clad. Measurements of final clad length and diameter are compared to BISON calculations. These comparisons showcase the fuel and clad mechanical behavior models such as thermal expansion, clad irradiation growth, clad creep, fuel relocation, fuel swelling, fuel densification, and, perhaps most importantly, the mechanical interaction of fuel and clad as the two come into contact.

2.5.1. Clad Elongation

One way to quantify the mechanical behavior of LWR fuel rods is clad elongation. The point in time at which fuel and clad interact mechanically itself depends on several factors including pellet fracturing and relocation. It is also important to recognize that the eccentric placement of fuel pellets in the clad allows mechanical interaction from very early times.

Once the mechanical interaction begins, the relative motion of the fuel and clad depends on the friction between them. The value of the friction coefficient is understood to come with a large amount of uncertainty.

One clad elongation case has been included to date: IFA-597. This case has been run with frictionless and glued (infinite friction) contact conditions to bound the solution. A plot of elongation vs. time is shown in Figure 2.6.

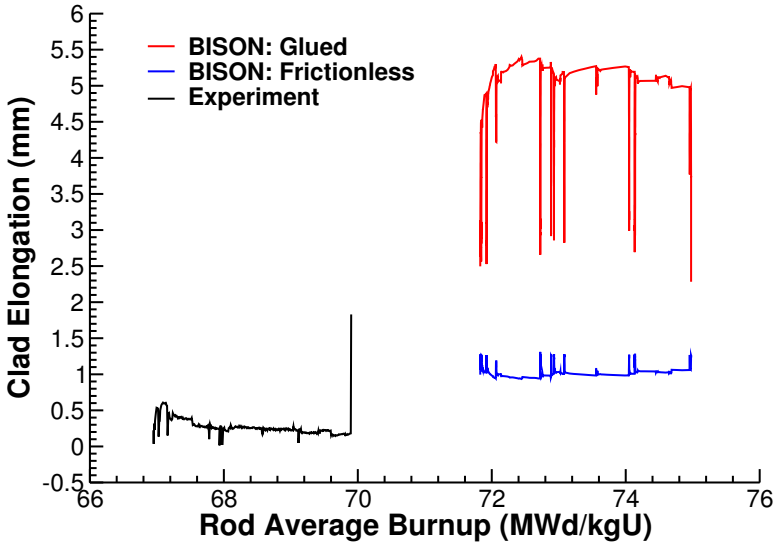

Figure 2.6.: IFA-597 elongation comparison.

There is data available for eight of the cases listed to compare fuel rod elongation, however, without frictional contact, it is not feasible to make these comparisons at this time.

2.5.2. Clad Final Diameter

Clad final diameter simulations and measurements are another way to quantify mechanical behavior models. The multiple experiments considered to date where final rod diameter measurements were made. Figure 2.7 is a summary plot of the measured minus predicted clad outer diameter after base irradiation and Figure 2.8 is a summary plot of the difference of the clad diameter change during the ramp. These experiments all consisted of a base irradiation followed by application of a power ramp before the end of the experiment.

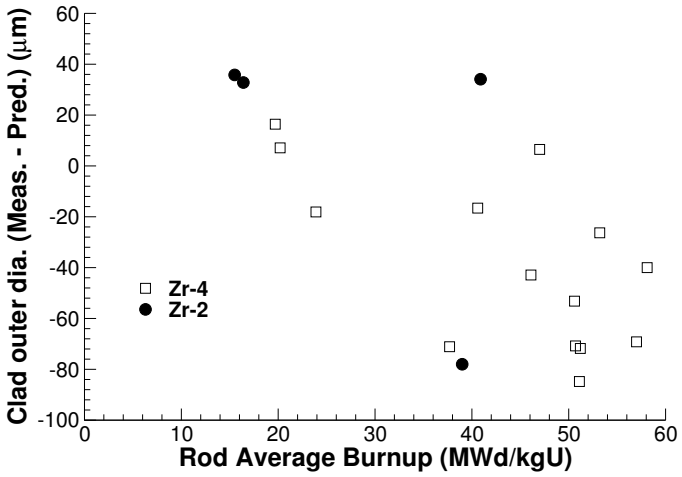

Figure 2.7.: The difference between measured and predicted cladding outer diameter as a function of burnup.

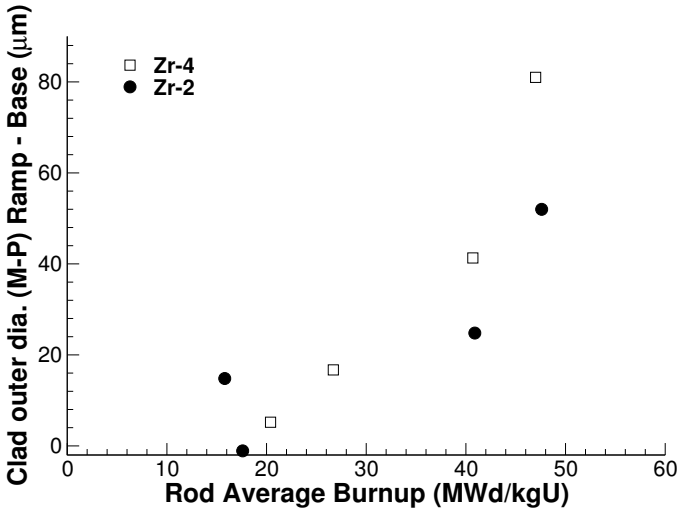

Figure 2.8.: The difference between measured and predicted difference between cladding outer diameter after and before the ramp as a function of burnup.

2.5.3. Mechanical Behavior Summary

Clad elongation and final diameter experimental measurments and BISON calculations have been presented for the purpose of quantifing the mechancial behavior and contact models in BISON. Overall, the comparisons are good but show a need for more accurate models. One possibility is to upgrade the nonlinear material models. For example the clad creep models (primary, secondary, and tertiary) and instantaneous plasticity could be coupled. Perhaps more importantly, more information regarding clad material characteristics (e.g. exact alloy specifications) and testing under realistic environments (thermal and irradiated) could be obtained via testing programs and incorporated into the material models. Further development work on nonlinear material modeling is an area of focus for next year.

3. TRISO-Coated Particle Fuel

3.1. Assessment Cases

As part of an International Atomic Energy Agency (IAEA) Coordinated Research Program (CRP-6) on High Temperature Gas Reactor (HTGR) reactor fuel technology, a set of benchmarking activities were developed to compare fuel performance codes under normal operation and operational transients [6]. Sixteen benchmark cases were identified, ranging in complexity from a simple fuel kernel having a single elastic coating layer, to realistic TRISO-coated particles under a variety of irradiation conditions. In each case, the particle geometry, constitutive relations, material properties, and operating conditions were carefully prescribed to minimize differences between the various code predictions; details are given in [6]. As an early code assessment exercise, BISON has been applied to 13 of the 16 benchmark cases, as summarized in Table 3.1.

Table 3.1.: IAEA CRP-6 benchmark cases considered in the BISON coated-particle assessment exercise. HFR-K3 and HFR-P4 are German pebble and fuel element experiments, respectively.

Case	Geometry	Description
1	SiC layer	Elastic only
2	IPyC layer	Elastic only
3	IPyC/SiC	Elastic with no fluence
4a	IPyC/SiC	Swelling and no creep
4b	IPyC/SiC	Creep and no swelling
4c	IPyC/SiC	Creep and swelling
4d	IPyC/SiC	Creep- and fluence-dependent swelling
5	TRISO	350 μm kernel, real conditions
6	TRISO	500 μm kernel, real conditions
7	TRISO	Same as 6 with high BAF PyC
8	TRISO	Same as 6 with cyclic temperature
10	HFR-K3	10% FIMA, 5.3×10^{-25}n/m^2 fluence
11	HFR-P4	14% FIMA, 7.2×10^{-25}n/m^2 fluence

The models for all benchmark cases used either six or eight quadratic axisymmetric finite elements across the width of each coating layer. A typical mesh with eight elements per layer is shown in Figure 3.1. Note that, in addition to the axisymmetry condition, a symmetry plane is also assumed along the top of the mesh. For cases 1 and 2, numerical solutions were also obtained with twelve elements across the coating layer to determine whether the mesh was sufficiently refined. Maximum tangential stresses obtained from the refined mesh models differed at most by 0.1%, demonstrating adequate mesh convergence with the coarser meshes. Since all of the cases are spherically symmetric, identical results (within machine precision) can be obtained using either 1D spherically symmetric or 3D elements.

The BISON input and all supporting files (mesh, mesh scripts, etc.) for the thirteen TRISO benchmark cases are provided with the code distribution at bison/assessment/TRISO_benchmarks. For users who wish to run these benchmarks, additional explanation is required. Because the IAEA CRP cases involved comparison of results from a large number and variety of codes, the particle geometry, boundary conditions and material models were prescribed for each case in detail. This was done principally to avoid differences in material models, which can be substantial between the various codes. In some cases these prescribed models differed from the standard BISON TRISO material models. Rather than

implement these numerous and specific models in the code, temporary models were developed and the necessary source code to use these models was stored with the individual cases. For the benchmark cases requiring these models (all except 1-3), users must overwrite the material model source code, re-compile, run the problem, and revert back to the original source. Refer to README files, included in each directory where such modifications are required, for more detail. This cumbersome process will be elimated in the future.

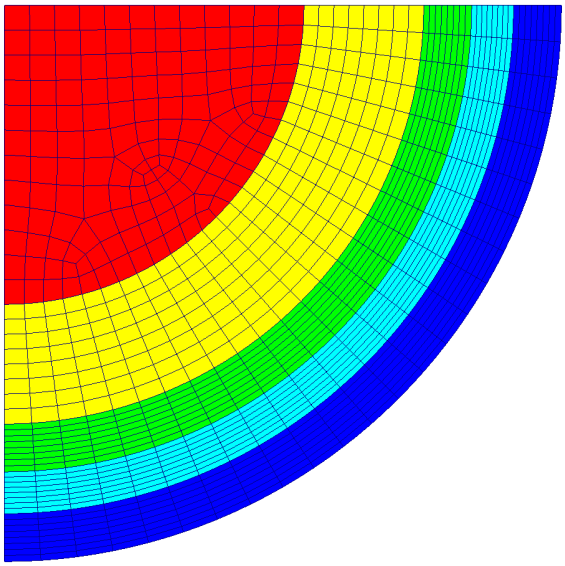

Figure 3.1.: Typical computational mesh used for the IAEA CRP-6 benchmark cases.

3.2. Results

Cases 1 to 3 were limited to single and double coating layers and tested simple elastic thermomechanical behavior against analytical solutions. A comparison of the analytical and BISON numerical solutions for the maximum tangential stress, which occurs at the inner surface of the various layers, is shown in Table 3.2. Comparisons are excellent.

Table 3.2.: Comparison of the BISON computed maximum tangential stress (MPa) to the analytical solution for Cases 1 to 3.

Case	Layer	Analytical	BISON	Error (%)
1	SiC	125.19	125.23	0.032
2	IPyC	50.200	50.287	0.173
3	IPyC/SiC	8.8/104.4	8.7/104.5	1.14/0.10

Cases 4a to 4d included both IPyC and SiC layers and investigated pyrolytic carbon layer behavior under a variety of conditions. Cases 5 to 8 considered a single TRISO particle with more complexity added with each subsequent case. For cases 1 to 4d, the internal gas pressure was fixed at 25 MPa while cases 5 to 8 included a linear pressure ramp. The particle temperature was held uniform at 1273 K for cases 1 to 7, but for case 8 was cycled ten times between 873 and 1273 K, characteristic of fuel in a pebble bed reactor. For cases 4 to 7, Table 3.3 compares BISON computed solutions to the range of solutions from eight coated-particle fuel codes included in the CRP-6 exercise [6]. Comparisons are of

the tangential stress at the inner surface of both the IPyC and SiC layers, at the end of irradiation. The BISON solutions are always within the range of values computed by the other codes. Note that tabulated values defining the ranges were extracted from plots in [6] and are thus not precise.

Table 3.3.: Comparison of the BISON computed tangential stress (MPa) to the range of values computed by the codes included in the CRP-6 exercise. Comparisons are at the inner surface of each layer and at the end of irradiation.

Case	Layer	CRP-6 codes [range]	BISON
4a	IPyC/SiC	[925, 970]/[-775, -850]	928/-819
4b	IPyC/SiC	[-25, -25]/[138, 142]	-25.0/139
4c	IPyC/SiC	[25, 27]/[83, 92]	26.0/89.4
4d	IPyC/SiC	[25, 35]/[71, 88]	27.8/87.0
5	IPyC/SiC	[40, 58]/[-56, -28]	41.9/-32.2
6	IPyC/SiC	[27, 38]/[28, 48]	29.2/44.9
7	IPyC/SiC	[37, 50]/[10, 25]	38.0/24.6

Although code comparisons in Table 3.3 are provided only at the end of irradiation, comparisons were made at various intermediate times during the irradiation period. The BISON solutions were always within the range of solutions produced by the CRP-6 codes.

Figure 3.2 compares solutions for case 8, which involved a cyclic particle temperature, during the full irradiation history. In this figure, BISON solutions of the tangential stress at the inner wall of the IPyC and SiC layers are compared to solutions from three codes from the CRP-6 exercise, namely PARFUME [19], ATLAS [20] and STRESS3 [21]. As above, data for the code comparisons were extracted from plots in [6]. For the IPyC layer, the four solutions essentially overlay each other during the entire irradiation period. In the SiC layer, the four solutions are quite similar but some differences are evident, particularly for the first four temperature cycles. The BISON solution falls roughly midway between the PARFUME and STRESS3 solutions and is essentially identical to the ATLAS solution.

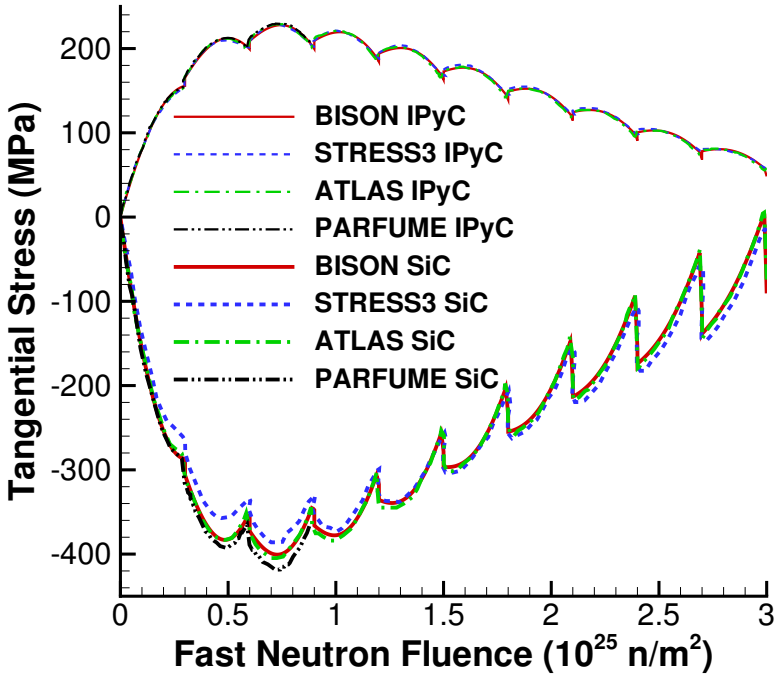

Figure 3.2.: Code comparison for case 8, which included a ten cycle temperature history. Plotted is the tangential stress at the inner wall of the IPyC and SiC layers.

Cases 9 to 13 in CRP-6 were more complicated benchmarks based on past or planned experiments with TRISO-coated particles. The two cases considered here (10 and 11) were based on German fuel from pebble and fuel element experiments. Again, details are provided in [6]. Although material properties and constitutive relations were prescribed for these cases, they differed from cases 1 to 8 in two ways: (1) the internal pressure was not fixed but instead determined by fission gas release and CO production and (2) the particle size was prescribed as a population (mean value and standard deviation) rather than a single value. BISON solutions were based on the gas release and CO production models described above; however, for simplicity, only a single particle size was considered based on the mean particle diameter.

Figure 3.3 provides code comparisons of the total gas pressure (Figure 3.3(a)) and tangential stress at the inner wall of the SiC layer (Figure 3.3(b)) for benchmark cases 10 and 11. Again, BISON is compared to three codes from the CRP-6 exercise. Substantial differences exist in these solutions, particularly for the gas pressure. The BISON solution histories, however, compare well to the range of solutions given by the three well-established codes chosen for comparison.

As stated in [6], the differences between various code predictions shown in Figures 3.3(a) and 3.3(b) can be largely attributed to the models used to calculate fission gas release and CO production in the kernel. A detailed description of these models is not available in [6], limiting more detailed investigation. One obvious and significant difference is that both BISON and ATLAS employ the simple Proksch et al. [22] empirical model for CO production while PARFUME [19] uses a detailed thermochemical model.

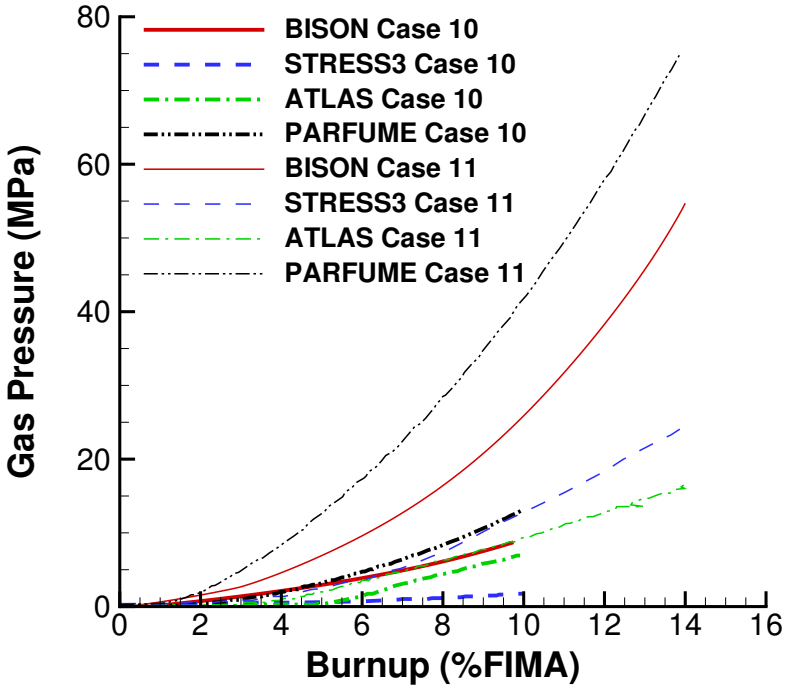

(a)

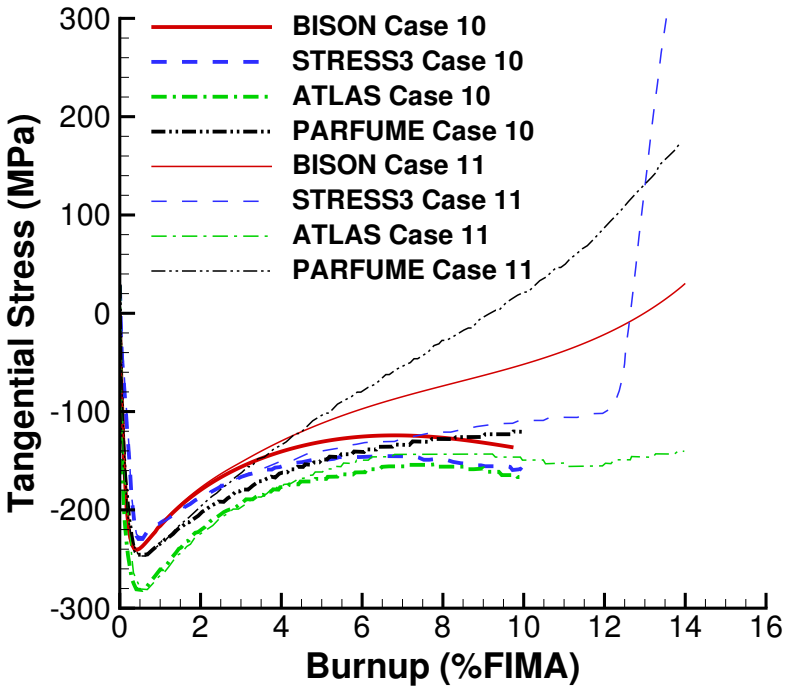

(b)

Figure 3.3.: Code comparisons of the total gas pressure (a) and tangential stress at the inner wall of SiC layer (b) for benchmark cases 10 and 11.

3.3. Summary

Since the IAEA CRP cases involved comparison of results from a large number and variety of codes, the particle geometry, boundary conditions and material models were prescribed for each case in detail. This was done principally to avoid differences in material models, which can be substantial between the various codes. In some cases these prescribed models differed from the standard BISON TRISO material models. Rather than implement these numerous and specific models in the code, temporary models were developed and the necessary source code to use these models was stored with the individual cases. BISON compares well with the other codes for these benchmark cases.

It is also important to assess the TRISO material models currently within BISON against experimental results. The beginning of this assessment work is planned to occur in FY 2015.

Appendices

A. IFA 431 Rod 1, Rod 2, and Rod 3

A.1. Overview

The IFA-431 experiment was part of an effort by the US NRC to obtain well-characterized experimental data under conditions that simulate long-term steady LWR operation [23]. IFA-431 was a heavily instrumented fuel assembly irradiated in the Halden boiling water reactor from 1975 to 1976. The test rods initially contained fresh fuel and were operated at power levels near the upper bound for full-length commercial fuel rods.

The IFA-431 assembly included six instrumented rods, each with centerline temperature instrumentation in both the top and bottom ends of the fuel column. Three of the six rods (Rods 1, 2, 3) are the focus of this assessment.

The IFA-431 assembly also contained neutron detectors, coolant thermocouples, a coolant flow meter, and a transducer to measure internal rod pressure.

A.2. Test Description

The three test rods considered here were designed to simulate BWR-6 rod cladding material and dimensions, and included only differences in fuel-cladding gap width. The general rod specifications are summarized in Table A.1 which contains data taken from Reference [24].

The fuel rod length was significantly shorter than full-length commercial rods to fit within the short length of the Halden reactor core. Slight differences in the pellet diameters, as defined in Table A.1, resulted in a variation in the initial radial fuel-clad gaps of 115 μm (Rod 1), 190 μm (Rod 2), and 25.5 μm (Rod 3).

A.2.1. Operating Conditions and Irradiation History

The reactor was operated with a coolant pressure of 3.4 MPa and an inlet temperature of 510 K. The power history was provided by experimentalists from Halden [25].

Table A.1.: IFA-431 Test Rod Specifications

Fuel Rod		
Overall length	m	0.635
Fuel stack height	m	0.5791
Nominal plenum height	mm	25.4
Number of pellets per rod		
Rod 1	mm	45
Rod 2	mm	44
Rod 3	mm	44
Fill gas composition		He
Fill gas pressure	MPa	0.1
Fuel		
Material		UO_2
Enrichment	%	10
Density	%	95
Inner diameter	mm	1.752
Outer diameter		
Rod 1	mm	10.681
Rod 2	mm	10.528
Rod 3	mm	10.858
Pellet geometry		flat end
Grain diameter	μm	22-77
Cladding		
Material		Zr-2
Outer diameter	mm	12.789
Inner diameter	mm	10.909
Wall thickness	mm	0.94

A.3. Model Description

A.3.1. Geometry and Mesh

All three fuels rods were meshed using 2-D axisymmetric quadratic elements. For simplicity, the pellet stack was modeled as a single continuous fuel column. The thermocouple holes were modeled as closely to the experiment as possible at the top and bottom of the fuel rod. Figure A.1 shows a scaled view of the mesh for rod 1. Rods 2 and 3 were identical with exceptions to the thermocouple hole length and the pellet-clad gap width.

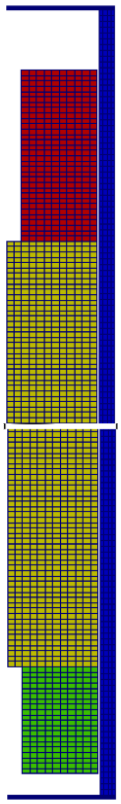

Figure A.1.: Scaled view of the finite element mesh for rod 1 (aspect ratio scaled 10x).

A.3.2. Material and Behavioral Models

The following material and behavioral models were used for the UO_2 fuel:

- ThermalFuel - NFIR: temperature and burnup dependent thermal properties
- RelocationUO2: relocation strains, relocation activation threshold power set to 5 kW/m.
- Sifgr: Simplified fission gas release model with the combined gaseous swelling model.

For the clad material, a constant thermal conductivity of 16 W/m-K was used and both thermal and irradiation creep were considered using the Limback model [26]. The fast neutron flux used in the irradiation creep model was 1.6e12 n/m^2-s per W/m [5]. This value was multiplied by the power history (W/m) and the axial peaking factors to approximate the fast neutron flux.

A.3.3. Boundary and Operating Conditions

The clad outer wall temperature was assumed constant at 513.3 K. The input BOL power histories for Rods 1, 2, and 3 are shown in Figure A.2.

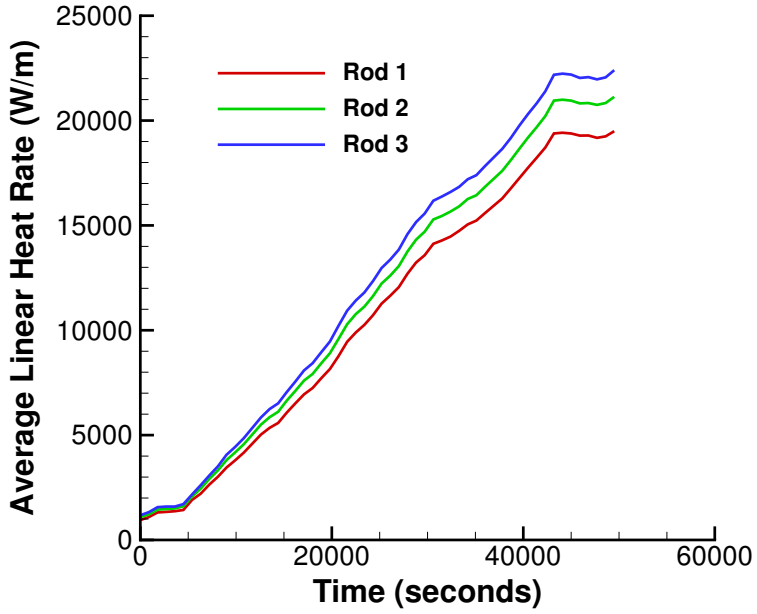

Figure A.2.: Input BOL power history for rods 1, 2, and 3.

A.3.4. Input files

The BISON input and all supporting files (power histories, axial power profile) are provided with the code distribution at bison/assessment/IFA_431/analysis.

A.3.5. Execution Summary

Table A.2.: Execution summary.

Rod	Machine	Operating System	Code Version
1	FALCON	LINUX	BISON 1.2
2	FALCON	LINUX	BISON 1.2
3	FALCON	LINUX	BISON 1.2

A.4. Results Comparison

BISON postprocessors were used to record the power and temperature histories at nodes corresponding to the upper and lower thermocouple positions.

A.4.1. Centerline Temperature at Beginning of Life

Initial comparisons were made to centerline fuel temperature measurements during the first rise to power, or the period referred to as the Beginning of Life (BOL). Comparisons during this period are important since they isolate several important aspects of fuel rod behavior before complexities associated with

higher burnups are encountered. For example, good prediction of BOL centerline temperature requires accurate models for the unirradiated fuel thermal conductivity, gap gas conductivity, thermal expansion of both the fuel and clad materials (which set the gap width), clad conductivity, and fuel relocation.

Figures A.3, A.4, and A.5 show centerline temperature comparisons at BOL for Rods 1, 2, and 3, respectively. Comparisons are excellent.

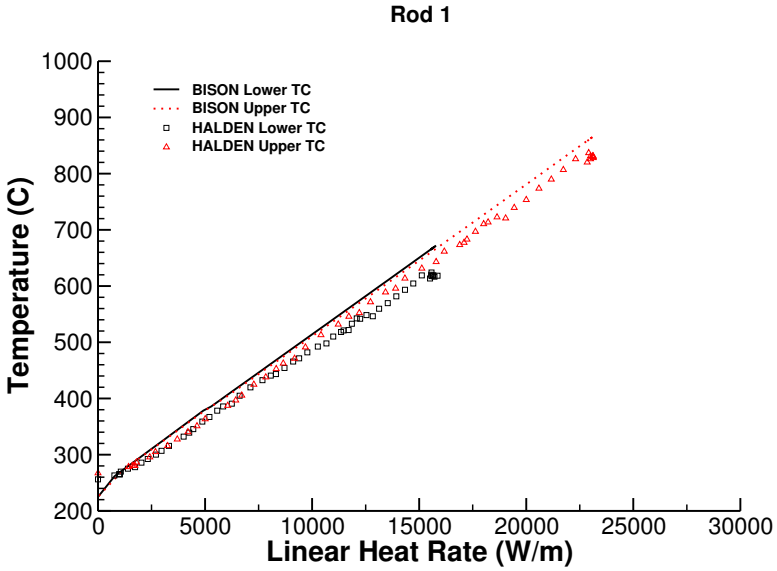

Figure A.3.: Comparison of measured and BISON predicted centerline temperatures at BOL for Rod 1.

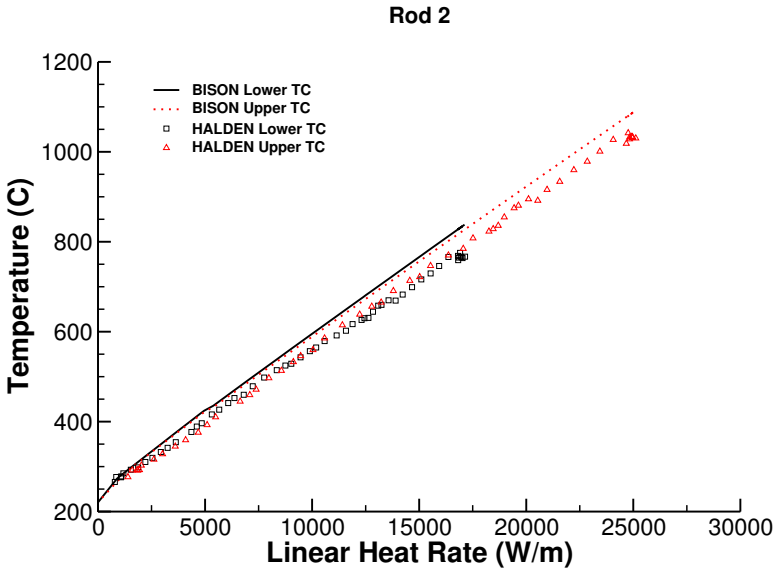

Figure A.4.: Comparison of measured and BISON predicted centerline temperatures at BOL for Rod 2.

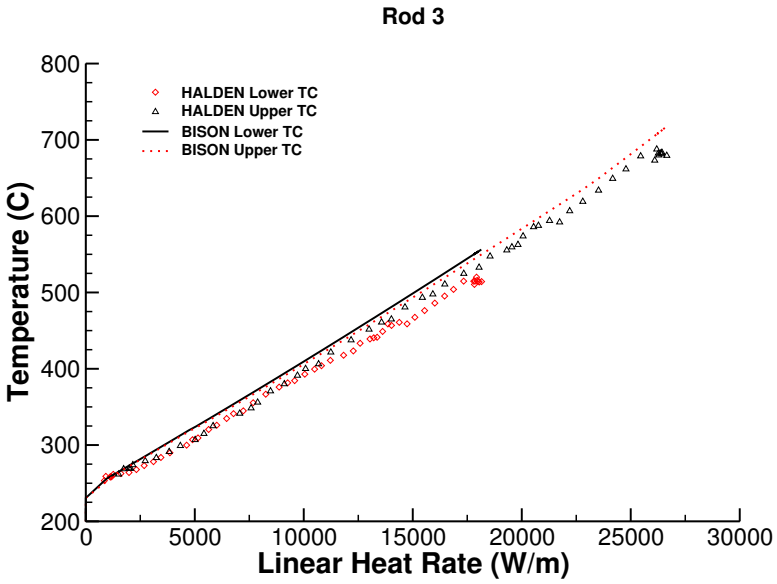

Figure A.5.: Comparison of measured and BISON predicted centerline temperatures at BOL for Rod 3.

A.5. Discussion

The recommended activation energy for the ESCORE relocation model implemented in BISON is 19.7 kW/m [27]. Based on experimental evidence of fuel cracking as a function of rod power, Wolfgang Wiesenack from Halden recommended lowering this activation threshold power to 5 kW/m. This lower value was further confirmed through a recent relocation calibration study [28] and is now used as the default value in BISON.

B. IFA 432 Rod 1, Rod 2, and Rod 3

B.1. Overview

The IFA-432 experiment was part of an effort by the US NRC to obtain well-characterized experimental data under conditions that simulate long-term steady LWR operation [23]. IFA-432 was a heavily instrumented fuel assembly irradiated in the Halden boiling water reactor from 1975 to 1984. The test rods initially contained fresh fuel and were operated at power levels near the upper bound for full-length commercial fuel rods.

The IFA-432 assembly included six instrumented rods, each with centerline temperature instrumentation in both the top and bottom ends of the fuel column. Three of the six rods (Rods 1, 2, 3) are the focus of this assessment. Rod 1 achieved a burnup of approximately 30 MWd/KgU, while rods 2 and 3 achieved burnups of approximately 45 MWd/kgU. Two of the temperature measurements failed prematurely. Rod 2 contained an ultrasonic thermometer at the top of the rod, which failed very early and no data were collected. The Rod 1 upper thermocouple failed after 150 days.

The IFA-432 assembly also contained neutron detectors, coolant thermocouples, a coolant flow meter, and a transducer to measure internal rod pressure.

B.2. Test Description

The three test rods considered here were designed to simulate BWR-6 rod cladding material and dimensions, and included only differences in fuel-cladding gap size. The general rod specifications are summarized in Table B.1 which contains data taken from Reference [24].

The fuel rod length was significantly shorter than full-length commercial rods to fit within the short length of the Halden reactor core. Slight differences in the pellet diameters, as defined in Table B.1, resulted in a variation in the initial radial fuel-clad gaps of 115 μm (Rod 1), 190 μm (Rod 2), and 38 μm (Rod 3).

B.2.1. Operating Conditions and Irradiation History

The reactor was operated with a coolant pressure of 3.4 MPa and an inlet temperature of 510 K. The power history was provided by experimentalists from Halden [29].

Table B.1.: IFA-432 Test Rod Specifications

Fuel Rod		
Overall length	m	0.635
Fuel stack height	m	0.5791
Nominal plenum height	mm	25.4
Number of pellets per rod		
Rod 1	mm	45
Rod 2	mm	44
Rod 3	mm	44
Fill gas composition		He
Fill gas pressure	MPa	0.1
Fuel		
Material		UO_2
Enrichment	%	10
Density	%	95
Inner diameter	mm	1.752
Outer diameter		
Rod 1	mm	10.681
Rod 2	mm	10.528
Rod 3	mm	10.833
Pellet geometry		flat end
Grain diameter	μm	22-77
Cladding		
Material		Zr-2
Outer diameter	mm	12.789
Inner diameter	mm	10.909
Wall thickness	mm	0.94

B.3. Model Description

B.3.1. Geometry and Mesh

All three fuels rods were meshed using 2-D axisymmetric quadratic elements. For simplicity, the pellet stack was modeled as a single continuous fuel column. The thermocouple holes were modeled as closely to the experiment as possible at the top and bottom of the fuel rod. Figure B.1 shows a scaled view of the mesh for rod 1. Rods 2 and 3 were identical with exceptions to the thermocouple hole length and the gap width.

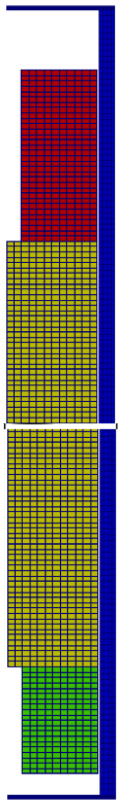

Figure B.1.: Scaled view of the finite element mesh for rod 1 (aspect ratio scaled 10x).

B.3.2. Material and Behavioral Models

The following material and behavioral models were used for the UO_2 fuel:

- ThermalFuel - NFIR: temperature and burnup dependent thermal properties
- RelocationUO2: relocation strains, relocation activation threshold power set to 5 kW/m.
- Sifgr: Simplified fission gas release model with the combined gaseous swelling model.

For the clad material, a constant thermal conductivity of 16 W/m-K was used and both thermal and irradiation creep were considered using the Limback model [26]. The fast neutron flux used in the irradiation creep model was 1.6e12 n/m^2-s per W/m [5]. This value was multiplied by the power history (W/m) and the axial peaking factors to approximate the fast neutron flux.

B.3.3. Boundary and Operating Conditions

The clad outer wall temperature was assumed constant at 513.3 K. The input BOL power histories for Rods 1 and 3 are shown in Figure B.2.

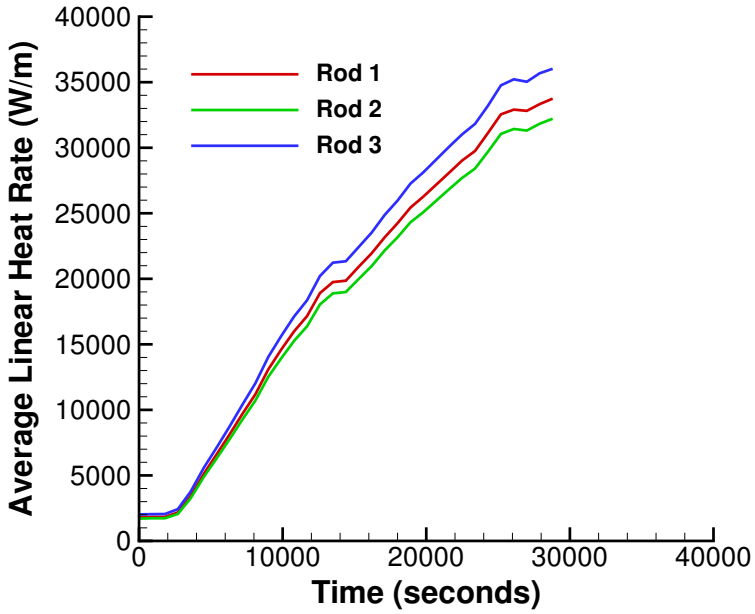

Figure B.2.: Input BOL power history for rods 1, 2, and 3

B.3.4. Input files

The BISON input and all supporting files (power histories, axial power profile) are provided with the code distribution at bison/assessment/IFA_432/analysis.

B.3.5. Execution Summary

Table B.2.: Execution summary.

Rod	Machine	Operating System	Code Version
1	FALCON	LINUX	BISON 1.2
2	FALCON	LINUX	BISON 1.2
3	FALCON	LINUX	BISON 1.2

B.4. Results Comparison

BISON postprocessors were used to record the power and temperature histories at nodes corresponding to the upper and lower thermocouple positions.

B.4.1. Centerline Temperature at Beginning of Life

Initial comparisons were made to centerline fuel temperature measurements during the first rise to power, or the period referred to as the Beginning of Life (BOL). Comparisons during this period are important since they isolate several important aspects of fuel rod behavior before complexities associated with

higher burnups are encountered. For example, good prediction of BOL centerline temperature requires accurate models for the unirradiated fuel thermal conductivity, gap gas conductivity, thermal expansion of both the fuel and clad materials (which set the gap width), clad conductivity, and fuel relocation.

Figures B.3, B.4, and B.5 show centerline temperature comparisons at BOL for Rods 1, 2, and 3, respectively. Note that for Rod 2, only lower thermocouple comparisons are possible since a gamma thermometer that failed to operate occupied this position in the rod [24]. Comparisons for all three rods are very good.

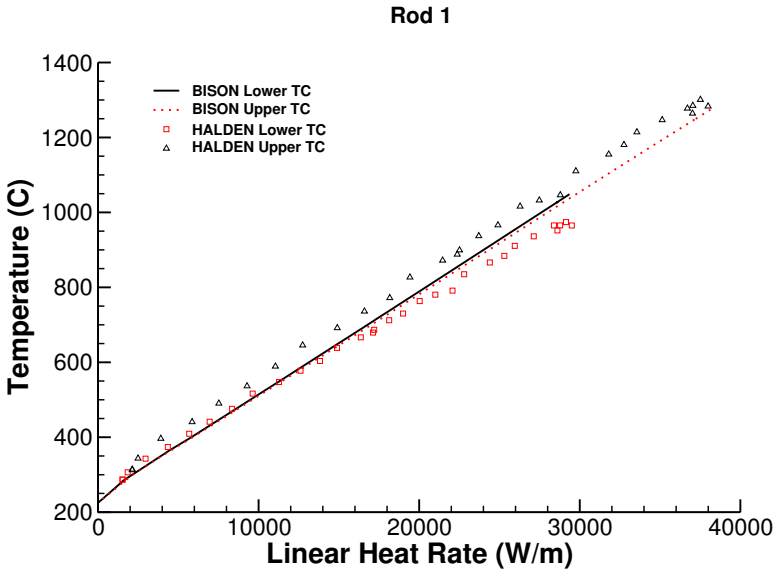

Figure B.3.: Comparison of measured and BISON predicted centerline temperatures at BOL for Rod 1.

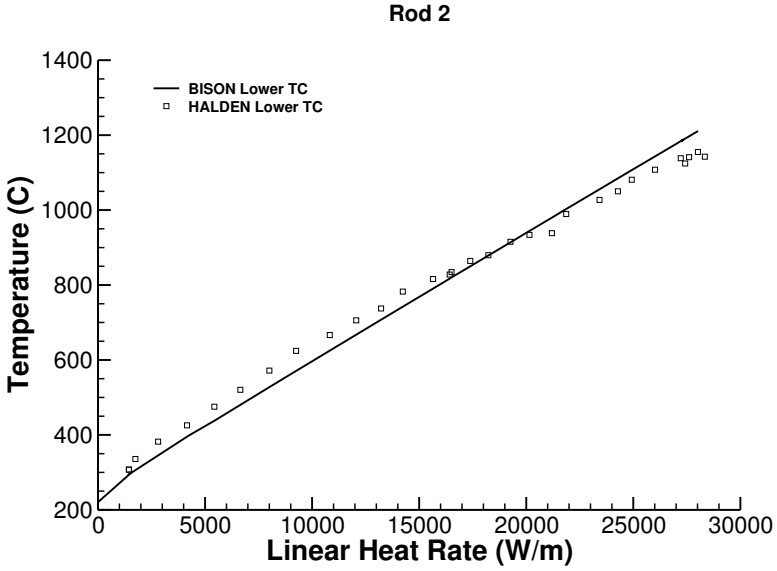

Figure B.4.: Comparison of measured and BISON predicted centerline temperatures at BOL for Rod 2.

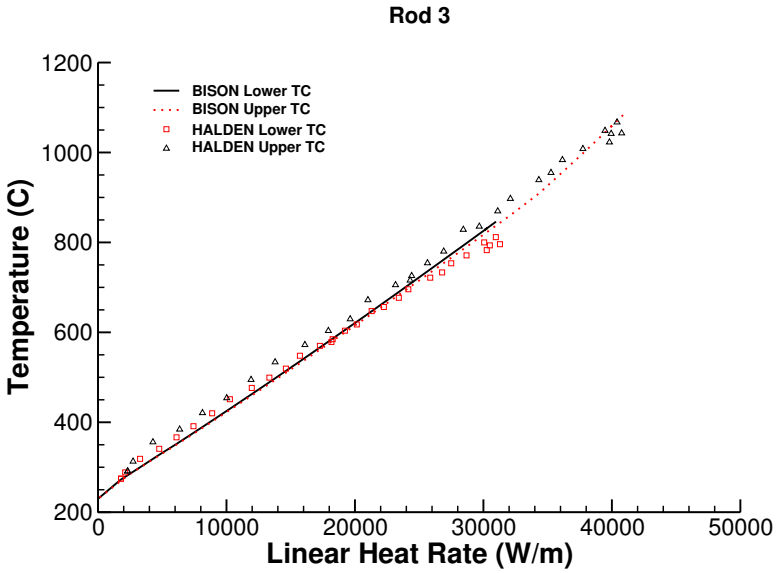

Figure B.5.: Comparison of measured and BISON predicted centerline temperatures at BOL for Rod 3.

B.5. Discussion

The recommended activation energy for the ESCORE relocation model implemented in BISON is 19.7 kW/m [27]. Based on experimental evidence of fuel cracking as a function of rod power, Wolfgang Wiesenack from Halden recommended lowering this activation threshold power to 5 kW/m. This lower value was further confirmed through a recent relocation calibration study [28] and is now used as the default value in BISON.

C. IFA 515.10 Rod A1

C.1. Overview

The IFA-515.10 Rod A1 experiment was irradiated in the Halden Boiling Water Reactor (HBWR) for approximately 6 years to a discharge burnup of $\sim$76 MWd/kgUO_2. Rod A1 was fitted with a fuel centerline expansion thermometer (ET) to measure the fuel centerline temperature during irradiation [15].

C.2. Test Description

C.2.1. Rod Design Specifications

Rod A1 in the IFA-515.10 series was an annular short rod (0.2455 m overall length) enriched to 11.5 %. The fuel and cladding specifications are tabulated in Table C.1.

Table C.1.: IFA-515.10 rod A1 Test Rod Specifications

Fuel Rod		
Overall length	m	0.2455
Fuel stack height	m	0.212
Nominal plenum height	mm	19.0
Fill gas composition		He
Fill gas pressure	MPa	1.0
Fuel		
Material		UO_2
Enrichment	%	11.5
Density	%	96.8
Inner diameter	mm	1.80
Outer diameter	mm	5.56
Pellet geometry		flat end
Average grain diameter	μm	15.5
Average fuel roughness	μm	0.28
Insulator Pellet		
Material		Al_2O_3
Inner diameter	mm	1.80
Outer diameter	mm	5.56
Pellet length	mm	5.0
Cladding		
Material		Zr-2
Outer diameter	mm	6.53
Inner diameter	mm	5.61
Zr-Barrier thickness	mm	0.05
Wall thickness	mm	0.46

C.2.2. Operating Conditions and Irradiation History

The HBWR operating conditions are tabulated in Table C.2. The reactor power history is shown in Figure C.1. The measured reactor coolant temperature was used as the boundary temperature on the cladding outer surface.

Table C.2.: Operational input parameters.

Average coolant temperature	C	195
Coolant pressure	MPa	3.4
Fast neutron flux	n/(cm^2·s) per (kW/m)	1.6·10^{11}

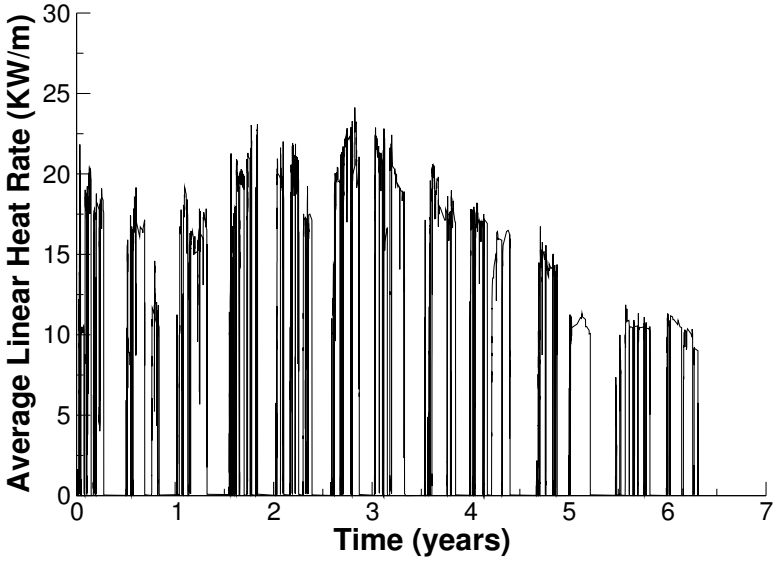

Figure C.1.: Halden irradiation through life power profile for IFA-515.10 rod A1.

C.3. Model Description

C.3.1. Geometry and Mesh

The assumed geometry and mesh are shown in Figure C.2. The fuel pellet stack was modeled as a smeared column with merged insulator pellets. The insulator pellets were modeled as UO_2 (ie. the same mechanical and thermal properties) to make the simulation easier to run. The expansion thermometer was modeled as a void in the pellet/insulator stack, this was also done to ease the simulation. The BISON fuel centerline temperature was calculated as an average of the pellet interior (BISON sideset 13). The plenum length for the mesh was adjusted from the experiment length to account for the difference in volume caused by the voided expansion thermometer. The initial gas volume in the simulation was 2.3 cc, as listed in [15].

A 2-dimensional axisymmetric quadratic mesh was used. The fuel column was meshed with 111 axial and 11 radial elements (aspect ratio 11.2) and the insulator pellets with 3 axial and 11 radial elements (aspect ratio 9.75). The cladding was meshed with 150 axial and 4 radial elements (aspect ratio 16.7).

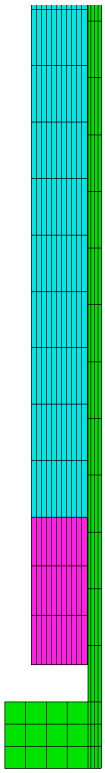

Figure C.2.: 2-D axisymmetric quadratic mesh for IFA-515.10 Rod A1 simulation. Note: This is only a cut from the bottom of the fuel rod meant to show the fuel and insulator pellet. The volume where the expansion thermometer would be in the experiment can also be seen.

C.3.2. Material and Behavioral Models

The following material and behavioral models were used for the UO_2 fuel:

- ThermalFuel - NFIR: temperature and burnup dependent thermal properties
- VSwellingUO2: free expansion strains (swelling and densification)
- RelocationUO2: relocation strains, relocation activation threshold power set to 5 kW/m.
- Sifgrs: fission gas generation and release

For the cladding material, a constant thermal conductivity of 16 W/m-K was used and both thermal and irradiation creep were considered using the Limback model [26].

C.3.3. Input files

The BISON input and all supporting files (power histories, axial power profile, cladding surface temperature boundary condition, fast neutron flux history, etc.) for this case are provided with the code distribution at bison/assessment/IFA_515_RodA1/analysis.

C.3.4. Simulation Parameters and Assumptions

As mentioned in the G.3.1 the mesh used is not an exact representation of the experiment. To make the simulation run easier the insulator pellets were modeled as UO_2 instead of Al_2O_3. Merged materials of the same type in the mesh make for easier mechanics (ie. thermal expansion and swelling). The insulator pellets were not included in the heat source term. The expansion thermometer was neglected in this mesh. This was done to alleviate troubles with thermal and mechanical properties between the thermometer and the fuel/insulator stack. The plenum length of the fuel rod was adjusted to account for the extra gas volume made from the voided thermometer. The initial gas volume is 2.3 cc as listed in [15]. The zirconium barrier on the cladding interior was not modeled, but the cladding thickness was modeled as specified in [15]. The initial fuel grain size and the fuel roughness were inputted in to BISON as averages of the numbers that were given in [15]. The test was short and located in a region were the axial flux variation average to peak is small, less than 1.03 [15]. Due to this peaking factors for power and temperature were not inputted into BISON.

C.3.5. Execution Summary

Table C.3.: Execution summary.

Machine	Operating System	Code Version
INL HPC Falcon	Linux	BISON 1.2

C.4. Results Comparison

A BISON postprocessor was used to extract the centerline temperature as an average of the interface of the pellet interior surface and the ET (BISON sideset 13). This provides an accurate representation of the average fuel centerline temperature since, in this case, no axial variation in fuel temperature.

C.4.1. Temperature

The BISON results for the fuel centerline temperature show that BISON approximates the actual experimental values well. A plot of the comparison can be seen below in Figure C.3. There are some noticeable differences between BISON and the experiment on the peaks at the beginning of the experiment. The difference between the BISON results and the experiment becomes less as the simulation progresses. This points to possible issues in the gap heat transfer model. As fuel centerline temperature was the only parameter that was measured we can only speculate on the other effects that may have contributed to this difference. Figure C.4 shows a comparison of fuel centerline temperature and linear heat rate. This plot shows that BISON does tend to under predict through the simulation at all powers. It should be noted that the experiment low outliers are from instrument issues and should be ignored. Figure C.5 is the same data as Figure C.4, but the results are compartmentalized by burnup level to investigate BISON performance throughout the simulation more closely. Figure C.5(a) shows that BISON does under predict during the early stages of the simulation. This is before the gap closes, which supports the previous hypothesis. As the simulation progresses the Figures C.5(b), C.5(c) and C.5(d) show that the comparison of BISON results to experiment data improves.

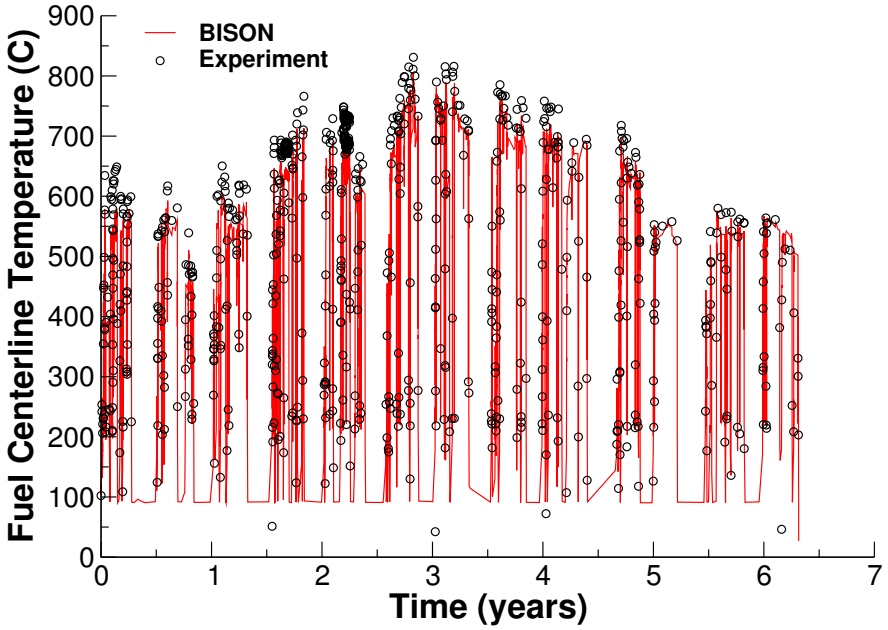

Figure C.3.: A comparison of fuel centerline temperatures from BISON calculations and experimental measurements.

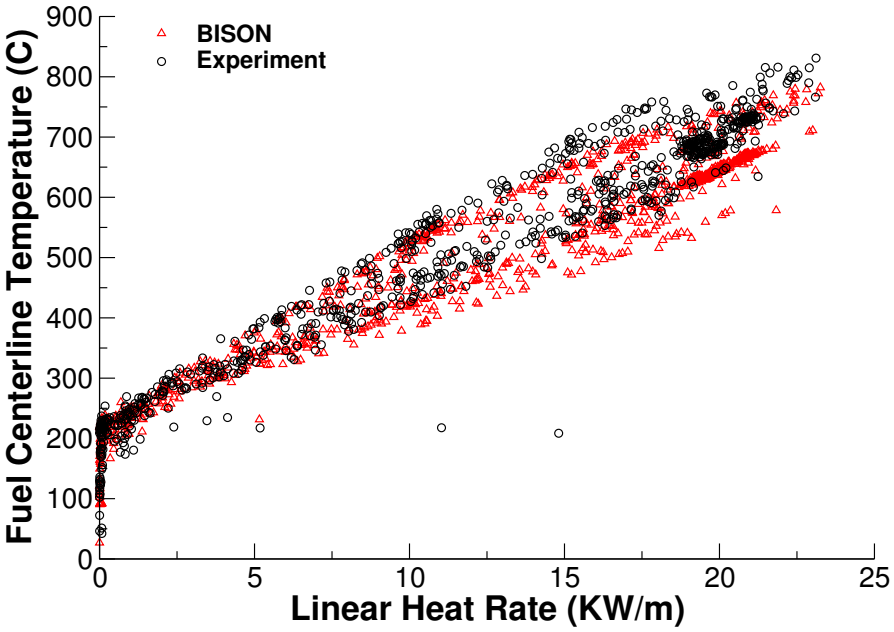

Figure C.4.: A comparison of measured and BISON predicted average fuel centerline temperature as a function of power.

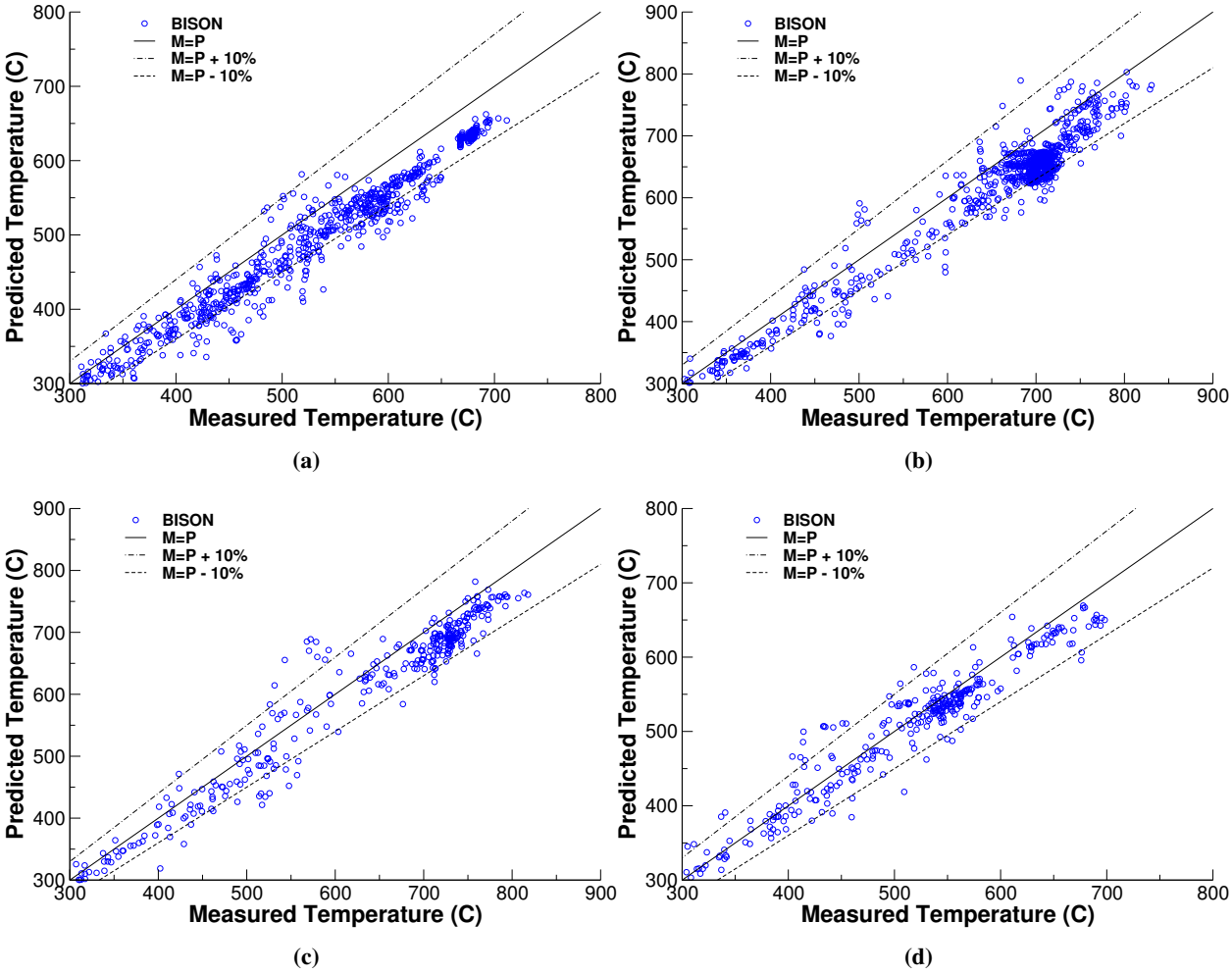

Figure C.5.: Comparison of the measured vs. predicted fuel centerline temperature for IFA-515.10 at four different burnup ranges: (a) $0 \leq Bu < 20$, (b) $20 \leq Bu < 40$, (c) $40 \leq Bu < 60$, and (d) $Bu \geq 60$ MWd/kgUO_2.

C.5. Discussion

The results show that the fuel centerline temperature compares well between the BISON predicted and experiment measurements. Although this is true the results also show that there are possible weaknesses in the gap conductance in the early stages of the simulation. Results and information from this simulation will help to guide future BISON developments.

D. IFA 519 Rod DH and Rod DK

D.1. Overview

The IFA-519.9 experiment was base irradiated in the Halden Boiling Water Reactor (HBWR), experiment IFA-429, to a burnup of 26-29 MWd/kgUO_2. The three rods (rods DC, DH, and DK) were then re-fabricated to include a bellows type pressure transducer and inserted back in to the HBWR to a burnup of approximately 90 MWd/kgUO_2 [30]. The bellows transducer in rod DC failed, therefore, in-pile data is only available for rod DH and rod DK.

D.2. Test Description

D.2.1. Rod Design Specifications

Summary of the rod specifications for rods DH and DK are shown in Table D.1.

Table D.1.: IFA-519 rod DH and DK Test Rod Specifications

		DH	**DK**
Fuel Rod			
Fuel stack height	m	0.244	0.245
Nominal plenum height	mm	25	24
Fill gas composition		He	He
Fill gas pressure	MPa	2.59	2.59
Fuel			
Material		UO_2	UO_2
Enrichment	%	13	13
Density	%	94.7	94.7
Outer diameter	mm	9.3	9.14
Pellet geometry		Dished both ends	Dished both ends
Dish radius	mm	16.8	16.8
Dish depth	mm	0.33	0.33
Land width	μm	1.4	1.4
Grain diameter (2D)	μm	6	17
Cladding			
Material		Zr-4	Zr-4
Outer diameter	mm	10.73	10.73
Inner diameter	mm	9.5	9.5
Wall thickness	mm	0.61	0.61

D.2.2. Operating Conditions and Irradiation History

The HBWR operating conditions are tabulated in Table D.2. The total reactor power history for rods DH and DK in the IFA-519.9 experiment is shown in Figure D.1. The measured reactor coolant temperature was used as the boundary temperature on the clad outer surface.

Table D.2.: Operational input parameters.

Coolant temperature	C	227
Coolant pressure	MPa	3.4
Fast neutron flux	n/(cm^2·s) per (kW/m)	1.6·10^{11}

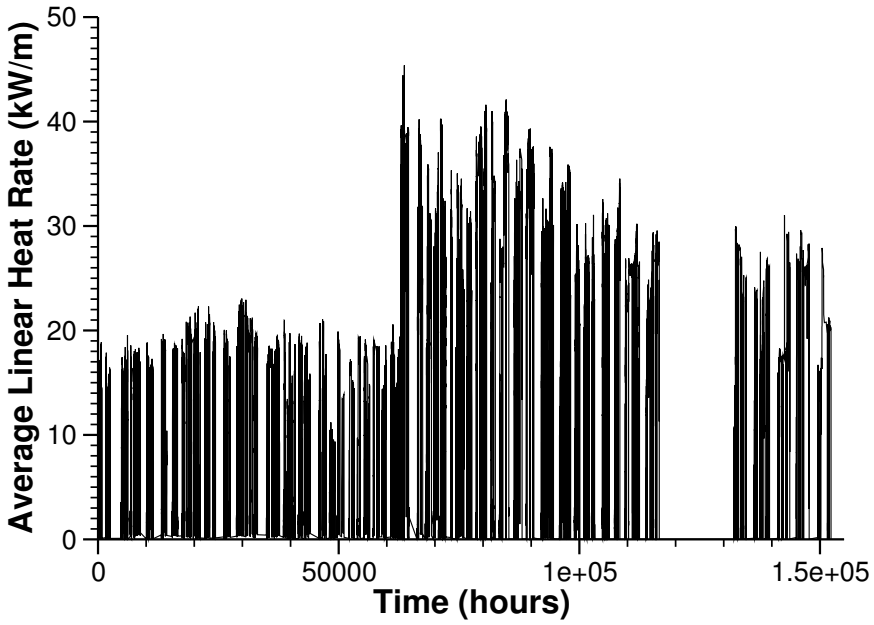

(a)

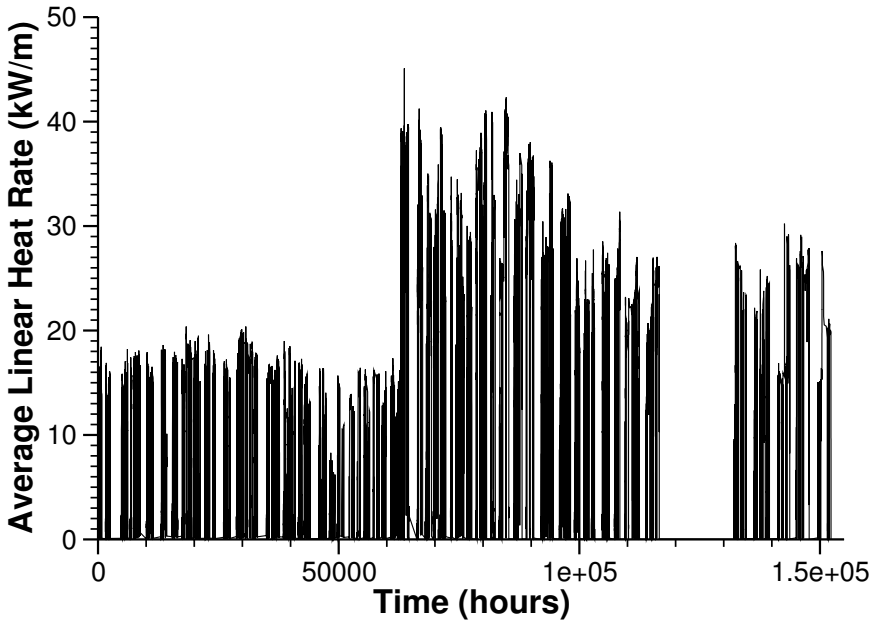

(b)

Figure D.1.: (a) Full irradiation power history for rod DH in the IFA-519.9 experiment. (b) Full irradiation power history for rod DK in the IFA-519.9 experiment.

D.3. Model Description

D.3.1. Geometry and Mesh

The assumed geometry and mesh for the two rods are shown in Figure D.2. The fuel pellet stack for each rod was modeled as a smeared column. A 2-dimensional axisymmetric quadratic mesh was used for each rod. The fuel columns were meshed with 48 axial and 11 radial element and the clad were meshed with 48 axial and 4 radial elements.

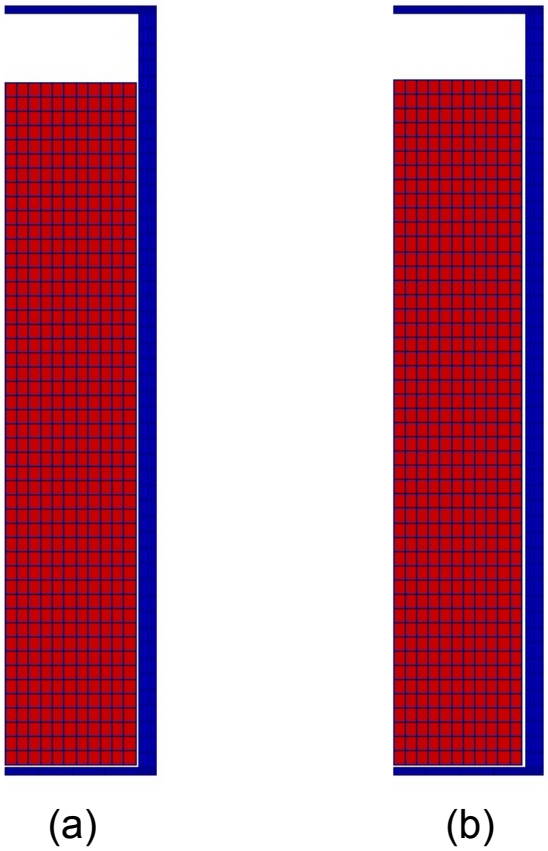

Figure D.2.: (a)2-D axisymmetric quadratic mesh for IFA-519 Rod DH simulation. (b)2-D axisymmetric quadratic mesh for IFA-519 Rod DH simulation. Note the figures above are scaled radially by a factor of 10.

D.3.2. Material and Behavioral Models

The following material and behavioral models were used for the UO_2 fuel:

- ThermalFuel - NFIR: temperature and burnup dependent thermal properties
- VSwellingUO2: free expansion strains (swelling and densification)
- RelocationUO2: relocation strains, relocation activation threshold power set to 5 kW/m.
- Sifgrs: fission gas generation and release

For the clad material, a constant thermal conductivity of 16 W/m-K was used and both thermal and irradiation creep were considered using the Limback model [26].

D.3.3. Input files

The BISON input and all supporting files (power histories, axial power profile, clad surface temperature boundary condition, fast neutron flux history, etc.) for this case are provided with the code distribution at bison/assessment/IFA_519/analysis/rod_DH and bison/assessment/IFA_519/analysis/rod_DK.

D.3.4. Execution Summary

Table D.3.: Execution summary.

Machine	Operating System	Code Version
Mac Workstation	OS X	BISON 1.2

D.4. Results Comparison

A BISON postprocessor was used to extract the data needed to compute the total fission gas released (FGR) from each rod. The total FGR is computed by dividing the fission gas released by the fission gas produced.

D.4.1. Fission Gas Release

Table D.4 summarizes the end of life (EOL) total fission gas release comparisons to the puncture results obtained durning post irradiation examination (PIE). It has been shown that the prediction of total FGR within a factor of 2 is considered acceptable [17]. Since the BISON FGR prediction is within this range, it is concluded that the FGR predictions are acceptable. As there is no fuel centerline temperature data available for comparisons, it is unknown if the underprediction of FGR is caused by a difference in the predicted and actual fuel temperature.

Table D.4.: End of Life Fission Gas Release for IFA-519.9 Rods DH and DK.

Rod	BISON Burnup ($MWd/kgUO_2$)	Halden Burnup ($MWd/kgUO_2$)	BISON FGR (%)	Halden FGR (%)	BU diff (%)	FGR diff (%)
DH	86.97	87.0	38.0	57.4	0.04	33.75
DK	83.16	88.5	33.8	52.8	6.03	36.02

E. IFA 534 Rod 18 and Rod 19

E.1. Overview

The purpose of the IFA-534 experiment was to investigate the effect of fuel grain size on fission gas release and pellet-clad mechanical interaction (PCMI) in high burnup fuel. [31]. IFA-534 consisted of two rods (rod 18 and rod 19) which were base irriated in the Goesgen PWR to 52-55 MWd/KgUO_2. These rods were then re-instrumented with internal pressure transducers and irradiated in the Halden Reactor. [18].

E.2. Test Description

The two test rods considered here were designed to test the effects of fuel grain size on fission gas release and PCMI. These two rods were instrumented with pressure transducers which provided on-line data as the experiment was irradiated in the Halden Reactor. The general rod specifications are summarized in Table E.1 which contains data taken from Reference [31] and [18].

Table E.1.: IFA-534 Test Rod Specifications

Fuel Rod		
Overall length	m	0.533
Fuel stack height	m	0.411
Nominal plenum height	mm	100
Number of pellets per rod		
Rod 18	mm	39
Rod 19	mm	39
Fill gas composition		He
Fill gas pressure	MPa	2.15
Fuel		
Material		UO_2
Enrichment		
Rod 18	%	3.84
Rod 19	%	3.79
Density	%	95
Outer diameter	mm	9.12
Pellet geometry		flat end
Grain diameter		
Rod 18	μm	22.1
Rod 19	μm	8.5
Cladding		
Material		Zr-4
Outer diameter	mm	10.75
Inner diameter	mm	9.29
Wall thickness	mm	0.73

E.2.1. Operating Conditions and Irradiation History

Rods 18 and 19 were base irradiated at the Goesgen PWR at a coolant pressure of 15.5 MPa and coolant inlet temperature of 308 C to approximatly 52 MWd/KgUO_2. The ramp testing was done in the Halden reactor and was operated with a coolant pressure of 3.2 MPa and an inlet temperature of 232 C. The Halden power history was provided by experimentalists from Halden [32].

E.3. Model Description

E.3.1. Geometry and Mesh

Both fuels rods were meshed using 2-D axisymmetric quadratic elements. For simplicity, the pellet stack was modeled as a single continuous fuel column. The rods were identical so the same mesh was used for both.The fuel pellets had 111 axial elements and 11 radial elements, and the cladding consisted of 117 axial elements and 4 radial elements.

E.3.2. Material and Behavioral Models

The following material and behavioral models were used for the UO_2 fuel:

- ThermalFuel - NFIR: temperature and burnup dependent thermal properties
- RelocationUO2: relocation strains, relocation activation threshold power set to 5 kW/m
- Sifgrs: Simplified fission gas release model with a gaseous swelling model

For the clad material, a constant thermal conductivity of 16 W/m-K was used and both thermal (primary and secondary) and irradiation creep were considered using the Limback creep model [26].

E.3.3. Input files

The BISON input and all supporting files (power histories, axial power profile) are provided with the code distribution at bison/assessment/IFA_534/analysis.

E.3.4. Execution Summary

Table E.2.: Execution summary.

Rod	Machine	Operating System	Code Version
18	FALCON	LINUX X	BISON 1.2
19	FALCON	LINUX X	BISON 1.2

E.4. Results Comparison

The purpose of the IFA-534 rod 18 and rod 19 experiments were to investigate the effect of fuel grain size on fission gas release. For this purpose the only parameter that was different in the build for these two rods was the fuel grain size. There is a slight difference in the enrichment of the two rods. This difference was accounted for by making a small modification to the individual rod power based on the acutal fuel weight to get 52 MWd/KgUO_2 at the beginning of the Halden run. [33] Fission gas relase is compared against the experiment numbers and other well known fuel performance codes. Pressure data for both rods was collected with an in-situ pressure transducer. Pressure is compared between BISON and the Halden data. The data for these comparisons was digitized from plots in the FUMEX-II Final Report [18]

E.5. IFA-534, Rod 18

E.5.1. Fission Gas Release

The BISON end result for fission gas release compared very well the the data that Halden collected. As one may note the BISON run does not start at zero like the Halden does. After the base irradiation the rod was refabricated so that the pressure transducer could be added. At this time the rod was also refilled with pure He gas. BISON currently misses rebasing the fission gas that was released prior to refabracation. We are currently discussing the best course of action to model this.

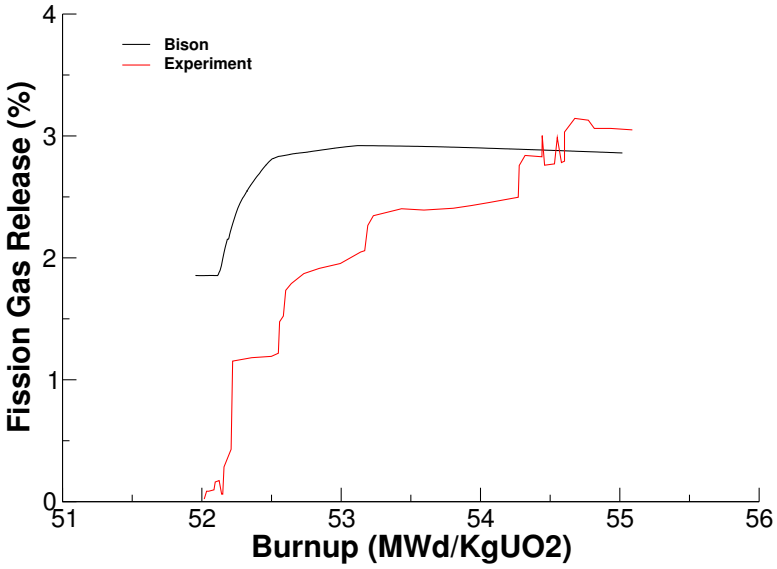

Figure E.1.: Comparison of measured and BISON predicted fission gas release during Halden irradiation for rod 18.

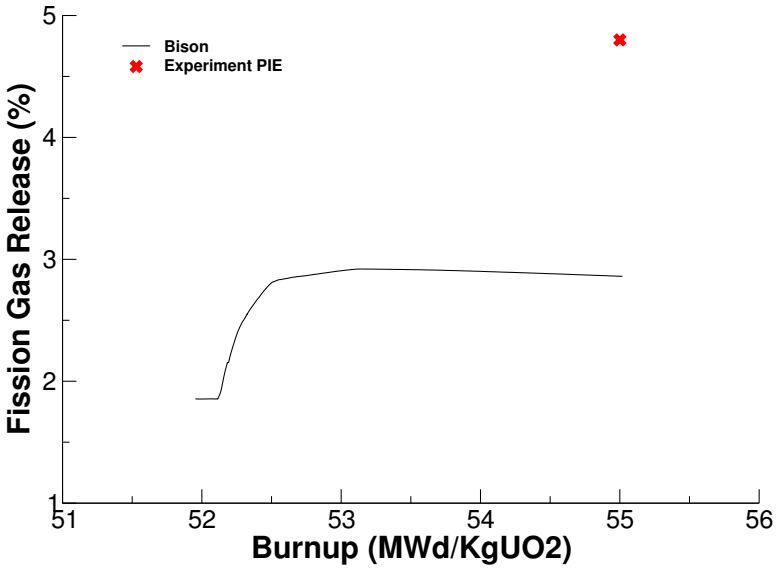

Figure E.2.: Comparison of the post irradiation examination and the BISON predicted fission gas release for rod 18.

E.5.2. Pressure

As stated previously the rod had an in-situ pressure transmitter installed at refabraction. Due to this we have real online data of the experiment's pressure. The BISON result for the pressure is off by a bit in the start and then compares very well in the end. One possible reason for the higher pressure at the start is the extra fission gas present in the model mentioned in the discussion above. Another problem that was encountered with pressure was the model predicted gas volume. The gas volume at the start of the BISON run (base irradiation) was correct, according to the FUMEX data. At refabracation the model underestimate gas volume leading to a much higher plenum pressure. As a temporary work around the mesh was adjusted such that the gas volume was high in the base irradiation and then was calculated by BISON to be correct in the Halden run. In this case the Fumex reported gas volume for the base irradiation and Halden run is 5.1 cm^3. A gas volume of 6.1 cm^3 was used for the BISON base irradiaion to achieve approximately 5.1 cm^3 for the Halden run.

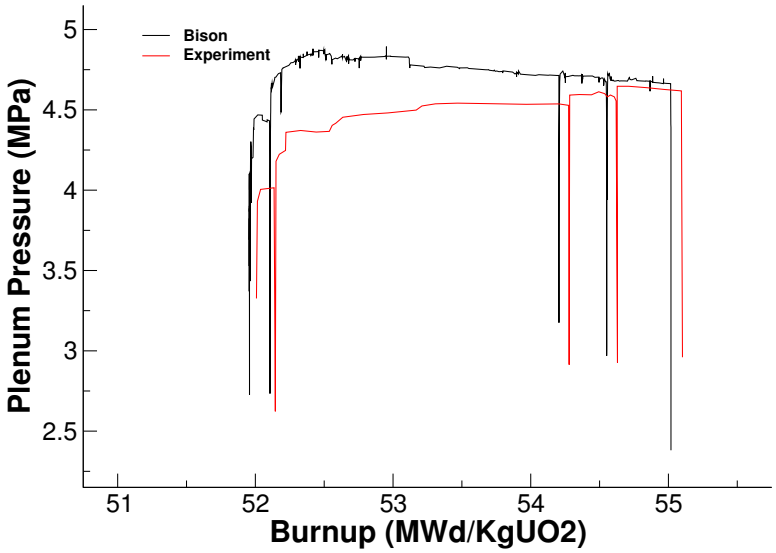

Figure E.3.: Comparison of measured and BISON predicted plenum pressure for rod 18.

E.6. IFA-534, Rod 19

E.6.1. Fission Gas Release

As with the the previous rod, 18, rod 19 compares well to the Halden data for fission gas release. Rod 19 does have the same issue as rod 18 in that fission gas does not start at zero. There is an added issue with the rod 19 data, there is a slight shift in the x-axis, burnup. This is common as burnup gets calculated in different manners with slightly different numbers and the shift is acceptable.

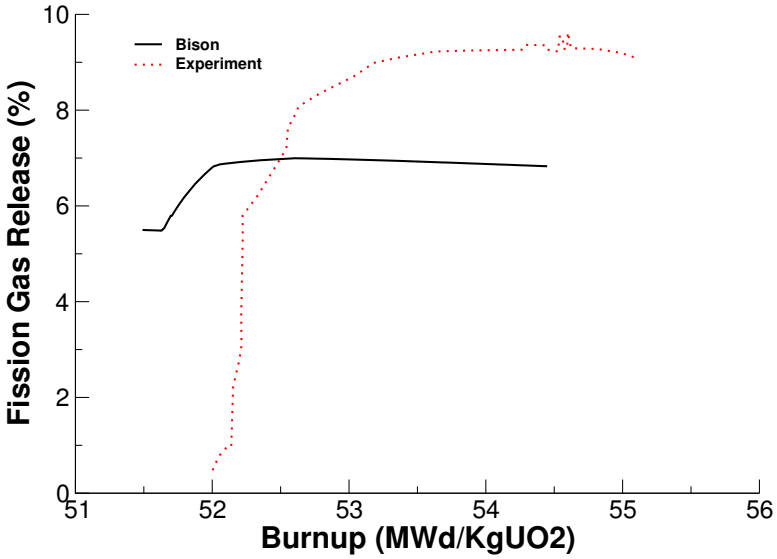

Figure E.4.: Comparison of measured and BISON predicted fission gas release during Halden irradiation for rod 19.

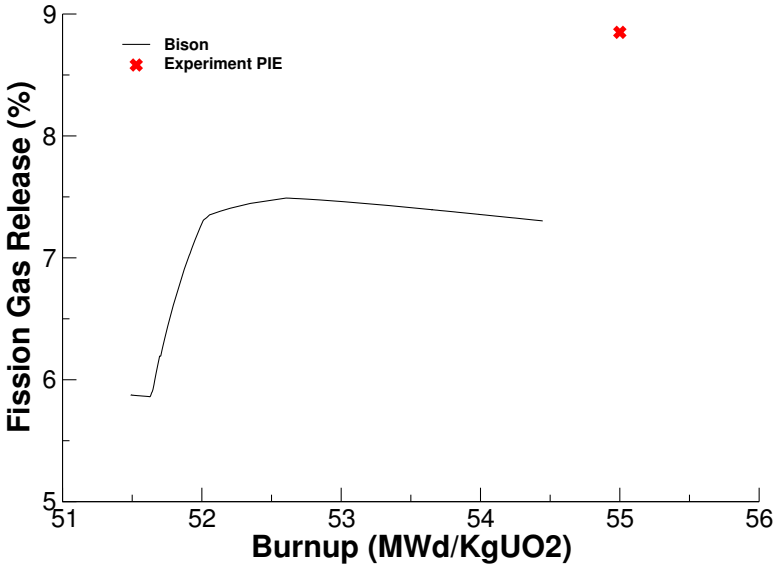

Figure E.5.: Comparison of the post irradiation examination and the BISON predicted fission gas release for rod 19.

E.6.2. Pressure

The pressure comparision is acceptable between BISON and the experiment. Once again, rod 19 has the same issues as rod 18 so the same methods where employed. These work arounds may account for the difference in the pressure. A gas volume of 6.1 cm ^{3} was used for the BISON base irradiaion to achieve approximately 5.1 cm^3 for the Halden run.

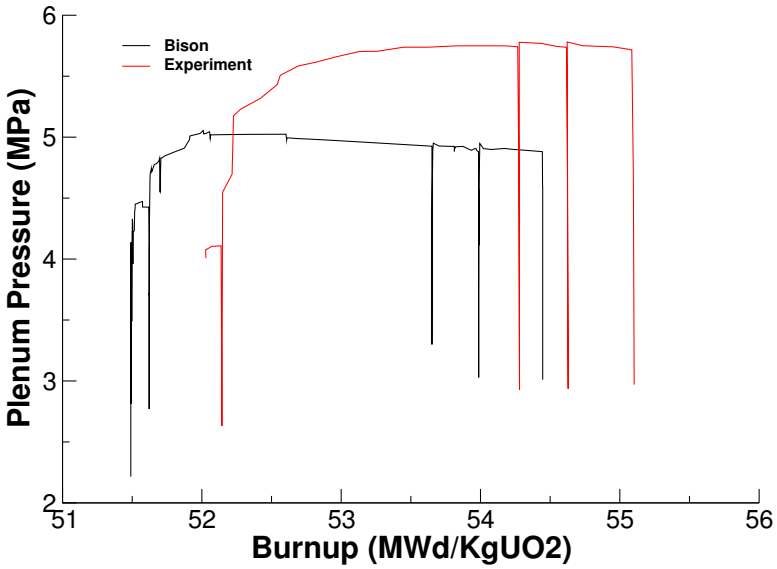

Figure E.6.: Comparison of measured and BISON predicted plenum pressure for rod 19.

E.7. Discussion

In modeling these two rods it came to the surface that how refabracation is modeled needs to be looked at more closely. This is a good thing as it will lead to a better overall BISON. Topics such as what to do with the released fission gas at refab and the BISON calculated gas volume are being worked out. As for how refabracation works currently a user enters plenum volume, gas temperature, gas content and gas pressure. BISON uses these to calulate the number of moles of gas in the plenum. BISON then looks to the postprocessors for the previous time step to calculate the gas volume that it is going to use for the continuation of the run. This was done to attempt to capture the fuel swelling and other physics that happened in the base irradiation. As stated better approaches are being looked in to.

F. IFA 535.5/6 Rod 809 and Rod 810

F.1. Overview

The IFA535 test is a test that was carried out during the Halden reactor project. This particular test was conducted to examine the effect of pre-pressurisation on fission gas release in high burnup BWR-type fuel rods. In this test four rods of identical design and base irradiation history were irradiated up to a burnup of 44 MWd/kgUO_2. At the end of the base irradiation the rods were reinstrumented with pressure transducers and clad elongation sensors. Two rods at a time were installed in the IFA-535 rig and rampe with one rod of each pair pressurized with He at 32 bar at room temperature. Rod 809, presented here was part of the first IFA535 test (IFA-535.5) which consisted of a slow ramp up to 52 kW/m. The base irradiation of the rods was completed in the upper cluster of IFA-409 from May 1973 to June 1985. Upon refabrication rods 809 and 810 were repressurized to 7.0 and 32.0 bar respectively, and fission gas from the base irradiation was measured. The rods were in reactor position 4-10 from November 1985 to February 1986 for the ramp test. After reaching a burnup of 48 MWd/kg$UO_2$the rods were removed from the reactor.

F.2. Test Description

F.2.1. Rod Design Specifications

The rod specifications for the IFA-535 test is are summarized in Table F.1. The clad thickness includes the 13μm niobium linear as the liner is not modeled for simplicity and is incorporated into the cladding thickness.

Table F.1.: IFA-535 Rod 809 and 810 Test Rod Specifications

Fuel Rod		
Overall length	m	0.560019
Fuel stack height	m	0.286
Nominal plenum height	mm	70.166
Base Irradiated Rod		
Fill gas composition		He
Fill gas pressure	MPa	0.1
Re-Fabricated Rod 809		
Fill gas composition		He
Fill gas pressure	MPa	7.0
Re-Fabricated Rod 810		
Fill gas composition		He
Fill gas pressure	MPa	32.0
Fuel		
Material		UO_2
Enrichment	%	9.88
Density	%	94.7
Inner diameter	mm	-
Outer diameter	mm	10.54
Pellet geometry		flat ends, chamfered
Grain diameter	μm	9.36 (not given assumed as per [34])
Pellet Dishing		
Chamfer width	cm	not given
Chamfer depth	cm	not given
Cladding		
Material		Zr-4
Outer diameter	mm	12.56
Inner diameter	mm	10.81
Wall thickness	mm	0.88

F.2.2. Operating Conditions and Irradiation History

The base irradiation average power is shown in Figure F.1. The average power during the bump test is shown in Figure F.2. According to Rossiter [34] the base irradition powers were given as average powers over a timestep. Therefore following the same format as Rossiter the power was ramped to the average power of the step at a rate of 10 kw/m per hour and then remained at the average power for the duration of the timestep. The ramp test values were given as point values and the power profile was linearly interpolated between these values. There was a signifcant axial profile on the fuel through both the base irradiation and the ramp test. There were minor fluctuations of the axial profile during irradiation. To illustrate the signifcance of the axial profile a plot of the profile at the end of base irradiation (prior to refabrication) and at the end of the ramp test (prior to shut down) are provided in Figure F.3.

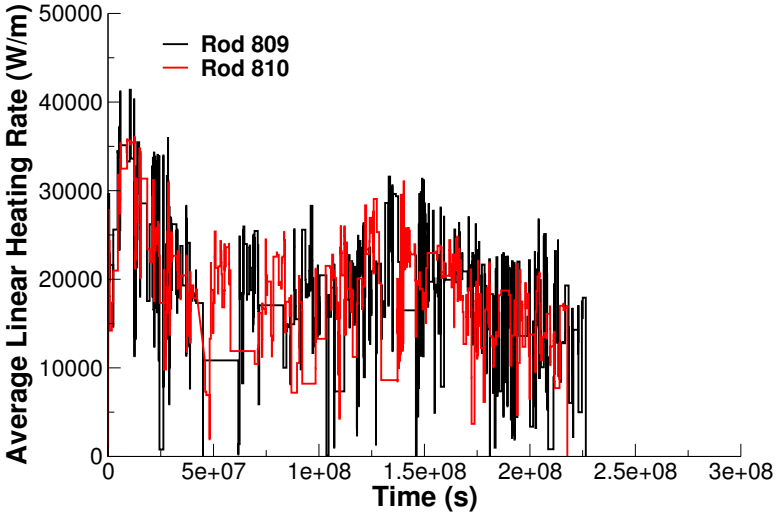

Figure F.1.: IFA-409 base irradiation used for all IFA535 tests.

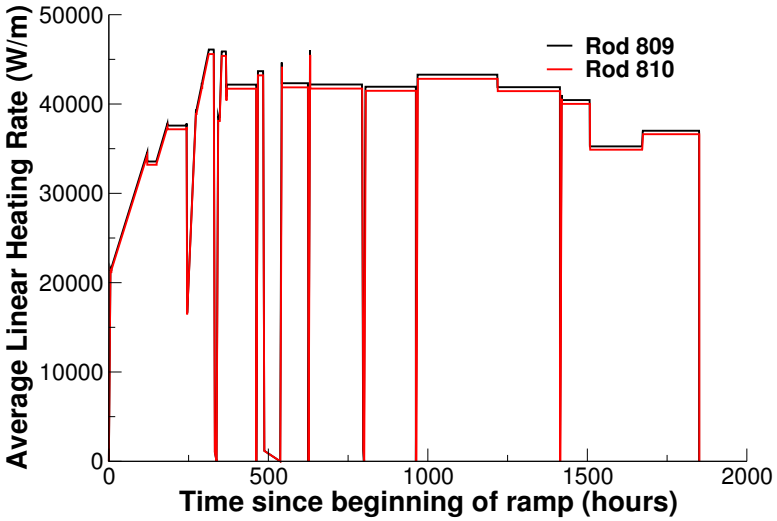

Figure F.2.: Average power history during the IFA-535.5 ramp test.

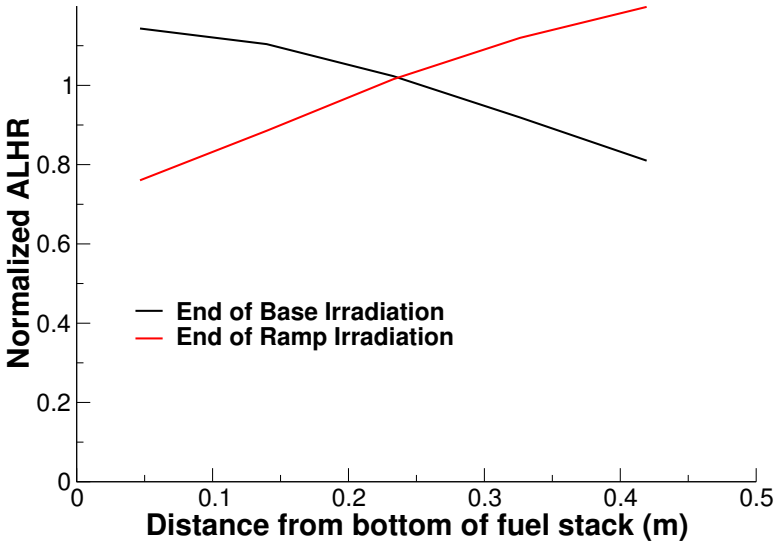

Figure F.3.: The axial power profile at the end of the base irradiation and the end of the ramp.

The clad surface temperature was input as a function, along with the fast neutron flux from data provided in the FUMEX-III data set [35]. The coolant inlet temperature and pressure for the base irradiation and power ramp is shown in Table F.2. The clad tempature, fast flux, and axial peaking factors were modified such that the same ramp rates as the power history are applied. This ensures that the times used are consistent throughout the model.

Table F.2.: Operational input parameters.

Base Irradiation		
Coolant inlet temperature	C	Not Given
Coolant pressure	MPa	3.2
Power Ramps		
Coolant inlet temperature	C	Not Given
Coolant pressure	MPa	3.2

F.3. Model Description

F.3.1. Geometry and Mesh

The geometric parameters specified in Table F.1 were used to create the mesh for this simulation. The fuel was meshed as a smeared fuel rod with 11 radial elements and 135 axial elements. The geometry was such that the refabricated rod length was modeled during the base irradiation and bump test. To account for the correct gas volume the plenum height was adjusted such that the overall voidage including radial gap, bottom plenum and top plenum were equivalent to the refabricated volume at the beginning of the ramp irradiation. The lower plenum was equal to the length of the insulator pellet that was not modeled.

F.3.2. Material and Behavioral Models

The thermal conductivity model used for the UO_2 fuel was NFIR. The fuel was modeled as elastic and fuel swelling was coupled to the fission gas release model. In addition fuel relocation was modeled using an activation power of 5 kW/m. Fission gas release was modeled using the Sifgrs model with a transient burst release model. The cladding material, was modeled using a constant thermal conductivity of 16 W/m-K. Primary and secondary thermal, and irradiation creep were modeled.

F.3.3. Input files

The BISON input and all supporting files (power histories, axial power profile, fast neutron flux history, etc.) for these cases are provided with the code distribution at bison/assessment/IFA_535/analysis/rod_809 and BISON/assessment/IFA_535/analysis/rod_810.

F.3.4. Execution Summary

The assessment case was completed on a Mac Workstation running OS X using BISON version 1.2.

Table F.3.: Execution summary.

Machine	Operating System	Code Version
FALCON	LINUX	BISON 1.2

F.4. Results Comparison

In this section the BISON simulation results are compared against the experimental data provided in the FUMEX-III data set. Measurements were provided for the rod internal pressure, fission gas release percentage and clad elongation. At the present time BISON is unable to predict clad elongation and therefore clad elongation comparisons are not included.

F.4.1. Rod Internal Pressure

The rod internal pressure results for rods 809 and 810 are presented in Figures F.4 and F.5 respectively. The initial pressure at the beginning of the ramp was 0.7 MPa nad 3.2 MPa for rods 809 and 810 respectively. It is observed that BISON overpredicts the internal pressure for 809 and slightly underpredicts the pressure for rod 810. BISON predicts the correct trends in both cases and the pressure drops during power decreases are much larger in magnitude then observed in the experimental data.

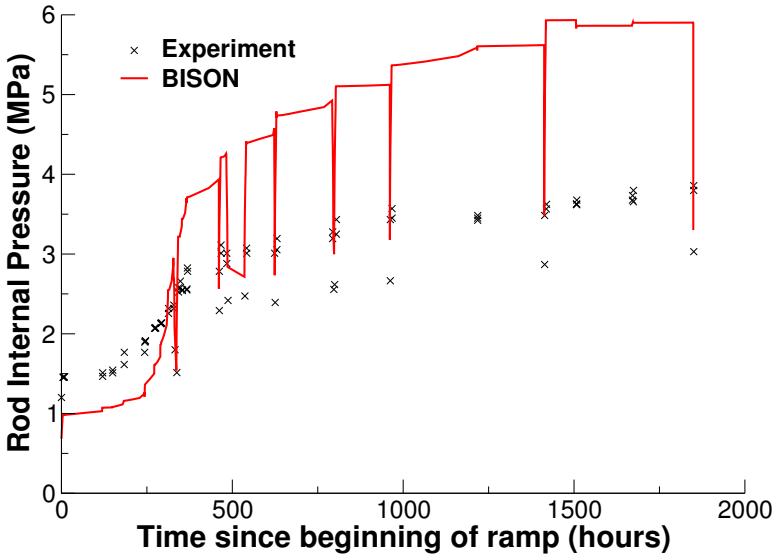

Figure F.4.: Rod internal pressure experimental comparison of IFA-535 rod 809 during the ramp test.

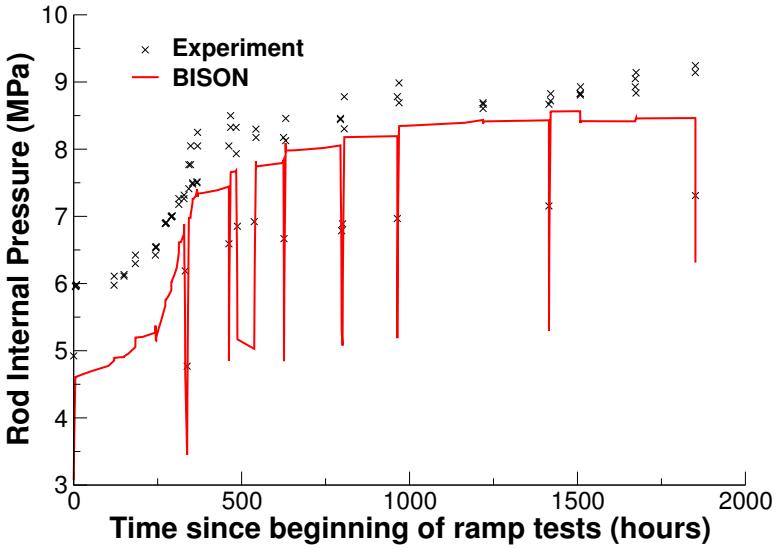

Figure F.5.: Rod internal pressure experimental comparison of IFA-535 rod 810 during the ramp test.

F.4.2. Fission Gas Release

The fission gas release results for rods 809 and 810 are presented in Figures F.6 and F.7. At the end of the base irradiation the PIE measurements obtained 19.6% and 16.2% fission gas for the two rods. However, the experimental data gives values that are slightly different at the end of the base irradiation (22% and 16.9%). BISON underpredicts the fission gas released in both cases however the results are within a factor of 2 which is considered acceptable for fission gas release predicts due to the complexity and uncertainties associated with the processes.

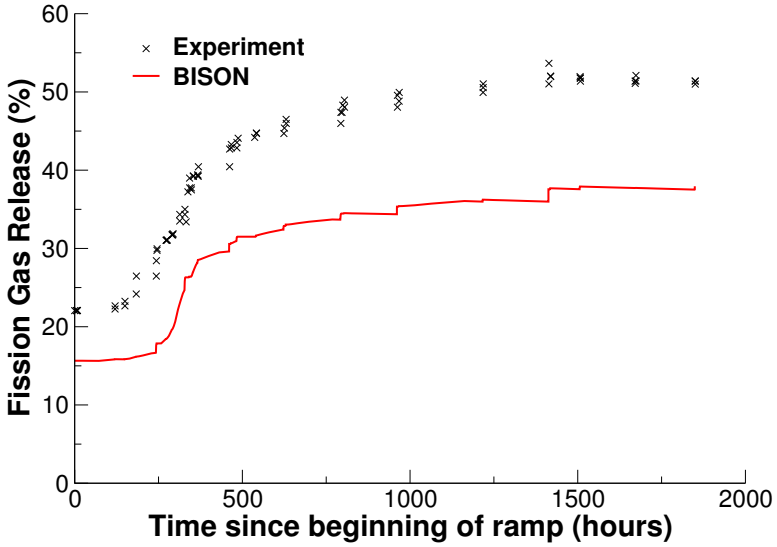

Figure F.6.: Fission gas release experimental comparison of IFA-535 rod 809 during the ramp test.

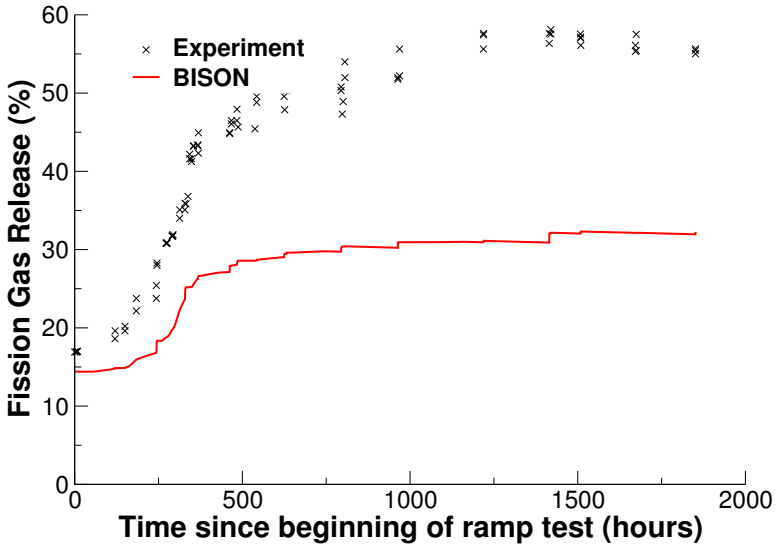

Figure F.7.: Fission gas release experimental comparison of IFA-535 rod 810 during the ramp test.

F.4.3. Discussion

There is some significant discrepancies in the experimental data provided in the FUMEX-III data files for the IFA-409 base irradiation history. Within the data the average linear heat rate is given and the linear heating rate at 5 axial locations. The axial peaking factors used within BISON are determined by taking the axial locations and dividing by the average. Therefore the average of the axial peaking factors should equal one. Using the data given in the FUMEX-III data base this is not the case. In many cases the average linear heating rate provided is less than the lowest value reported for the axial zones, which does not make sense. Therefore to ensure the correct axial profile is applied to the fuel the average linear heat rate is recalculated by taking the average of the 5 axial values provided in the data file. Moreover at certain locations in the datat files, there are two points for a specific time. Usually one lists adt value of 0 and was therefore removed. In one case the second data point contains a negative value for power at the fifth axial location. Thus for this data point the axial peaking profile was set to completely flat and the average linear heating rate to zero to remove the unphysical negative power. The effect of this change to the base irradiation on the final results is expected to be minimal. Moreover the base irradiation given in the data files for both rods 809 and 810 were significantly different even when they were irradiated in the same IFA-409 rig. Therefore, the corresponding base irradiation provided in the data files in each case was used.

In addition to the experimental data provided in the FUMEX-III dataset, numerous well known codes also completed the simulation of rod 809. Figure F.8 presents the rod internal pressure of BISON, TRANSURANUS, FRAPCON and ENIGMA-B alongside the experimental comparison. It can be seen that BISON's predictions are within the range predicted by other codes.

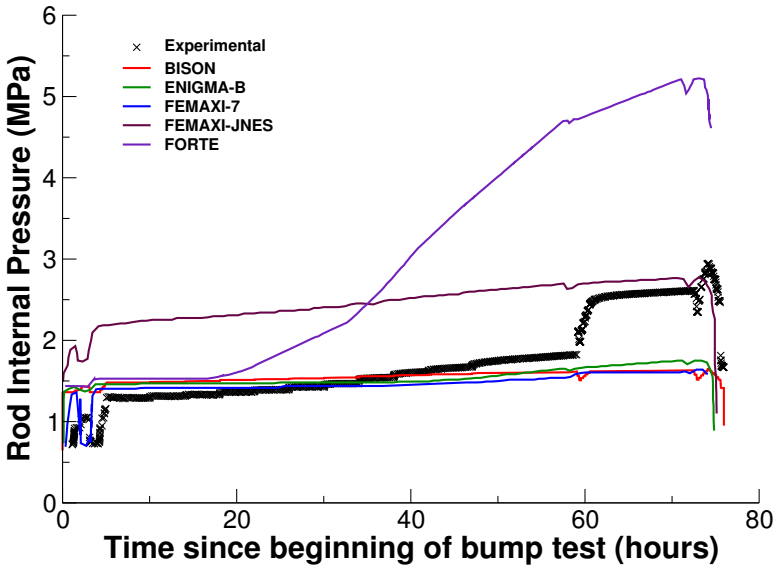

Figure F.8.: Rod internal pressure comparison of IFA-535 rod 809 during the ramp test.

G. IFA 562 Rod 15, Rod 16, and Rod 17

G.1. Overview

The IFA-562.2 experiments centered on through life fuel centerline temperature and were part of the Ultra High Burnup (UHB) program. They were irradiated in the Halden Boiling Water Reactor (HBWR) for 2.68 years to a average burnup of approximately 50 MWd/kgUO_2. The rods were fitted with a fuel centerline expansion thermometer (ET) to measure the fuel centerline temperature during irradiation [16].

G.2. Test Description

G.2.1. Rod Design Specifications

The IFA-562.2 rods were short rods of annular fuel and were enriched to 13% U-235. The fuel and cladding specifications are tabulated in Table G.1.

Table G.1.: IFA-562.2 Test Rod Specifications

Fuel Rod		
Fuel stack height	mm	442.5
Nominal plenum height	mm	31.0
Fuel pellet height	mm	7.5
Fill gas composition		He
Fill gas pressure	MPa	1.0
Fuel		
Material		UO_2
Enrichment	%	13
Density	%	94
Inner diameter	mm	2
Outer diameter	mm	5.915
Pellet geometry		flat end
Insulator Pellet		
Material		natural UO_2
Inner diameter	mm	1.80
Outer diameter	mm	5.56
Pellet length	mm	7.5
Cladding		
Material		Zr-2
Outer diameter	mm	7.015
Inner diameter	mm	6.015
Wall thickness	mm	0.5

G.2.2. Operating Conditions and Irradiation History

The HBWR operating conditions are tabulated in Table G.2. The reactor power history is shown in Figure G.1. The measured reactor coolant temperature was used as the boundary temperature on the cladding outer surface.

Table G.2.: Operational input parameters.

Average coolant temperature	C	230
Coolant pressure	MPa	3.4

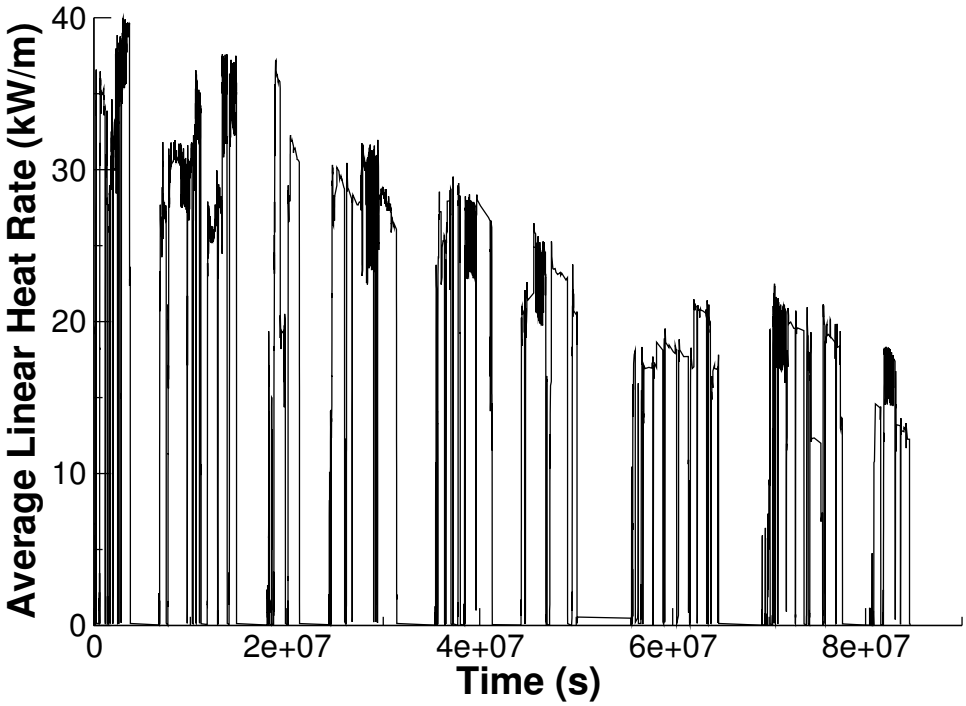

Figure G.1.: Through life power profile for IFA-562.2 rod 15. Note: Rods 15-17 power histories were very similar.

G.3. Model Description

G.3.1. Geometry and Mesh

The assumed geometry and mesh are shown in Figures G.2 and G.3. The fuel pellet stack was modeled as a smeared column with merged insulator pellets. The insulator pellets were modeled as UO_2, meaning they the same mechanical and thermal properties of the rest of the column. The expansion thermometer was modeled as a void in the pellet/insulator stack; this was done to ease the simulation. The BISON fuel centerline temperature was calculated as an average of the pellet interior (BISON sideset 13). The plenum length for the mesh was adjusted from the experiment length to account for the difference in volume caused by the voided expansion thermometer. The initial gas volumes for the simulations were as listed in [16]. A 2-dimensional axisymmetric quadratic mesh was used. The fuel column was meshed with 177 axial and 11 radial elements (aspect ratio 14) and the insulator pellets with 3 axial and 11 radial elements (aspect ratio 14). The cladding was meshed with 183 axial and 4 radial elements (aspect ratio 23.3).

Figure G.2.: 2-D axisymmetric quadratic mesh for IFA-562.2 rod 15. Note: magnified radially 10x.

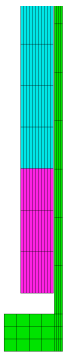

Figure G.3.: Close-up view of the IFA-562.2 rod 15. Note: This is only a cut from the bottom of the fuel rod meant to show the fuel and insulator pellet. The volume where the expansion thermometer would be in the experiment can also be seen.

G.3.2. Material and Behavioral Models

The following material and behavioral models were used for the UO_2 fuel:

- ThermalFuel - NFIR: temperature and burnup dependent thermal properties
- VSwellingUO2: free expansion strains (swelling and densification)
- RelocationUO2: relocation strains, relocation activation threshold power set to 5 kW/m.
- Sifgrs: fission gas generation and release

For the cladding material, a constant thermal conductivity of 16 W/m-K was used and both thermal and irradiation creep were considered using the Limback model [16].

G.3.3. Input files

The BISON input and all supporting files (power histories, axial power profile, cladding surface temperature boundary condition, fast neutron flux history, etc.) for this case are provided with the code distribution at bison/assessment/IFA_515_RodA1/analysis.

G.3.4. Simulation Parameters and Assumptions

As mentioned in the G.3.1 the mesh used is not an exact representation of the experiment. The insulator pellets were not included in the heat source term. The expansion thermometer was physically neglected in this mesh. This was done to alleviate troubles with thermal and mechanical properties between the thermometer and the fuel/insulator stack. The plenum length of the fuel rod was adjusted to account for the extra gas volume made from the voided thermometer. The simulation initial gas volumes were as listed in [16]. The initial fuel grain size and the fuel roughness were not given in [16]. The value of 7.75e-6 m was used for the initial grain size. This value was taken from IFA-515A1. The BISON default value of 2e-6 was used for the fuel roughness. Peaking factors were not given for this experiment. It is assumed that the rod were short enough that they did not experience much power tilting.

G.3.5. Execution Summary

Table G.3.: Execution summary.

Machine	Operating System	Code Version
INL HPC Falcon	Linux	BISON 1.2

G.4. Results Comparison

A BISON postprocessor was used to extract the centerline temperature as an average of the interface of the pellet interior surface and the ET (BISON sideset 13). This provides an accurate representation of the average fuel centerline temperature since, in this case, no axial variation in fuel temperature.

G.4.1. Temperature

The BISON results for the fuel centerline temperature show that BISON over predicts the actual experimental. Plots of the comparisons can be seen below in Figures G.4, G.5 and G.6. The peak fuel centerline temperatures are over estimated by 40-100 degrees C. One possible reason for the higher predicted temperature is that the fuel and cladding roughnesses were not reported. While running the initial simulations it was noticed that a smaller roughness affects the peak FCT greatly, improving the result comparisons. Fission gas release is another possible player with the FCT results. Initial fuel grain radius was not reported either and due to this 7.75e-6 m was taken from another simulation. The end of life FGR was reported by BISON to be about 3.5% for all three rods. This small amount would not affect the temperature much. The difference in the BISON results and the experiment measured can be seen as soon as the simulation starts. Meaning that the FGR is not the reason for the FCT difference. FCT were the only data measured from this experiment. Figures G.7, G.8 and G.9 show a comparison of measured and predicted fuel centerline temperatures. These plots show that BISON does tend to over predict through the simulation at all powers. Included in these plots are the results from the test simulation that was run with a smaller fuel roughness. The rod 17 R_f=0.2μm results show a significant improvement in the comparison of measured and predicted. As mentioned before the fuel roughness was not reported so these results are purely academic.

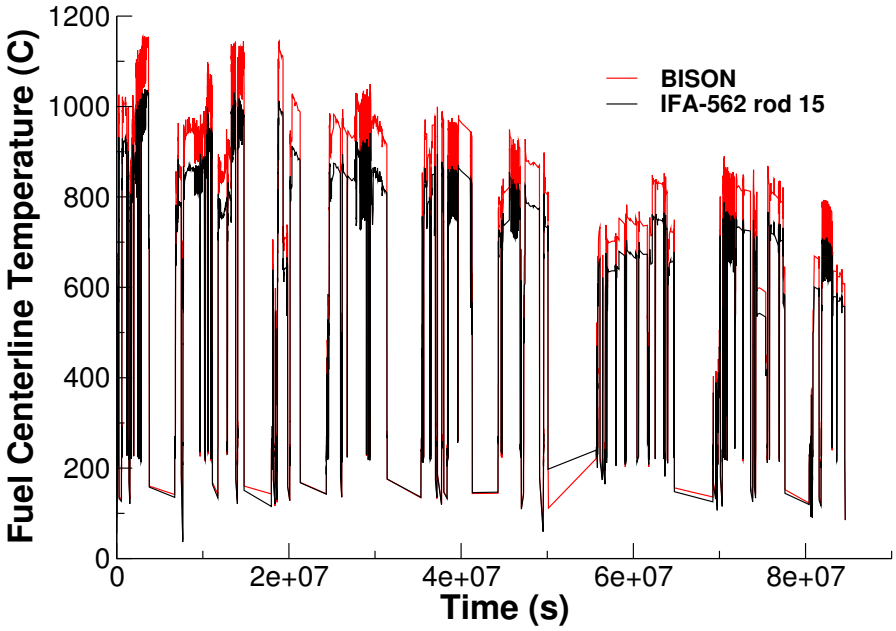

Figure G.4.: A comparison of fuel centerline temperatures for IFA-562.2 rod 15 from BISON calculations and experimental measurements.

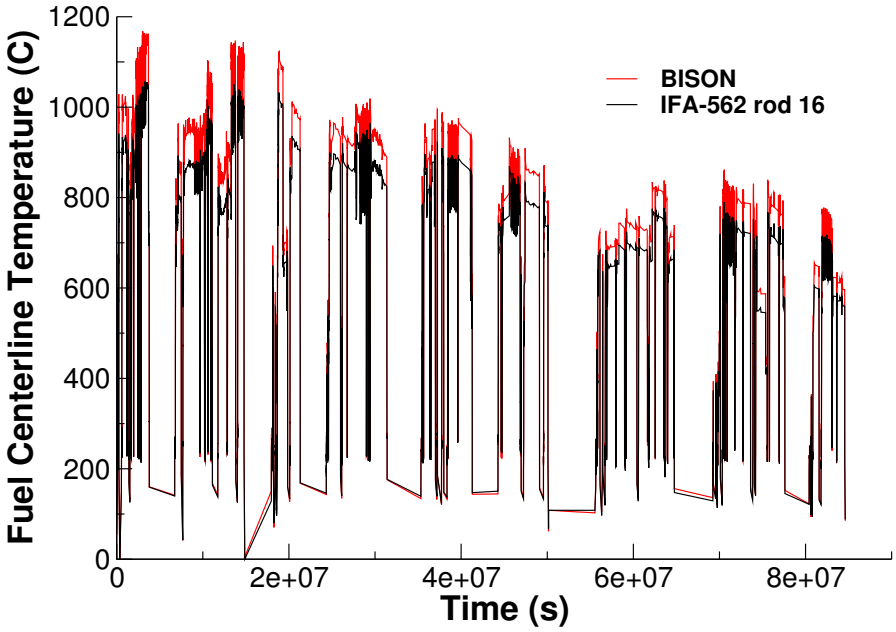

Figure G.5.: A comparison of fuel centerline temperatures for IFA-562.2 rod 16 from BISON calculations and experimental measurements.

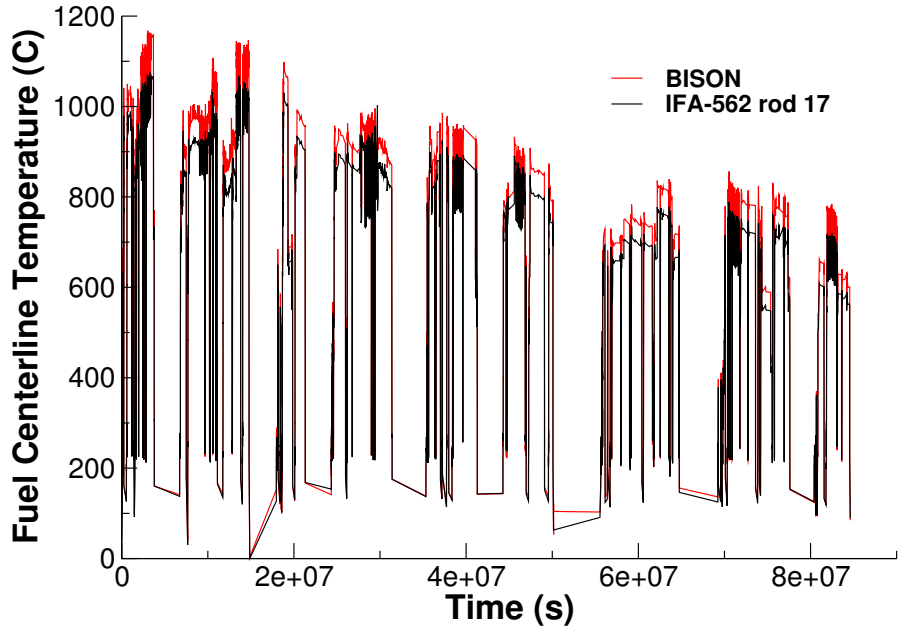

Figure G.6.: A comparison of fuel centerline temperatures for IFA-562.2 rod 17 from BISON calculations and experimental measurements.

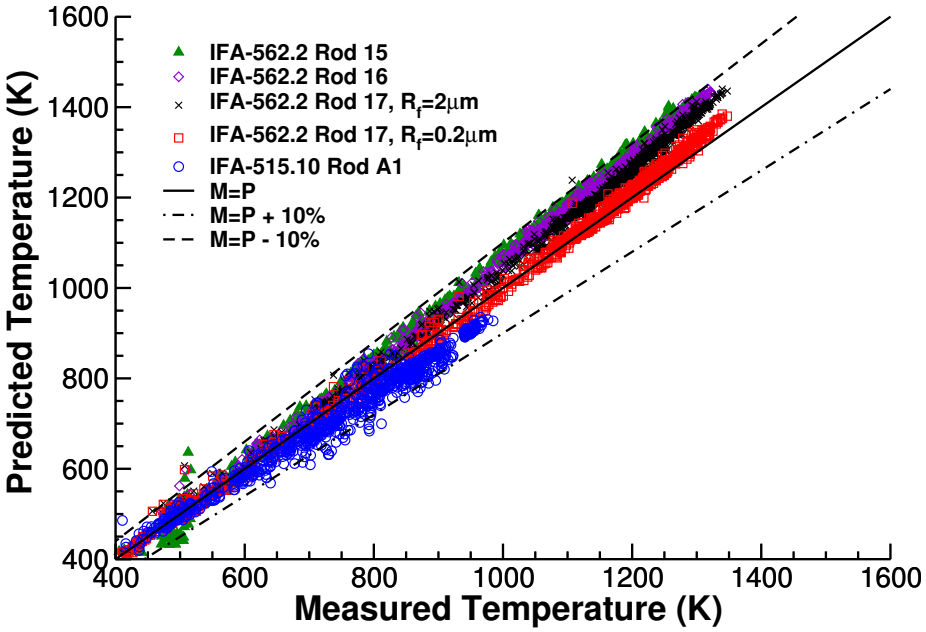

Figure G.7.: Comparison of measured vs. predicted fuel centerline temperature for IFA-562.2 at burnup 0-19 MWd/kgUO_2.

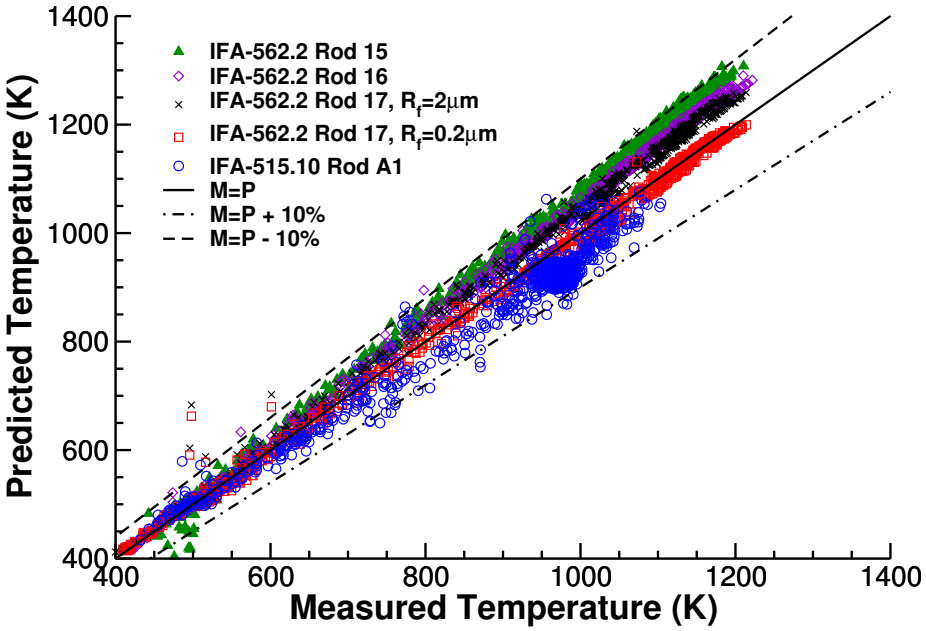

Figure G.8.: Comparison of measured vs. predicted fuel centerline temperature for IFA-562.2 at burnup 20-39 MWd/kgUO_2.

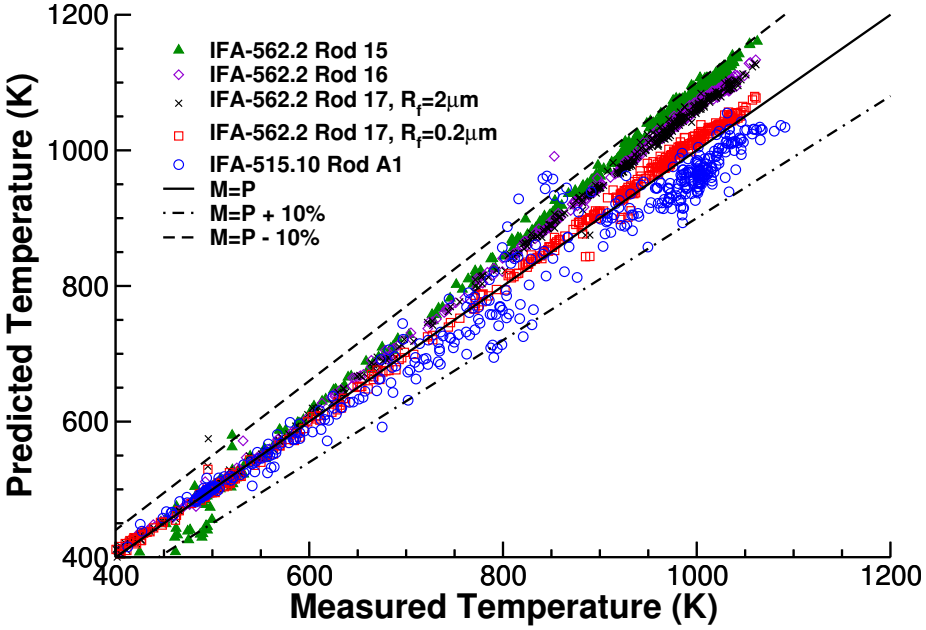

Figure G.9.: Comparison of measured vs. predicted fuel centerline temperature for IFA-562.2 at burnup 40-59 MWd/kgUO_2.

G.5. Discussion

Fuel centerline temperature comparisons between BISON and the measured results show obvious differences, although the BISON results are within 10% of the experiment measured data. Fuel roughness was shown to be a sensitive parameter and one that we are stuck using a default value for. As mentioned previously FCT was the only data recorded from this experiment leaving us with only speculation as to what may be causing the result differences.

H. IFA 636 Rod 5

H.1. Overview

The IFA-636 fuel performance test was an experiment completed in the Halden reactor as part of the OECD Halden Reactor Project. The main objective of this experiment was to extend the database on the performance of UO_2-Gd_2O_3 fuel compared with commerical UO_2. The rod of interest investigated in this report is rod 5 which contained standard UO_2fuel pellets and had online measurements of fuel elongation. Fuel elongation prior to contact can provide information on whether or not the thermal expansion, densification, solid fuel swelling and gaseous fuel swelling models are behaving as expected. Upon contact with the cladding the fuel elongation behavior becomes dependent upon the friction between the fuel stack and cladding. In the experiment it was observed that densification only occured in the UO_2fuel whearas fuel elongation measurements in the Gd-doped fel rolds indicated essentially constant sweeling with burnup. At burnups above 5 MWd/kgUO_2 the swelling rate was observed to be about 0.5 - 0.6 % ΔV/V per 10 MWd/kgUO_2 for both fuel types. The total burnup in rod 5 is approximately 34 MWd/kgUO_2.

H.2. Test Description

H.2.1. Rod Design Specifications

The specifications for IFA-636 rod 5 is are summarized in Table H.1.

Table H.1.: IFA-636 Rod 5 Rod Specifications

Fuel Rod		
Overall length	m	0.7288
Fuel stack height	m	0.393
Nominal plenum height	mm	20.2
Fill gas composition		He
Fill gas pressure	MPa	0.1
Fuel		
Material		UO_2
Enrichment	%	4.25
Density	%	96.1
Inner diameter	mm	-
Outer diameter	mm	8.195
Pellet geometry		dished, chamfered
Grain diameter	μm	9.36
Pellet Dishing		
Chamfer width	mm	0.51
Chamfer depth	mm	0.13
Dish diameter	mm	4.95
Dish depth	mm	0.24
Cladding		
Material		Zr-4
Outer diameter	mm	9.5
Inner diameter	mm	8.357
Wall thickness	mm	0.5715

H.2.2. Operating Conditions and Irradiation History

The power history of the IFA-636 experiment was provided by Halden as part of the Halden Research Project (HRP). Throughout the duration of the experiment there was an axial profile that resulted in higher power to the fuel at the top of the rod. The average linear heating rate applied to the fuel is presented in Figure H.1

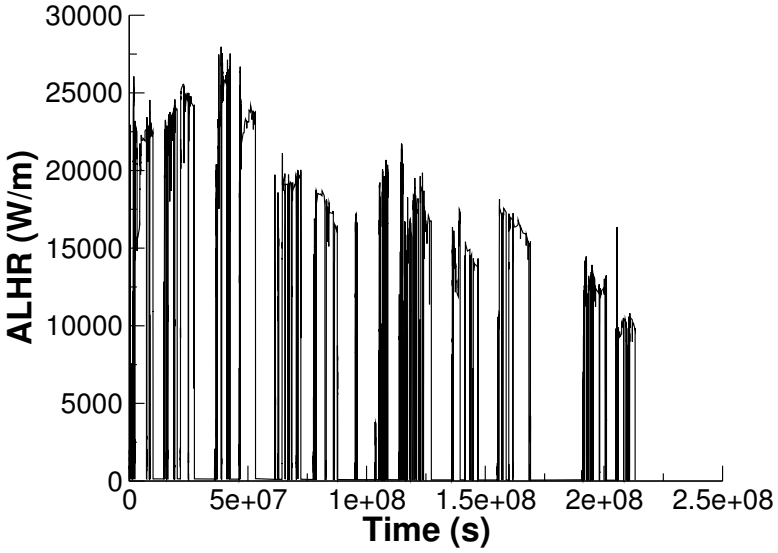

Figure H.1.: Average linear heating rate to the fuel for the IFA-636 rod 5 test.

The outer clad surface temperature was given in the Halden data and prescribed as function Dirichlet boundary condition. For the fast flux to the cladding factor of 1.6 $\times 10^{12}$ n m^{-2} s^{-1} per W/m was multiplied by the power profile. This factor is a typical value for the Halden Boiling Water Reactor. The coolant pressure for the duration of the experiment was set to 3.33 MPa.

H.3. Model Description

H.3.1. Geometry and Mesh

The geometric parameters specified in Table H.1 were used to create the mesh for this simulation. The fuel was meshed as a smeared fuel rod with 11 radial elements and 40 axial elements. The plenum length was adjusted such that the initial void volume within the fuel element is equal to 5.4 cubic centimeters as given in the Halden report. A segment of the mesh is illustrated in Figure H.2.

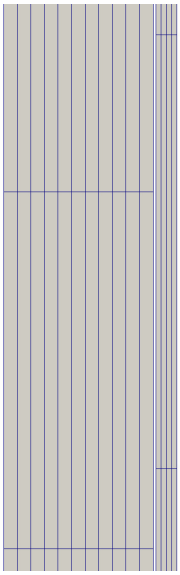

Figure H.2.: Segment of the mesh used for the fuel and cladding for the IFA-636 rod 5 simulation.

H.3.2. Material and Behavioral Models

The thermal conductivity model used for the UO_2 fuel was NFIR. The fuel was modeled as elastic and fuel swelling was coupled to the fission gas release model. In addition fuel relocation was modeled using an activation power of 5 kW/m. Fission gas release was modeled using the Sifgrs model with a transient burst release model. The cladding material, was modeled using a constant thermal conductivity of 16 W/m-K, and primary and secondary thermal, and irradiation creep were modeled.

H.3.3. Input files

The BISON input and all supporting files (power histories, axial power profile, fast neutron flux history, etc.) for this case are provided with the code distribution at bison/assessment/IFA_636/analysis/

H.3.4. Execution Summary

The assessment case was completed on a Mac Workstation running OS X using BISON version 1.2.

Table H.2.: Execution summary.

Machine	Operating System	Code Version
FALCON	LINUX	BISON 1.2

H.4. Results Comparison

In this section the BISON simulation results are compared against the experimental data and information provided by Halden. Measurements were provided for fuel elongation for rod 5. From the fuel elongation measurements a calculation of the volumetric strain in the fuel was determined. Halden takes experimental measurements every 15 minutes during the irradiation. To make the amount of data points manageable the program PowerCondense4 was used to condense the power history, axial profile, cladding temperature and cladding elongation. All condensed measurements were synchronized in time. Halden noted that the fuel elongation sensor present in rod 5 failed during irradiation. This failure is observed when the experimental data falls close to zero at an irradiation time of approximately 60 000 hours as illustrated in H.3. BISON underpredicts the fuel elongation early in life and overpredicts the fuel elongation late in life. To gain a better understanding of the behavior early in the irradiation a zoomed in version on the first 500 hours of irradiation is provided in Figure H.5. The sharp increase in the BISON results immediately after the simulation starts is due to the fact that BISON assumes a reference temperature of 297 for the thermal expansion. The systematic underprediction during part of the irradiation is due to the use of a constant thermal expansion coefficient currently employed in BISON.

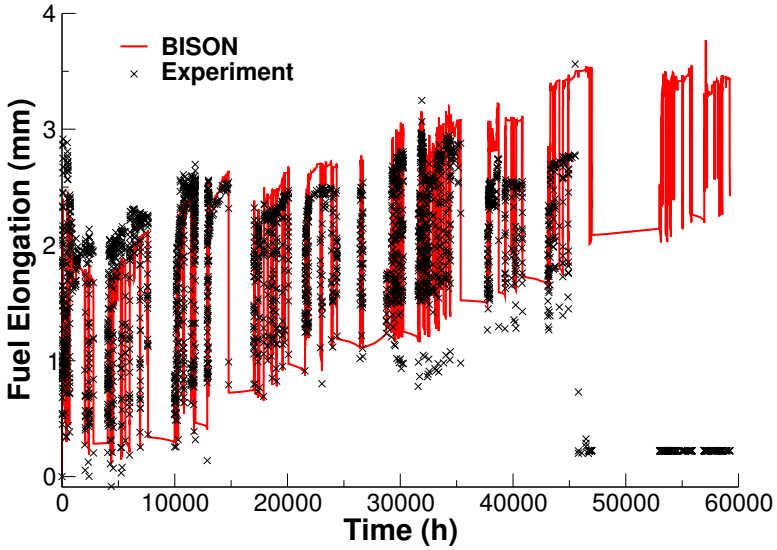

Figure H.3.: Comparison of BISON simulation results to the experimental measurements for fuel elongation for IFA-636 rod 5.

Halden stated in the report that the volumetric swelling rate was between 0.5% and 0.6% per 10 MWd/kgUO2 after a burnup of 5 MWd/kgUO2 as presented in Figure H.4. It is observed that BISON overpredicts this swelling rate by approximately 10

To gain a better understanding of the behavior early in the irradiation a zoomed in version on the first 500 hours of irradiation is provided in Figure H.5. The sharp increase in the BISON results immediately after the simulation starts is due to the fact that BISON assumes a reference temperature of 297 for the thermal expansion. The systematic underprediction during part of the irradiation is likely due to the use of a constant thermal expansion coefficient currently employed in BISON.

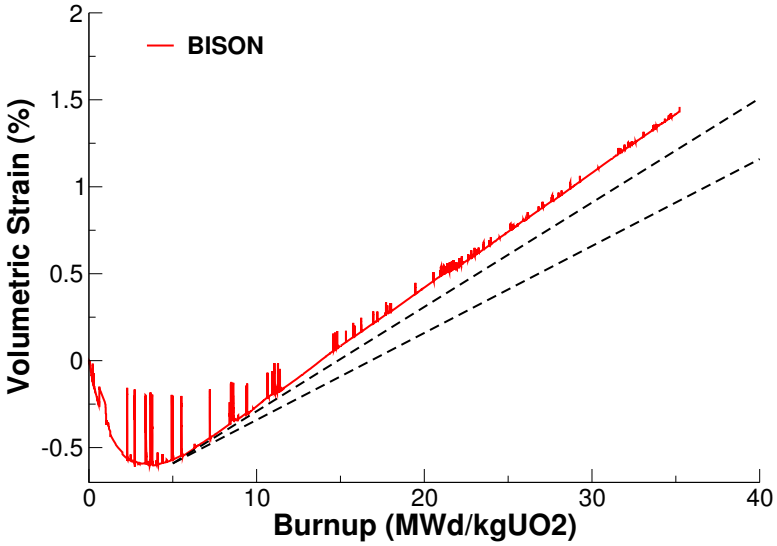

Figure H.4.: Volumetric strain predicted by BISON. The minimum and maximum swelling rates (0.5% and 0.6% per 10 MWd/kgUO2) given by Halden are superimposed. BISON appears to overpredict the volumetric strain.

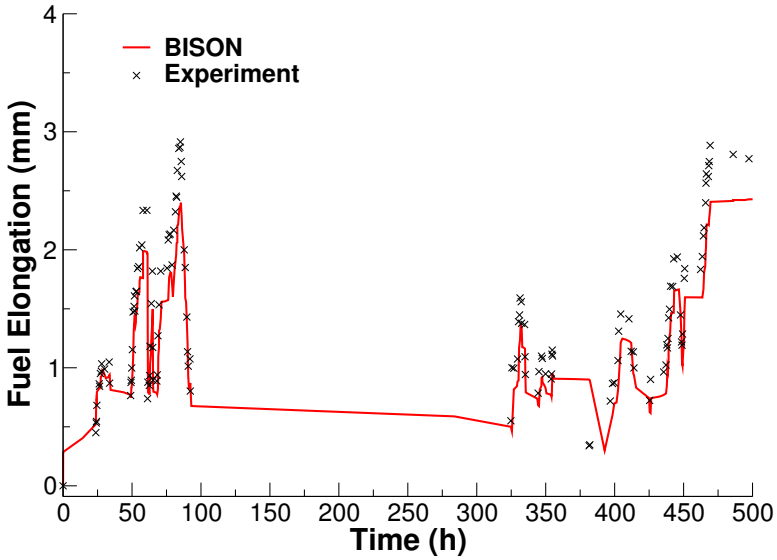

Figure H.5.: Comparison of BISON simulation results to the experimental measurements for fuel elongation for IFA-636 rod 5 for the first 500 hours of irradiation.

I. US PWR 16x16

I.1. Overview

The US PWR 16x16 lead test assembly (LTA) extended burnup demonstration (refered to as US PWR 16x16 from here on out) was conducted during the 1980's in a US commercial pressurized water reactor (PWR) [35]. The purpose of this series of exeperiments was to increase final discharge burnup and to demonstrate improved fuel utilization through more effecient fuel management. Two rods out of this series, TSQ002 and TSQ022, were discharged at a burnup of approximately 58 MWd/kgU and are the subjects of this report. TSQ002 is a full length fuel rod with standard (solid) fuel pellets, whereas TSQ022 is a full length fuel rod with annular fuel pellets.

I.2. Test Description

I.2.1. Rod Design Specifications

As mentioned in the previous section, both rods considered in the US PWR16x16 experiment were full length rods. TSQ002 was a standard fuel rod with solid fuel pellets whereas TSQ022 had annular fuel pellets. Both fuel rods were clad with Zr-4. The rod specifications are tabulated in Table I.1.

I.2.2. Operating Conditions and Irradiation History

The power history for rod TSQ002 is shown in Figure I.1. The power history for rod TSQ022 is shown in Figure I.2. A prescribed axial profile for this experiment was provided in the FUMEX-III data [35]. The measured clad surface temperature, as a function of time, was also provided in the FUMEX-III data [35] and used as a boundary condition for this simulation. The fast neutron flux was provided in the FUMEX-III data [35] as well, and is input in to the code as a function of time. The other reactor operation parameters are tabulated in Table I.2.

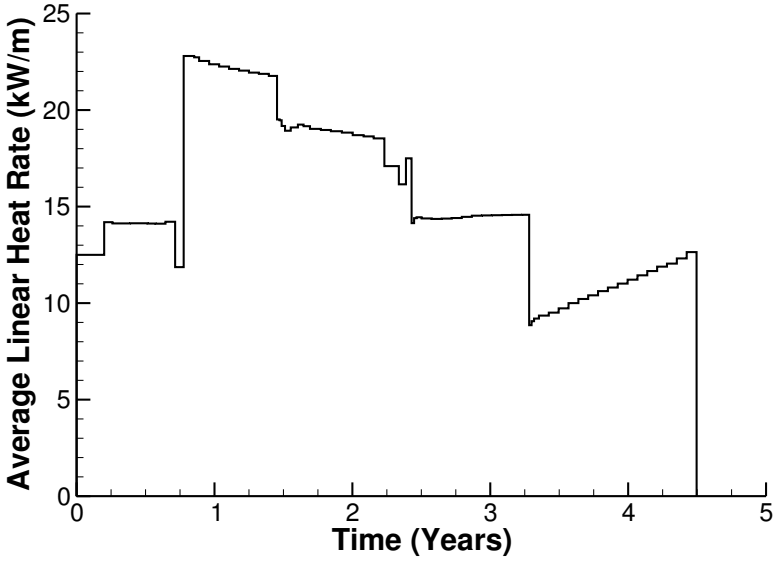

Figure I.1.: Power history for the TSQ002 fuel rod.

Table I.1.: Rod Specifications for US PWR 16x16 rods TSQ002 and TSQ022.

Fuel Rod		
Overall length	m	4.094
Fuel stack height	m	3.81
Nominal plenum height	mm	284
Number of pellets per rod		385
Fill gas composition		He
Fill gas pressure	MPa	2.62
Fuel		
Material		UO_2
Enrichment	%	3.48
Density	%	95
Inner diameter (TSQ022 only)	mm	2.337
Outer diameter	mm	8.255
Pellet geometry		dished both ends
Grain diameter	μm	7-12
Pellet Dishing		
Dish diameter	cm	0.5
Dish depth	cm	0.03
Chamfer width	cm	0.05
Chamfer depth	cm	0.016
Cladding		
Material		Zr-4
Outer diameter	mm	9.7028
Inner diameter	mm	8.4328
Wall thickness	mm	0.635

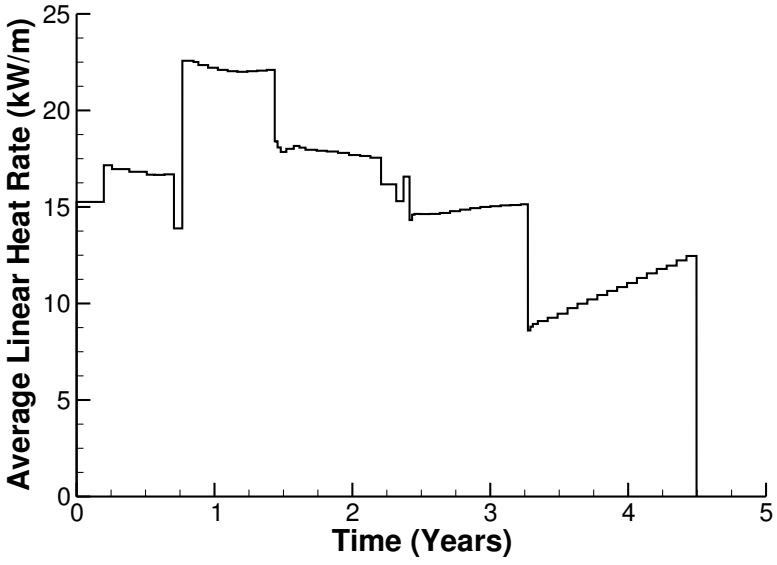

Figure I.2.: Power history for the TSQ022 fuel rod.

Table I.2.: Operational input parameters for the US commercial PWR.

Coolant inlet temperature	C	290
Coolant pressure	MPa	15.517
Fast neutron flux	n/(cm^2∗s) per (kW/m)	$5.41*10^{12}$

I.3. Model Description

I.3.1. Geometry and Mesh

A 2-dimensional axi-symmetric quadratic mesh was used to model the geometry for both rods. The fuel pellets were modeled using a single cylindrical fuel column, refered to as a smeared pellet mesh. Both meshes consisted of 1925 axial elements and 11 radial elements. The clad mesh for both rods consisted of 1931 axial elements and 4 radial elements.

I.3.2. Material and Behavioral Models

The following material and behavioral models were used for the UO_2 fuel:

- ThermalFuel - NFIR: temperature and burnup dependent thermal properties
- RelocationUO2: relocation strains, relocation activation threshold power set to 5 kW/m.
- Sifgrs: fission gas release model with a couple gaseous swelling model

For the clad material, a constant thermal conductivity of 16 W/m-K was used and both thermal (primary and secondary) and irradiation creep were considered using the Limback creep model [26].

I.3.3. Input files

The BISON input and all supporting files (power histories, axial power profile, fast neutron flux history, etc.) for this case are provided with the code distribution at ..bison/assessment/US_PWR_16x16/analysis.

I.3.4. Execution Summary

Table I.3.: Execution summary.

Rod	Machine	Operating System	Code Version
TSQ002	Falcon	Linux	BISON 1.2
TSQ022	Falcon	Linux	BISON 1.2

I.4. Results Comparison

The purpose of this series of experiments was to increase final fuel discharge burnup and to demonstrate improved fuel utilization through more effcient fuel management. The two rods of interest, for this study, are TSQ002 and TSQ022, which compare the difference between annular and solid pellets with the standard PWR fuel design [35]. Experimental data is sparse as these are commercial rods irradiated in a commercial plant. The through life fuel centerline temperature and the through life rod internal pressure results were compared to other well know fuel performance codes. The data for these comparisons were digitized from the plots in the FUMEX-III Summary Report [35]. The total fission gas release and the end of life final rod diameter calculations were compared to experimental data.

I.4.1. TSQ002

Temperature

As there is no experimental data to compare the fuel centerline temperature to, BISON results were compared to other well know fuel performance codes [35]. As show in Figure I.3, the BISON predictions for fuel centerline temperature compare well with the other codes. Note: The fuel centerline temperature was taken at a node near the axial mid-plane of the rod.

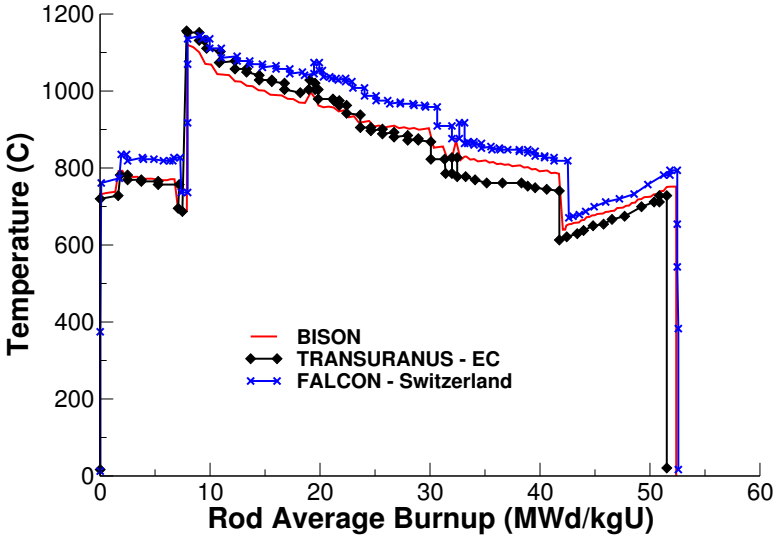

Figure I.3.: Fuel centerline temperature comparisons for rod TSQ002.

Fission Gas Release

The only fission gas release data available for this experiment is from post irradiation examination (PIE) puncture tests at the end of the fuel life. Figure I.4 shows BISON's comparisons with the end of life experimental data.

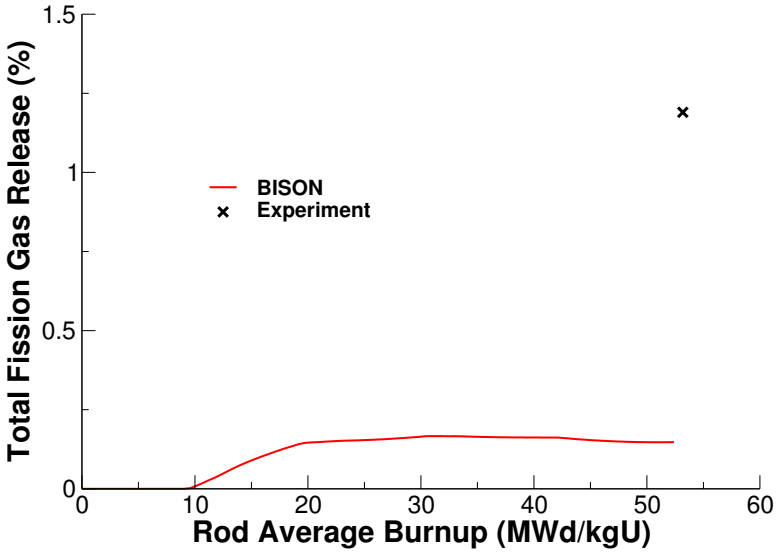

Figure I.4.: Fission gas release comparisons for rod TSQ002.

Internal Rod Pressure

As there is no rod internal pressure data to compare to, BISON calculations are compared to other well known fuel performance codes [35]. As shown in Figure I.5, the BISON predictions of rod internal pressure compare well with the other codes.

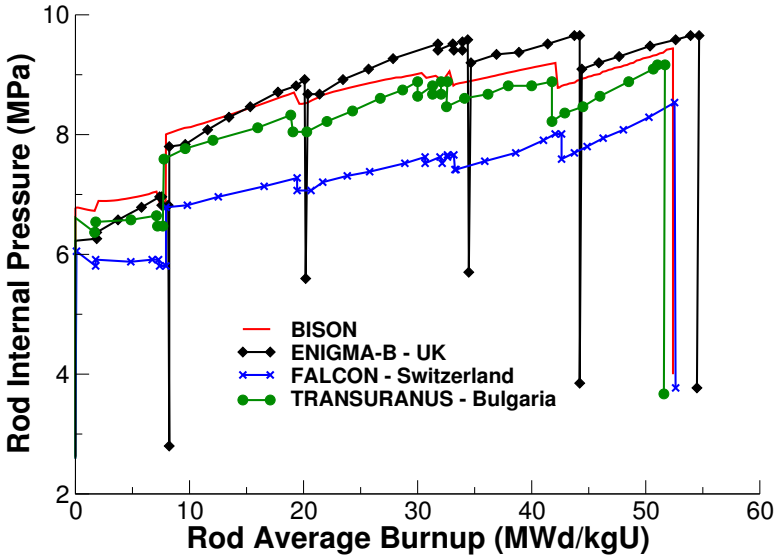

Figure I.5.: Through life code comparisons for the rod internal pressure for fuel rod TSQ002.

Rod Diameter

The final rod diameter is an indication of how well the solid mechinics featured in BISON are predicting fuel swelling and clad creep. Figure I.6 has the BISON to experimental comparisons for the end of life final rod diamter. The BISON predictions over estimate the end of life rod diameter, with a difference of appoximatly 0.02 mm. Results of the other fuel performance codes can be found in reference [35].

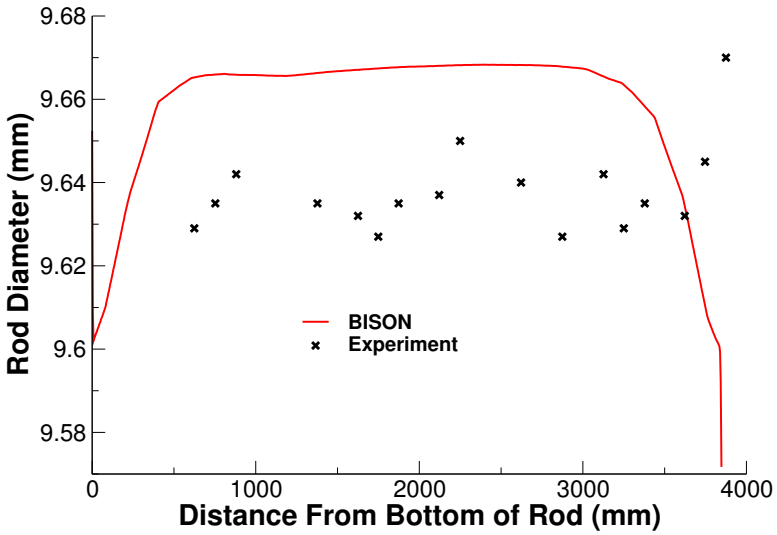

Figure I.6.: Final rod diameter comparisons for fuel rod TSQ002.

I.4.2. TSQ022

Temperature

As there is no experimental data to compare the fuel centerline temperature to, BISON results were compared to other well known fuel performance codes [35]. As show in Figure I.7, the BISON predictions for fuel centerline temperature compare well with the other codes. Note: The fuel centerline temperature was take at a node near the axial mid-plane of the rod.

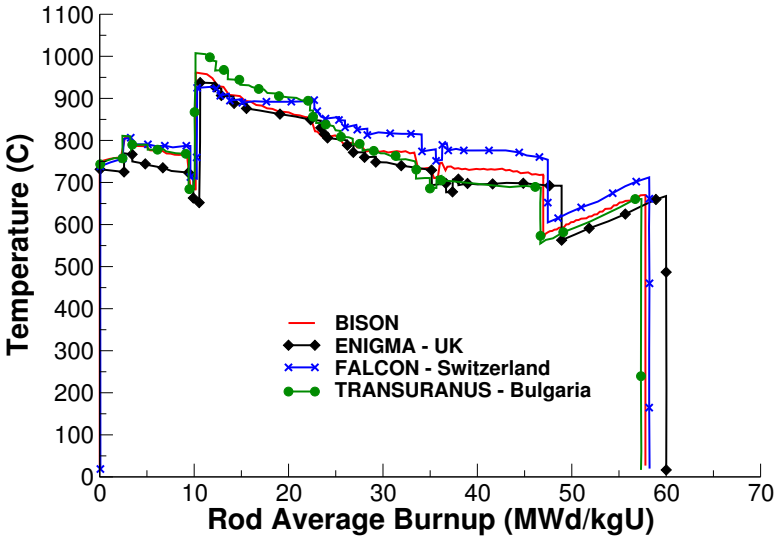

Figure I.7.: Fuel centerline temperature comparisons for rod TSQ022.

Fission Gas Release

The measured fission gas released was 0.85%, BISON did not predict any fission gas release for this experiment.

Rod Internal Pressure

As there is no rod internal pressure data to compare to, BISON calculations are compared to other well known fuel performance codes [35]. As shown in Figure I.8, the BISON predictions for the rod internal pressure are lower than the other codes plotted. The lack of fission gas release in the BISON simulation could account for the lower pressure calculated.

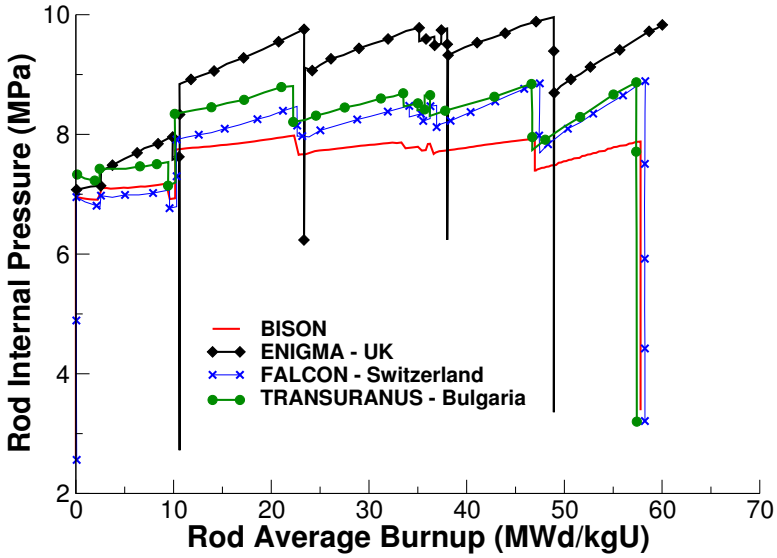

Figure I.8.: Through life code comparisons for the rod internal pressure for fuel rod TSQ022.

Rod Diameter

The final rod diameter is an indication of how well the solid mechanics featured in BISON are predicting fuel swelling and clad creep. Figure I.9 shows the BISON to experimental comparisons for the end of life final rod diamter. The BISON predictions over estimate the end of life rod diameter, with a difference of appoximatly 0.03 mm. Results of the other fuel performance codes can be found in reference [35].

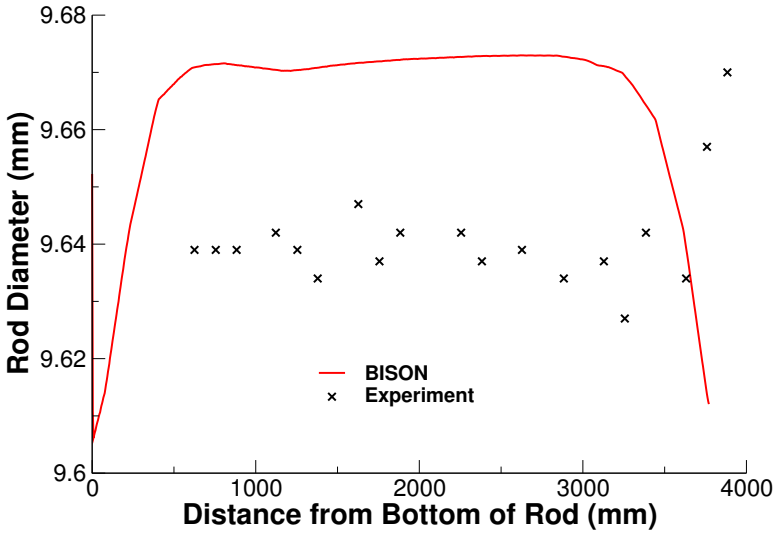

Figure I.9.: Final rod diameter comparisons for fuel rod TSQ022.

I.5. Discussion

Data for these two simulations, TSQ002 and TSQ022, where provided in a histogram format from the FUMEX-III database. A script was written at Idaho National Laboratory to convert this histogram style formatting in to a linear style format for BISON's PiecewiseLinear function call. This script can be found with the code distribution at ..bison/assessment/US_PWR_16x16/analysis. From the results shown above it is plain to see that BISON results differ from the other codes mainly in the end of life rod diameter. Pellet-cladding interactions are extremely complex and modeling them is not a trivial matter.

The BISON code is constantly undergoing changes and revisions to rectify weaknesses and results will be revisited as new and improved features are made available.

J. IFA 597.3 Rods 7 and 8

J.1. Overview

The IFA-597.3 rod 8 experiment conducted at Halden utilized a re-fabricated rod from the Ringhals boiling water reactor (BWR) [18]. The mother rod was irradiated at a low average power of around 16 kW/m for approximately 12 years. The mother rod was then re-fabricated to a shorter length and fitted with a fuel centerline thermocouple and an internal pressure sensor [36], [37].

The IFA-597.3 rod 7 experiment is similiar to the IFA-597.3 rod 8 experiment with the exception that it was instrumented with an elongation detector. The two experiments saw similarl powers (differed by approximately 2 kW/m). However, since the maximum power is approximately 30 kW/m this 2 kW/m difference is a significant percentage of the total power and the two simulations were run as separate rods with only the power history being changed. The fuel temperature and fission gas release results were obtained from the rod 8 simulation and the cladding elongation was obtained from the rod 7 simulation.

J.2. Test Description

J.2.1. Rod Design Specifications

As stated in the previous section, both rods were nearly identical and comparisons for both experiments were modeled with one simulation. The specifications for rod 8 were used for the simulation. Rod 8 was a re-fabricated rod extracted from a full length rod. The hole for the thermocouple was at the top of the fuel stack and did not penetrate the entire fuel stack. The re-fabricated rod geometry is tabulated in Table J.1.

Table J.1.: IFA-597.3 Rod 8 Test Rod Specifications

Fuel Rod		
Overall length	m	0.3539
Fuel stack height	m	0.4098
Nominal plenum height	mm	0.0513
Mother Rod		
Fill gas composition		He
Fill gas pressure	MPa	0.1
Re-Fabricated Rod		
Fill gas composition		He
Fill gas pressure	MPa	0.5
Fuel		
Material		UO_2
Enrichment	%	3.347
Density	%	95.5
Inner diameter	mm	2.5
Outer diameter	mm	10.439
TC hole length	mm	34.0
Pellet geometry		dishing one end
Grain diameter	μm	7.83
Pellet Dishing		
Dish diameter	cm	0.5
Dish depth	cm	0.01
Chamfer width	cm	0.07
Chamfer depth	cm	0.02
Cladding		
Material		Zr-2
Outer diameter	mm	12.25
Inner diameter	mm	10.65
Wall thickness	mm	0.8

J.2.2. Operating Conditions and Irradiation History

The power history for the base irradiation carried out at the Ringhals BWR is the same for both rods 7 and 8 and is shown in Figure J.1. The experiment power history carried out at the Halden boiling water reactor (HBWR) is shown in Figure J.2. The measured clad surface temperature as a function of time is shown in Figure J.3. The other reactor operational parameters are tabulated in Table J.2.

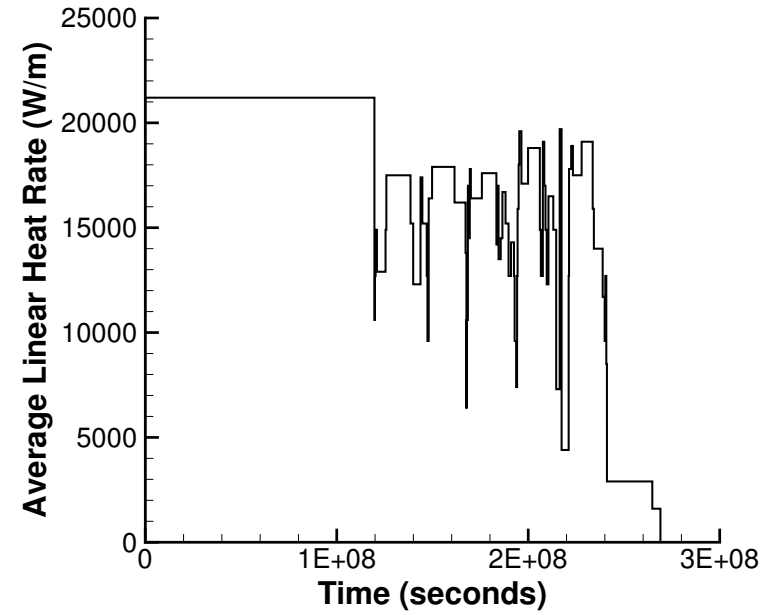

Figure J.1.: Base irradiation history for IFA-597.3, carried out at Ringhals BWR.

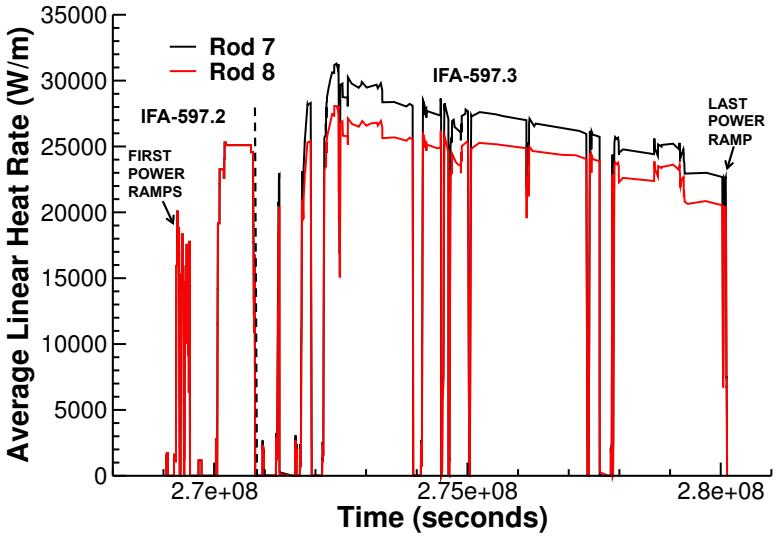

Figure J.2.: Halden irradiation periods for rods 7 and 8. The irradiations include IFA-597.2 and IFA-597.3.

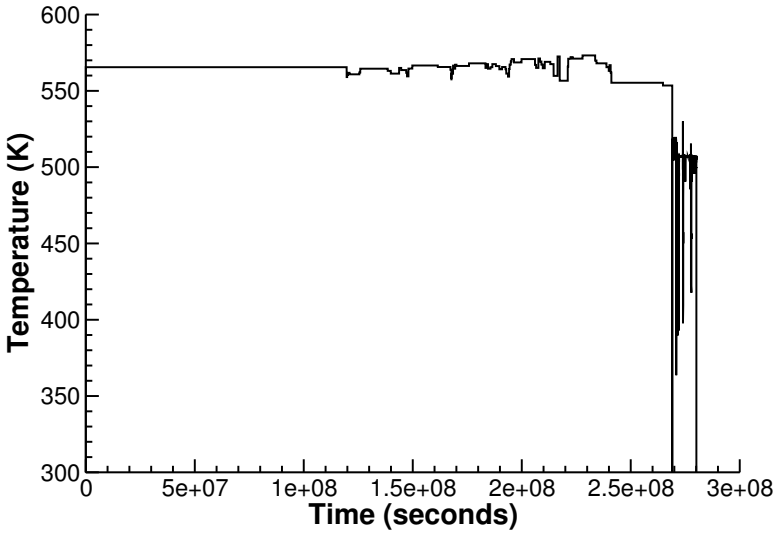

Figure J.3.: Temperature on the outside surface of the cladding for both the base irradiation and Halden irradiations for Rods 7 and 8.

Table J.2.: Operational input parameters.

Base Irradiation		
Coolant inlet temperature	C	286
Coolant pressure	MPa	7.0
Fast neutron flux	n/(cm^2·s) per (kW/m)	2.3·10^{12}
Power Ramps		
Coolant inlet temperature	C	232
Coolant pressure	MPa	3.2
Fast neutron flux	n/(cm^2·s) per (kW/m)	1.6·10^{11}

J.3. Model Description

J.3.1. Geometry and Mesh

The re-fabricated rod geometry was modeled for the entire simulation. The rod was modeled with two smeared pellet blocks, one annular and one solid, to account for the thermocouple at the top of the fuel rod.

A 2D-RZ axisymmetric quadratic mesh was used to model the geometry of rod 8. The fuel mesh consisted of 128 axial nodes and 14 radial nodes (11 radial elements for the annular section) and the clad was meshed with 4 radial elements through the thickness. A section of the meshed fuel rod at the thermocouple location is shown in Figure J.4.

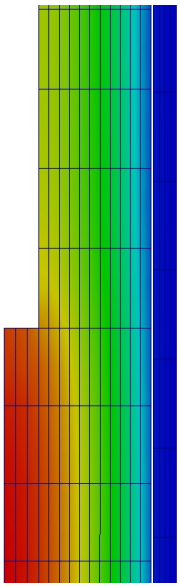

Figure J.4.: 2D-RZ axisymmetric mesh for IFA-597.3 Rod 8 simulation with temperature contour plot at thermocouple location.

J.3.2. Material and Behavioral Models

The following material and behavioral models were used for the UO_2 fuel:

- ThermalFuel - NFIR: temperature and burnup dependent thermal properties
- RelocationUO2: relocation strains
- Sifgrs: Simplified fission gas release model with a combined solid/gaseous swelling model based on fission gas release.

Material models for Zr-4 were used as a replacement for the Zr-2 clad. For the clad material, a constant thermal conductivity of 16 W/m-K was used and both thermal (primary and secondary) and irradiation creep were considered using the Limback model [26].

J.3.3. Input files

The BISON input and all supporting files (power histories, axial power profile, fast neutron flux history, etc.) for this case are provided with the code distribution at bison/assessment/IFA_597_3/analysis.

J.3.4. Execution Summary

Table J.3.: Execution summary.

Machine	Operating System	Code Version
FALCON	LINUX	BISON 1.2

J.4. Results Comparison

The IFA-597.3 Rod 8 experiment irradiated at Halden is used to demonstrate the code's capability to capture the fuel centerline temperature and the total fission gas released. The IFA-597.3 Rod 7 experiment is used to assess the code's capability to predict clad elongation during irradiation.

J.4.1. Temperature

Comparison of the measured and predicted fuel centerline temperature during the first four and final power ramps are shown in Figure J.5. Although BISON tends to under predict the temperature, considering uncertainties in the power and temperature measurements the comparisons are reasonable.

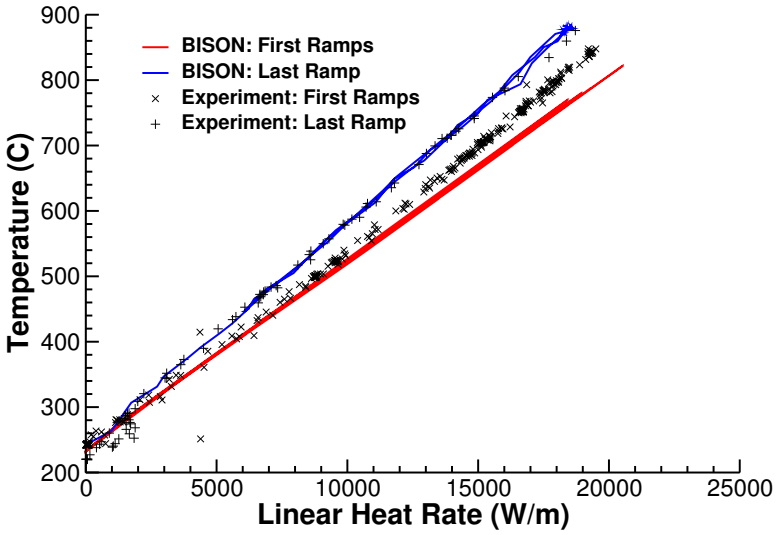

Figure J.5.: BISON fuel centerline temperature comparison to Halden experimental data.

A comparison of the predicted (P) and measured (M) fuel centerline temperatures for the entire IFA-597.3 ramp section is shown in Figure J.6. Superimposed on the graph are a M=P, M=P+10%, and M=P−10% lines to illustrate how well BISON is predicting the fuel centerline temperature. Given the uncertainty in thermal conductivity and measurements of linear power, predictions within ±10% are considered acceptable.

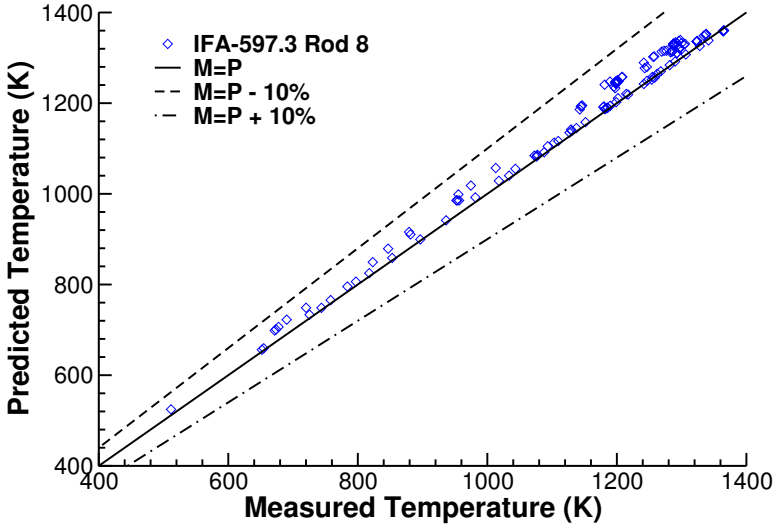

Figure J.6.: Predicted versus measured temperature throughout the IFA-597.3 Halden ramp.

J.4.2. Fission Gas Release

BISON under predicts the total FGR at the end of base irradiation and at the end of the power ramps. The pressure transducer that was used to measure the FGR reached its maximum operating limit at 68

MWd/kgU. The total fission gas release measured during the PIE puncture test was 15.8%. BISON predicts 1.8%. The BISON results compared to experimental data is shown in Figure J.7.

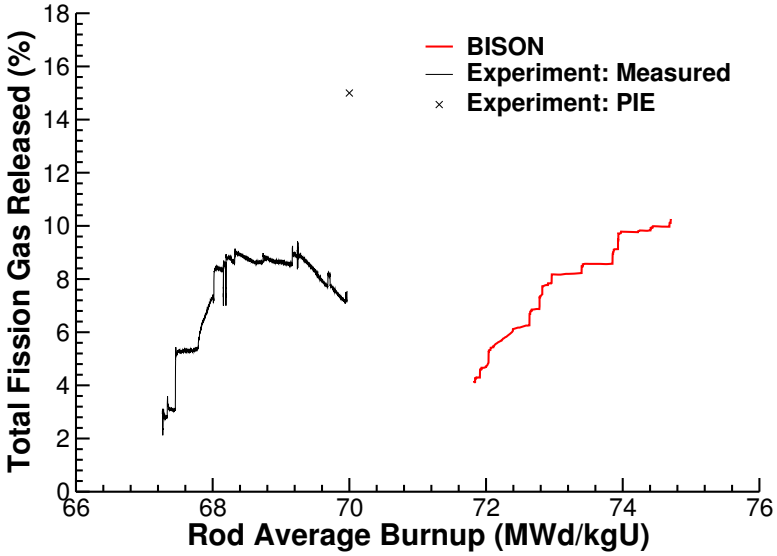

Figure J.7.: BISON fuel centerline temperature comparison to Halden experimental data.

J.4.3. Clad Elongation

The clad elongation was predicted with both frictionless contact between the fuel and clad and with glued contact between the fuel and clad, with the actual clad elongation lying between the two predictions.

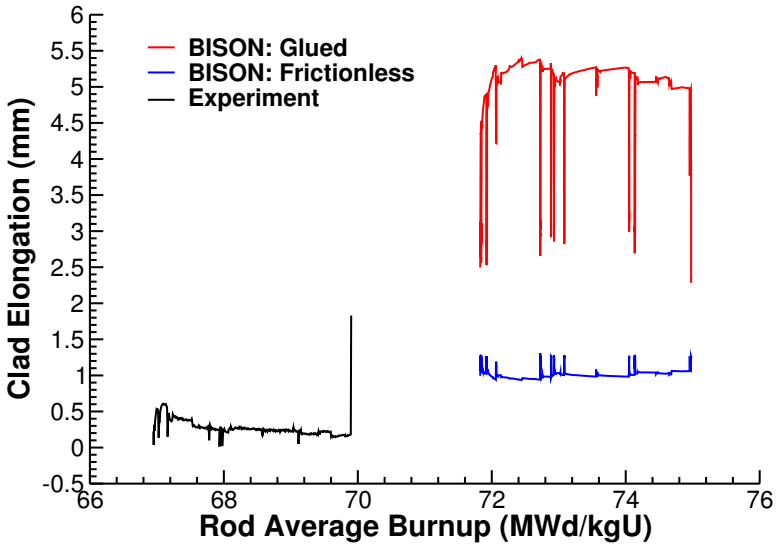

Figure J.8.: BISON fuel centerline temperature comparison to Halden experimental data.

J.5. Discussion

BISON over predicts the burnup which leads to a shift in the comparisons; this is currently being investigated.

It is recommended that this problem be revisited when frictional contact is ready for use in order to better predict the clad elongation during the power ramps.

K. R. E. Ginna Rod 2 and Rod 4

K.1. Overview

The objective of the Siemens Power Corporation (SPC)- R. E. Ginna fuel irradiation program was to test proposed fuel designs with increased margin to PCI failure and potential for higher burnup. The lead fuel assemblies were fabricated by Exxon Nuclear Company (ENC, later acquired as SPC) under a cooperative program jointly sponsored by Empire State Electric Energy Research Corporation (ESEERCo), Rochester Gas and Electric Corporation (RG&E), and ENC [38]. The irradiation program conducted at the R. E. Ginna nuclear power plant evaluated 14x14 fuel rod designs with both full length and segmented test rods featuring annular or solid pellets combined with standard (CWSRA Zr-4) or Zr-barrier (Zr-lined, CWSRA Zr-4) cladding. For the purposes of this fuel analysis problem, two rodlets from a segmented fuel rod in lead fuel assembly XT03 were evaluated: one with solid pellets and one with annular pellets. Both rods used standard cladding without a Zr-barrier. This experiment was chosen for analysis because of the availability of measured data for evaluation of several fuel rod performance characteristics including fission gas release, cladding hydrogen pick-up fraction, fuel column length changes, and end-of-life internal free volume and rod internal pressure.

K.2. Test Description

K.2.1. Rod Design Specifications

Two segmented rodlets from lead test assembly XT03 were chosen for analysis: Rodlet-2 type SSN5 and Rodlet-4 type ASN5. The fuel rodlet cross reference identification data is shown below in Table K.1 [39]. The geometric input parameters for the R.E. Ginna Rodlet-2 and Rodlet-4 test are summarized in Table K.2.

Table K.1.: R.E. Ginna Fuel Rodlet Cross Reference

Rodlet Number	Assembly	Rod Position	Rod Serial Number	Segment Number	Segment Serial No.	Rodlet Type
2	XT03	M07	XV00-2604	3	S003L	SSN5
4	XT03	L02	XU10-2303	2	S015U	ASN5

Table K.2.: R. E. Ginna Rodlet-2 and Rodlet-4 Test Rod Specifications.

Fuel Rod		
Overall length	m	0.653
Fuel stack height	m	0.5418
Nominal plenum height	mm	70.8
Fill gas composition		He
Fill gas pressure	MPa	2.1
Fuel		
Material		UO_2
Enrichment (Rodlet-2)	%	3.52
Enrichment (Rodlet-4)	%	3.7
Density	%	94
Inner diameter (Rodlet-4 only)	mm	2.814
Outer diameter	mm	8.903
Nominal diametral gap	μm	190
Average grain size (Rodlet-2)	μm	22
Average grain size (Rodlet-4)	μm	20
Cladding		
Material		Zr-4
Outer diameter	mm	10.592
Inner diameter	mm	9.093
Wall thickness	mm	0.749

K.2.2. Operating Conditions and Irradiation History

The XT03 segmented rod was irradiated for 5 cycles in the R.E Ginna reactor to a final discharge average assembly burnup of 52.07 MWd/kgU. The reactor operated at or near full power throughout the five cycles of irradiation. The power mode selected is PiecewiseLinear. The power histories for Rodlet-2 and Rodlet-4 are shown in Figures K.1 and K.2, respectively. These two power histories assumed a 24 hour startup time to reach full power, and a ramp rate of 0.33 kW/m/hr for large power increases. The ramp rate of 0.33 kW/m/hr was applied for Rodlet-2 at time step 18 to increase linear power from 21700 W/m to 33200 W/m in 125454.4 seconds and at time step 74 to increase linear power from 8200 W/m to 21300 W/m in 142909.1 seconds. The ramp rate was also applied for Rodlet-4 at time step 16 to go from LHGR of 16200 W/m to 33200 W/m in 185454.5 seconds and at time step 97 to go from 12600 W/m to 21400 W/m in 96000 seconds.

The startup times and ramp rates selected are based on ANATECH's experience with fuel rod modeling for steady state operation and are intended to minimize the introduction of computational artifacts from unrealistic power changes and ramp rates into the analyses . The ramp rate guidelines for typical power maneuvers are shown in Table K.3. The axial profile was calculated from the SPC-RE-Ginna data package [40]. The measured cladding outer surface temperature as a function of time was also provided in the SPC- RE-Ginna data package [40] and was used as a boundary condition for these simulations. The cladding outer surface temperature ranged from 568 K to 601.2 K. The initial fill-gas (Helium) pressure was 2.1 MPa, and the coolant system pressure was corrected to be 15.51 MPa instead of 155.1 MPa as shown in the QA report for SPC Irradiation in RE Ginna Reactor data [41]. The fast neutron flux as a function time was calculated from the fluence data provided in the SPC-RE- Ginna data package [40]. The fast neutron flux profile was scaled to 4.8e17. Operational input parameters are summarized in Table K.4.

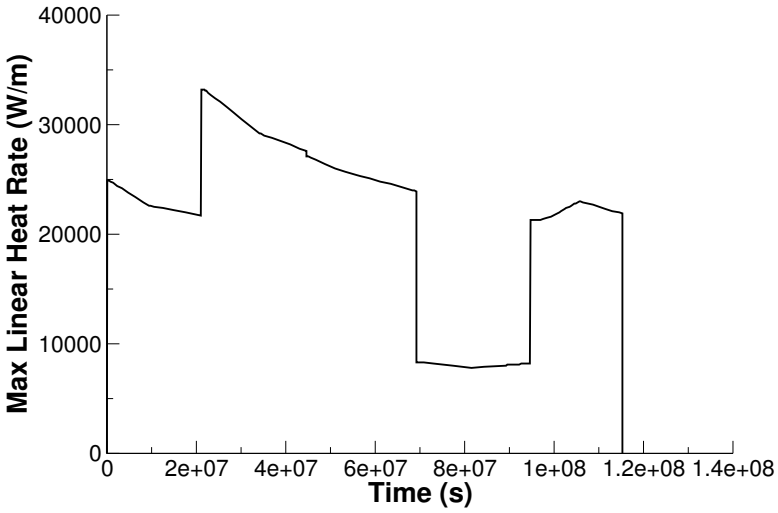

Figure K.1.: Rodlet-2 power history with 24 hours startup and ramp rate of 0.33 kW/m/hr

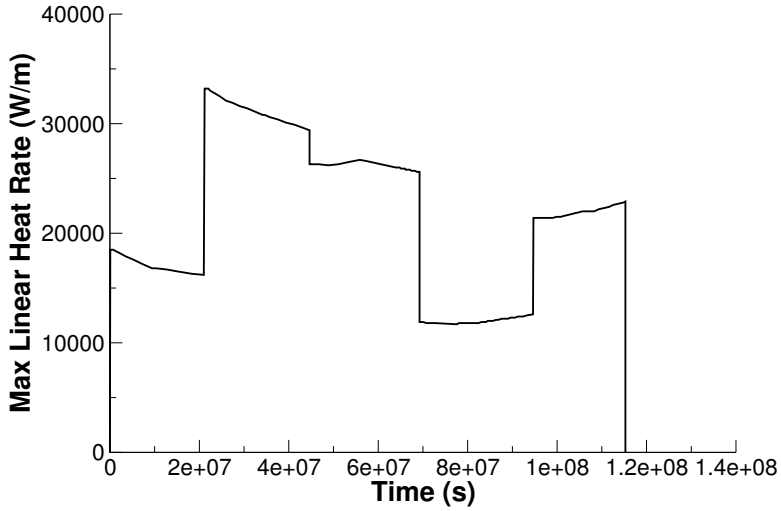

Figure K.2.: Rodlet-4 power history with 24 hours startup and ramp rate of 0.33 kW/m/hr

Table K.3.: Ramp Rate Guidelines for typical power maneuvers

Steady State Operation	**kW/ft/hr**	**kW/m/hr**
Typical operating maneuvers	0.1	0.33
Start-Ups	0.3 - 1.0	1.0 - 3.3
Fast Transients		
LOCA tests	2.2E3	7.2E3

Table K.4.: Operational input parameters

Base Irradiation		
Coolant inlet temperature	K	550.15
Coolant pressure	MPa	15.51

K.3. Model Description

K.3.1. Geometry and Mesh

The rod specifications in Table K.2 were used to define the geometry for these simulations. Each rodlet was modeled as a 2-dimensional axi-symmetric linear mesh with quadratic elements. The Rodlet-2 fuel mesh consisted of 102 axial elements and 11 radial elements, whereas the Rodlet-4 fuel mesh consisted of 102 axial elements and 8 radial elements due to the presence of the fuel pellet annulus. The cladding mesh for both rodlets consisted of 4 radial elements.

In order to accurately model the fuel rod initial free volume, the overall fuel rod length and upper plenum height were adjusted during the mesh generation to account for the volume of the plenum spring which is not explicitly modeled. The overall fuel rod lengths for Rodlet-2 and Rodlet-4 were reduced from 653 mm to 600.853 mm and 593.578 mm, respectively. The plenum heights for Rodlet-2 and Rodlet-4 were reduced from 70.8 mm to 53.59 mm and 46.316 mm, respectively. The meshes for each rodlet are shown in Figures K.3 and K.4.

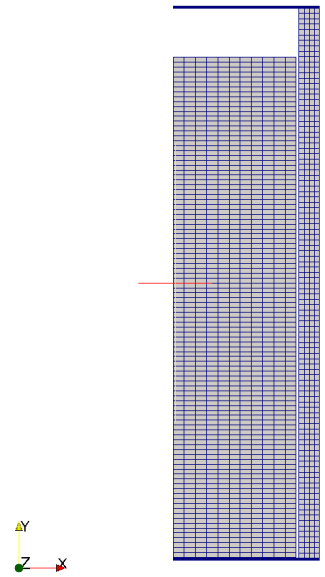

Figure K.3.: Rodlet-2 mesh

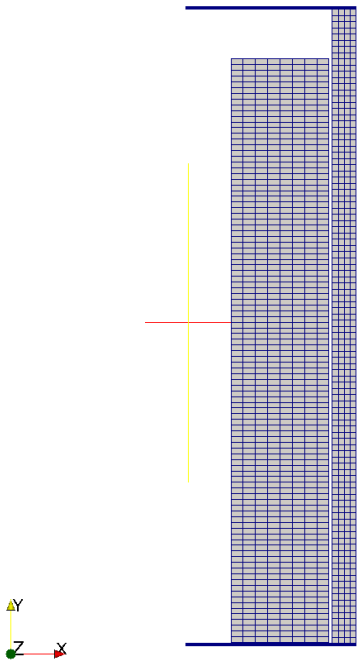

Figure K.4.: Rodlet-4 mesh

K.3.2. Material and Behavioral Models

The following material and behavioral models were used for the UO_2 fuel:

- ThermalFuel - NFIR: temperature and burnup dependent thermal properties.

- RelocationUO2: relocation strains, relocation activation threshold power set to 5 kW/m.
- Sifgrs: fission gas release model with the combined gaseous swelling model.
- MechZry: model irradiation growth.

For the cladding material, a constant thermal conductivity of 16 W/m-K was used and both thermal and irradiation creep were considered using the Limback model [26].

K.3.3. Input files

The BISON input and all supporting files (power histories, axial power profile, etc.) for Rodlet-2 and Rodlet-4 are provided with the code distribution at bison/assessment/RE_Ginna_Rodlets/analysis/RE_Ginna_Rodlet-2 and bison/assessment/RE_Ginna_Rodlets/analysis/RE_Ginna_Rodlet-4, respectively.

K.3.4. Execution Summary

Table K.5.: Execution summary.

Rod	Machine	Operating System	Code Version
2	FALCON	LINUX	BISON 1.2
4	FALCON	LINUX	BISON 1.2

K.4. Results Comparison

Data from the SPC-R. E. Ginna fuel irradiation program was used to assess the codes capability to capture the integral fuel rod fission gas release, rod internal pressure, fuel column length changes and cladding hydrogen pick-up fraction. A comparison of the predicted values from BISON calculations versus measured values from experimental data are shown in Table K.6 and Table K.7 for Rodlet-2 and Rodlet-4 respectively. Because the feature to calculate oxide thickness, cladding hydrogen concentration and pick-up fraction are not currently available in BISON, these comparisons will be performed in the future. The final burnup calculated for Rodlet-2 and Rodlet-4 were 51.508 MWd/kgU and 57.57 MWd/kgU compared to 51.6 MWd/kgU and 57.04 MWd/kgU burnup, respectively in the test documentation.

Table K.6.: Bison prediction versus measured data for Rodlet-2.

	BISON prediction	Measured Data
Burnup (MWd/kgU)	51.508	51.69
Fission Gas Release (%)	1.903	2.36
EOL Rod Internal Pressure (MPa)	4.25	2.88
Column changes (mm)	3.578	7.3 (Length Increase)
Initial free volume (cc)	5.0	5.0
Final free volume (cc)	3.599	3.7
Rod average diametral creepdown (%)	0.1944	0.793

Table K.7.: Bison prediction versus measured data for Rodlet-4.

	BISON prediction	Measured Data
Burnup (MWd/kgU)	57.57	57.04
Fission Gas Release %	0.843	0.92
EOL Rod Internal Pressure (MPa)	3.604	2.32
Column changes (mm)	4.75	4.7 (Length Increase)
Initial free volume (cc)	7.897	7.9
Final free volume (cc)	6.565	7.0
Rod average diametral creepdown (%)	0.19	0.769

K.4.1. Fission Gas Release

The only fission gas release (FGR) data available for this experiment is from post irradiation examination (PIE) puncture tests at the end of the fuel life. Figure K.5 and Figure K.6 show BISONs comparisons with the end-of-life experimental data for Rodlet-2 and Rodlet-4, respectively. BISON computes a reasonable FGR value that only slightly under predicts the measured result for both rodlets.

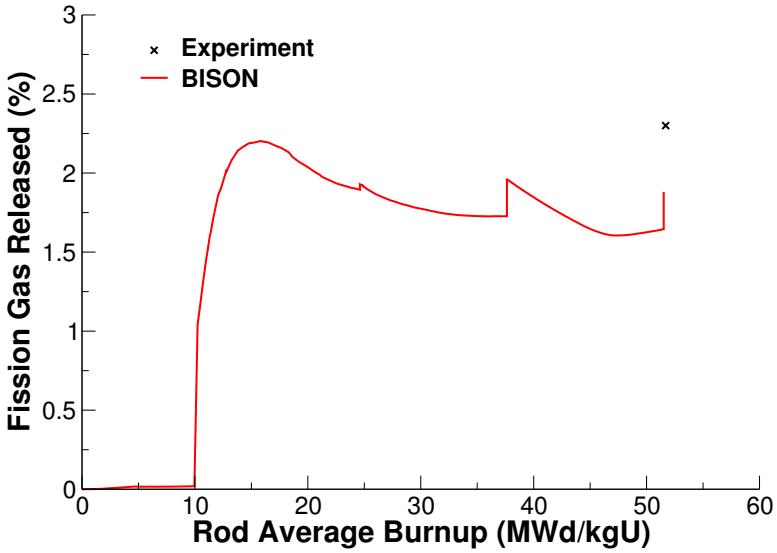

Figure K.5.: Fission gas release comparisons for Rodlet-2

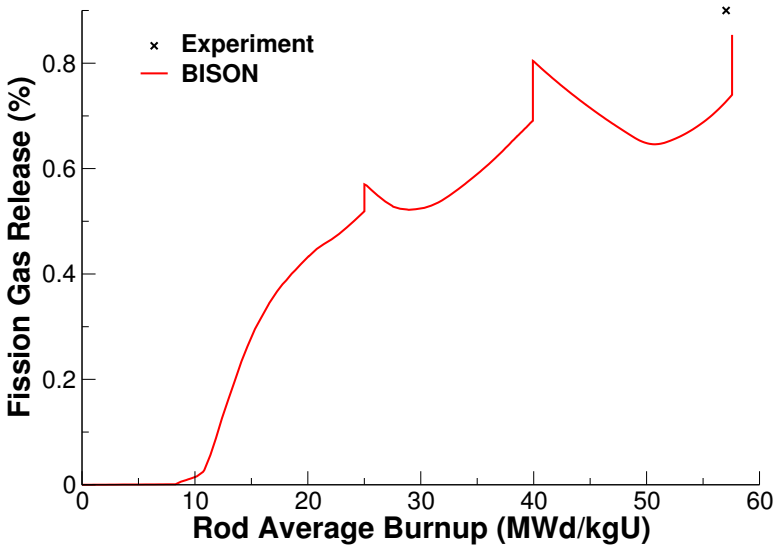

Figure K.6.: Fission gas release comparisons for Rodlet-4

K.4.2. Rod Internal Pressure

The only rod internal pressure data available for this experiment is from PIE puncture tests at the end-of-life. Figure K.7 and Figure K.8 show BISONs comparisons with the experimental data for Rodlet-2 and Rodlet-4, respectively. Both figures show BISON over predicts the rod internal pressure at the end of life.

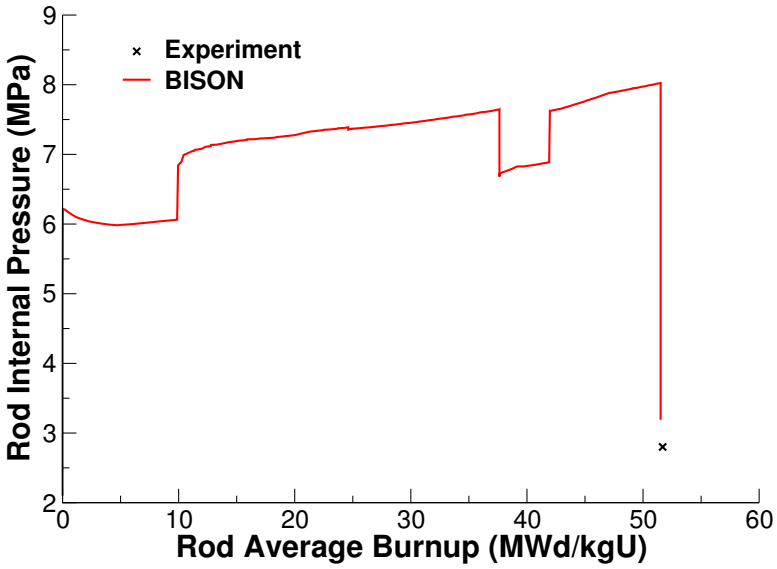

Figure K.7.: Rod internal pressure comparisons for Rodlet-2

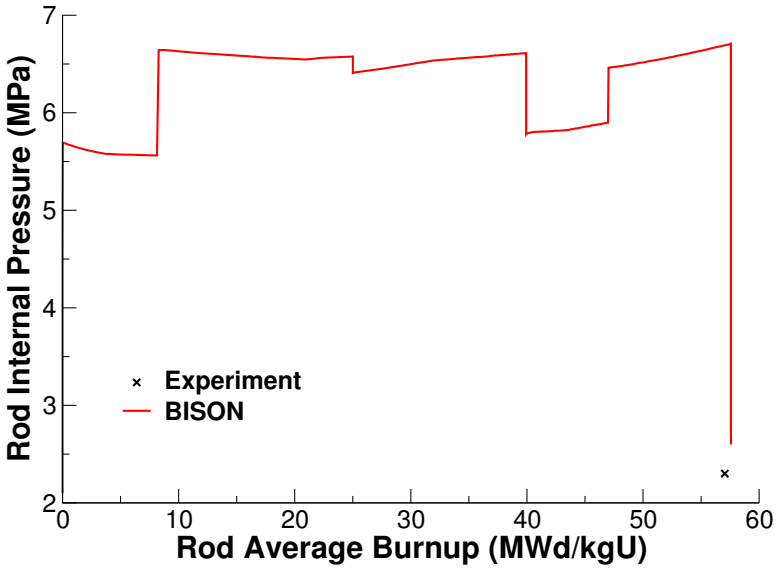

Figure K.8.: Rod internal pressure comparisons for Rodlet-4

K.4.3. Cladding Diametral Creep

The calculated final rod diameter as a function of axial position is compared to measured data. Figure K.9 and Figure K.10 show BISONs comparisons with the measured end-of-life rod average diameter data for Rodlet-2 and Rodlet-4, respectively. Both figures show BISON under predicts the cladding creep down which results in larger rod computed diameters than measured.

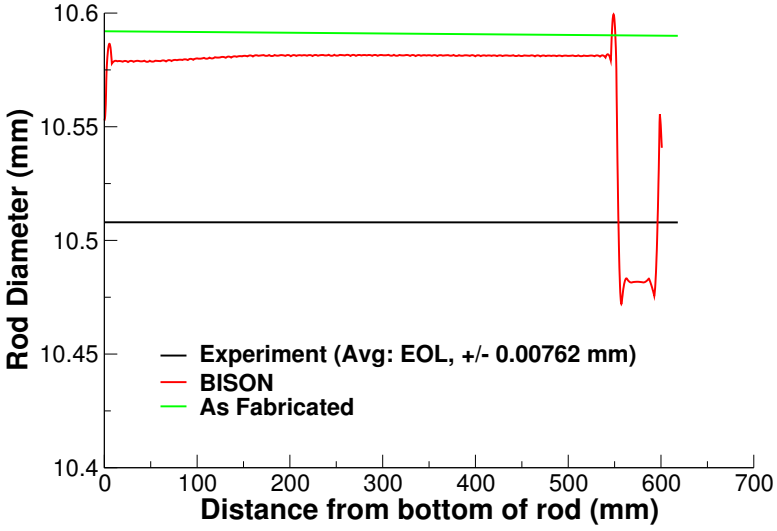

Figure K.9.: Rod diameter comparisons for Rodlet-2

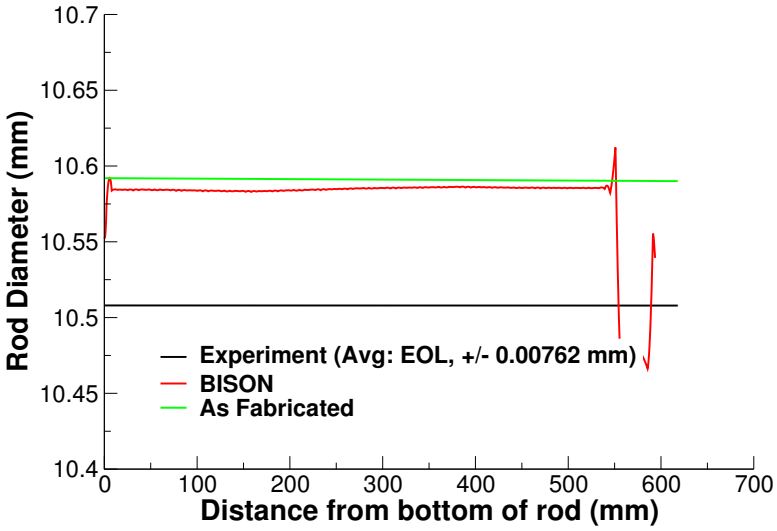

Figure K.10.: Rod diameter comparisons for Rodlet-4

K.4.4. Discussion

Based on the data presented above, several observations can be made regarding the results obtained from BISON analyses of Rodlets 2 and 4.

- BISON predicts the EOL FGR reasonably well for both cases.
  - From Figures K.5 and K.6, sharp increases in FGR can be seen that correspond to large power drops. This rapid release of fission gas during power drop appears to be characteristic of the SIFGRs model implemented in BISON. This response may not be representative of FGR kinetics and warrants further review.
- BISON over predicts the measured rod internal pressure for both cases by a fairly large margin.
- BISON over predicts measured EOL cladding diameter except in the plenum region.
  - Based on evaluation of these and other assessment cases, this behavior appears to be related to fuel swelling after fuel/cladding contact. Additionally, other effects on fuel deformation including relocation, densification, fuel creep, etc. could influence the behavioral response in these analyses.

Since cladding oxide thickness and hydrogen concentration data are available for Rodlet-2 and Rodlet-4, these characteristics should be evaluated in the future once these features are available in BISON.

L. Risø AN2

L.1. Overview

The Risø AN2 experiment conducted at the Risø DR3 water-cooled HP1 rig utilized a non re-fabricated rod from the Biblis A pressurized water reactor (PWR) [18],[42]. The rod, CB6, was irradiated over four reactor cycles up to about 41 GWd/t and inserted into the DR3 reactor without any modifications made. The rod diameter at the end of the base and experimental irradiation periods and the final fission gas release can be used for comparison.

L.2. Test Description

L.2.1. Rod Design Specifications

Fuel pin CB6 was the upper-middle segment of four, ~675 mm-long barrier clad segments (from top CB9, CB6, CB7, CB8) which together with a top and a bottom segment constituted a fuel rod stringer. CB6 was bump tested in the unopened condition. The CB6 rod geometry is tabulated in Table L.1.

Table L.1.: Risø AN2 Test Rod Specifications

Fuel Rod		
Overall length	m	0.65354
Fuel stack height	m	0.5418
Nominal plenum height	mm	61.0
Mother Rod		
Fill gas composition		He
Fill gas pressure	MPa	2.31
Fuel		
Material		UO_2
Enrichment	%	2.95
Density	%	93.74
Outer diameter	mm	9.053
Pellet geometry		both ends
Grain diameter (3D)	μm	9.36
Pellet Dishing		
Dish diameter	cm	0.665
Dish depth	cm	0.013
Chamfer width	cm	0.046
Chamfer depth	cm	0.016
Cladding		
Material		Zr-4
Outer diameter	mm	10.811
Inner diameter	mm	9.261
Wall thickness	mm	0.775

L.2.2. Operating Conditions and Irradiation History

The power history for the base irradiation carried out at the Biblis A PWR is shown in Figure L.1. The experiment power history carried out at the Risø DR3 facility is shown in Figure L.2. A prescribed axial profile for this experiment was provided in the FUMEX-II data [18]. The measured clad surface temperature as a function of time was also provided in the FUMEX-II data [18] and was used as a boundary condition for this simulation. The other reactor operation parameters are tabulated in Table L.2.

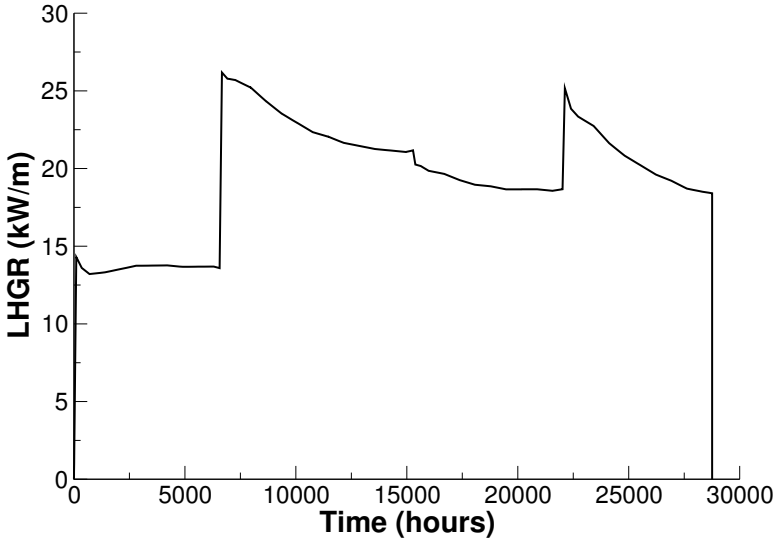

Figure L.1.: Base irradiation history for fuel segment CB6, carried out at Biblis A PWR.

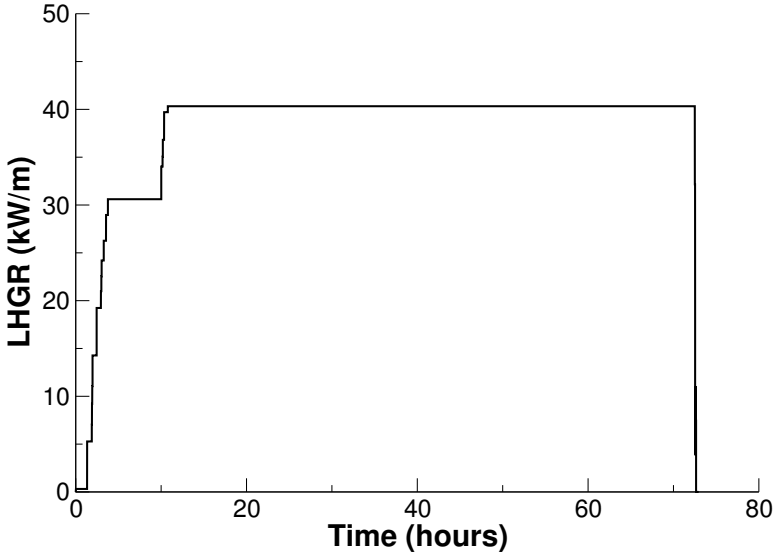

Figure L.2.: Risø DR3 irradiation period for test AN2 (CB6).

L.3. Model Description

L.3.1. Geometry and Mesh

The CB6 section rod geometry was modeled for the entire simulation considering a smeared column of flat ended pellets. The entire fuel stack was shifted up from the bottom of the clad by 5.1 mm, which is

Table L.2.: Operational input parameters.

Base Irradiation		
Coolant inlet temperature	C	284.7
Coolant pressure	MPa	15.52
Fast neutron flux	n/(cm^2·s) per (kW/m)	3.4·10^{12}
Power Ramps		
Coolant inlet temperature	C	NA
Coolant pressure	MPa	15.3
Fast neutron flux	n/(cm^2·s) per (kW/m)	4.0·10^{11}

the height of the insulator pellet at the bottom of the fuel rod.

A 2-dimensional axisymmetric quadratic (Quad8 elements) mesh was used to model the geometry of the rod used in the AN2 experiment. The fuel was meshed so that the total active fuel length would equal 0.54 m, leaving a total upper plenum length of 61 mm. The fuel mesh consisted of elements 2.31 mm in the axial direction and 0.4115 mm in the radial direction (for an aspect ratio of 5.613). The clad mesh consisted of elements 2.57565 mm in the axial direction and 0.19375 mm in the radial direction (for an aspect ratio of 13.29).

L.3.2. Material and Behavioral Models

The following material and behavioral models were used for the UO_2 fuel:

- ThermalFuel - NFIR: temperature and burnup dependent thermal properties
- RelocationUO2: relocation strains, relocation activation threshold power set to 5 kW/m.
- Sifgrs: fission gas release model with coupled gaseous swelling.

For the clad material, a constant thermal conductivity of 16 W/m-K was used, and both thermal and irradiation creep were considered using the Limback creep model [26]. Thermal expansion modeling utilized the CTHEXP sub-code with its correlations for zircaloy [43].

L.3.3. Boundary and Operating Conditions

The Risø DR3 irradiation period for the AN2 test shown in Figure L.2 was appended to the base irradiation power history shown in Figure L.1. It was assumed that the clad temperature during the down time between base irradiation and the Risø test was 300K. The fast neutron flux was input as a function of power and scaled to 4.9e17.

L.3.4. Input files

The BISON input and all supporting files (power histories, axial power profile, fast neutron flux history, etc.) for this case are provided with the code distribution at bison/assessment/Riso_AN2/analysis.

L.3.5. Execution Summary

Table L.3.: Execution summary.

Machine	Operating System	Code Version
FALCON	LINUX	BISON 1.2

L.4. Results Comparison

The Risø AN2 experiment is used to assess the code's capability to capture the total radial displacement of the cladding surface as well as the final amount of fission gas that is released. Cladding surface displacement measurements were given with the AN2 data packet taken at ten different locations along the cladding which are used for comparison. A final fission gas release point was also taken after all testing by puncturing the rod to obtain all gasses.

L.4.1. Cladding Displacement

BISON predicts the final cladding surface displacement with sufficient accuracy, as seen in Figure L.3 where the sudden diameter decrease denotes the pellet-stack's edge. The cladding displacement was measured at 10 equidistant node lengths at both the pellet end and mid sections.

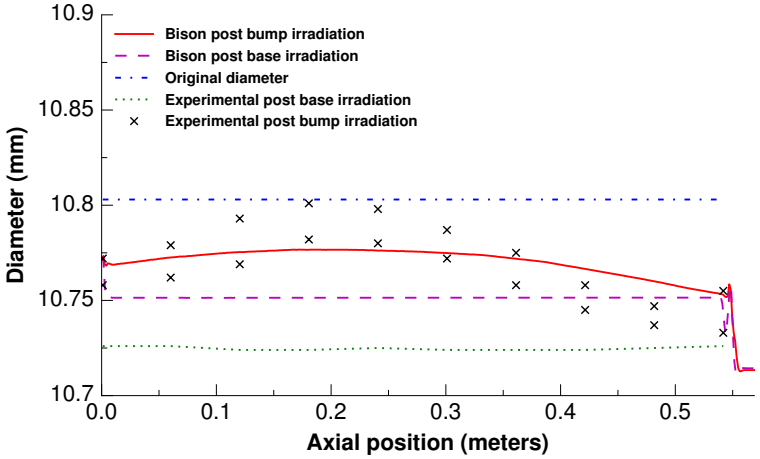

Figure L.3.: BISON fuel cladding displacement comparison to Risø experimental data.

L.4.2. Fission Gas Release

The calculated integral fuel rod fission gas release is compared to the measured data point, in Figure L.4. In view of the uncertainties involved in FGR modeling, the predictive accuracy is satisfactory.

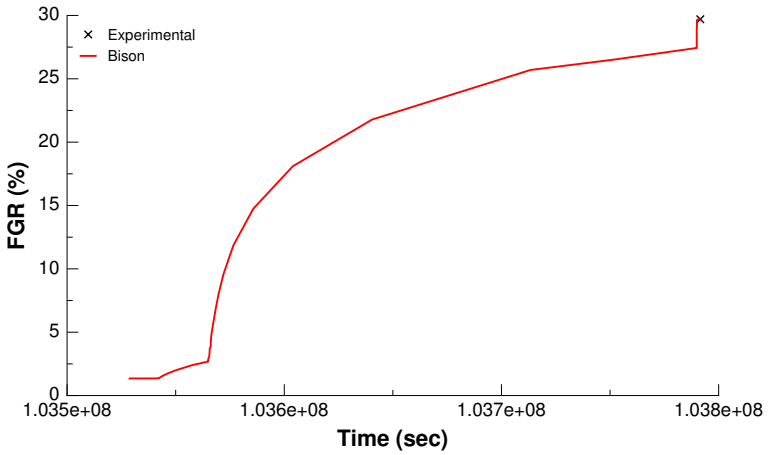

Figure L.4.: BISON total fission gas release comparison to Risø experimental data.

M. Risø AN3

M.1. Overview

The Risø AN3 experiment conducted at the Risø DR3 water-cooled HP1 rig utilized a re-fabricated rod from the Biblis A pressurized water reactor (PWR) [18],[44]. The mother rod, CB8, was irradiated over four reactor cycles up to about 41 GWd/t, and re-fabricated to a shorter length. The re-fabricated rod, CB8-2R, was instrumented with a fuel centerline thermocouple and a pressure transducer. The fuel centerline temperature, fission gas release and rod internal pressure can be used for comparison.

M.2. Test Description

M.2.1. Rod Design Specifications

Rod CB8-2R was a re-fabricated rod extracted from a full length rod. The hole for the thermocouple was at the top of the fuel rod and did not penetrate the entire fuel stack. The re-fabricated rod geometry is tabulated in Table M.1.

Table M.1.: Risø AN3 Test Rod Specifications

Fuel Rod		
Overall length	m	0.39058
Fuel stack height	m	0.286
Nominal plenum height	mm	61.0
Mother Rod		
Fill gas composition		He
Fill gas pressure	MPa	2.31
Re-Fabricated Rod		
Fill gas composition		He
Fill gas pressure	MPa	1.57
Fuel		
Material		UO_2
Enrichment	%	2.95
Density	%	93.74
Inner diameter	mm	2.5
Outer diameter	mm	9.053
Pellet geometry		both ends
Grain diameter	μm	6.0
Pellet Dishing		
Dish diameter	cm	0.665
Dish depth	cm	0.013
Chamfer width	cm	0.046
Chamfer depth	cm	0.016
Cladding		
Material		Zr-4
Outer diameter	mm	10.81
Inner diameter	mm	9.258
Wall thickness	mm	0.776

M.2.2. Operating Conditions and Irradiation History

The power history for the base irradiation carried out at the Biblis A PWR is shown in Figure M.1. The experiment power history carried out at the Risø DR3 facility is shown in Figure M.2. A prescribed axial profile for this experiment was provided in the FUMEX-II data [18]. The measured clad surface temperature as a function of time was also provided in the FUMEX-II data [18] and used as a boundary condition for this simulation. The other reactor operation parameters are tabulated in Table M.2.

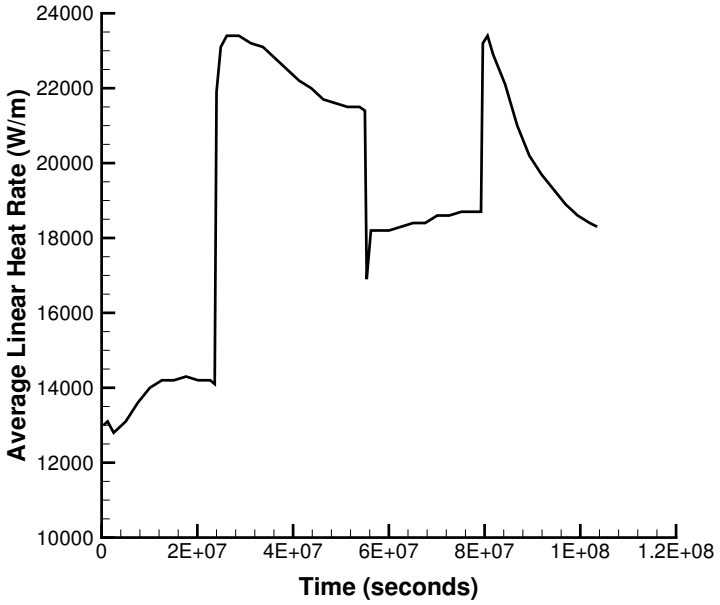

Figure M.1.: Base irradiation history for fuel segment CB8, carried out at Biblis A PWR.

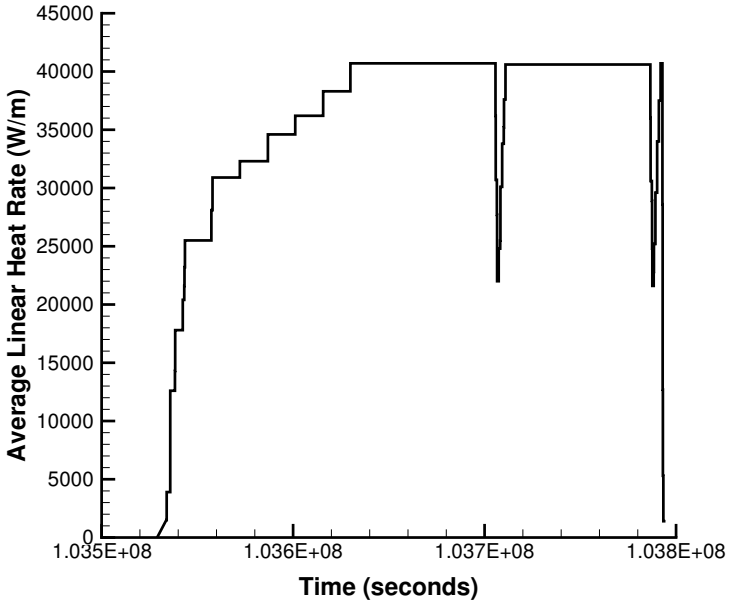

Figure M.2.: Risø DR3 irradiation period for test AN3 (CB8-2R).

Table M.2.: Operational input parameters.

Base Irradiation		
Coolant inlet temperature	C	287.7
Coolant pressure	MPa	15.52
Fast neutron flux	n/(cm^2·s) per (kW/m)	3.4·10^{12}
Power Ramps		
Coolant inlet temperature	C	NA
Coolant pressure	MPa	15.3
Fast neutron flux	n/(cm^2·s) per (kW/m)	4.0·10^{11}

M.3. Model Description

M.3.1. Geometry and Mesh

The re-fabricated rod geometry was modeled for the entire simulation considering a smeared column of flat ended pellets, with the top pellets containing the hole for the thermocouple. The plenum height was adjusted such that the plenum volume at the beginning of the bump test was approximately 7.0 cm^3. The entire fuel stack was shifted up from the bottom of the clad by 5.1 mm, which is the height of the insulator pellet at the bottom of the fuel rod.

A 2-dimensional axi-symmetric quadratic (Quad8 elements) mesh was used to model the geometry of the rod used in the AN3 experiment. The fuel was meshed considering two fuel pellet types. The first pellet type was 4.1 cm in length with a hole down the center, the second pellet type was 24.5 cm in length with no hole down the center. The first pellet type's mesh consisted of 29 axial nodes and 10 radial nodes (for an aspect ratio of 4.07). The second pellet type's mesh consisted of 166 axial nodes and 13 radial nodes (for an aspect ratio of 3.93). The clad mesh consisted of 131 axial nodes and 3 radial nodes. Figure M.3 shows the top section of the mesh at the thermocouple location with a temperature contour plot.

M.3.2. Material and Behavioral Models

The following material and behavioral models were used for the UO_2 fuel:

- ThermalFuel - NFIR: temperature and burnup dependent thermal properties
- RelocationUO2: relocation strains, relocation activation threshold power set to 5 kW/m.
- Sifgrs: fission gas release model with the combined gaseous swelling model.

For the clad material, a constant thermal conductivity of 16 W/m-K was used and both thermal and irradiation creep were considered using the Limback model [26].

M.3.3. Boundary and Operating Conditions

The Risø DR3 irradiation period for the AN3 test shown in Figure M.2 was appended to the base irradiation power history shown in Figure M.1. It was assumed that the clad temperature during the down time between base irradiation and the Risø test was 500K. The fast neutron flux was input as a function of power and scaled to 4.9e17.

M.3.4. Input files

The BISON input and all supporting files (power histories, axial power profile, fast neutron flux history, etc.) for this case are provided with the code distribution at bison/assessment/Riso_AN3/analysis.

M.3.5. Execution Summary

Table M.3.: Execution summary.

Machine	Operating System	Code Version
FALCON	LINUX	BISON 1.2

M.4. Results Comparison

The Risø AN3 experiment is used to assess the code's capability to capture the fuel centerline temperature and the integral fuel rod fission gas release. Fuel centerline temperature and fission gas release data from the TRANSURANUS and ENIGMA codes were digitized from the FUMEX-II report [5] for comparison with the BISON predictions.

M.4.1. Temperature

BISON predicts the fuel centerline temperature well (see Figure M.3) and is comparable with other well known fuel performance codes. The fuel centerline temperature is taken at a node approximately 36.4 mm from the top of the fuel stack (black dot on mesh in Figure M.3).

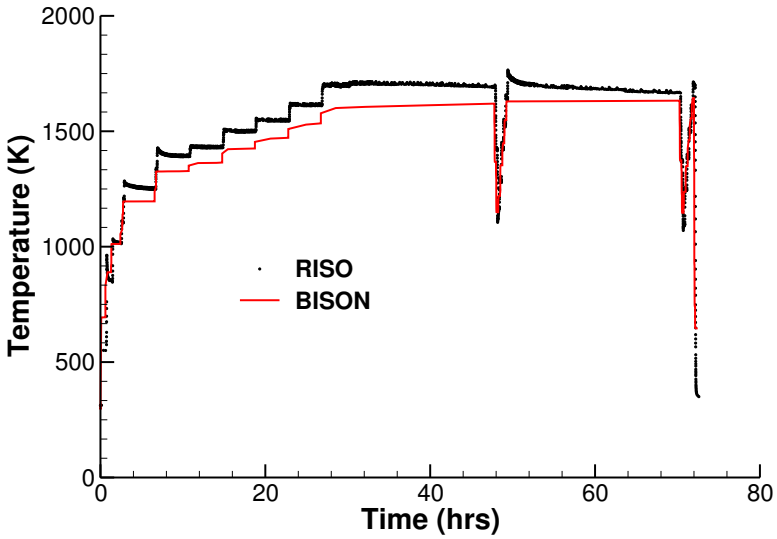

Figure M.3.: BISON fuel centerline temperature comparison to Risø experimental data.

M.4.2. Fission Gas Release

The calculated integral fuel rod fission gas release is compared to the measured data, as well as with the TRANSURANUS and ENIGMA predictions, in Figure M.4. In view of the uncertainties involved in FGR modeling, the predictive accuracy is satisfactory. When compared to other codes, BISON's prediction of total FGR is excellent, with many codes underpredicting the fission gas release at the end of life by more than a factor of 2 [5].

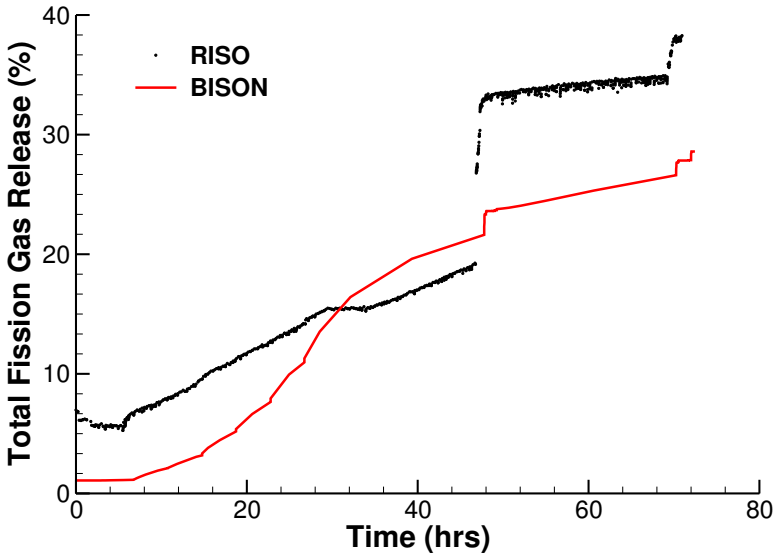

Figure M.4.: BISON total fission gas release comparison to Risø experimental data.

M.4.3. Rod Internal Pressure

The fission gas release as a function of time during the ramp test is calculated based off the measured pressure of the rod. When compared to the measured rod internal pressure, BISON slightly over predicts the rod pressure, see Figure M.5. This is likely due to the conditions of the rod at the refabrication time. It is reported that the fill gas is measured at room temperature, however, the temperature of the gap is higher than that of ambient temperature due to the decay heat of the already irradiated fuel.

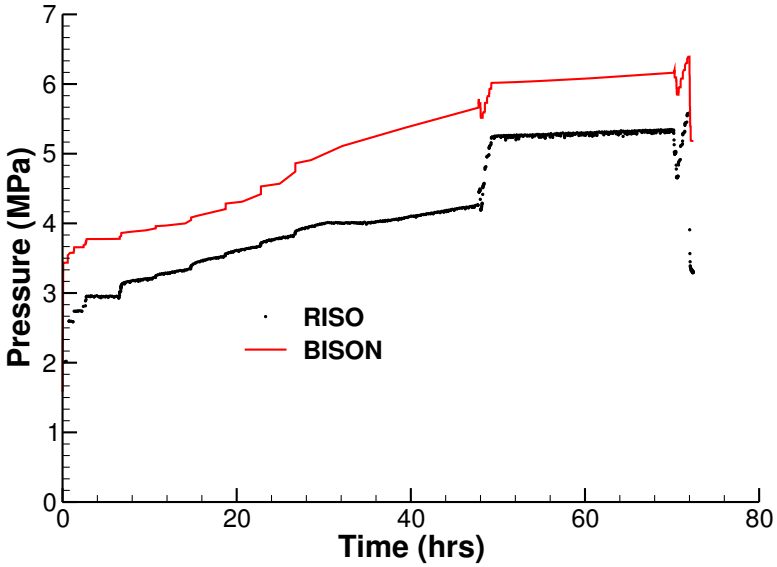

Figure M.5.: BISON rod internal pressure comparison to Risø measured data.

N. Risø AN4

N.1. Overview

The Risø AN4 experiment conducted at the Risø DR3 water-cooled HP1 rig utilized a re-fabricated rod from the Biblis A pressurized water reactor (PWR) [45], [18]. The mother rod, CB7, was irradiated over four reactor cycles then re-fabricated to a shorter length. The re-fabricated rod, CB7-2R, was fitted with a fuel centerline thermocouple and a pressure transducer. The fuel centerline temperature, fission gas release and rod internal pressure can be used for comparison.

N.2. Test Description

N.2.1. Rod Design Specifications

ROB CB7-2R was a re-fabricated rod extracted from a full length rod. The hole for the thermocouple was at the top of the fuel rod and did not penetrate the entire fuel stack. The re-fabricated rod geometry is tabulated in Table N.1.

Table N.1.: Risø AN4 Test Rod Specifications

Fuel Rod		
Overall length	m	0.330483
Fuel stack height	m	0.292
Nominal plenum height	mm	34.0
Mother Rod		
Fill gas composition		He
Fill gas pressure	MPa	2.31
Re-Fabricated Rod		
Fill gas composition		Xe
Fill gas pressure	MPa	0.1
Fuel		
Material		UO_2
Enrichment	%	2.97
Density	%	93.74
Inner diameter	mm	2.5
Outer diameter	mm	9.053
Pellet geometry		both ends
Grain diameter	μm	6.0
Pellet Dishing		
Dish diameter	cm	0.665
Dish depth	cm	0.013
Chamfer width	cm	0.046
Chamfer depth	cm	0.016
Cladding		
Material		Zr-4
Outer diameter	mm	10.81
Inner diameter	mm	9.258
Wall thickness	mm	0.776

N.2.2. Operating Conditions and Irradiation History

The power history for the base irradiation carried out at the Biblis A PWR is shown in Figure N.1. The experiment power history carried out at the Risø DR3 facility is shown in Figure N.2. The axial profile for this experiment is shown in Figure N.3. The measured clad surface temperature as a function of time is shown in Figure N.4. The other reactor operation parameters are tabulated in Table N.2.

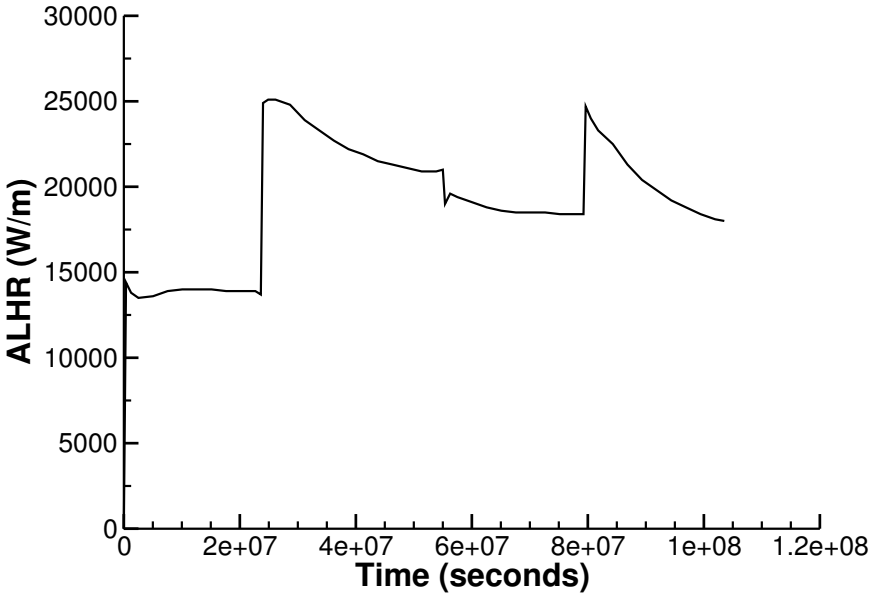

Figure N.1.: Base irradiation history for fuel segment CB7, carried out at Biblis A PWR.

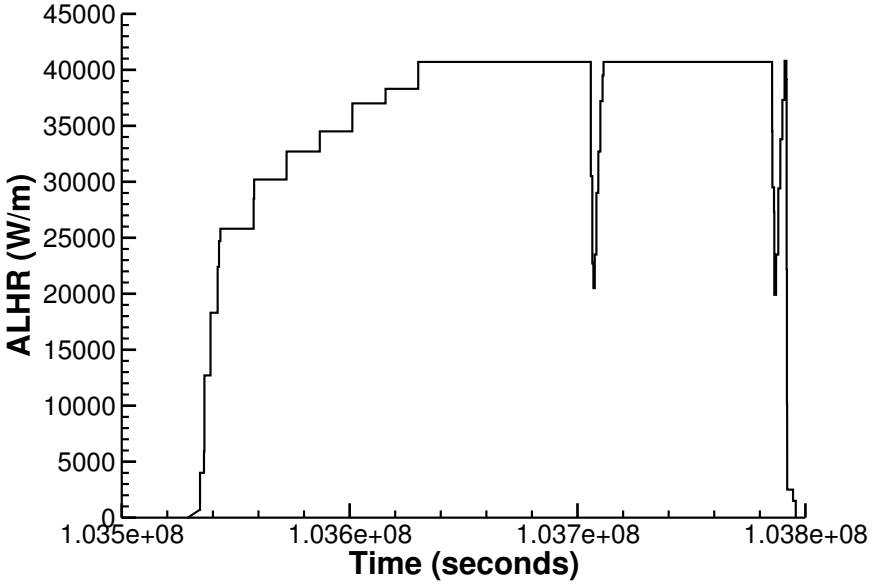

Figure N.2.: Risø DR3 irradiation period for test AN4 (CB7-2R).

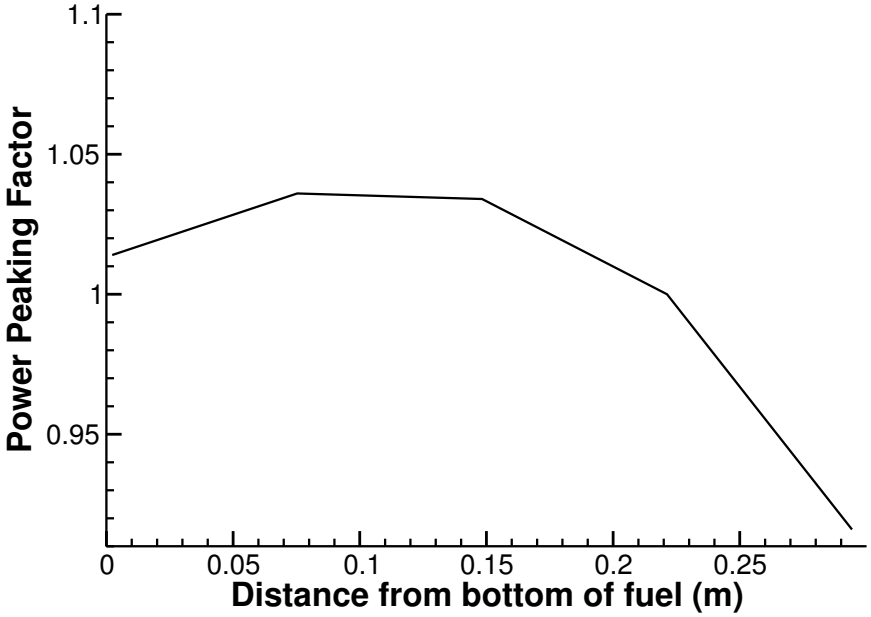

Figure N.3.: Axial power profile for Risø AN4.

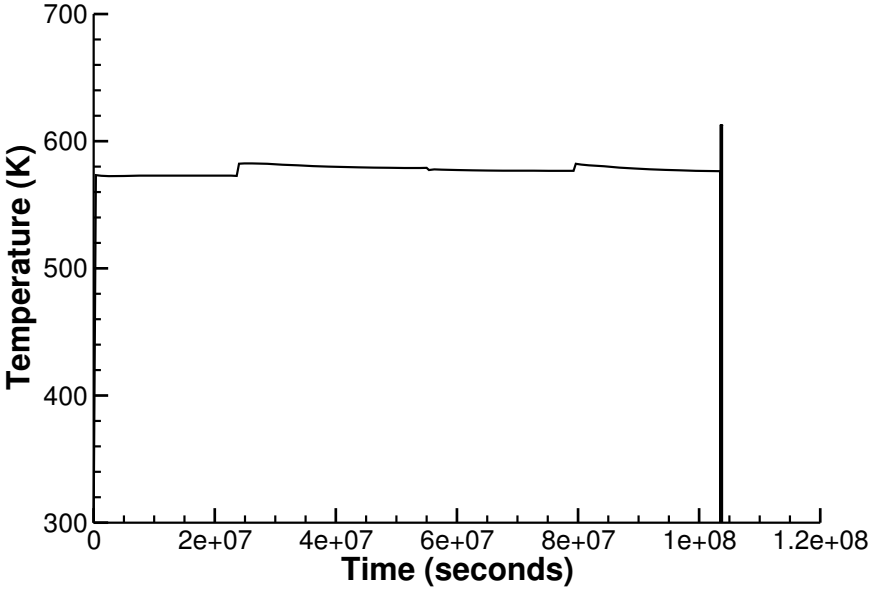

Figure N.4.: Measured clad surface temperature as a function of time.

Table N.2.: Operational input parameters.

Base Irradiation		
Coolant inlet temperature	C	287.7
Coolant pressure	MPa	15.52
Fast neutron flux	n/(cm^2$*$s) per (kW/m)	$3.4*10^{12}$
Power Ramps		
Coolant inlet temperature	C	NA
Coolant pressure	MPa	15.3
Fast neutron flux	n/(cm^2$*$s) per (kW/m)	$4.0*10^{11}$

N.3. Model Description

N.3.1. Geometry and Mesh

The re-fabricated rod geometry was modeled for the entire simulation as a single dished pellet. The entire fuel stack was shifted up from the bottom of the clad by 5.1 mm, which is the height of the insulator pellet at the bottom of the fuel rod.

A 2-dimensional axi-symmetric linear mesh was used to model the geometry of the rod used in the AN4 experiment. The fuel mesh consisted of 141 axial nodes and 9 radial nodes (for an aspect ratio of 5.1), the clad mesh consisted of 113 axial nodes and 5 radial nodes, see Figure N.5.

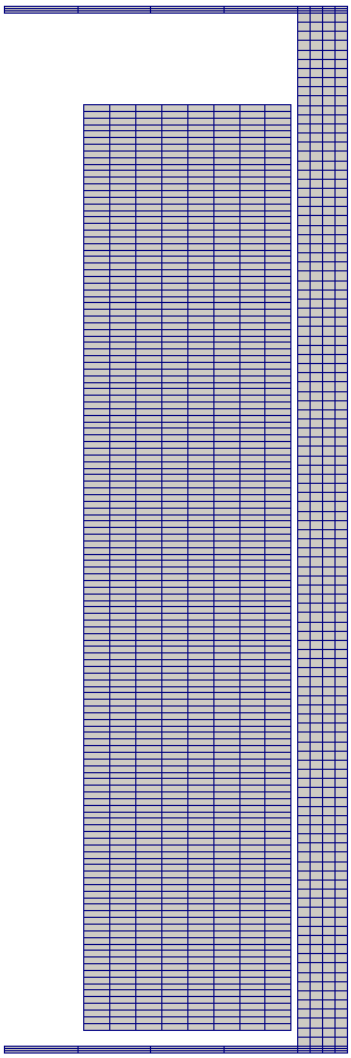

Figure N.5.: 2-D axi-symmetric mesh for Risø AN4 simulation. Note: Mesh plot is scaled axially by 0.05

N.3.2. Material and Behavioral Models

The following material and behavioral models were used for the UO_2 fuel:

- ThermalFuel - NFIR: temperature and burnup dependent thermal properties
- RelocationUO2: relocation strains, relocation activation threshold power set to 5 kW/m.
- Sifgrs: fission gas release model with the combined gaseous swelling model.

For the clad material, a constant thermal conductivity of 16 W/m-K was used and both thermal and irradiation creep were considered using the Limback model [26].

It has been observed during late in life that the interaction layer between the fuel and clad has some contribution to the heat transfer in the gap. The effect of an interaction layer is not as obvious with helium in the gap. However, the presence of this interaction layer is magnified with xenon in the gap. The gap heat transfer model for this problem included the presence of an interaction layer between the fuel and clad. The fuel centerline temperature comparisons were extremely off when this interaction layer was not taken into consideration for this problem.

N.3.3. Boundary and Operating Conditions

The Risø DR3 irradiation period for the AN4 test shown in Figure N.2 was appended to the base irradiation power history shown in Figure N.1. The power history used as an input parameter for this particular simulation is shown in Figure N.6. The clad temperature as a function of time shown in Figure N.4 was used as the clad boundary condition for this simulation. The fast neutron flux was input as a function of power and scaled to 4.9e17.

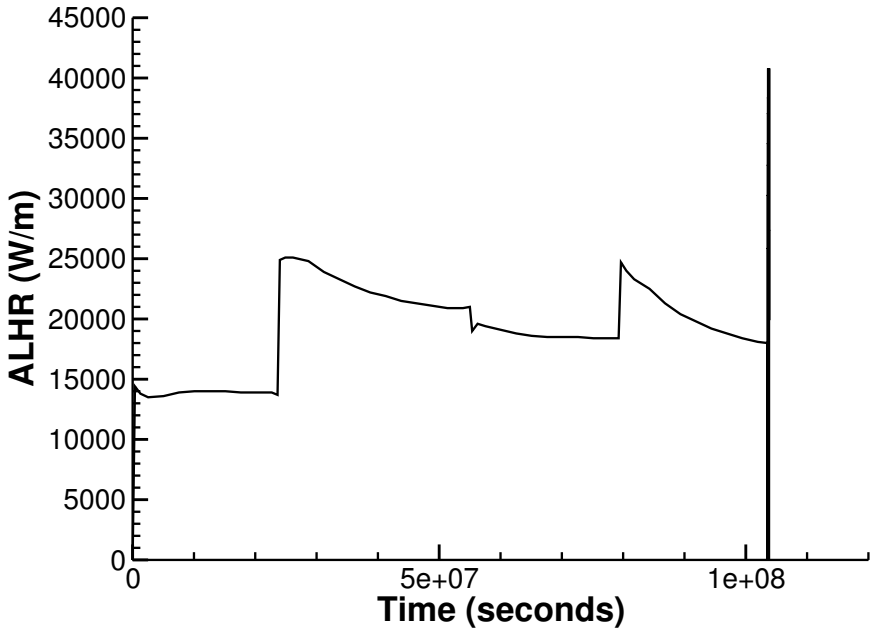

Figure N.6.: BISON input power history for Risø AN4.

N.3.4. Input files

The BISON input and all supporting files (power histories, axial power profile, fast neutron flux history, etc.) for this case are provided with the code distribution at bison/assessment/Riso_An4/analysis.

N.3.5. Execution Summary

Table N.3.: Execution summary.

Machine	Operating System	Code Version
FALCON	LINUX	BISON 1.2

N.4. Results Comparison

The Risø AN4 experiment is used to assess the codes' capability to capture the fuel centerline temperature, plenum pressure and the total fission gas released. At this time BISON is not capable of capturing the total fission gas release during transient analysis, therefore, the only comparisons made were the fuel centerline temperature and plenum pressure.

N.4.1. Temperature

The fuel centerline temperature predicted with BISON compared extremely well with the experimental data. The maximum difference between measured temperature and predicted temperature was approximately 72 degress C at the top of the ramp. (see Figure N.7).

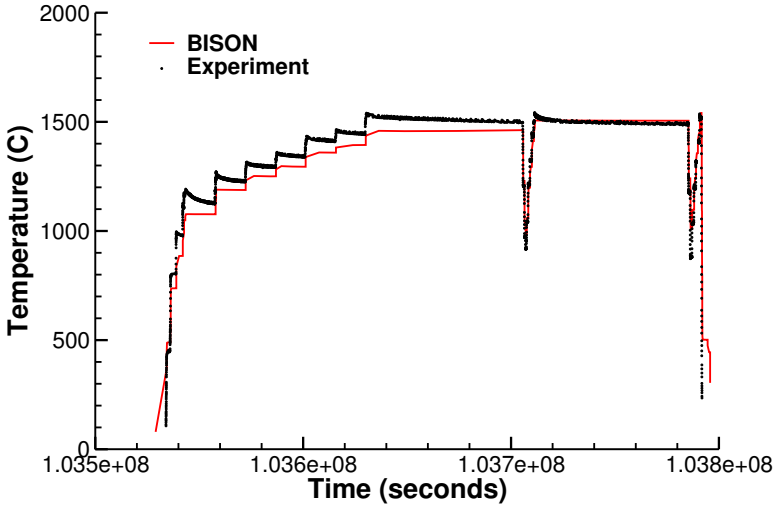

Figure N.7.: BISON fuel centerline temperature comparison to Risø experimental data.

N.4.2. Fission Gas Release

BISON predicts the total fission gas released well with some over prediction during the first flat power section of the ramp test (see Figure N.8).

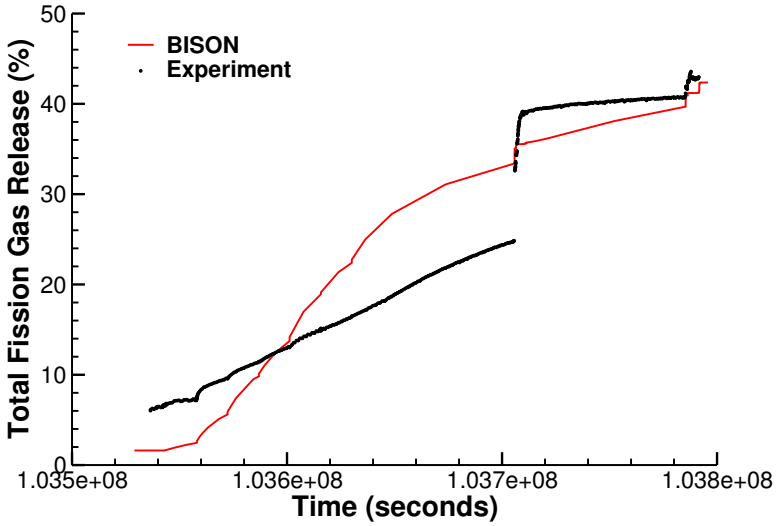

Figure N.8.: BISON total fission gas release comparison to Risø experimental data.

N.4.3. Plenum Pressure

The calculated plenum pressure increases throughout the entire ramp test (see Figure N.9). The pressure prediction follows the fission gas release behavior which could be the reason for the constant increase in plenum pressure during the ramp test.

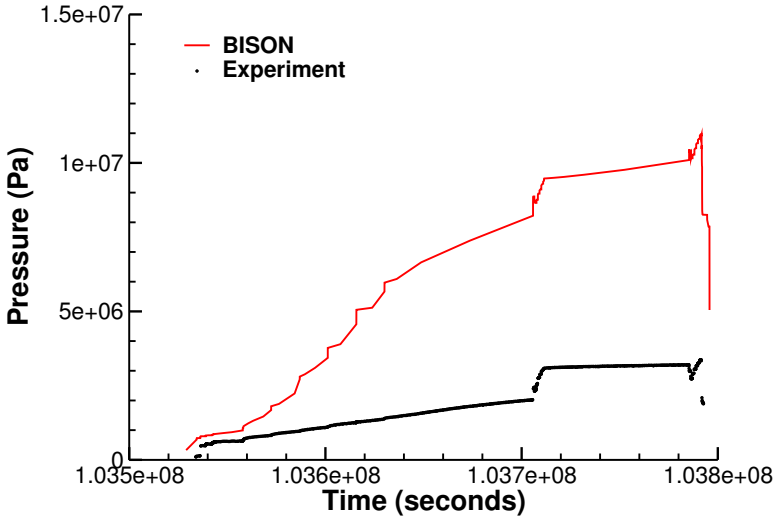

Figure N.9.: BISON plenum pressure comparison to Risø experimental data.

O. HBEP Rod BK363, Rod BK365, and Rod BK370

O.1. Overview

The purpose of the High Burnup Effects Programme (HBEP) task 3 rods BK363, BK365 and BK370 was to provide high burnup data on fission gas release (FGR) and fission product distributiions [18]. Rods BK363,BK365 and BK370 were irratiated to 66.7 MWd/KgU, 69.4 MWd/KgU and 50.9 MWd/KgU, respectivly, in the BR-3 pressurized water reactor (PWR) [18]. Only end of life FGR predictions were requested from the modellers.

O.2. Test Description

The three rods in this series were manufactured by CEA and are identical. The fuel stack consisted of annular pellets and was one meter long. The only difference in experiment build was the initial plenum fill gas pressure(See Table O.1). This portion of the HBEP experiments was designed to study the effects of fill gas pressure on FGR. It also provided data on FGR of annual pellets for use against the solid pellets in the HBEP series [18].

O.2.1. Operating Conditions and Irradiation History

Rods BK363, BK365 and BK370 were irratited in the BR-3 pressurized water reactor (PWR) in Belgium [46] at a coolant pressure of 13.73 MPa and coolant inlet temperature of 255 C [18]. Rods BK363 and BK365 were irratiated four cycles to burnups of 66.7 MWd/KgU and 69.4 MWd/KgU, respectively. Rod BK370 was irratiated three cycle to a burnup of 50.9 MWd/KgU. Clad temperatures and local power histories were taken at 10 axial locations and obtained from the FUMEX II data.

Table O.1.: HBEP Test Rod Specifications

Fuel Rod		
Overall length	m	1.0895
Fuel stack height	m	1.017
Nominal plenum height	mm	72.5
Number of pellets per rod		102
Pellet Height		
BK363	mm	9.98
BK365	mm	9.98
BK370	mm	9.98
Fill gas composition		He
Fill gas pressure		
BK363	MPa	1.40
BK365	MPa	2.88
BK370	MPa	2.88
Fuel		
Material		UO_2
Enrichment		
BK363	%	7.07
BK365	%	7.07
BK370	%	7.07
Density	%	93.2
Outer diameter	mm	8.188
Inner diameter	mm	2.475
Grain diameter		
All Rods	μm	13.5
Cladding		
Material		Zr-4
Outer diameter	mm	9.515
Inner diameter	mm	8.3536

O.3. Model Description

O.3.1. Geometry and Mesh

All three fuel rods were meshed using 2-D axisymmetric quadratic elements. For simplicity, the pellet stack was modeled as a single continuous fuel column. The rods were identical so the same mesh was used for all runs. The fuel pellets had 306 axial elements and 11 radial elements, and the cladding consisted of 312 axial elements and 4 radial elements.

O.3.2. Material and Behavioral Models

The following material and behavioral models were used for the UO_2 fuel:

- ThermalFuel - NFIR: temperature and burnup dependent thermal properties
- RelocationUO2: relocation strains, relocation activation threshold power set to 5 kW/m
- Sifgrs: Simplified fission gas release model (model 2) with a gaseous swelling model

For the clad material, a constant thermal conductivity of 16 W/m-K was used and both thermal (primary and secondary) and irradiation creep were considered using the Limback creep model [26].

O.3.3. Input files

The BISON input and all supporting files (power histories, axial power profile) are provided with the code distribution at bison/assessment/HBEP/analysis.

O.3.4. Execution Summary

Table O.2.: Execution summary.

Rod	Machine	Operating System	Code Version
BK363	FALCON	LINUX	BISON 1.2
BK365	FALCON	LINUX	BISON 1.2
BK370	FALCON	LINUX	BISON 1.2

O.4. Results Comparison

HBEP rods BK363, BK365 and BK370 were designed and built to investigate the effects of initial fill gas pressure on fission gas release. To achieve this the rods were built identical and for BK363 and BK365 only the initial fill gas pressure was changed. These 2 rods were then irradiated to approximately the same burnup. Rod BK370 was filled to the same pressure as BK365, but was only irratiated 3 cycles as opposed to 4 cycles.

O.5. HBEP, BK363

O.5.1. Fission Gas Release

The BISON end result of fission gas release for this rod did not compare very well to the experimental data. It is thought that the BISON high burnup structure model needs some work. There is also a new fission gas burst release model under development that may prove to improve the FGR numbers in Figure O.1.

O.6. HBEP, BK365

O.6.1. Fission Gas Release

The BISON result for this rod compares well to the experimental data Figure O.1.

O.7. HBEP, BK370

O.7.1. Fission Gas Release

No experimental data was collected from this rod.

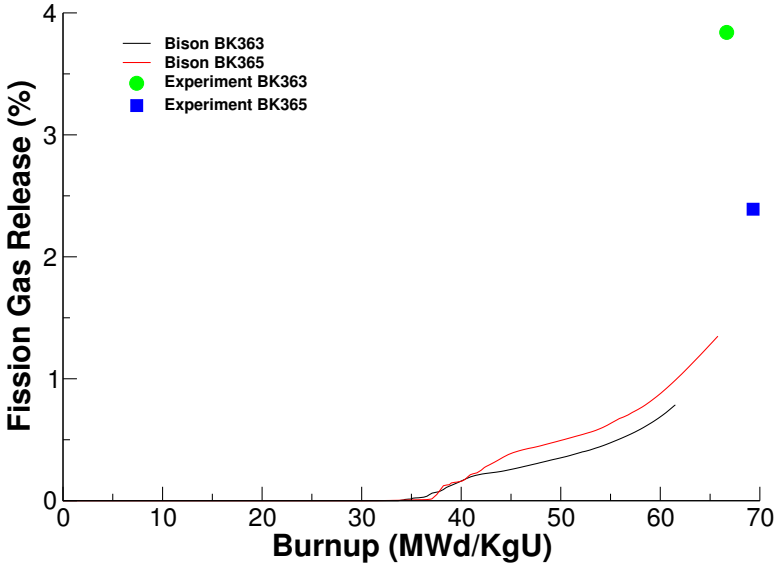

Figure O.1.: Comparison of measured fission gas release and the BISON prediction

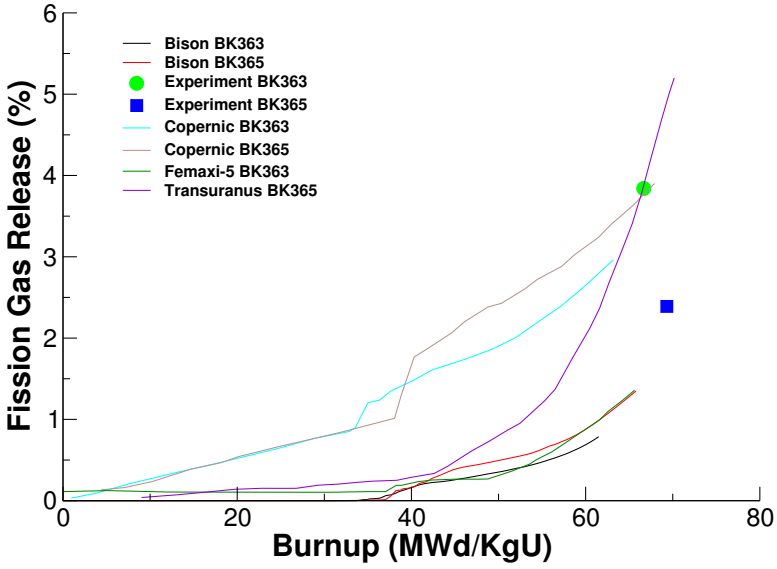

Figure O.2.: Comparison of measured fission gas release and the predictions of other codes

O.8. Discussion

Modeling these three rods was useful to the BISON developement as it shows that there is possible work needed in the high burnup structure. BISON seems to have similar issues to other codes as the overall results, comparing all codes, appears more random than real (see Figure O.2). As mentioned above there is current work being done with the fission gas models and these HBEP cases will be rerun as they become available. Another piece of future work for this test would be modeling the plutonium concentration with BISON.

P. AREVA Idealized Case

P.1. Overview

The AREVA Idealized Case is an optimal case designed to simulate idealized commercial power plant operation. This case was based on measurements for three rods operatedf or 3, 4, and 7 cycles in a commercial French pressurized water reactor (PWR). The three rods chosen experienced similar power histories, allowing for three fission gas release measurements for a single power history. The maximum fuel rod burnup is approximately 81.5 MWd/kgU with a total fission gas release of approximately 9% [35].

P.2. Test Description

P.2.1. Rod Design Specifications

The rod simulated for this particular case was based on an idealized commercial reactor fuel rod. Details of the rod geometry and specifications are summarized in Table P.1.

Table P.1.: AREVA Idealized Case Test Rod Specifications

Fuel Rod		
Fuel stack length	m	3.65
Nominal plenum volume	cm^3	8.04
Number of pellets per rod		275
Fill gas composition		He
Fill gas pressure	MPa	1.6
Fuel		
Material		UO_2
Enrichment	%	4.5
Density	%	95
Outer diameter	mm	8.085
Pellet geometry		dished
Grain diameter	μm	15.6
Pellet Dishing (if applicable)		
Dish diameter	mm	6.0
Dish depth	mm	0.31
Chamfer width	mm	0.5425
Chamfer depth	mm	0.27
Cladding		
Material		Zr-4 (stress-relieved)
Outer diameter	mm	9.5
Inner diameter	mm	8.25
Wall thickness	mm	0.625

P.2.2. Operating Conditions and Irradiation History

The operating conditions for this simulation were based on power cycles in a commercial French PWR. The operating conditions used are shown in Table P.2.

Table P.2.: Operational input parameters.

Coolant inlet temperature	C	282
Coolant pressure	MPa	15.5
Coolant mass flow rate	kg/m^2-sec	3700

P.3. Model Description

P.3.1. Geometry and Mesh

The fuel rod geometry specified in Table P.1 was used as a basis for the mesh used in this simulation. The fuel pellets were meshed as a single smeared fuel column. The mesh consists of 1375 axial elements and 12 radial elements in the fuel, and 1375 axial elements and 4 radial elements in the clad, see Figure P.1. This simulation was meshed as a 2D-RZ axisymmetric geometry with quadratic elements.

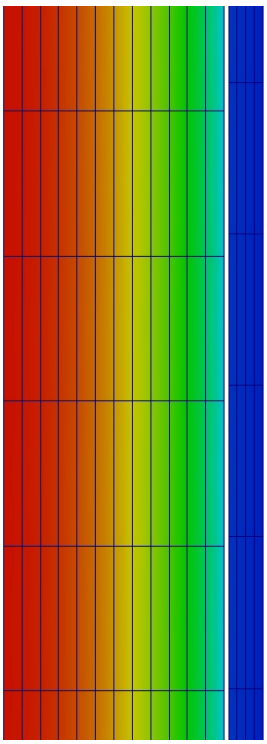

Figure P.1.: Section of BISON mesh with temperature contour.

P.3.2. Material and Behavioral Models

The following material and behavioral models were used for the UO_2 fuel:

- ThermalFuel - NFIR: temperature and burnup dependent thermal properties
- RelocationUO2: relocation strains, relocation activation threshold power set to 5 kW/m.
- Sifgrs: coupled fission gas release and swelling model

For the clad material, a constant thermal conductivity of 16 W/m-K was used and both thermal and irradiation creep were considered using the Limback model [26].

P.3.3. Boundary and Operating Conditions

The power history used for this simulation is shown in Figure P.2, with axial peaking factors shown in Figure P.3. The average fast neutron flux was input as a function as well and is shown in Figure P.4 with axial peaking factors shown in Figure P.5. The clad temperature was calculated using the coolant channel model.

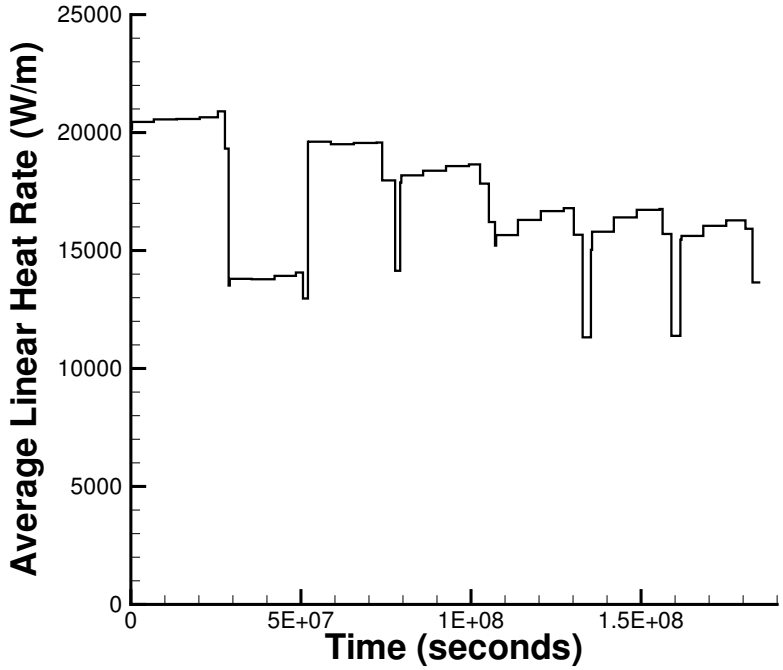

Figure P.2.: BISON input power history for the AREVA Idealized Case.

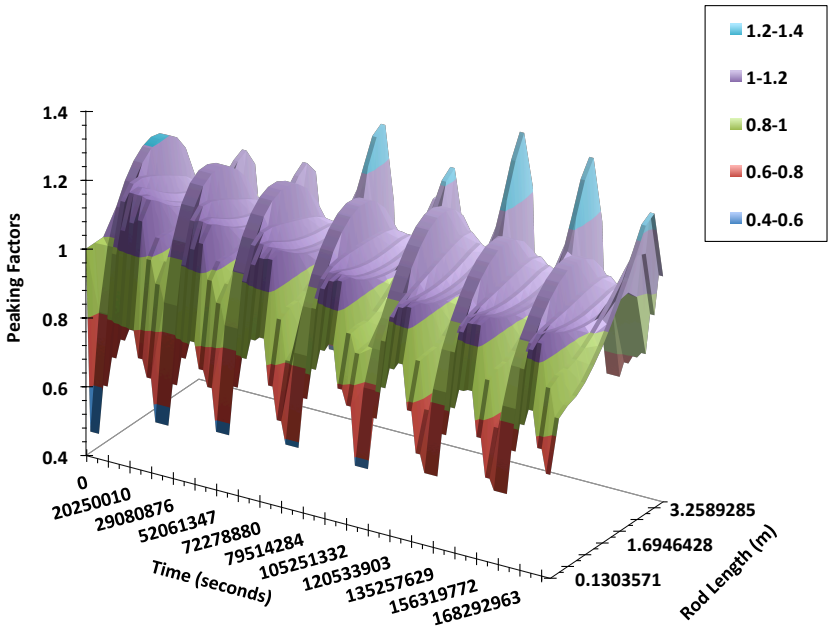

Figure P.3.: BISON input power axial peaking factors for the AREVA Idealized Case.

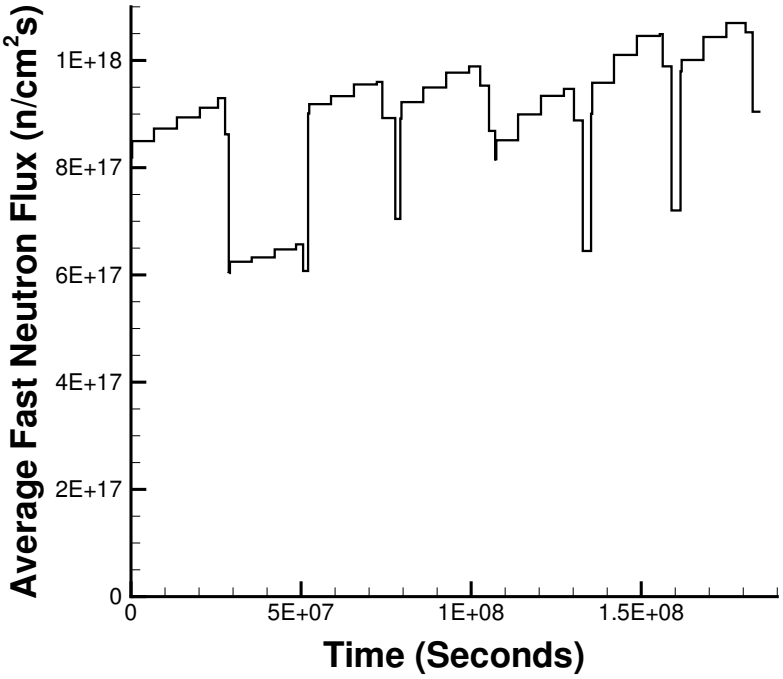

Figure P.4.: BISON input average fast neutron flux for the AREVA Idealized Case.

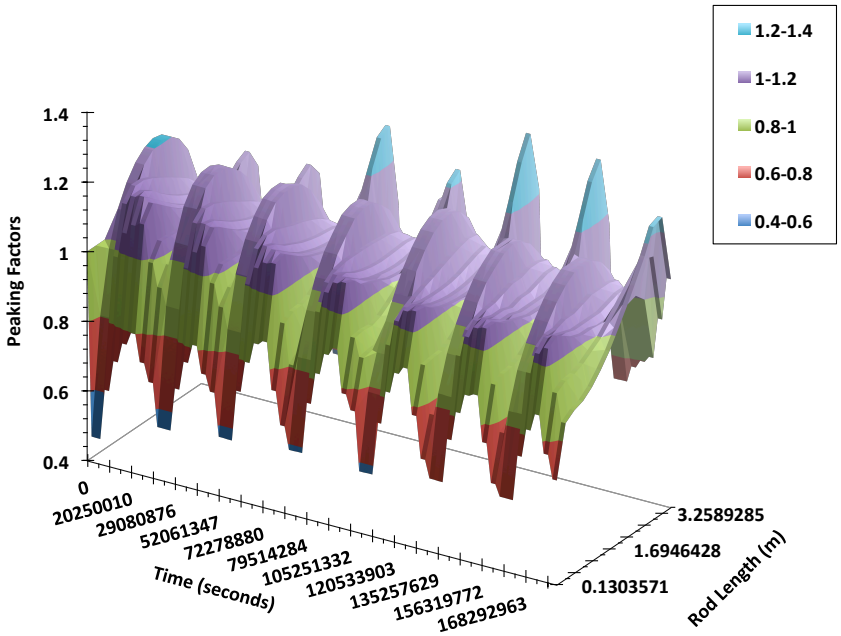

Figure P.5.: BISON input fast neutron flux axial peaking factors for the AREVA Idealized Case.

P.3.4. Input files

The BISON input and all supporting files (power histories, axial power profile, fast neutron flux history, etc.) for this case are provided with the code distribution at bison/assessment/AREVA_idealized_case/analysis.

P.3.5. Execution Summary

Table P.3.: Execution summary.

Machine	Operating System	Code Version
FALCON	LINUX X	BISON 1.2

P.4. Results Comparison

P.4.1. Fission Gas Release

The expected fission gas release values are shown in Table P.4 [35].

Table P.4.: Expected FGR values.

End of cycle	Insertion time (d)	Burnup (MWd/kg(HM))	Expected FGR value (%)
3	916.4	36.6	0.5+0.5/-0.2
4	1239.1	49.7	1.9+1.0/-0.7
7	2141.9	81.5	9.0+2.5/-2.0

BISON predicts the total fission gas release reasonably well during the early and mid-burnup regimes, however FGR is under predicted at high burnup. BISON also compares well with other well known fuel performance codes, see Figure P.6.

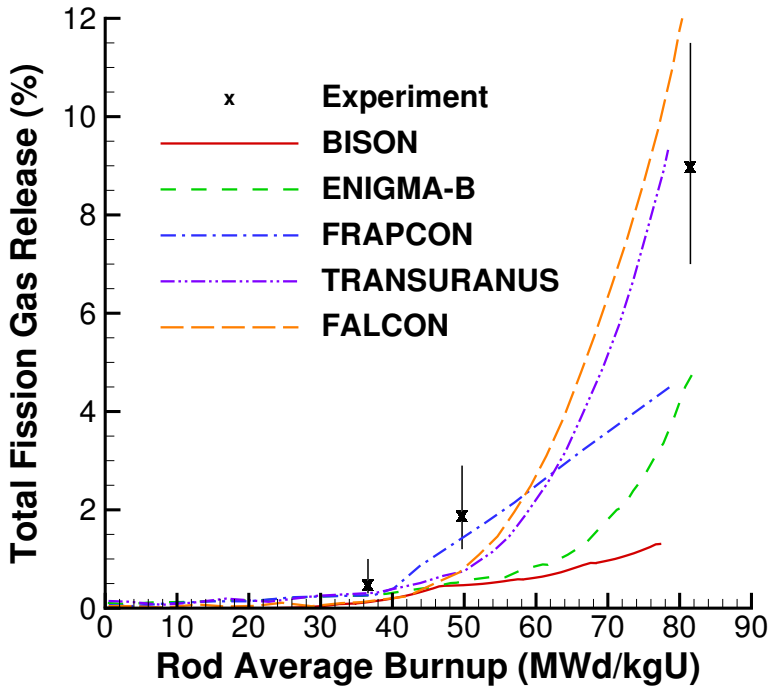

Figure P.6.: BISON predicted fission gas release in comparison to measured data and multiple fuel performance codes (code data digitized from FUMEX-III report [35]).

P.5. Discussion

Fuel creep was not modeled at this time. Fuel creep will be considered upon availablitly of some type of fuel cracking model.

Q. FUMEX-II Simplified Cases

Q.1. Overview

Over the last few decades, the International Atomic Energy Agency (IAEA) has supported several programs related to nuclear power reactor fuel behavior and fuel behavior modeling. These efforts have collected fuel behavior experimental data, fuel irradiation experiment and hardware descriptions, and fuel modeling code results to develop a useful database of information for code assessment and to determine the maturity of currently existing fuel performance codes. One such program was the Fuel Modeling at Extended Burnup (FUMEXII [18]) program. This program, conducted from 1999-2007, outlined relevant collections of analytical exercises and appropriate experiments and encouraged participants to submit calculation results for a wide variety of fuel performance experiments in a format that readily allowed comparisons between specific codes and to experiment data when available. Given the success of this approach and ready access to the results, we chose to use some test cases from the FUMEXII program for initial assessment of certain BISON code elements. In particular, FUMEXII participants devoted significant effort to fission gas release (FGR) and an impressive compilation of experiment data and code results is given in Ref. [18].

FGR is of particular interest for the present BISON assessment since calculation of fuel centerline temperature and radial and axial temperature distribution depends heavily on fission gas generation in the pellets, migration of the gas to grain boundaries, and eventual release to the fuel pin gap and plenum. FUMEXII Case No. 27, so-called 'Simplified cases', provide an ideal basis for examining the BISON FGR model(s) performance and comparison of BISON results with results from other fuel performance codes that participated in the FUMEXII exercises. The first of the simplified cases, 27(1) focused on the Vitanza criterion [47], which is the comparison of fuel centerline temperature versus burnup at onset of FGR (e.g. 1% release). The second case was to assess the codes' ability to predict total FGR as a function of burnup up to 100 MWd/kgU. Four separate simulations were used for this case:

- 27(2a) a constant power of 15 kW/m from BOL to 100 MWd/kgU,
- 27(2b) a linearly decreasing power from 20 kW/m at BOL to 10 kW/m at 100 MWd/kgU,
- 27(2c) more realistic power history supplied by G Rossiter of BNFL,
- 27(2d) idealized 'real' history supplied by F Sontheimer of FANP.

Q.2. Test Description

Q.2.1. Rod Design Specifications

For Case 27(1), 27(2a), and 27(2b), a standard fuel description representative of a boiling water reactor (BWR) fuel rod typically irradiated in the Halden reactor was specified. The rod plenum was specified as being large as to avoid thermal feedback, the rod plenum fill gas was helium at 0.5 MPa (5 bar). The fuel pellet was solid and flat ended (no chamfer, no dish) UO_2 with 13% ^{235}U enrichment and a grain diameter of 15 microns. Cladding consisted of standard Zr-2. In the Halden reactor, fast neutron flux is typically assumed negligible and thus irradiation induced cladding creep is negligible. Also, the axial power profile in Halden is flat. The detailed specification of the pellet, cladding, and other information relevant to the exercise is shown in Table Q.1.

Table Q.1.: FUMEX-II 27(1), 27(2a), and 27(2b) Fuel Rod/Pellet Specifiactions.

Fuel Rod		
Fuel stack length	m	0.0127
Number of pellets per rod		1
Fill gas composition		He
Fill gas pressure	MPa	0.5
Fuel		
Material		UO_2
Enrichment	%	13
Density	%	95
Outer diameter	mm	10.61
Pellet geometry		Flat Ended
Grain diameter	μm	15
Cladding		
Material		Zr-2
Outer diameter	mm	12.7
Inner diameter	mm	10.8
Wall thickness	mm	0.95

Table Q.2.: FUMEX-II 27(2c) Fuel Rod/Pellet Specifications.

Fuel Rod		
Fuel stack length	m	3.658
Nominal plenum length	mm	162
Number of pellets per rod		275
Fill gas composition		He
Fill gas pressure	MPa	2.5
Fuel		
Material		UO_2
Enrichment	%	8
Density	%	95
Outer diameter	mm	8.2
Pellet length	mm	9.8
Pellet geometry		dished
Grain diameter	μm	75
Pellet Dishing (no chamfers)		
Dish diameter	mm	5.24
Dish depth	mm	0.3
Cladding		
Material		Zr-4
Outer diameter	mm	9.5
Inner diameter	mm	8.36
Wall thickness	mm	0.57

For case 27(2c) and 27(2d) the fuel rod specifications were provided by BNFL (Table Q.2) and FANP (Table Q.3), respectively.

Table Q.3.: FUMEX-II 27(2d) Fuel Rod/Pellet Specifications.

Fuel Rod		
Fuel stack length	m	3.5
Total free volume	cm^3	30
Number of pellets per rod		318
Fill gas composition		He
Fill gas pressure	MPa	2.2
Fuel		
Material		UO_2
Enrichment	%	4
Density	%	95.5
Outer diameter	mm	9.12
Pellet length	mm	11.0
Pellet geometry		standard UO_2
Grain diameter	μm	10
Cladding		
Material		Zr-4
Outer diameter	mm	10.75
Inner diameter	mm	9.29
Wall thickness	mm	0.73

Q.2.2. Operating Conditions and Irradiation History

To match the Vitanza Threshold (described above) multiple simulations are ran at multiple powers until 1% FGR is reached. This was done for 20, 25, 30, 35, 40, and 45 kW/m. For case 27(2a) a constant power of 15 kW/m was used up to a burnup of 100 MWd/kgU. The power for case 27(2b) linearly decreased from 20 kW/m at BOL to 10 kW/m at a burnup of 100 MWd/kgU. Typical Halden BWR (HBWR) conditions were used for the operating conditions (fast neutron flux of 1.6E11 n/cm^2-sec per kW/m, coolant temperature of 232 C, and a coolant pressure of 3.2 MPa) for cases 27(1), 27(2a), and 27(2b).

The power history used for case 27(2c) is shown in Figure Q.1(a), the power is provided as a thermal power in the fuel. The ratio of thermal heat to total heat for the rod is 0.975, thus the input power is scaled by a factor of 1.025641 as BISON requires the total fission power as input. The fast neutron flux was specified as a function and is shown in Figure Q.1(b). The coolant pressure was specified as 15.5 MPa with an average clad temperature of 325 C.

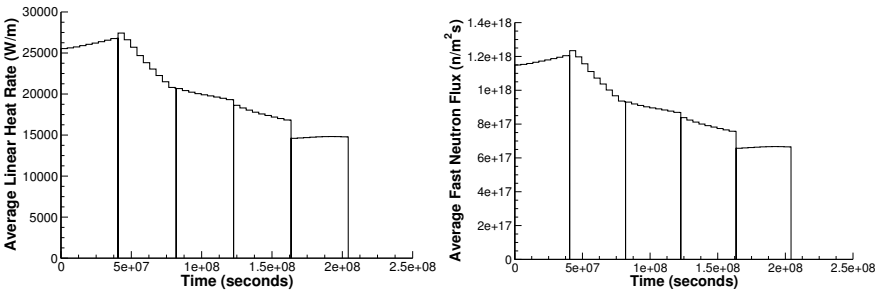

Figure Q.1.: (a) Case 27(2c) average linear heat rate (b) Case 27(2c) average fast neutron flux.

The power history used for case 27(2d) is shown in Figure Q.2. The fast neutron flux had a suggested value of 4E16 n/m^2-sec per kW/m. The coolant pressure was 15.5 MPa, with a coolant temperature of 290 C and a mass flow rate of 0.4 kg/s.

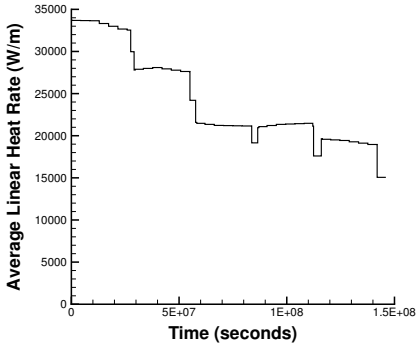

Figure Q.2.: Case 27(2d) average linear heat rate.

Q.3. Model Description

Q.3.1. Geometry and Mesh

Case 27(1)

For this exercise, the main interest was interaction between the fission gas generation and release and the thermal behavior of the fuel. As such, several simplifications could be made. First, since fractional fission gas release was of prime interest, only a single fuel pellet reflecting the parameters given in Table Q.1 was modeled. Second, since fuel-cladding interaction was not of interest, the cladding was removed and only the fuel pellet was modeled. A convective boundary condition representative of Halden operating conditions was applied directly to the pellet outer radius and the top and bottom of the pellet were insulated.

Figure Q.3 shows the mesh used for BISON calculation of the Vitanza criteria. This mesh represents a 2D-RZ axi-symmetric geometry and with 12 radial and 8 axial quadratic elements.

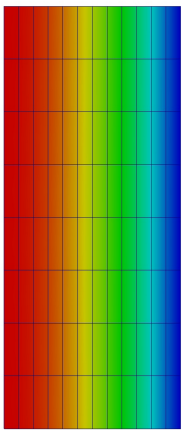

Figure Q.3.: BISON single pellet mesh used for Vitanza Criteria calculation. Fuel temperature profile shown at 1% FGR for LHR of 45 kW/m.

Cases 27(2a) and 27(2b)

A similar mesh was used for cases 27(2a) and 27(2b), except the clad was modeled in these two cases. This mesh consisted of 12 radial and 8 axial quadratic elements in the fuel and 4 radial elements in the clad (see Figure Q.4).

Case 27(2c)

Fuel rod specifications in Table Q.2 were used to generate the mesh for case 27(2c). The fuel rod was meshed as a 2D-RZ axi-symmetric geometry, with 11 radial and 5 axial quadratic elements per fuel pellet. The clad thickness was meshed with 4 radial quadratic elements. A section of the fuel rod is shown in Figure Q.5.

Case 27(2d)

Fuel rod specifications in Table Q.3 were used to generate the mesh for case 27(2d). The fuel rod was meshed as a 2D-RZ axi-symmetric geometry, with 11 radial and 4 axial quadratic elements per fuel pellet. The clad thickness was meshed with 4 radial quadratic elements. A section of the fuel rod is shown in Figure Q.6.

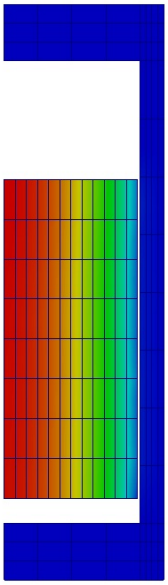

Figure Q.4.: BISON mesh used for cases 27(2a) and 27(2b). Temperature contour of 27(2a) at a burnup of 100 MWd/kgU.

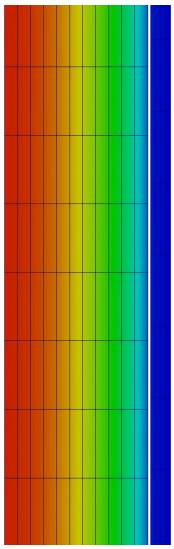

Figure Q.5.: BISON mesh used for cases 27(2c). Temperature contour at a burnup of approximately 100 MWd/kgU.

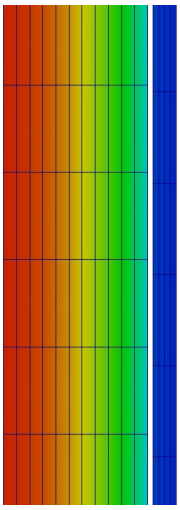

Figure Q.6.: BISON mesh used for cases 27(2d). Temperature contour at a burnup of approximately 67.5 MWd/kgU.

Q.3.2. Material and Behavioral Models

The following material and behavioral models were used for the UO_2 fuel:

- ThermalFuel - NFIR: temperature and burnup dependent thermal properties
- RelocationUO2: provides burnup dependent relocation, with a relocation activation power of 5 kW/m
- Sifgrs: provides mechanistic fission gas release calculation with coupled gaseous swelling

Since the case 1 model did not include cladding, no cladding irradiation growth, cladding thermal, or cladding solid mechanics material models were included. For the case 2 series, the clad material had a constant thermal conductivity of 16 W/m-K was used and both thermal (primary and secondary) and irradiation creep were considered using the Limback model [26].

Q.3.3. Input files

The BISON input and all supporting files (power histories, axial power profile, mesh input, etc.) for this case are provided with the code distribution at bison/assessment/FUMEXII_simplified_cases/analysis.

Q.3.4. Execution Summary

Assessment cases are ran nightly with the most recent version of the code. Table Q.4 summarizes the date and version of the code used to generate results shown in this document.

Table Q.4.: Execution summary.

Experiment	Machine	Operating System	Code Version
27(1)	FALCON	LINUX X	BISON 1.2
27(2a)	FALCON	LINUX X	BISON 1.2
27(2b)	FALCON	LINUX X	BISON 1.2
27(2c)	FALCON	LINUX X	BISON 1.2
27(2d)	FALCON	LINUX X	BISON 1.2

Q.4. Results Comparison

Q.4.1. Fission Gas Release

As mentioned above, the Vitanza criteria is an empirical relationship derived from operational data at the Halden reactor. The empirical relationship has the form

$$T_{CL} = \frac{9800}{ln(\frac{Bu}{0.005})} \tag{Q.1}$$

where T_{CL} is the fuel pellet centerline temperature in C and Bu is the burnup in MWd/kgUO_2. Equation Q.1 provides the locus of centerline temperature-Bu pairs at the onset of fission gas release (onset taken to be approximately 1% FGR) for Halden operational history (e.g. various LHR with standard BWR flow, pressure, and fluid temperature values). The computational process described above was implemented with BISON to determine the onset of 1% FGR for several different LHR. Table Q.5 shows BISON numerical results for linear heat rates ranging from 15 to 45 kW/m.

The BISON predictions and other code comparisons (data digitized from FUMEX-II report [18] are shown with the Vitanza Criteria in Figure Q.7.

Table Q.5.: BISON fuel centerline temperature versus burnup at onset of FGR (various linear heat rates) for the simplified case FUMEXII 27(1).

Burnup (MWd/kgU)	FCT (C)	LHR (kW/m)
80.0	956.5	20.0
49.6	1033.0	25.0
32.9	1093.3	30.0
22.0	1147.3	35.0
14.1	1198.9	40.0
7.8	1248.0	45.0

The Vitanza criteria was derived from pressure, burnup, and centerline temperature data gathered during Halden reactor operations. Most of the experimental data base for the threshold development was for maximum Bu of about 40 MWd/kgU. Reference [18] suggests that the threshold may be somewhat conservative at higher burnups as recent high burnup data shows enhancement of FGR due to rim effect (enhanced porosity) development at the pellet surface. Several of the codes shown in Figure Q.7 have FGR models that predict gas release to be independent of fuel temperature above some burnup limit. Predictions that become vertical are indicative of this feature. BISON results are generally in good agreement with the other code results though it is clear that considerable scatter exists among the predictions.

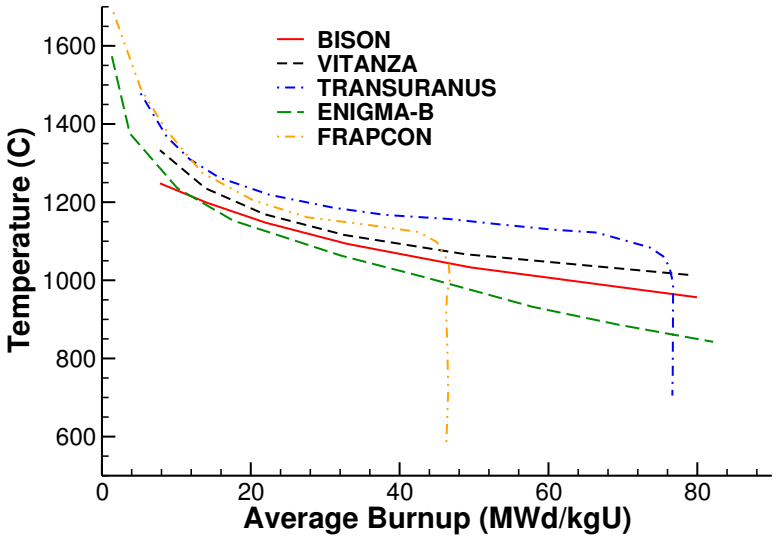

Figure Q.7.: 27(1) BISON and other code results compared to Vitanza criteria [18].

BISON compares well with other well known fuel performance codes. All of the data for the other codes were digitized from plots in the FUMEX-II report [18]. Code comparisons for cases 27(2a) and 27(2b) are shown in Figure Q.8 and Figure Q.9, respectively.

BISON under predicts the total FGR at high burnup, but is within an acceptable range at low and moderate burnup. The BISON comparisons to other fuel performance codes for case 27(2c) are shown in Figure Q.10. The BISON comparisons to expected FGR values and other fuel performance codes for case 27(2d) are shown in Figure Q.11.

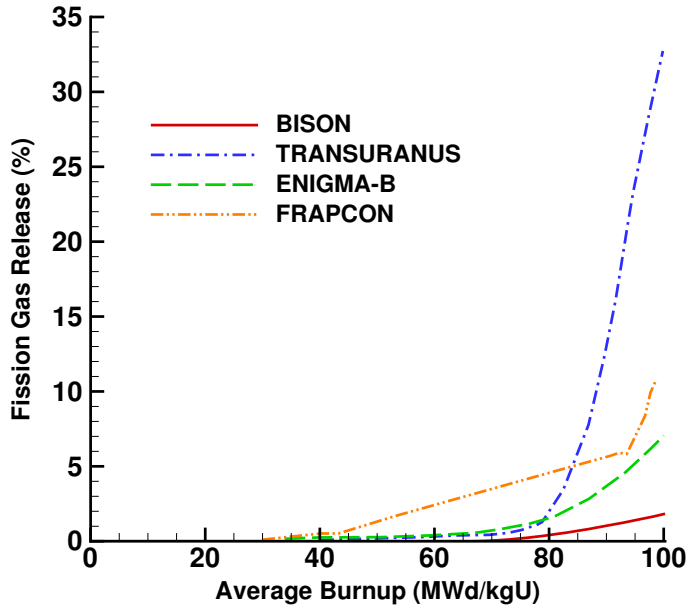

Figure Q.8.: Case 27(2a) BISON comparisons with other well known fuel performance codes [18].

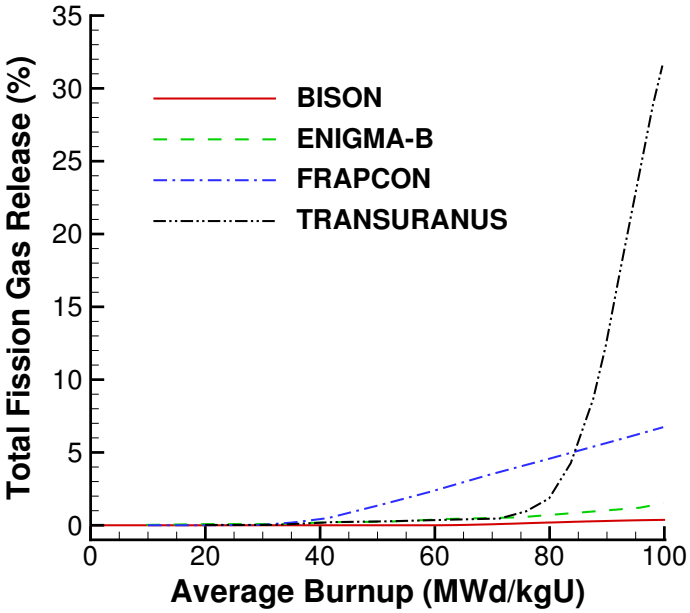

Figure Q.9.: Case 27(2b) BISON comparisons with other well known fuel performance codes [18].

Q.5. Discussion

As discussed above, the mesh shown in Figure Q.3 includes only the fuel pellet. Specifications for FUMEXII 27(1) problem suggested that modelers use a large fuel rod plenum to preclude thermal feedback effects from the plenum and gap on FGR. After some experimentation with this concept, it became

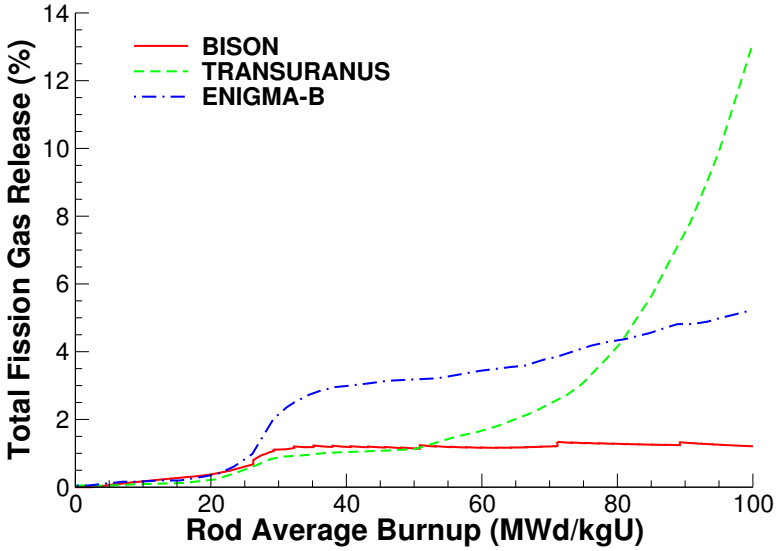

Figure Q.10.: Case 27(2c) BISON comparisons with other well known fuel performance codes [18].

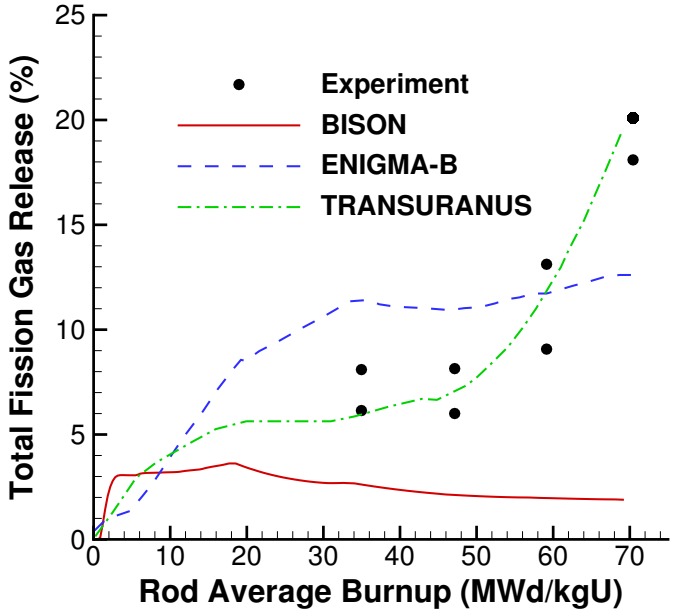

Figure Q.11.: Case 27(2d) BISON comparisons with other well known fuel performance codes [18].

apparent that in BISON it was computationally more efficient to eliminate the cladding and plenum altogether since unrestricted fission gas release was the matter of interest.

The overall results from the FUMEX-II simplified cases study indicate that a more accurate high burnup release model is needed in BISON. At low and moderate burnup, BISON does an adequate job predicting total fission gas release.

R. Risø GEm

R.1. Overview

The Risø-2 GE-m test is a bump test that was carried out during the second Risø Transient Fission Gas Release Project in 1985 [48]. The fuel pin STR013 was supplied by General Electric Company and was punctured and refabricated prior to the bump test. The STR013 fuel element measured 973.50 mm long tip-to-tip. The length of fuel irradiated during the bump test was 271 mm long. The fuel segment was base irradiated in the Millstone reactor at low powers ranging from 10-15 kW/m to a burnup of approximately 14 MWd/kgUO_2. A unique feature of the GE fuel used for this test is that it has a Niobium liner buried 0.075 mm from the clad inner diameter to resist failure due to Pellet-to-Cladding Interaction (PCI). For simplicity this liner was ignored in the simulation. The bump test was performed in the water-cooled HP-1 rig under BWR conditions in the DR3 test reactor.

R.2. Test Description

R.2.1. Rod Design Specifications

The rod specifications for the Risø-2 GE-m test is are summarized in Table R.1.

R.2.2. Operating Conditions and Irradiation History

The base irradiation average power is shown in Figure R.1. The average power during the bump test is shown in Figure R.2. The axial power profile is nearly linear for the duration of the base irradiation and bump test. During the base irradiation there are small fluctuations in the axial power profile as a function of time. The axial profile for the duraction of the bump test is shown in Figure R.3.
Since the data was provided in a histogram form the input power profile used by BISON was modified to add additional points that are 10 s later than the supplied points to provide a short ramp time between plateaus in the histogram. The small duration of the ramp results in the use of a power profile that is very close to a histogram which permits the use of a piecewise linear algorithm. Moreover the first ramp in power has been broken down into 24 short ramps as per recommendations by ANATECH.

The clad surface temperature was input as a function, along with the fast neutron flux from data provided in the FUMEX-III data set [35]. The coolant inlet temperature and pressure for the base irradiation and power ramp is shown in Table R.2. The clad tempature, fast flux, and axial peaking factors were modified such that the 10 s ramps are also applied. This ensures that the times used are consistent throughout the model.

Table R.1.: Rod specifications of rods STR013 and Risø-2 GE-m

Base Fuel Rod (STR013)		
Tip-to-tip length	m	0.9735
Fuel Length	m	0.778
Active Fuel Length	m	0.7557
Nominal plenum height	mm	0.1444
Number of pellets in rod		63
Fill gas composition		He
Fill gas pressure (0 C)	MPa	1.7
Fuel		
Material		UO_2
Enrichment	%	2.89
Density	%	95.73
Outer diameter	mm	10.89
Pellet geometry		Chamfered
Grain diameter	μm	19.0
Pellet Chamfer (both ends)		
Dish diameter	cm	–
Dish depth	cm	–
Chamfer width	mm	0.25
Chamfer depth	mm	0.38
Cladding		
Material		Zr-2
Outer diameter	mm	12.54
Inner diameter	mm	11.11
Wall thickness	mm	0.71
Refabricated Fuel Rod (GE-m)		
Fuel stack height	m	0.271
Number of pellets in rod		23
Fill gas composition		He
Fill gas pressure (0 C)	MPa	0.49

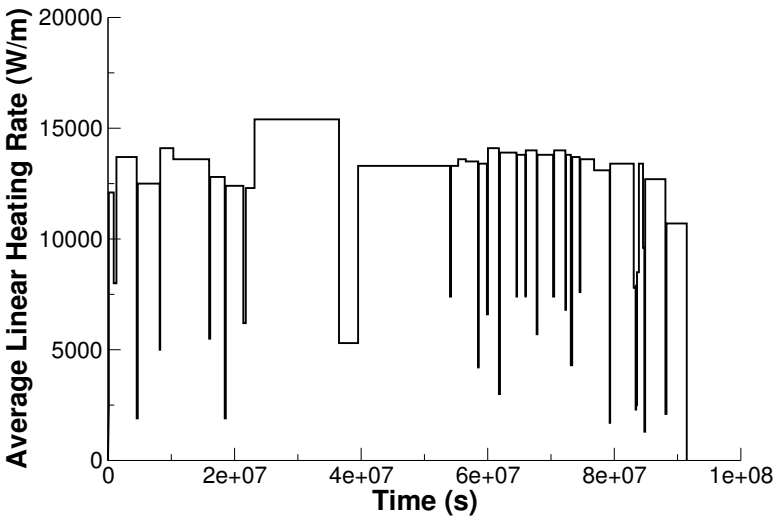

Figure R.1.: Base irradiation average power history for test pin STR013.

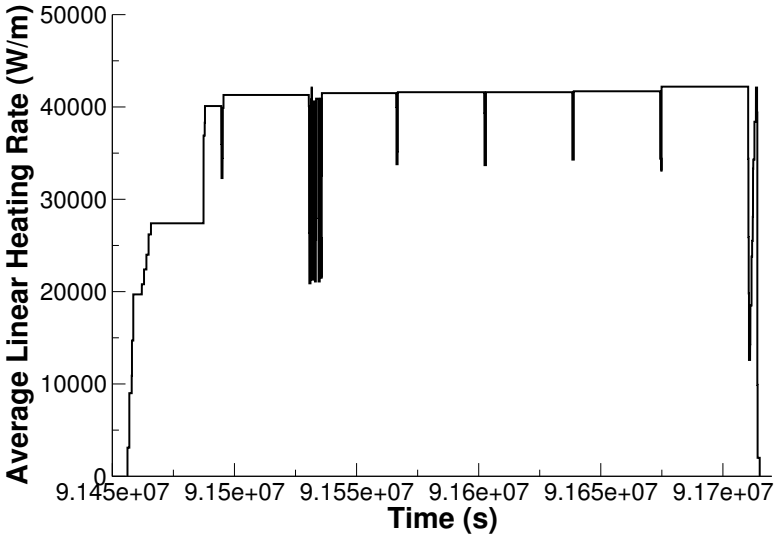

Figure R.2.: Average power history during the bump test.

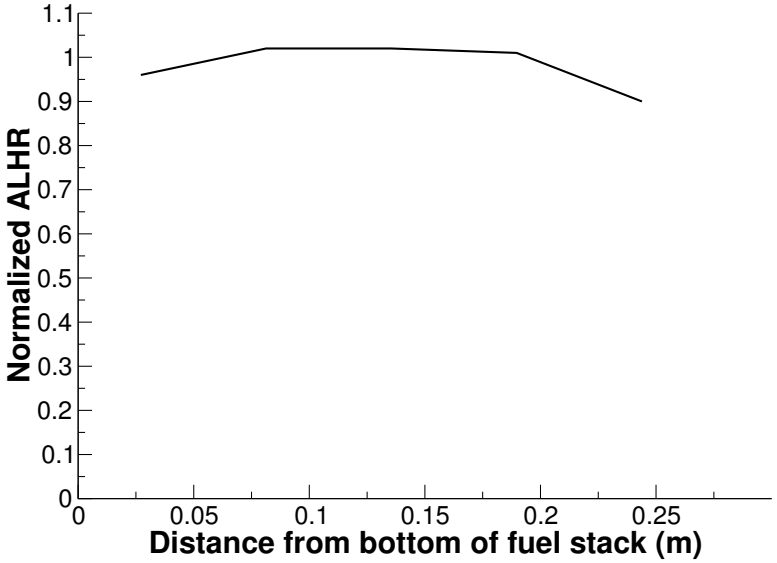

Figure R.3.: The axial power profile during the bump test

Table R.2.: Operational input parameters.

Base Irradiation		
Coolant inlet temperature	C	287.8
Coolant pressure	MPa	7.24
Power Ramps		
Coolant inlet temperature	C	289
Coolant pressure	MPa	7.2

R.3. Model Description

R.3.1. Geometry and Mesh

The geometric parameters specified in Table R.1 were used to create the mesh for this simulation. The fuel was meshed as a smeared fuel rod with 11 radial elements and 184 axial elements. Figure R.4 shows a section of the mesh with a temperature contour plot. The geometry was such that the refabricated rod length was modeled during the base irradiation and bump test. To account for the correct gas volume the plenum height was adjusted such that the overall voidage including chamfers, radial gap, bottom plenum and top plenum were equivalent to the refabricated volume at the base irradiation. The lower plenum was equal to the length of the Hafnium Oxide insulator pellet that was not modeled. Due to fuel swelling and cladding creep down the initial volume at the beginning of the bump test is slightly lower than the refabrication.

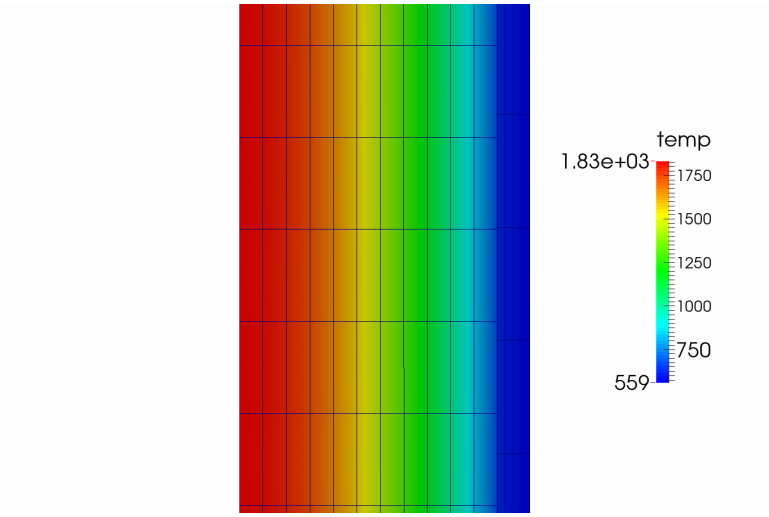

Figure R.4.: A section of the mesh with a temperature contour at t = 9.15662×10^7s.

R.3.2. Material and Behavioral Models

The thermal conductivity model used for the UO_2 fuel was NFIR. The fuel was modeled as elastic and fuel swelling was coupled to the fission gas release model. In addition fuel relocation was modeled using an activation power of 5 kW/m. Fission gas release was modeled using the Sifgrs model with a transient burst release model. The cladding material, was modeled using a constant thermal conductivity of 16 W/m-K. Primary and secondary thermal, and irradiation creep were modeled.

R.3.3. Input files

The BISON input and all supporting files (power histories, axial power profile, fast neutron flux history, etc.) for this case are provided with the code distribution at bison/assessment/Riso_GEM_STR013/analysis.

R.3.4. Execution Summary

The assessment case was completed on a Mac Workstation running OS X using BISON version 1.2.

Table R.3.: Execution summary.

Machine	Operating System	Code Version
FALCON	LINUX	BISON 1.2

R.4. Results Comparison

R.4.1. Clad Diameter

A comparison of the predicted and measured rod outer diameter is shown in Table R.4. The comparisons include the average rod diameter prior to the bump test, and the maximum and average changes in diameter during the test. No ridging was observed before the bump test and there is little to unclear evidence at the conclusion of the bump test.

Table R.4.: Clad diameter comparisions before and after the bump test.

	Average Diameter before Ramp (mm)	Maximum Diameter Increase (μm)	Average Diameter Increase (μm)
Experimental	12.536	8	5
Refab T=273 K Smeared	12.500	2.169	-5.434
Refab T=273 K Discrete	12.500	2.740	2.120
Refab T=373 K Smeared	12.506	0.406	-7.219
Refab T=373 K Discrete	12.506	0.470	-7.216

R.4.2. Fission Gas Release

A comparison of the predicted and measured total fission gas release is shown in Figure R.5. Since the base irradiation is a low power and low burnup irradiation BISON accurately predicts FGR of approximately zero percent. However, at the end of the ramp test, BISON under predicts the total FGR. Although the end of life percentage of FGR was underpredicted by the BISON simulation it is an acceptable result as it is within a factor of two of the experimental data.

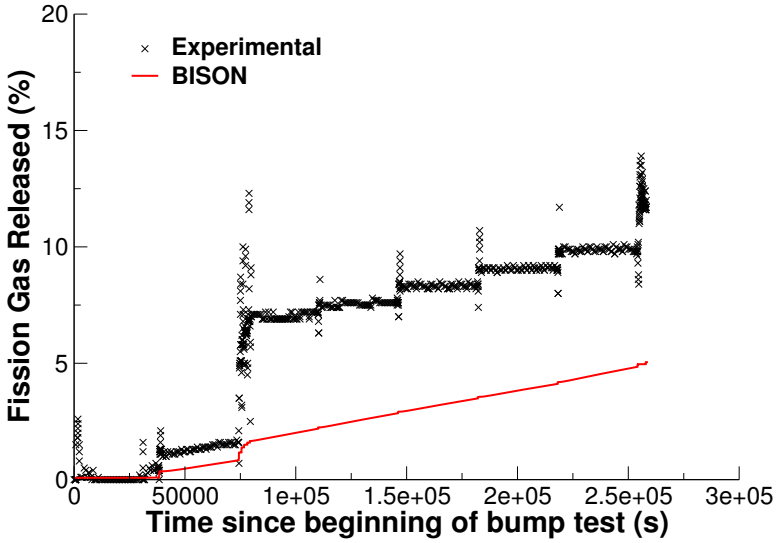

Figure R.5.: Fission gas release comparison of GE-m during the bump test.

R.4.3. Rod Internal Pressure

A comparison of the predicted and measured internal rod pressure is shown in Figure R.6. BISON overpredicts the rod internal pressure from the beginning of the bump test. This is likely due with the refabrication calculation. The trend observed is encouraging as it is exactly the same as the experimental

data. However, there appears to be an systematic offset in the internal pressure from the beginning of the bump test. Further investigation is required to determine the cause of this offset.

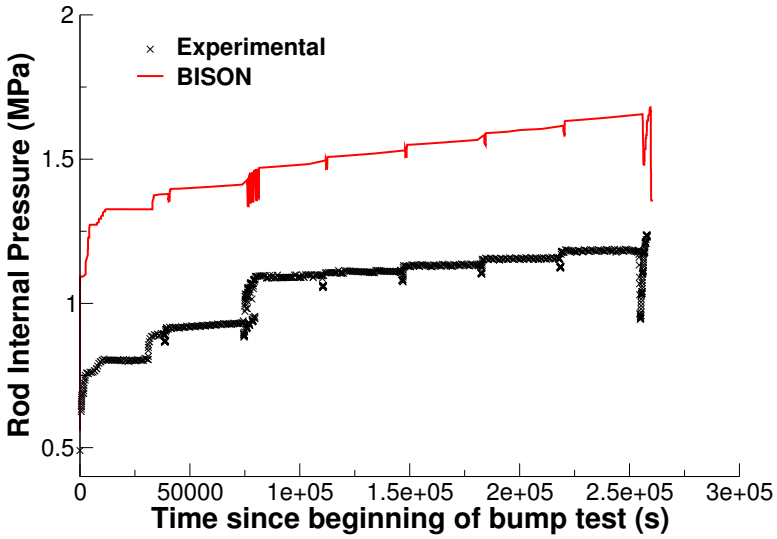

Figure R.6.: Rod internal pressure comparison of GE-m during the bump test.

R.4.4. Discussion

The comparisons of the results against the experimental data for the refabrication supplied in the FUMEX-III data were examined in the previous two subsections. It appears that the rod internal pressure strongly depends upon the refabrication temperature. Therefore a sensitivity analysis of the plenum pressure behavior as a function of the refabrication temperature was completed. By keeping the refabrication temperature and volume constant and varying the refabrication temperature the amount of initial moles after refabrication can be varied. BISON uses the refabrication data provided in the input file to calculate the initial moles after refabrication. Then the calculated moles and the postprocessor values for the average gas temperature and the gas volume are used to determine the internal gas pressure. To ensure the calculated pressure is close to the refabrication pressure the cladding temperature during the refabrication process must be set equal to the refabrication temperature. The sensitivity analysis was completed for refabrication temperatures of 273 K (given in the experimental data), 373 K, 473 K and 546 K. The rod internal pressure results of the analysis are presented in Figure R.7 and the fission gas release results are presented in Figure R.8.

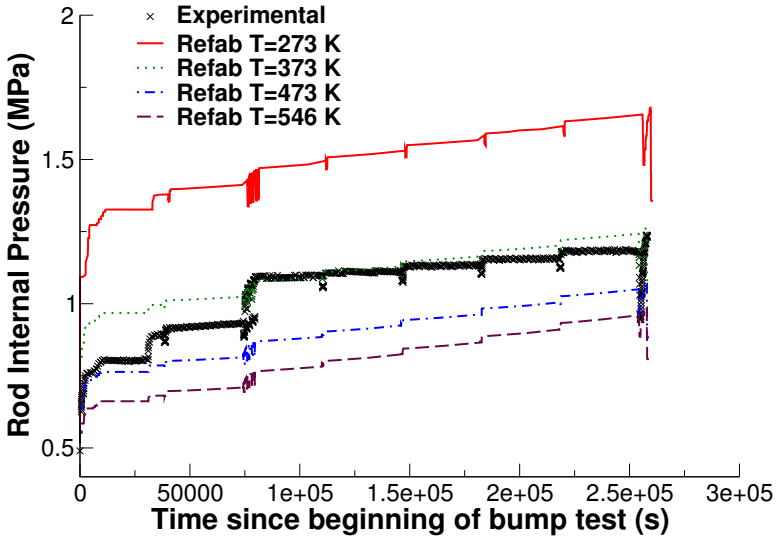

Figure R.7.: Sensitivity analysis of the rod internal pressure as a function of the refabrication temperature.

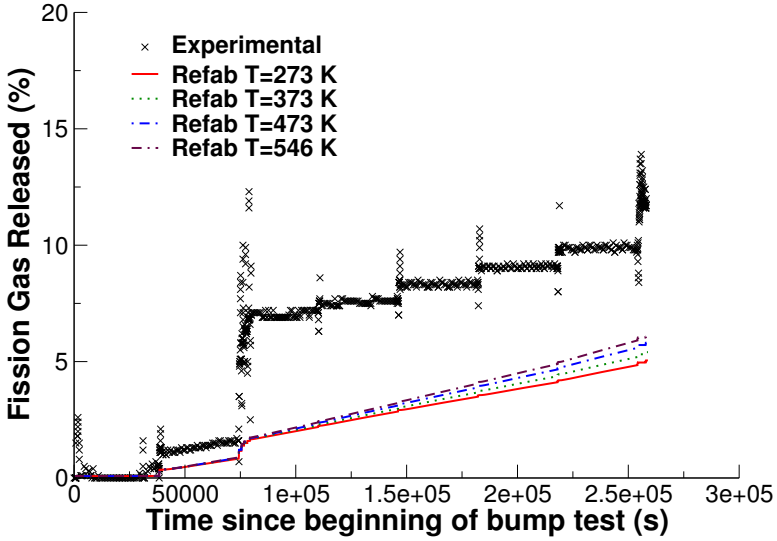

Figure R.8.: Sensitivity analysis of the fission gas release as a function of the refabrication temperature

Based upon the sensitivity analysis it is observed that as the refabrication temperature increases from 273 K to 546 K the internal rod pressure decreases and the fission gas released increases. This is expected because by changing the refabrication time the number of moles decreases. Less initial moles results in a lower internal rod pressure. The increasing temperature contributes to the increase fission gas release that is observed. The key takeaway of the sensitivity analysis is that the internal rod pressure for the duration of irradiation is strongly influenced by the refabrication temperature, or more importantly the difference between the refabrication temperature and the cladding temperature after refabrication. For example if the cladding temperature is brought down to 273 K during the refabrication process to be equal to the internal gas temperature. Once refabrication is complete the cladding surface temperature is increased to 562 K (the supplied boundary condition). This change in temperature is more than double the refabrication temperature and by the ideal gas law when the volume and initial moles remain relatively constant, the pressure more than doubles. Therefore, the largest contributing factor to the rod internal pressure discrepancy is the difference between the reported refabrication temperature and the cladding boundary condition.

The refabrication data is provided to calculate the initial moles in the void volume within the rod. Then using the gas volume and temperature postprocessors the plenum pressure is calculated using the determined initial moles. By examining the ideal gas law it should not matter what temperature the refabrication pressure is reported at because the refabrication volume remains constant. However, to correctly model the evolution of the rod internal pressure, the temperature at which the refabrication was completed at is required to ensure the temperature change from refabrication to bump test operation is correct.

S. Risø II3

S.1. Overview

The Risø II3 experiment conducted at the Risø DR3 water-cooled HP1 rig utilized a re-fabricated rod from the Millstone-1 BWR [35],[49]. The mother rod, STR014, was irradiated over three reactor cyclers up to about 14.5 GWd/t, and re-fabricated to a shorter length. The re-fabricated rod, II3 (STR014-3R), was instrumented with a fuel centerline thermocouple and a pressure transducer. The fuel centerline temperature, fission gas release, rod internal pressure, and rod outer diameter can be used for comparison.

S.2. Test Description

S.2.1. Rod Design Specifications

Rod II3 was a re-fabricated rod extracted from a full length rod. The hole for the thermocouple was at the top of the fuel rod and did not penetrate the entire fuel stack. The re-fabricated rod geometry is tabulated in Table S.1.

Table S.1.: Risø II3 Test Rod Specifications

Fuel Rod		
Overall length	m	0.3616
Fuel stack height	m	0.291
Nominal plenum height	mm	51.0
Mother Rod		
Fill gas composition		He
Fill gas pressure	MPa	1.53
Re-Fabricated Rod		
Fill gas composition		He
Fill gas pressure	MPa	0.684
Fuel		
Material		UO_2
Enrichment	%	2.89
Density	%	95.77
Inner diameter	mm	2.5
Outer diameter	mm	10.89
Pellet geometry		both ends
Grain diameter	μm	12.2
Pellet Dishing		
Dish diameter	cm	0.0
Dish depth	cm	0.0
Chamfer width	cm	0.038
Chamfer depth	cm	0.018
Cladding		
Material		Zr-2
Outer diameter	mm	12.53
Inner diameter	mm	11.11
Wall thickness	mm	0.71

S.2.2. Operating Conditions and Irradiation History

The power history for the base irradiation carried out at the Millstone-1 BWR is shown in Figure T.1. The experiment power history carried out at the Risø DR3 facility is shown in Figure T.2 and run at BWR conditions by reducing the system pressure to 7.24 MPa. A prescribed axial profile for this experiment was provided in the FUMEX-III data [35]. The measured clad surface temperature as a function of time was also provided in the FUMEX-III data [35] and used as a boundary condition for this simulation. The other reactor operation parameters are tabulated in Table S.2.

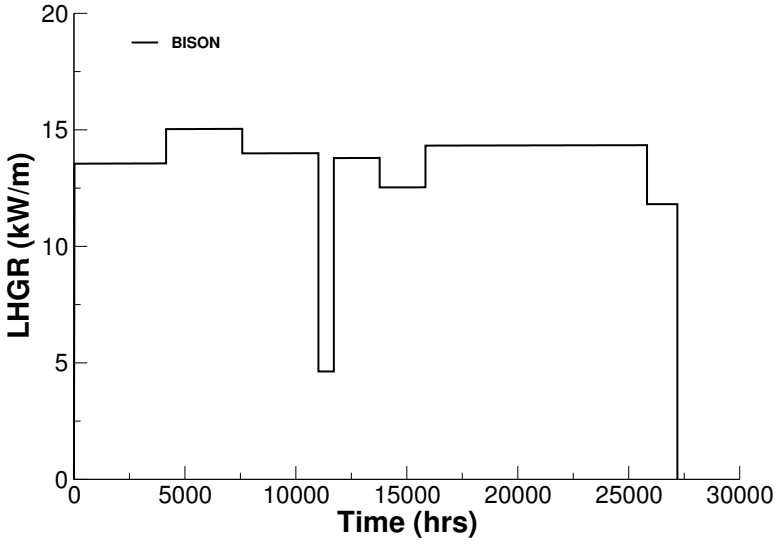

Figure S.1.: Base irradiation history for fuel segment STR014, carried out at Millstone-1 BWR.

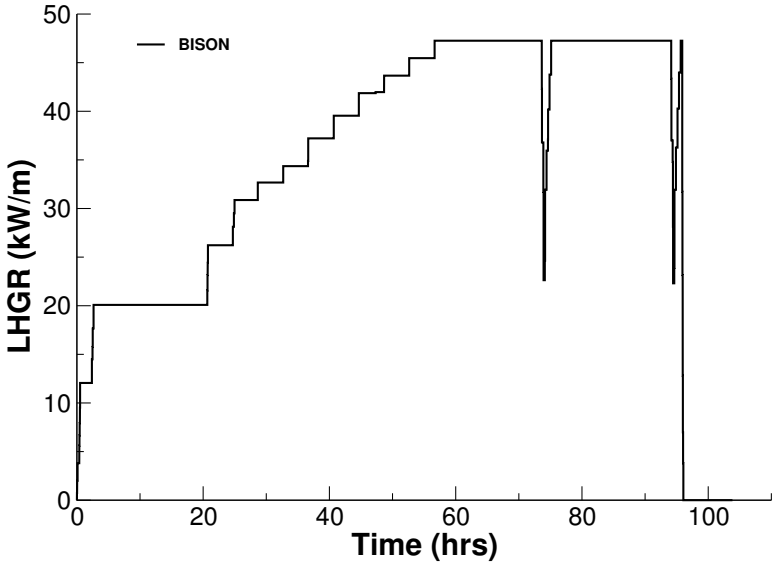

Figure S.2.: Risø DR3 irradiation period for test II3 (STR014-3R).

Table S.2.: Operational input parameters.

Base Irradiation		
Coolant inlet temperature	C	287.8
Coolant pressure	MPa	7.24
Fast neutron flux	n/(cm^2·s) per (kW/m)	1.6·10^{12}
Power Ramps		
Coolant inlet temperature	C	NA
Coolant pressure	MPa	7.24
Fast neutron flux	n/(cm^2·s) per (kW/m)	4.0·10^{11}

S.3. Model Description

S.3.1. Geometry and Mesh

The re-fabricated rod geometry was modeled for the entire simulation considering a smeared column of flat ended pellets, with the top pellets containing the hole for the thermocouple. The plenum height was adjusted such that the plenum volume at the beginning of the bump test was approximately 7.41 cm^3.

A 2-dimensional axi-symmetric quadratic (Quad8 elements) mesh was used to model the geometry of the rod used in the II3 experiment. The fuel was meshed considering two fuel pellet types. The first pellet type was 4.2 cm in length with a hole down the center, the second pellet type was 24.9 cm in length with no hole down the center. The first pellet type's mesh is comprised of elements 3.953 mm in the axial direction and 0.3889 mm in the radial direction (for an aspect ratio of 10.16). The second pellet type's mesh is comprised of elements 2.0 mm in the axial direction and 0.3813 mm in the radial direction (for an aspect ratio of 5.244). The clad mesh is comprised of elements 4.278 mm in the axial direction and 0.1775 mm in the radial direction (for an aspect ratio of 24.1).

S.3.2. Material and Behavioral Models

The following material and behavioral models were used for the UO_2 fuel:

- ThermalFuel - NFIR: temperature and burnup dependent thermal properties
- RelocationUO2: relocation strains, relocation activation threshold power set to 5 kW/m.
- Sifgrs: fission gas release model with the combined gaseous swelling model.

For the clad material, a constant thermal conductivity of 16 W/m-K was used and both thermal and irradiation creep were considered using the Limback model [26].

S.3.3. Boundary and Operating Conditions

The Risø DR3 irradiation period for the II3 test shown in Figure T.2 was appended to the base irradiation power history shown in Figure T.1. It was assumed that the clad temperature during the down time between base irradiation and the Risø test was 373K. The fast neutron flux was input as a function of power.

S.3.4. Input files

The BISON input and all supporting files (power histories, axial power profile, fast neutron flux history, etc.) for this case are provided with the code distribution at bison/assessment/Riso_II3/analysis.

S.3.5. Execution Summary

Table S.3.: Execution summary.

Machine	Operating System	Code Version
FALCON	LINuX	BISON 1.2

S.4. Results Comparison

The Risø II3 experiment is used to assess the code's capability to capture the fuel centerline temperature, the integral fuel rod fission gas release, rod internal pressure, and rod outer diameter. All results were compared against the II3 data found in the FUMEX-III data sets [35].

S.4.1. Temperature

BISON predicts the shape of temperature curve well, but fails to reach measured thermocouple temperatures as shown in Figure T.3. One possible explaination for the lower predicted temperature is the underprediction of fission gas release as seen in Figure T.4. The fuel centerline temperature is taken at a node approximately 38 mm from the top of the fuel stack.

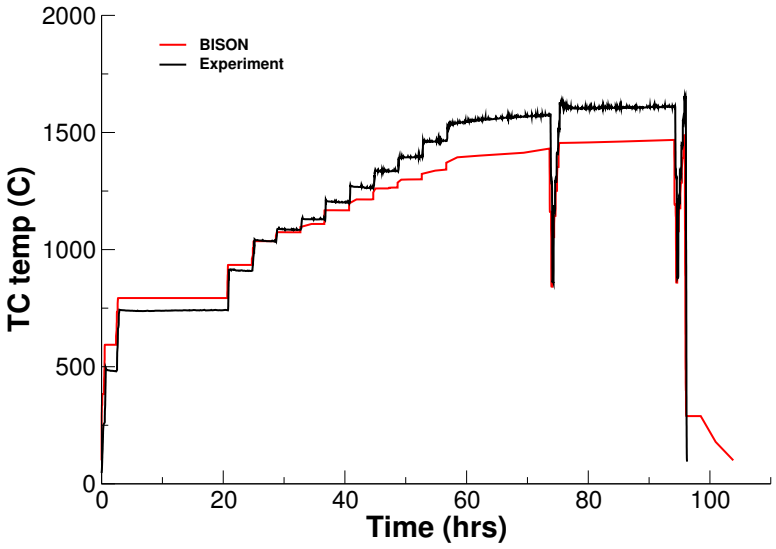

Figure S.3.: BISON fuel centerline temperature comparison to Risø experimental data

S.4.2. Fission Gas Release

The calculated integral fuel rod fission gas release is compared to the measured data in Figure T.4. In view of the uncertainties involved in FGR modeling, the predictive accuracy is satisfactory, falling well within the uncertainty factor of 2 [5].

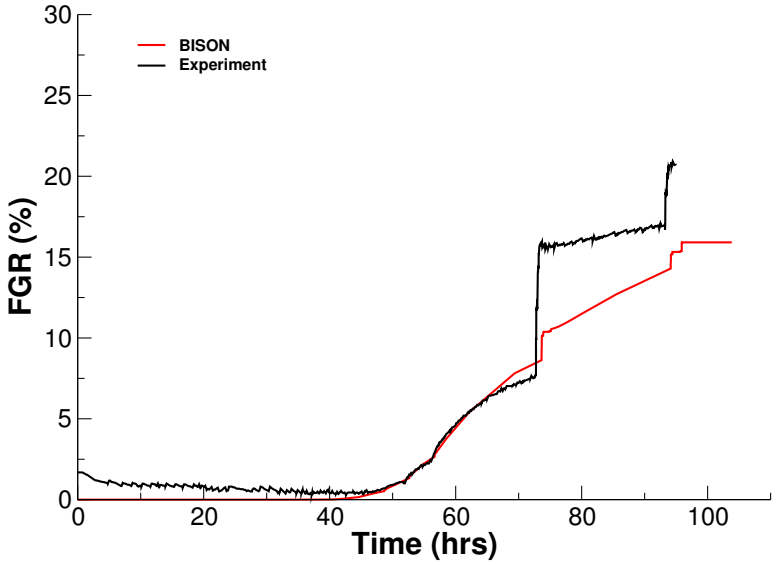

Figure S.4.: BISON ramp test fission gas release comparison to Risø experimental data.

S.4.3. Rod Internal Pressure

The calculated rod internal pressure matches the measured data set well as seen in Figure T.5 following the given shape of the measured cuve accurately.

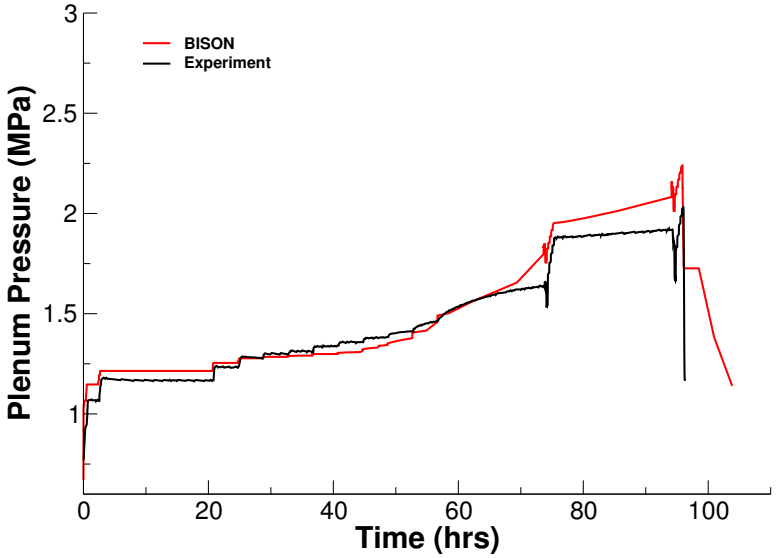

Figure S.5.: BISON rod internal pressure comparison to Risø experimental data.

S.4.4. Rod Outer Diameter

The calculated rod diameter seems to predict more cladding creepdown than experiment results suggest as shown in Figure S.6. Since BISON currently does not have a cladding option for cold worked Zry2, a SRA Zry4 cladding was chosen instead.

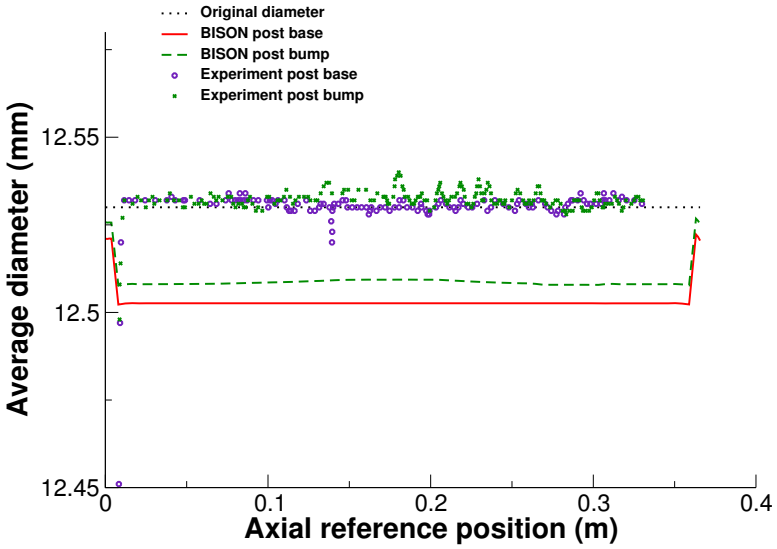

Figure S.6.: BISON rod outer diameter comparison to Risø experimental data.

S.5. Discussion

For the grain size, a chosen diameter of 12.2 μm was used. A brief discussion of how the grain size had already been multiplied by the correction factor of 1.56 can be found in the PRECHAR.II3 file included in the FUMEX-II3 data sets [35].

T. Risø II5

T.1. Overview

The Risø II5 experiment conducted at the Risø DR3 water-cooled HP1 rig utilized a re-fabricated rod from the Halden BWR [35]. The mother rod, M72-2, was one of the six ZR-2 clad UO_2fuel pins in the IFA161 test rig. This base irradiation was completed between July 14, 1968 and October 2, 1981. Upon compleiton of the base irradiation the mother rod was refabricated and bump tested as part of the II5 experiment. The refabricated rod II5 was instrumented with a fuel centerline thermocouple and a pressure transducer. The fuel centerline temperature, fission gas release, rod internal pressure, and rod outer diameter can be used for comparison.

T.2. Test Description

T.2.1. Rod Design Specifications

Rod II5 was a re-fabricated rod extracted from a full length rod. The hole for the thermocouple was at the top of the fuel rod and did not penetrate the entire fuel stack. The re-fabricated rod geometry is tabulated in Table T.1.

Table T.1.: Risø II5 Test Rod Specifications

Fuel Rod		
Overall length	m	0.3563
Fuel stack height	m	0.2878
Nominal plenum height	mm	65.47
Mother Rod		
Fill gas composition		He
Fill gas pressure	MPa	0.09
Re-Fabricated Rod		
Fill gas composition		He
Fill gas pressure	MPa	0.641
Fuel		
Material		UO_2
Enrichment	%	5.078
Density	%	94.7
Inner diameter	mm	0
Outer diameter	mm	12.625
Pellet geometry		dished both ends
Grain diameter	μm	9.984
Pellet Dishing		
Dish diameter	mm	11.125
Dish depth	mm	0.3
Chamfer width	mm	0.0
Chamfer depth	mm	0.0
Cladding		
Material		Zr-2
Outer diameter	mm	14.00
Inner diameter	mm	12.85
Wall thickness	mm	0.56

T.2.2. Operating Conditions and Irradiation History

The power history for the base irradiation carried out at the Halden BWR is shown in Figure T.1. The experiment power history carried out at the Risø DR3 facility is shown in Figure T.2 and run at BWR conditions by reducing the system pressure to 7.24 MPa. A prescribed axial profile for this experiment was provided in the FUMEX-III data [35]. The measured clad surface temperature as a function of time was also provided in the FUMEX-III data [35] and used as a boundary condition for this simulation. The other reactor operation parameters are tabulated in Table T.2.

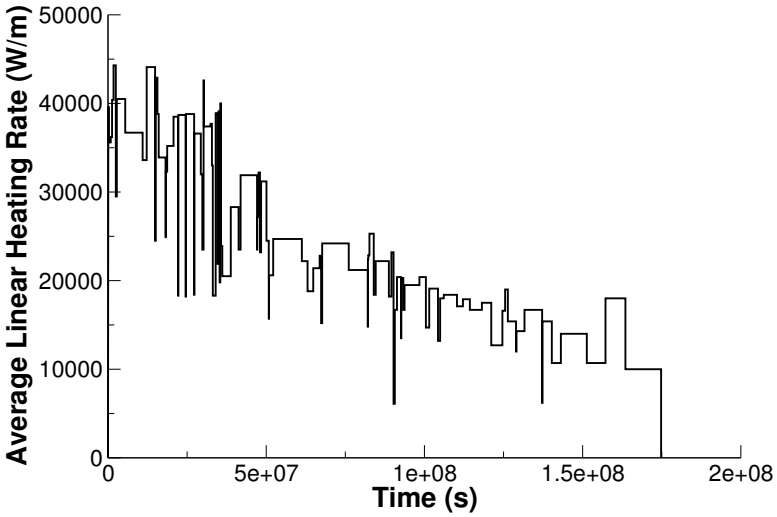

Figure T.1.: Base irradiation history for fuel segment STR014, carried out at Halden BWR.

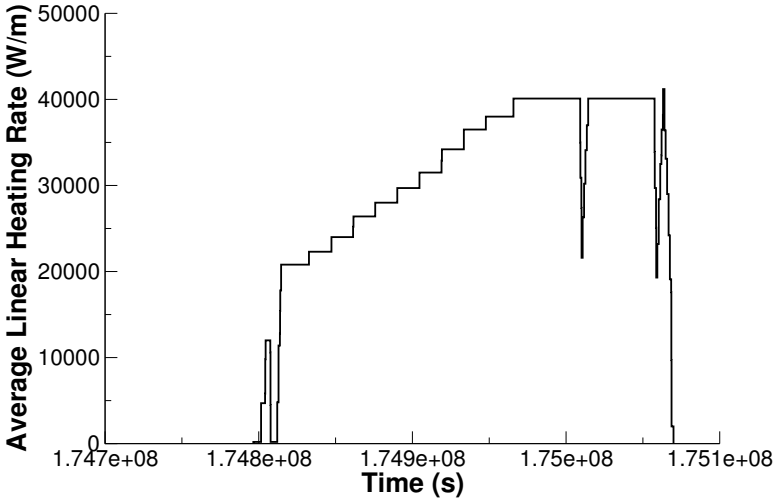

Figure T.2.: Risø DR3 irradiation period for test II5.

T.3. Model Description

T.3.1. Geometry and Mesh

The re-fabricated rod geometry was modeled for the entire simulation considering a smeared column of flat ended pellets, with the top pellets containing the hole for the thermocouple. The plenum height was adjusted such that the plenum volume at the beginning of the bump test was approximately 8.68 cm^3.

Table T.2.: Operational input parameters.

Base Irradiation		
Coolant inlet temperature	C	287.8
Coolant pressure	MPa	3.2
Fast neutron flux	n/(m^2·s) per (W/m)	$5.5 \cdot 10^{12}$
Power Ramps		
Coolant inlet temperature	C	NA
Coolant pressure	MPa	7.2
Fast neutron flux	n/(m^2·s) per (W/m)	$4.0 \cdot 10^{12}$

A 2-dimensional axi-symmetric quadratic (Quad8 elements) mesh was used to model the geometry of the rod used in the II5 experiment. The fuel was meshed considering two fuel pellet types. The first pellet type was 1.38 cm in length with a 0.125 cm diameter hole down the center, the second pellet type was 1.297 cm in length with no hole down the center. The first pellet type's mesh is comprised of elements 4.6 mm in the axial direction and 0.460227 mm in the radial direction (for an aspect ratio of 9.995). The second pellet type's mesh is comprised of elements 4.323 mm in the axial direction and 0.4602 mm in the radial direction (for an aspect ratio of 9.393). The clad mesh is comprised of elements 5.353 mm in the axial direction and 0.1438 mm in the radial direction (for an aspect ratio of 37.22).

T.3.2. Material and Behavioral Models

The following material and behavioral models were used for the UO_2 fuel:

- ThermalFuel - NFIR: temperature and burnup dependent thermal properties
- RelocationUO2: relocation strains, relocation activation threshold power set to 5 kW/m.
- Sifgrs: fission gas release model with the combined gaseous swelling model.

For the clad material, a constant thermal conductivity of 16 W/m-K was used and both thermal and irradiation creep were considered using the Limback model [26].

T.3.3. Boundary and Operating Conditions

The Risø DR3 irradiation period for the II5 test shown in Figure T.2 was appended to the base irradiation power history shown in Figure T.1. It was assumed that the clad temperature during the down time between base irradiation and the Risø test was 273K as per the experimental data. The fast neutron flux was input as a function of power.

T.3.4. Input files

The BISON input and all supporting files (power histories, axial power profile, fast neutron flux history, etc.) for this case are provided with the code distribution at bison/assessment/Riso_II5/analysis.

T.3.5. Execution Summary

Table T.3.: Execution summary.

Machine	Operating System	Code Version
FALCON	LINUX	BISON 1.2

T.4. Results Comparison

The Risø II5 experiment is used to assess the code's capability to capture the fuel centerline temperature, fission gas release, rod internal pressure, and rod outer diameter. All results were compared against the II5 data found in the FUMEX-III data sets [35].

T.4.1. Centerline Temperature

BISON predicts the shape of temperature curve well, but fails to reach measured thermocouple temperatures as shown in Figure T.3. One possible explaination for the lower predicted temperature is the underprediction of fission gas release as seen in Figure T.4. The fuel centerline temperature is taken at a node approximately 38 mm from the top of the fuel stack.

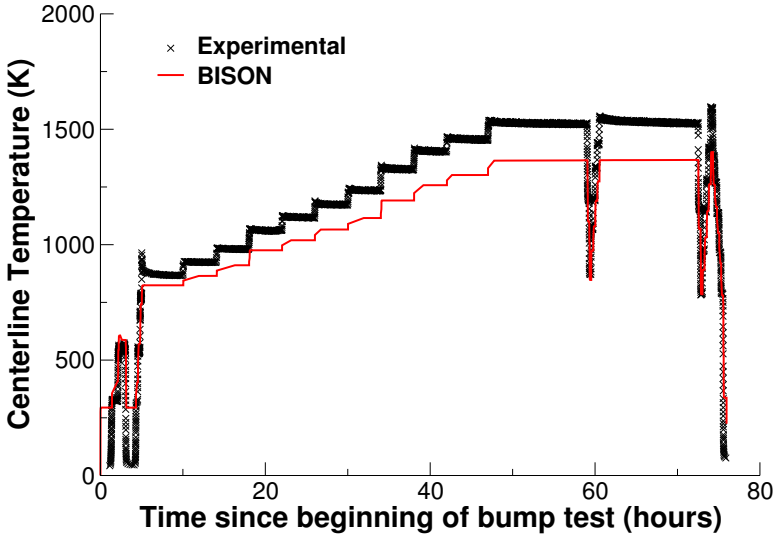

Figure T.3.: BISON fuel centerline temperature comparison to Risø experimental data

T.4.2. Fission Gas Release

The calculated integral fuel rod fission gas release for the ramp tests is compared to the measured data in Figure T.4. For this prediction the fission gas released during the base irradiation is not included. It is observed that BISON significantly underpredicts the fission gas release. The experiment predicts 11% and BISON predicts approximately 0.33%. This significant difference is partly due to the fact the transient burst release model in the Sifgrs fission gas release model in BISON was turned off due to convergence issues. In order to have the burst release model work the interpenteration of the fuel and

clad was enormously large at about 12 microns. Therefore, to have acceptable penetration results (less then 3 microns) the transient release model was not used.

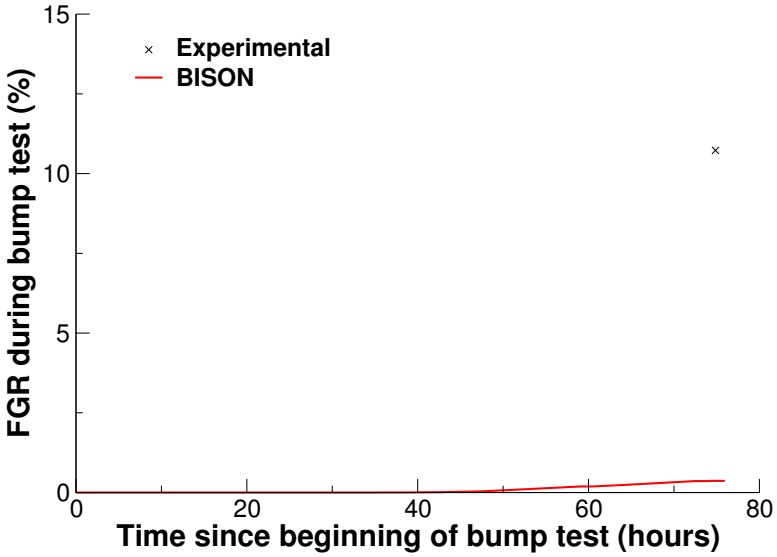

Figure T.4.: BISON ramp test fission gas release comparison to Risø experimental data.

T.4.3. Rod Internal Pressure

Figure T.5 illustrates the comparison between BISON and the experimental data for the rod internal pressure during the bump test. It is observed that BISON immediately rises to a larger pressure after refabrication. This is due to the difference in temperature between the cladding boundary and the refabrication temperature immediately after refabrication. A further analysis of these results is provided in the Discussion section.

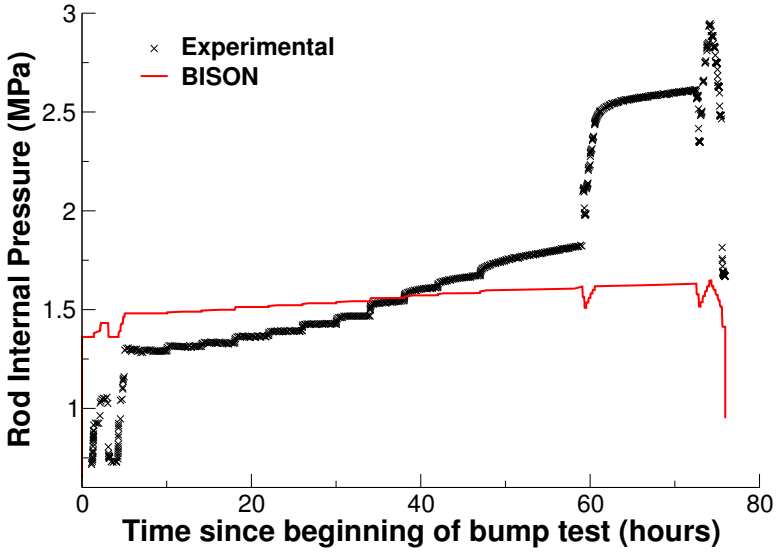

Figure T.5.: BISON rod internal pressure comparison to Risø experimental data.

T.4.4. Clad Diameter

Figure T.6 shows the comparison between BISON and the experimental data for the cladding diameter for two cases: pre-ramp and post-ramp. In general bison does a reasonable job at predicting the cladding

diameter pre-ramp but significantly underpredicts the diameter post-ramp. For the experimental data, the 2 points above one another using the same symbols indicate the maximum and minimum diameters observed at that location due to pellet hourglassing. Since a smeared model was used in BISON a single value was obtained. Ideally this line should fall between the 2 data points. The cause of the discrepancy between BISON and the experimental predictions is because the transient release model was not used for fission gas release. If the burst release model was used a large internal gas pressure would be observed and a higher amount of fission gas swelling would occur within the fuel pellets. A larger swelling would result in a large cladding diameter. In addition, a discrete pellet model would be ideal to capture the hourglassing effect and to predict the maximum and minimum diameter values.

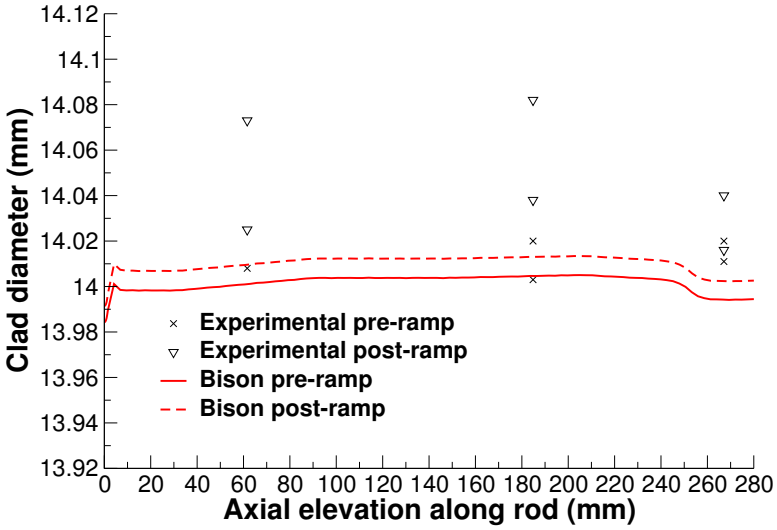

Figure T.6.: BISON clad diameter comparison to Risø experimental data pre-ramp and post-ramp

T.5. Discussion

In this section, comparison plots of BISON against the experimental data and a variety of well known fuel performance codes is completed for rod internal pressure and fission gas release. Figure T.7 illustrates the rod internal pressure comparison. It is observed that despite BISON not matching the experimental data that well it falls within the range of the other codes. In fact ENIGMA-B, FEMAXI-7 and BISON all predict relatively similar trends in the pressure behavior. Similar results are presented in Figure T.8 for fission gas release. All the codes presented underpredict the fission gas release. Although BISON predicts the lowest fission gas release, if penetration can be minimized such that the burst release model could be used, BISON would fall within the spread of the fuel performance codes.

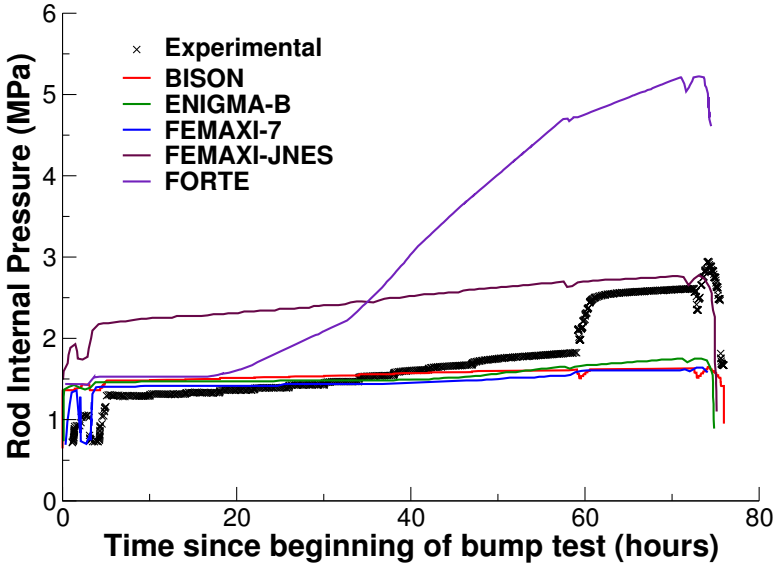

Figure T.7.: BISON rod internal pressure comparison to experimental data and other well known codes.

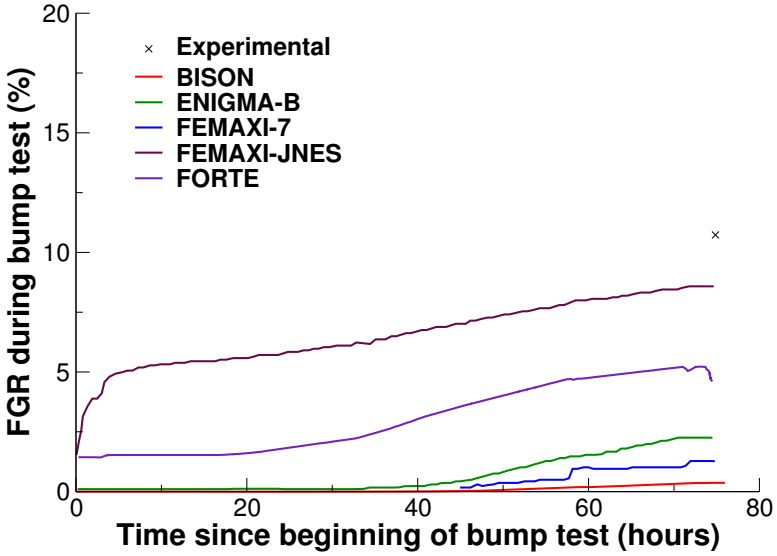

Figure T.8.: BISON ramp test fission gas release comparison experimental data and other well known codes.

U. Risø GE7

U.1. Overview

The Risø-3 GE7 test is a bump test that was carried out during the third Risø Transient Fission Gas Release Project in 1989 [50]. The fuel pin ZX115 was supplied by General Electric Company and was neither punctured nor re-fabrication prior to the test. The test pin was the lower middle segment of four approximately 0.975 m long segments assembled to a stringer. The fuel segment was base irradiated in the Quad Cities-1 boiling water reactor (BWR) over four reactor cycles. The bump test was performed in the water-cooled HP-1 rig under BWR conditions in the Risø DR3 test reactor.

U.2. Test Description

U.2.1. Rod Design Specifications

The rod specifications for the Risø-3 GE7 test is are summarized in Table U.1.

Table U.1.: Risø-3 GE7 rod specifications.

Fuel Rod		
Fuel stack height	mm	752.1
Nominal plenum height	mm	143.4
Fill gas composition		He
Fill gas pressure	MPa	0.29
Fuel		
Material		UO_2
Enrichment	%	3.0
Density	%	95.2
Outer diameter	mm	10.41
Pellet geometry		Chamfered
Grain diameter	μm	11.3-12.8
Pellet Chamfer (both ends)		
Dish diameter	cm	–
Dish depth	cm	–
Chamfer width	mm	0.18
Chamfer depth	mm	0.38
Cladding		
Material		Zr-2
Outer diameter	mm	12.26
Inner diameter	mm	10.63
Wall thickness	mm	0.815

U.2.2. Operating Conditions and Irradiation History

The base irradiation average power is shown in Figure U.1. The average power during the ramp test is shown in Figure U.2. The axial power profile is nearly linear for the base irradiation, however, during

the ramp test, the power is shifted heavily to the bottom of the rod (see Figure U.3). The clad surface temperature was input as a function, along with the fast neutron flux from data provided in the FUMEX-III data set [35]. The coolant inlet temperature and pressure for the base irradiation and power ramp is shown in Table U.2.

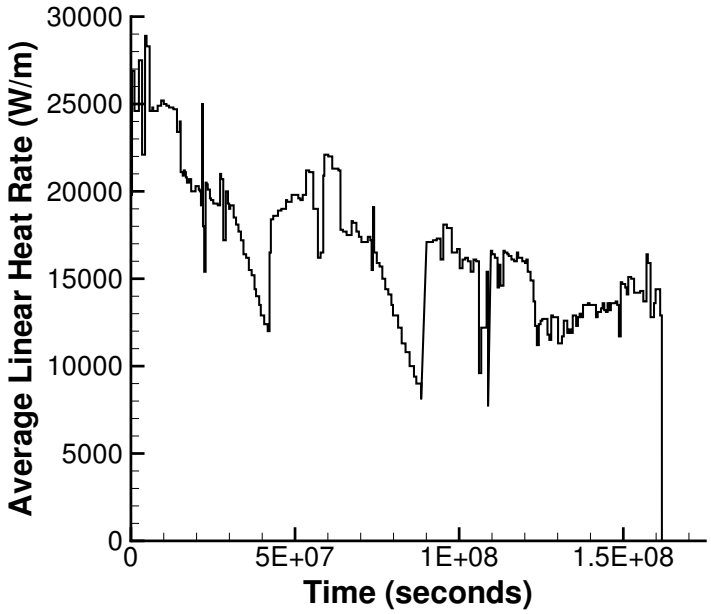

Figure U.1.: Base irradiation average power history for test pin ZX115.

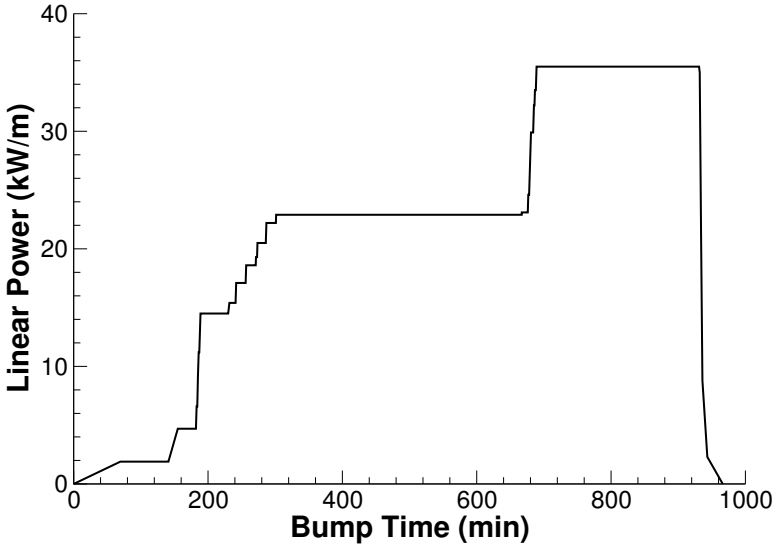

Figure U.2.: Average power history during power ramp. Note: The time has been zeroed to the start of the ramp.

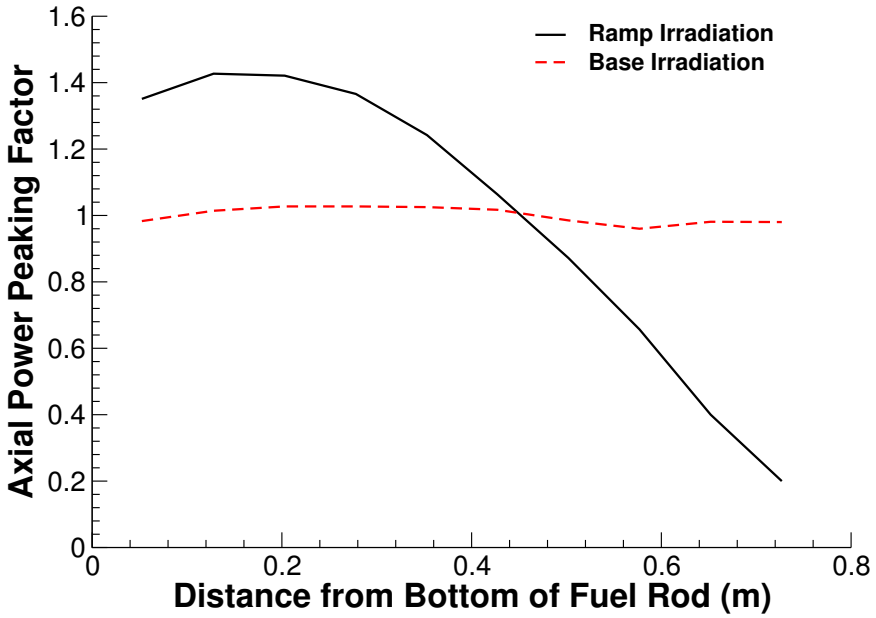

Figure U.3.: Axial power profile during base irradiation and ramp test.

Table U.2.: Operational input parameters.

Base Irradiation		
Coolant inlet temperature	C	295
Coolant pressure	MPa	7.24
Power Ramps		
Coolant inlet temperature	C	289
Coolant pressure	MPa	7.24

U.3. Model Description

U.3.1. Geometry and Mesh

The Risø GE7 ZX115 rod was modeled both as a smeared fuel pellet stack and as a discrete fuel pellet stack. The geometric parameters specified in Table U.1 were used to create the meshes for these simulations. The smeared fuel was meshed as a single smeared fuel column with 11 radial elements and 432 axial elements. The discrete fuel was meshed as 72 individual pellets, each with 8 axial and 11 radial elements. Figure U.4 shows a section of the mesh with a stress contour plot. This contour plot was made near the end of the run. Actual numbers are irrelevant in this case as this plot is only meant to show the discretization.

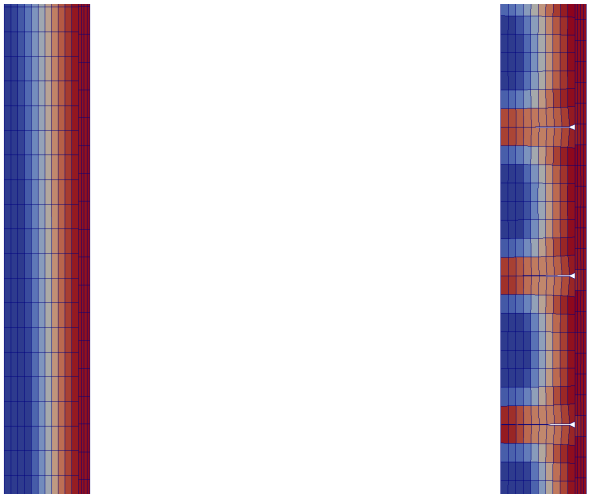

Figure U.4.: A section of the GE7 ZX115 fuel rod mesh with a temperature contour plot.

U.3.2. Material and Behavioral Models

The following material and behavioral models were used for the UO_2 fuel:

- ThermalFuel - NFIR: temperature and burnup dependent thermal properties.
- RelocationUO2: relocation strains, relocation activation threshold power set to 5 kW/m.
- Sifgrs: Simplified fission gas release model with physics based gaseous swelling model.

For the clad material, a constant thermal conductivity of 16 W/m-K was used. Both thermal (primary and secondary creep) and irradiation creep were considered and combined with a J_2 plasticity model to simulate rapid cladding deformation during power ramps.

U.3.3. Input files

The BISON input and all supporting files (power histories, axial power profile, fast neutron flux history, etc.) for this case are provided with the code distribution at bison/assessment/Riso_GE7_ZX115/analysis.

U.3.4. Execution Summary

Table U.3.: Execution summary.

Machine	Operating System	Code Version
INL HPC Falcon	Linux	BISON 1.2

U.4. Results Comparison

U.4.1. Clad Diameter

A comparison of the predicted and measured rod outer diameter at post base irradiation and post ramp is shown in Figure U.5. Starting with the post base irradiation it can be seen from Figure U.5 that

BISON over predicted the Under predicted the rod diameter for both the smeared and discrete cases. This is most likely cause by over predicting the cladding creep down. At this point in the irradiation the cladding creep is mostly a function of thermal creep. It can also be seen that the post base profile matches the base irradiation peaking factors seen in Figure U.3. The diameter matching the axial profile so well supports the thought that the cladding creep is over predicted. As mentioned, Figure U.5 also shows the post bump results. BISON under predicts the rod diameter for both the smeared and discrete cases here as well. The ramp test for this experiment had a strong axial profile by design. The diameter profile for both BISON cases does match the axial profile. The difference between the post ramp measured results and the discrete average diameter in the power tilted region is about 0.005 mm.

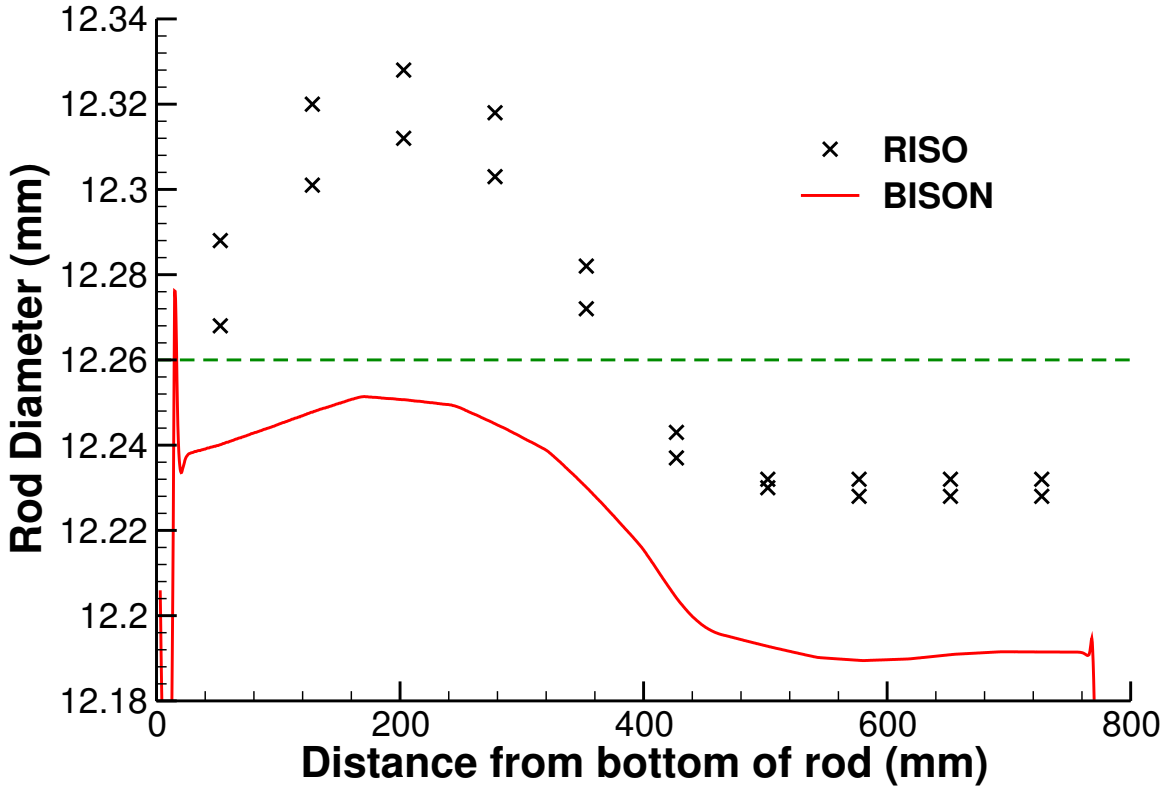

Figure U.5.: Risø GE7 experimental rod diameter comparisons before and after the power ramp.

U.4.2. Other Results

The Risø GE7 experiment was centered around fuel rod diameter, but other parameters were measured as well. Figure U.6 is a composite of the other parameters measured during the ramp. Figure A plots the fuel centerline temperature of the smeared pellet simulation against the discrete pellet model. The plot shows that the two models compare very closely with the discrete pellet having a slightly higher temperature in the ramp. Figure B is of the fission gas released. The measured results were taken at the end of the ramp test by puncture method. Both the smeared and the discrete models compare well to the measured results. The discrete compares better with slightly more fission gas release, this is due to the higher temperature the discrete pellets saw. Figure C plots the plenum pressure of the test. Once again the smeared and the discrete models compare well to the post ramp puncture test. The discrete model shows a higher internal pressure during the ramp caused by the combination of higher temperature and increased fission gas release. Figure D plots the internal gas volume of the rod. The smeared and discrete cases follow each other until just after the start of the high power ramp. Current thoughts on what is happening here are as follows: As the temperature increases the fuel stack volume increases due to thermal expansion and fuel swelling causing the gas volume it decrease. Shortly after the start of the ramp the smeared and discrete cased diverge and the discrete gains volume. Thoughts are that the thermal expansion takes over and opens the gap between the pellets. This also starts to cause the bamboo effect on the cladding as it creeps down. The gaps opening and possible clad lift due to bambooing could account for the gas volume increase. It should be noted that the abrupt down spike at the end of the run is from numerical error. The end results for free gas volume are under estimated.

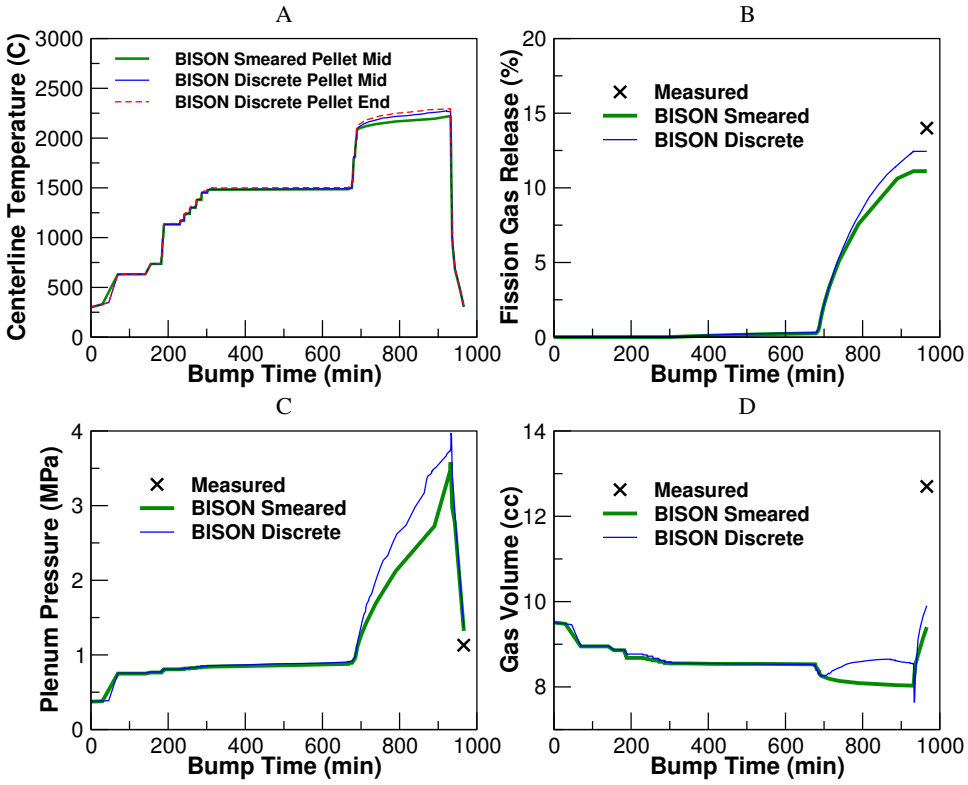

Figure U.6.: BISON and Risø GE7 results for A) BISON calculated fuel centerline temperature B) fission gas release C) plenum pressure D) free gas volume during and after the power ramp.

U.4.3. Discussion

From the results shown above it can be seen that BISON over predicts the cladding creep in both the base irradiation and the ramp phases of this experiment. Going in to this experiment there were a couple

assumptions made that will affect the outcome of the diameter. Cladding oxidation was omitted, due to this BISON should always under predict the rod diameter. The fuel was modeled as elastic and there was no frictional contact between the fuel and cladding. Both of these will change the overall results of this simulation. As mentioned in the previous section both smeared and discrete post ramp FGR, plenum pressure and gas volume all compare to each other and the measured results. As new methods are implemented in to BISON this simulation will be revisited.

V. OSIRIS J12

V.1. Overview

This test is of a segmented PWR rod base-irradiated in the Electricity of France (EDF) Gravline 5 PWR [35]. The segment was then re-fabricated and ramp-tested in the French Alternative Energies and Atomic Energy Commission (CEA) OSIRIS reactor to investigate PCMI resistance. This experiment was chosen because it allows for an evaluation of several aspects of the code, including fully coupled thermo-mechanics, contact, and several nonlinear material models.

V.2. Test Description

V.2.1. Rod Design Specifications

The geometric input parameters for the OSIRIS J12 test are summarized in Table V.1.

Table V.1.: OSIRIS J12 Test Rod Specifications

Fuel Rod		
Overall length	m	0.5224
Fuel stack height	m	432.95
Nominal plenum height	mm	89.44
Number of pellets per rod		32
Fill gas composition		He
Fill gas pressure	MPa	2.6
Fuel		
Material		UO_2
Enrichment	%	4.5
Density	%	95.73
Outer diameter	mm	8.192
Pellet geometry		Dished
Grain diameter	μm	10
Pellet Dishing (no chamfers)		
Dish diameter	mm	6
Dish depth	mm	0.32
Cladding		
Material		Zr-2
Outer diameter	mm	9.5
Inner diameter	mm	8.36
Wall thickness	mm	0.57

V.2.2. Operating Conditions and Irradiation History

The approximately 0.522 m segmented Zircaloy-4 clad rod was irradiated for 2 cycles in the EDF Gravline 5 PWR to a final discharge burn-up of 23.852 MWd/kgU. The average powers in the 2 cycles were approximately 16 and 23 kW/m. The rod segment designated J12-5, which was irradiated in the fifth span from the lower end of the assembly, was refabricated with new end plugs without altering either the fuel column or the internal fill gas. After a conditioning period of 762 minutes at 21 kW/m, the power was increased quickly (9 kW/m/min.) and held at 39.5 kW/m for 739 minutes. The axial profile was flat during base irradiation. The peaking factors during the bump test varied from approximately 0.75 at the ends of the segment to 1 at the center. The power history is presented in Figure V.1, and the power ramp is shown in Figure V.2. The initial fill-gas (Helium) pressure was 2.6 MPa, and the coolant pressure was 15.5 MPa. The external clad temperature was defined as a function of time and constant in space over the section of rod, the specified clad temperature in Figure V.3 was used in this simulation. The clad temperature was about 585 K during base irradiation and about 615 K during the ramp. The fast neutron flux in the clad was supplied via input using experimental data supplied with the experiment. Operational input parameters are summarized in Table V.2.

Table V.2.: Operational input parameters.

Base Irradiation		
Coolant inlet temperature	C	
Coolant pressure	MPa	15.5
Fast neutron flux	n/(m^2·s) per (W/m)	4.8·10^{13}
Power Ramp		
Coolant inlet temperature	C	
Coolant pressure	MPa	14.7
Fast neutron flux	n/(m^2·s) per (W/m)	4.8·10^{13}

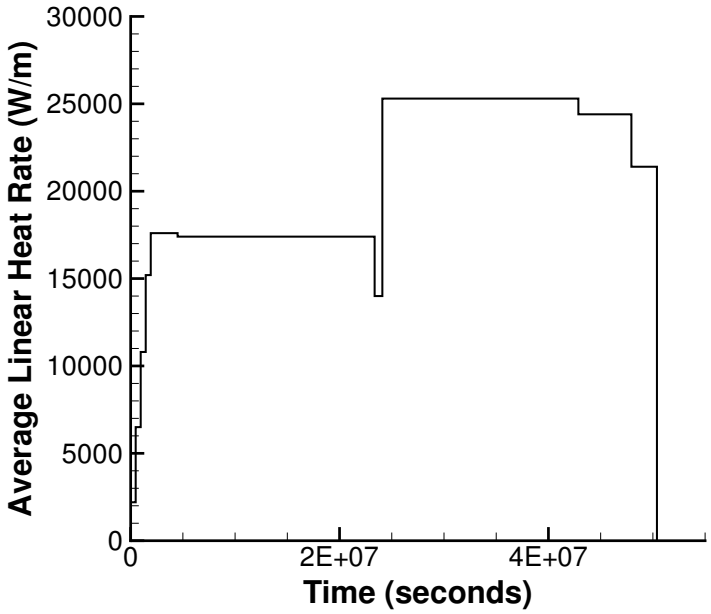

Figure V.1.: OSIRIS J12 power history in the Gravlines 5 PWR.

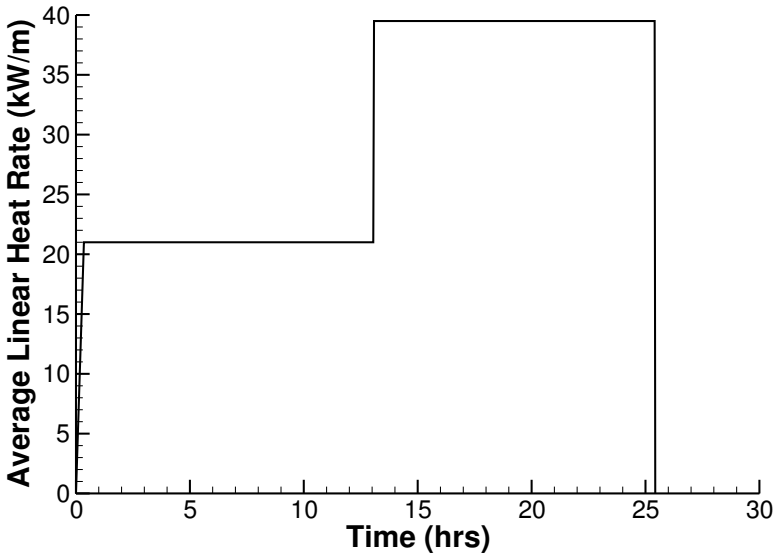

Figure V.2.: OSIRIS J12 power ramp

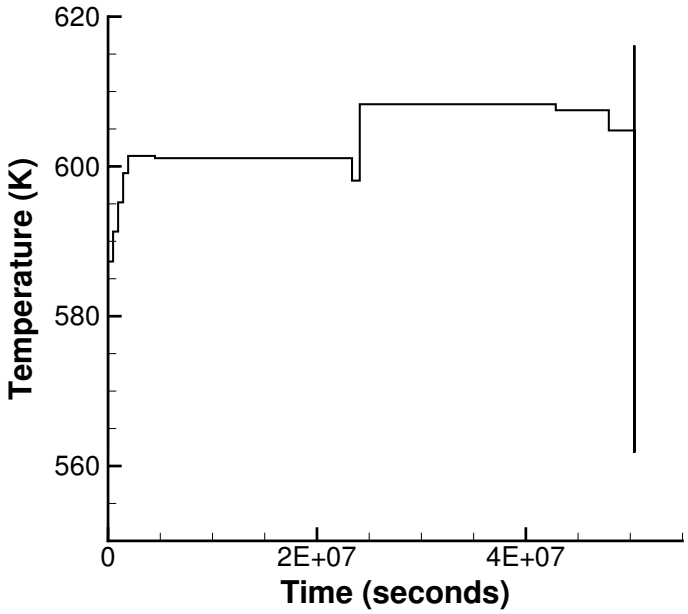

Figure V.3.: OSIRIS J12 clad temperature

V.3. Model Description

V.3.1. Geometry and Mesh

The rod specifications in Table V.1 were used as input for the geometry for this simulation. The J12-5 rod was modeled as a 2D-RZ axisymmetric discrete pellet mesh with quadratic elements. Each pellet consisted of 16 axial elements and 9 radial elements. The clad was meshed with 4 elements through the thickness. Figure V.4 is a section of the mesh with a temperature contour.

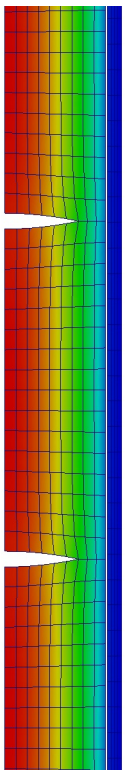

Figure V.4.: OSIRIS J12-5 mesh with temperature contour.

V.3.2. Material and Behavioral Models

The following material and behavioral models were used for the UO_2 fuel:

- ThermalFuel - NFIR: temperature and burnup dependent thermal properties
- RelocationUO2: relocation strains, relocation activation threshold power set to 5 kW/m.
- Sifgrs: Simplified fission gas release model with a combined solid/gaseous swelling model based on fission gas release.

For the clad material, a constant thermal conductivity of 16 W/m-K was used and both thermal (primary and secondary) and irradiation creep were considered.

V.3.3. Input files

The BISON input and all supporting files (power histories, axial power profile, fast neutron flux history, etc.) for this case are provided with the code distribution at bison/assessment/OSIRIS_J12/analysis.

V.3.4. Execution Summary

Table V.3.: Execution summary.

Machine	Operating System	Code Version
FALCON	LINUX	BISON 1.2

V.4. Results Comparison

V.4.1. Clad Diameter

A comparison of the predicted and measured rod outer diameter is shown in Figure V.5. The solid blue line is the as-manufactured rod diameter, prior to irradiation. The experimental data, shown as "+" (post-ramp) and "x" (pre-ramp) symbols, indicate the measured average rod diameter at both the end and middle fuel pellet locations, giving an indication of rod ridging due to pellet hour-glassing. The green solid line is the predicted rod diameter following the power bump and the red solid line is the predicted rod diameter prior to the ramp.

BISON under predicts clad creep down resulting in a larger than measured diameter. The overall shape of the rod after the ramp is captured well with BISON, as well as the clad ridging caused by the hour glassing (bamboo effect) of the discrete pellets.

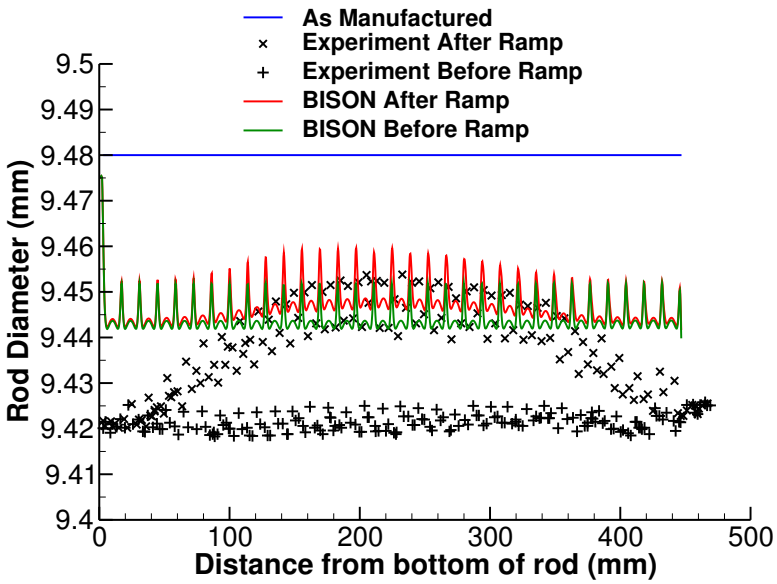

Figure V.5.: OSIRIS J12 experimental measurements and BISON calculation results from before and after the power ramp.

W. OSIRIS H09

W.1. Overview

The OSIRIS H09 test rod is a standard full length PWR rod that was irradiated for 4 cycles in the Electricity of France (EDF) Cruas 2 PWR to a final discharge rod average burn-up of 46.06 MWd/kgU [51]. This experiment was chosen for analysis because of the availability of measured data for evaluation of several fuel rod performance characteristics including fission gas release, cladding hydrogen content, fuel column length changes, rod growth, oxide thickness, rod internal pressure, whole pellet density, end-of-life internal free volume, and radial distribution of Cs, Nd, Pu and Xe.

W.2. Test Description

W.2.1. Rod Design Specifications

The geometric input parameters for the OSIRIS H09 rod are summarized in Table W.1.

Table W.1.: OSIRIS H09 Test Rod Specifications.

Fuel Rod		
Overall length	m	3.8517
Fuel stack height	m	3.66038
Nominal plenum height	m	0.13932
Fill gas composition		He
Fill gas pressure	MPa	3.1
Fuel		
Material		UO_2
Enrichment	%	3.249
Density	%	95.31
Outer diameter	mm	8.190
Nominal diametral gap	μm	160
Average grain size	μm	9.060
Cladding		
Material		Zr-4
Outer diameter	mm	9.508
Inner diameter	mm	8.35
Wall thickness	mm	0.575

W.2.2. Operating Conditions and Irradiation History

The H09 rod was irradiated for 4 cycles in the OSIRIS reactor to a final discharge average burnup of 46.06 MWd/kgU. The power mode selected for this simulation is PiecewiseConstant. The average linear powers in the 4 cycles were approximately 22, 20, 18, and 15 kW/m [51]. The average power history for is shown in Figure W.1. The power history assumed a 24 hour startup time that was broken into 24 timesteps in one hour increments. Because the axial power shapes and boundary conditions are modeled as PieceswiseBilinear, a ramp time of 360 seconds (0.1 hours) was assumed at each power step for the axial power shape and boundary condition input. The startup time of 24 hours and the ramp time of 360 seconds (0.1 hours) are based on ANATECH's experience with fuel rod modeling for steady state operation and the development of Falcon Verification and Validation cases. They are intended to minimize the introduction of computational artifacts from unrealistic power changes and ramp rates into the analyses. The axial power profile was calculated from the OSIRIS data package [51] taken from the IFPE database. The cladding outer surface temperature as a function of time was also provided in the OSIRIS data package [51], and was used as a boundary condition for this simulation. The cladding outer surface temperature ranged from 562.55 K to 611.95 K. The initial fill-gas (Helium) pressure was 3.1 MPa, and the coolant system pressure was 15.5 MPa. The fast neutron flux as a function time was calculated from the data provided in the OSIRIS data package [51]. Operational input parameters are summarized in Table W.2.

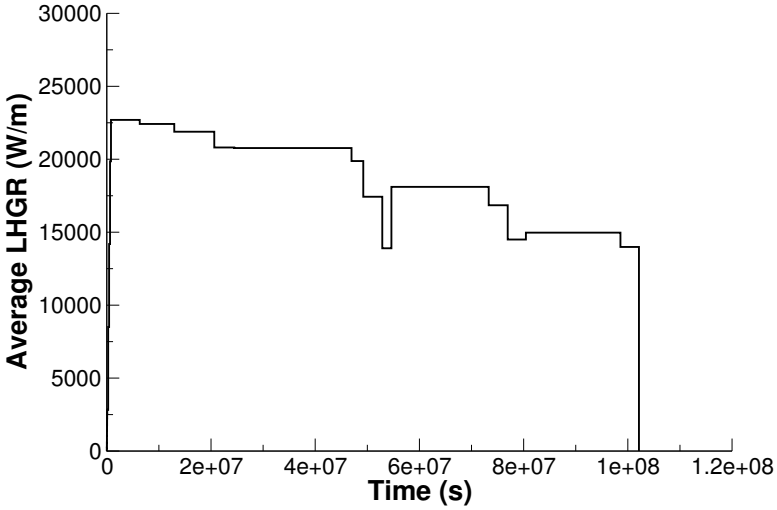

Figure W.1.: OSIRIS H09 power history with 24 hours startup

Table W.2.: Operational input parameters

Base Irradiation		
Coolant inlet temperature	K	562.55
Coolant pressure	MPa	15.5
Fast Neutron Flux		
Cycle 2	n/(m^2·s) per (W/m)	4.2·10^{13}
Cycle 3	n/(m^2·s) per (W/m)	4.6·10^{13}
Cycle 4	n/(m^2·s) per (W/m)	4.8·10^{13}
Cycle 6	n/(m^2·s) per (W/m)	4.8·10^{13}

W.3. Model Description

W.3.1. Geometry and Mesh

The rod specifications in Table W.1 were used to define the geometry for this simulation. The OSIRIS H09 rod was modeled as a two-dimensional, axi-symmetric linear mesh with quadratic elements. The fuel mesh consisted of 11 radial elements and the cladding mesh consisted of four radial elements to form a clad thickness of 0.575 mm. The fuel stack length is 3.66 m and the plenum height is 0.139 m. The mesh of the top portion of the rod is shown in Figure W.2.

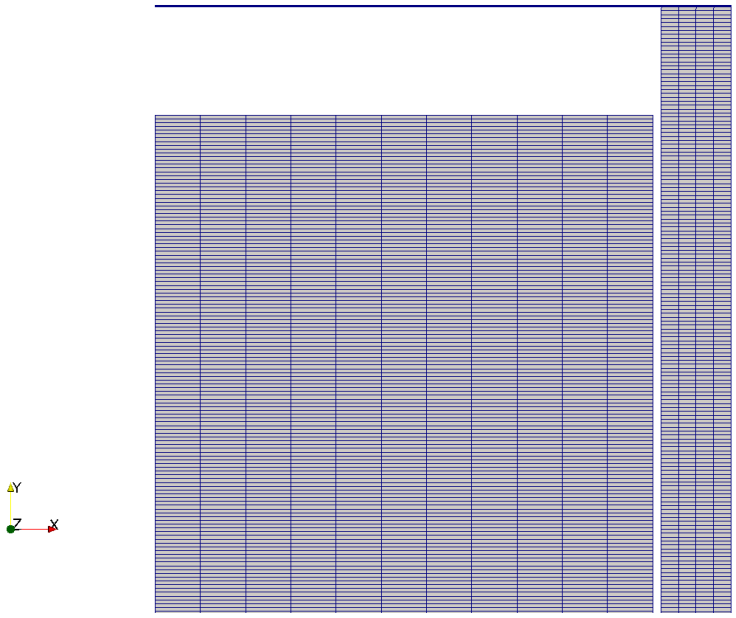

Figure W.2.: OSIRIS H09 mesh (not to scale)

W.3.2. Material and Behavioral Models

The following material and behavioral models were used for the UO_2 fuel:

- ThermalFuel - NFIR: temperature and burnup dependent thermal properties.
- RelocationUO2: relocation strains, relocation activation threshold power set to 5 kW/m.
- Sifgrs: fission gas release model with the combined gaseous swelling model.
- MechZry: model irradiation growth for Zircaloy-4.

For the cladding material, a constant thermal conductivity of 16 W/m-K was used and both thermal and irradiation creep were considered using the Limback model [26].

W.3.3. Input files

The BISON input and all supporting files (power histories, axial power profiles, etc.) OSIRIS H09 rod are provided with the code distribution at folder bison/assessment/OSIRIS_H09/analysis in the code repository.

W.3.4. Execution Summary

Table W.3.: Execution summary.

Machine	Operating System	Code Version
FALCON	LINUX	BISON 1.2

W.4. Results Comparison

Data from the OSIRIS fuel irradiation program was used to assess the code's capability to capture the integral fuel rod fission gas release, rod internal pressure, rod growth, fuel column length changes, axial cladding diameter, cladding hydrogen content and oxide thickness at the end of life. A comparison of the predicted values from BISON calculations versus measured values from experimental data are shown in Table W.4. Because the feature to calculate cladding hydrogen concentration and oxide thickness are not currently available in BISON, these comparisons will be performed in the future. The final burnup calculated was 44.64 MWd/kgU compared to 46.06 MWd/kgU burnup in the test documentation.

Table W.4.: Bison prediction versus measured data for OSIRIS H09.

	BISON prediction	Measured Data
Burnup (MWd/kgU)	44.65	46.06
Fission Gas Release (%)	0.21	0.8
EOL Rod Internal Pressure at RT (MPa)	6.67	4.338
EOL Internal free volume (cc)	9.35	11.1
Fuel column changes (mm)	22.41	26.62
Fuel rod growth (mm)	23.08	28.8

W.4.1. Fission Gas Release

The fission gas release data available for this experiment is from post irradiation examination (PIE) puncture tests. Figure W.3 show BISON's comparisons with the end-of-life measurement for the OSIRIS H09 rod. BISON computes a reasonable FGR value that under predicts the measured result.

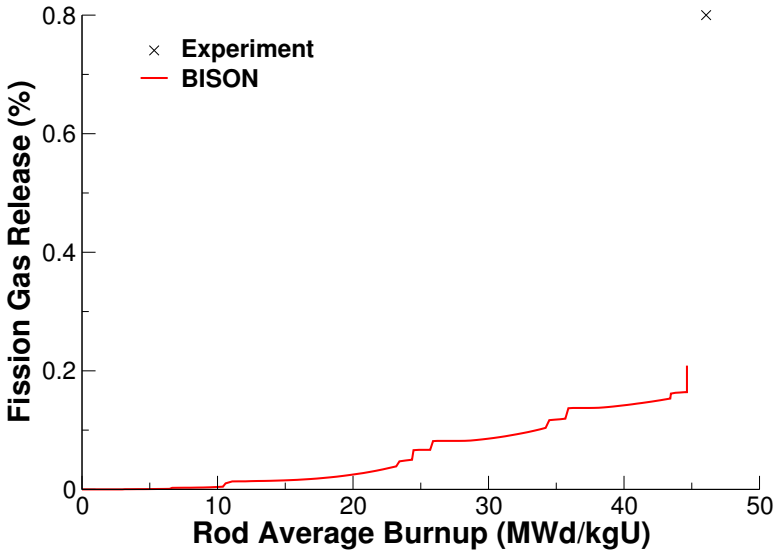

Figure W.3.: Fission gas release comparisons for OSIRIS H09

W.4.2. Rod Internal Pressure

The only rod internal pressure data available for this experiment is from PIE puncture tests at the end-of-life. Figure W.4 shows BISON's comparisons to the experimental data for the OSIRIS H09 rod. The figure shows BISON over predicts the rod internal pressure.

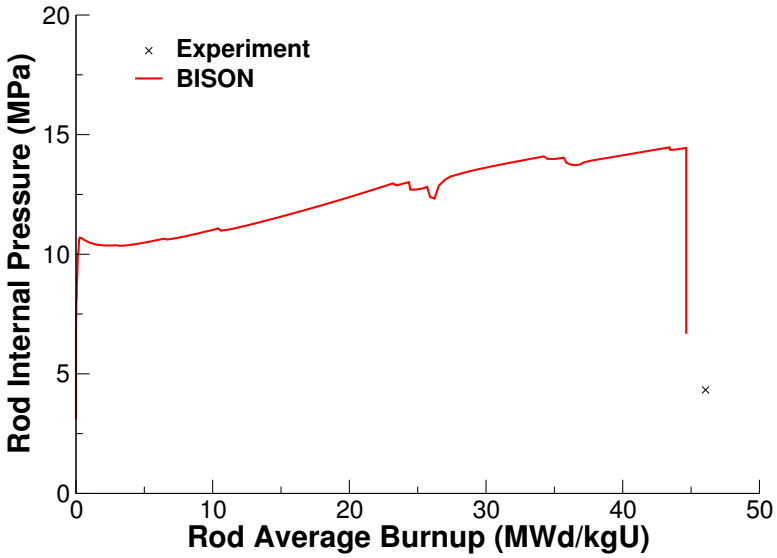

Figure W.4.: Rod internal pressure comparison for OSIRIS H09

W.4.3. Cladding Diameter

The calculated final rod diameter as a function of axial position is compared to measured data. A comparison of the computed and measured end-of-life rod diameter data (excluding oxide thickness) is shown in Figure W.5. The figure shows BISON over predicts the cladding diameter at the end of life which results in less cladding computed creep down than measured.

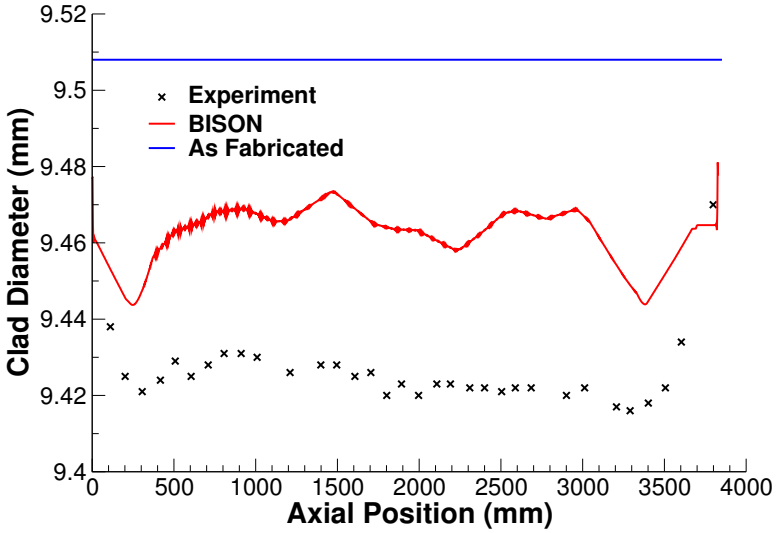

Figure W.5.: EOL average cladding diameter comparisons for OSIRIS H09

W.4.4. Discussion

Based on the data presented above, several observations can be made regarding the results obtained from BISON analyses of the OSIRIS H09 test rod.

- BISON's prediction the EOL FGR is reasonable, but somewhat low.
- BISON over predicts the measured rod internal pressure by a fairly large margin.
- BISON over predicts measured EOL cladding diameter.

- Based on evaluation of these and other assessment cases, this behavior appears to be related to fuel swelling after fuel/cladding contact. Additionally, other effects on fuel deformation including relocation, densification, fuel creep, etc. could influence the behavioral response in these analyses.

Since cladding oxide thickness and hydrogen concentration data are available for OSIRIS H09 rod, these characteristics should be evaluated in the future once these features are available in BISON.

X. REGATE

X.1. Overview

Regate is one of the experiments of the Fuel Modeling at Extended Burnup (FUMEX-II) program [18]. This experiment was carried out in order to provide data on Fission Gas Release (FGR) and clad diameter change. The rod is a short fuel segment irradiated in a commercial PWR and ramped in the french SILOE test reactor. The original segment was base irradiated in the Gravlines 5 PWR up to 47.415 MWd/kgHM.

Non-destructive post-irradiation examination (PIE) was performed on the fuel segment after discharge from the Gravlines 5 PWR with measurements on clad diameter and total fission gas release (based on Kr-85 gamma scan measurements), the total measured FGR after base irradiation was 1.5%. It is important to note that the fuel segment was not subject to any re-fabrication after base irradiation in Gravlines 5 PWR (power history shown in Figure X.1).

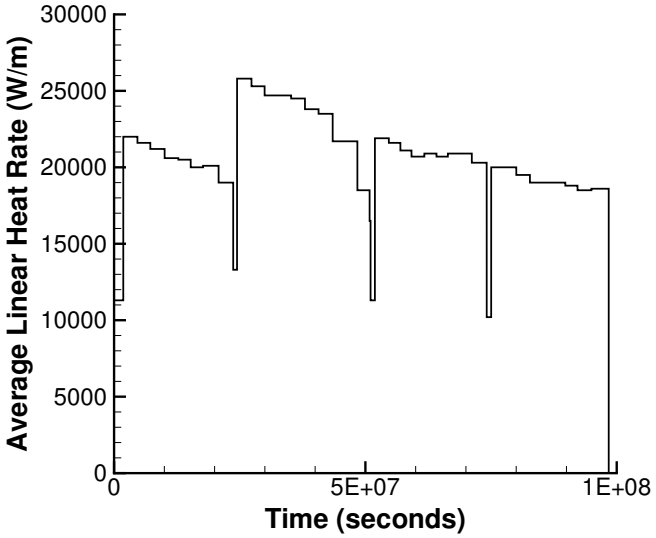

Figure X.1.: Rod average power history in the Gravlines 5 reactor.

The Kr-85 concentration was also measured with gamma scanning to measure a total of 9.3% FGR after the ramp test in the SILOE reactor. Puncturing tests were done after the power ramp in the SILOE reactor, to measure the total FGR of 10.2%. The oxide layer thickness and total clad diameter were also measured in PIE after the ramp test.

BISON comparisons to clad diameter and FGR are reported herein.

X.2. Test Description

X.2.1. Rod Design Specifications

The geometric input parameters for the FumexII–Regate case are summarized in Table X.1.

Table X.1.: Regate geometric input parameters

Fuel Rod		
Overall length	m	0.522
Fuel stack height	m	0.43595
Nominal plenum height	mm	48.15
Number of pellets per rod		32
Fill gas composition		He
Fill gas pressure	MPa	2.5
Fuel		
Material		UO_2
Enrichment	%	4.487
Density	%	94.8
Outer diameter	mm	8.192
Pellet geometry		dished
Grain diameter	μm	8.7
Pellet Dishing		
Dish diameter	mm	6
Dish depth	mm	0.32
Chamfer width	mm	0.531
Chamfer depth	mm	0.16
Cladding		
Material		Zr-2
Outer diameter	mm	9.5
Inner diameter	mm	8.36
Wall thickness	mm	0.57

X.2.2. Operating Conditions and Irradiation History

The irradiation was adjusted by varying the distance of the rig from the SILOE core. The ramp test irradiation history consisted of a pre-condition power step of 19.5 kW/m (peak power) for 48 hours, prior to ramping at 1.0 kW/m/min up to 38.5 kW/m (peak power) which was held for 1.5 hours. The rod average power history during the SILOE irradiation is shown in Figure X.2. As the height of the SILOE reactor ($\sim$0.6 m) is comparable to the segment length ($\sim$0.44 m), the axial power is not flat during the ramp test, leading to values of $P_{average}/P_{max}$ of 0.9 and P_{min}/P_{max} of 0.65.

Table X.2.: Operational input parameters.

Base Irradiation		
Clad temperature	C	317
Coolant pressure	MPa	15.5
Fast neutron flux		Figure X.3
Power Ramps		
Clad temperature	C	77 -338
Coolant pressure	MPa	13
Fast neutron flux	n/(cm^2·s)	2.0·10^{13}

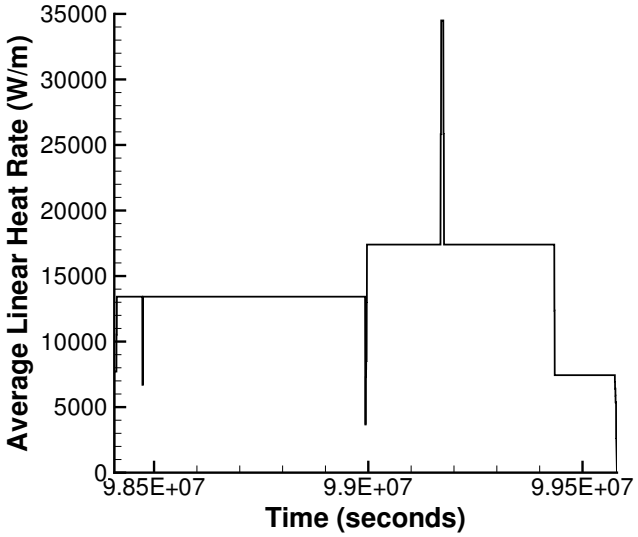

Figure X.2.: Rod average power history in the SILOE reactor.

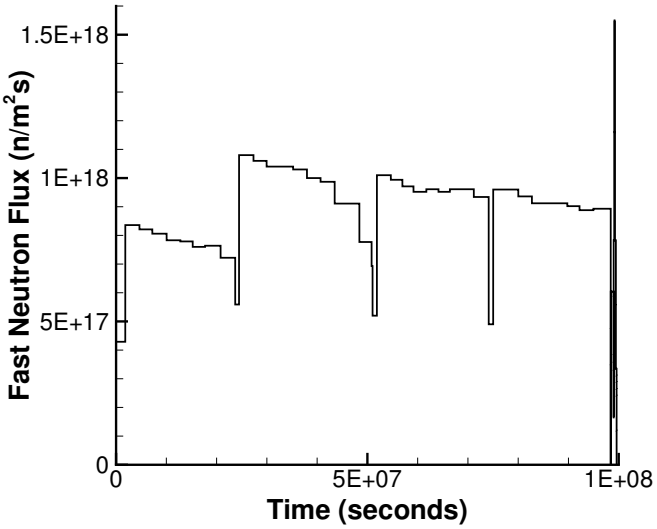

Figure X.3.: Fast neutron flux history. This history was supplied with the experimental data.

X.3. Model Description

X.3.1. Geometry and Mesh

A 2D-RZ axisymmetric discrete pellet mesh with quadratic elements was used to model this experiment. Each pellet was meshed with 16 axial and 9 radial elements. The clad was meshed with 4 axial elements. Figure X.4 shows a section of the meshed with a temperature contour plot during the ramp test.

X.3.2. Material and Behavioral Models

The following material and behavioral models were used for the UO_2 fuel:

- ThermalFuel - NFIR: temperature and burnup dependent thermal properties

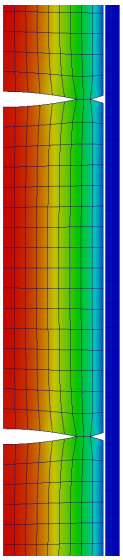

Figure X.4.: Section of mesh used for Regate simulation with temperature contour during the ramp test in the SILOE reactor.

- RelocationUO2: relocation strains, relocation activation threshold power set to 5 kW/m.
- Sifgrs: Simplified fission gas release model with a combined solid/gaseous swelling model based on fission gas release.

For the clad material, a constant thermal conductivity of 16 W/m-K was used and both thermal and irradiation creep were considered using the Limback model [26]. Due to the high mises stress in the clad, plasticity was also used to get the proper deformation during the power ramp in the Risø DR3 reactor.

X.3.3. Input files

The BISON input and all supporting files (power histories, axial power profile, fast neutron flux history, etc.) for this case are provided with the code distribution at bison/assessment/FUMEXII_Regate/analysis.

X.3.4. Execution Summary

Table X.3.: Execution summary.

Machine	Operating System	Code Version
FALCON	LINUX	BISON 1.2

X.4. Results Comparison

X.4.1. Fission Gas Release

BISON over predicts FGR after the base irradiation in the Gravlines 5 PWR and under predicts the FGR at the end of the ramp test. The comparisons are plotted in Figure X.5.

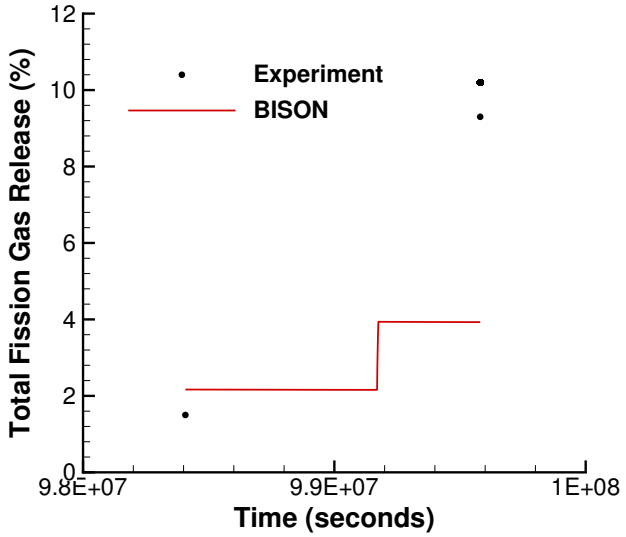

Figure X.5.: BISON FGR comparisons to experimental data.

X.4.2. Clad Diameter

BISON over predicts clad creep down which results in a smaller diameter than measured during PIE. The BISON comparisons to experimental measurements before and after the ramp are shown in Figure X.6.

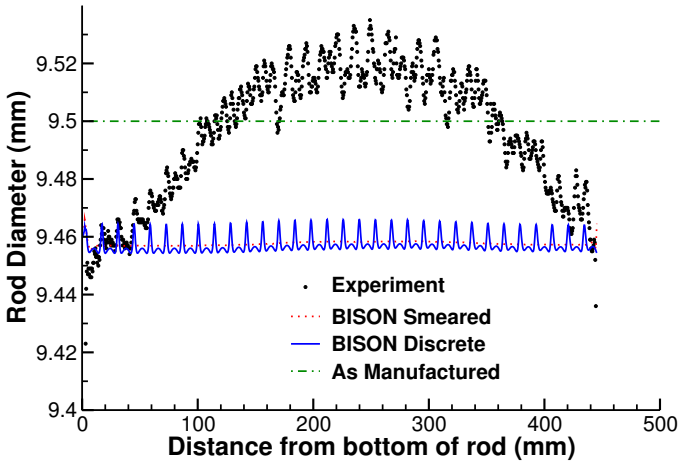

Figure X.6.: BISON rod diameter comparisons to experimental measurements before and after the power ramp.

Y. TRIBULATION Rod BN1/3, rod BN1/4, and Rod BN3/15

Y.1. Overview

The objectives of the TRIBULATION (Tests Relative to High BUrnup Limitations Arising Normally in LWR's) International Programme were to 1) assess fuel rod behaviour at high burnup with an earlier transient and 2) to investigate the behaviour of different fuel rod designs and manufacturers when subjected to a steady state irradiation history to high burn-up. The program was organized jointly by BelgoNucleaire and the Nuclear Energy Centre at Mol (CEN/SCK) with the co-sponsorship of 14 participating organizations [52]. For the purpose of this fuel analysis problem, three out of the 19 fuel rods from the TRIBULATION Database [53] were evaluated with BISON. The three fuel rods were fabricated by BelgoNucleaire (BN) and are referred to as test rods BN1/3, BN1/4 and BN3/15 in this document. All three rods used standard Zircaloy-4 cladding and were discharged at rod average burnups of approximately 51.6, 51.2, and 51.1 MWd/kgU, respectively. Non-destructive post irradiation examination (PIE) was performed at various stages throughout testing of the BN rods for cladding creep down, cladding ovalization, rod growth and fuel column length changes. Destructive PIE was performed at the end-of-life for fission gas release and internal void volume. This experiment was chosen for analysis because of the availability of measured data for evaluation of several fuel rod performance characteristics including fission gas release, cladding creep down, fuel column length changes, rod growth and end-of-life internal free volume.

Y.2. Test Description

Y.2.1. Rod Design Specifications

An overview of the test matrix and cross reference identification data for BN1/3, BN1/4 and BN3/15 are shown below in Table Y.1 [53]. The specific geometric input parameters for the test rods are summarized in Table Y.2. BN1/3 contained fuel pellets from two different batches with slightly different pellet mean densities. This simulation assumed the same pellet density of 10.408 g/cm^3 for test BN1/3 because the two densities were close to each other. The fuel pellets for BN1/3 and BN1/4 have an initial enrichment of 8.25% while BN3/15 had an initial enrichment of 5.76%. The cladding material for all three rods was Zircaloy-4. The cladding was stress relieved at 460 C for 2.5 hours. BN1/3 and BN1/4 were pressurized with helium to 1.96 MPa (20 kg/cm^2) while BN3/15 was pressurized to 0.098 MPa (1 kg/cm^2).

Table Y.1.: Overview of test matrix for test rods BN1/3, BN1/4 and BN3/15

Matrix No.	Test No.	Rod No.	BR3 cycle Nos.	BR2 transient Power (kW/m)	BR3 cycle Nos.	History
3	BN1/3	3-47	4B	34.7(for 540 sec)	4C, 4D1	NDT, T, NDT, BR3(4C+4D), NDT, DT
4	BN1/4	3-342	4B		4C, 4D1	NDT, BR3(4C+4D), NDT, DT
15	BN3/15	1-610	4A, 4B		4D2	NDT, BR3(4D), NDT, DT

NDT = non destructive tests
DT = destructive tests
T = transient irradiation in BR2

Table Y.2.: BN1/3, BN1/4 and BN3/15 Rod Specifications.

Fuel Rod	Unit	BN1X3	BN1X4	BN3X15
Overall length	m	1.1352	1.1360	1.1358
Fuel stack height	m	1.0019	0.9976	0.9956
Upper plenum height	mm	88.3	93.4	95.2
Fill gas composition		He	He	He
Fill gas pressure	MPa	1.96133	1.96133	0.09807
Fuel	Unit	BN1/3	BN1/4	BN3/15
Material		UO_2	UO_2	UO_2
Enrichment	%	8.25	8.25	5.76
Pellet mean density	g/cm3	10.408-10.340	10.355	10.435
Pellet mean density	$\%TD$	94.965-94.345	94.474	95.037
Outer diameter	mm	8.04	8.04	8.04
Nominal diametral gap	μm	200	200	200
Average grain size	μm	11	11	10
Cladding	Unit	BN1/3	BN1/4	BN3/15
Material		Zr-4	Zr-4	Zr-4
Outer diameter	mm	9.50 +/- 0.04	9.50 +/- 0.04	9.50 +/- 0.04
Inner diameter	mm	8.24 +/- 0.04	8.24 +/- 0.04	8.24 +/- 0.04
Wall thickness	mm	not $<$0.58	not $<$0.58	not $<$0.58

Y.2.2. Operating Conditions and Irradiation History

The irradiation of the BelgoNucleaire (BN) fuel rods chosen for the TRIBULATION programme was carried out in the BR2 and BR3 reactors of the Nuclear Energy Centre at Mol at Mol-Belgium (CEN/SCK). The base irradiation for BN1/3, BN1/4 and BN3/15 was performed in the BR3 reactor up to a specified preconditioning burnup between 20 and 40 GWd/tM peak pellet. Following the base irradiation, the rods were non-destructively examined. BN1/3 was transferred to the BR2 reactor for fast operational transient testing and then continued further irradiation in BR3. The fast operational transient for test BN1/3 consisted of a preconditioning period of at approximately 2 days 26600 W/m, followed by a rapid power increase to 35400 W/m at a ramp rate of approximately 1960 W/m/s. After a hold period of about 9 minutes, the power was then rapidly decreased to near the preconditioning level. Following the base irradiation and non-destructive exmaination, BN1/4 and BN3/15 were transferred back to the BR3 reactor for further irradiation.

The power mode selected for this simulation is PiecewiseConstant. The power histories for BN1/3, BN1/4, and BN3/15 are shown in Figures Y.1, Y.2 and Y.3, respectively. These three power histories assumed a 24 hour startup time that was broken into 24 timesteps of one hour increments. Because the axial power shapes and boundary conditions are modeled as PieceswiseBilinear, a ramp time of 360 seconds (0.1 hours) was assumed at each power step for the axial power shape and boundary condition input. The startup time of 24 hours and the ramp time of 360 seconds (0.1 hours) are based on ANATECH's experience with fuel rod modeling for steady state operation and the development of Falcon Verification and Validation cases. They are intended to minimize the introduction of computational artifacts from unrealistic power changes and ramp rates into the analyses. The axial power profile and cladding outer surface temperature profile as a function of time were calculated from the TRIBULATION data package [53]. The initial fill-gas (Helium) pressure was 1.96 MPa for BN1/3 and BN1/4 and 0.098 MPa for BN3/15. The coolant system pressure was 13.729 MPa for the BR3 irradiation and 14.0 MPa for the BR2 irradiation. The fast neutron flux profile was scaled to a factor of 4.8e17. Operational input parameters are summarized in Table Y.3.

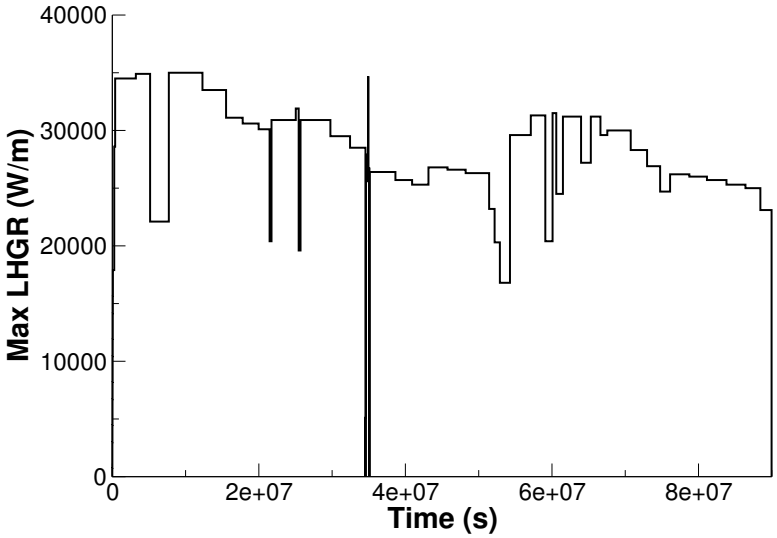

Figure Y.1.: BN1/3 power history

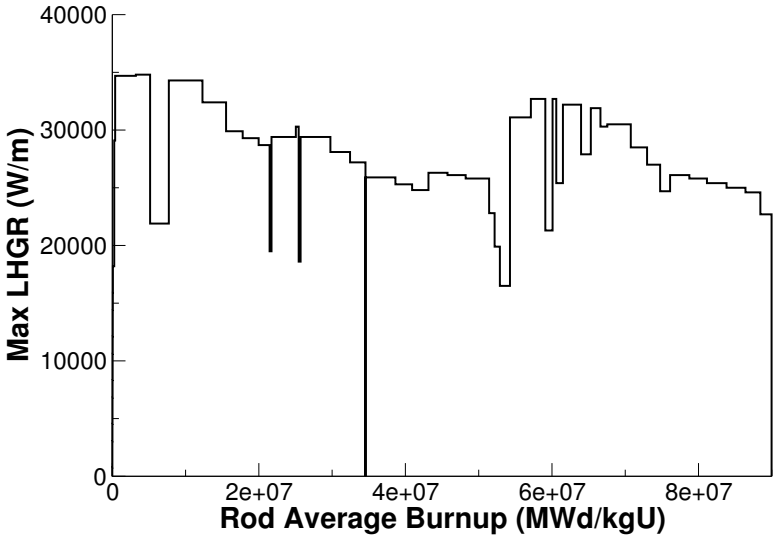

Figure Y.2.: BN1/4 power history

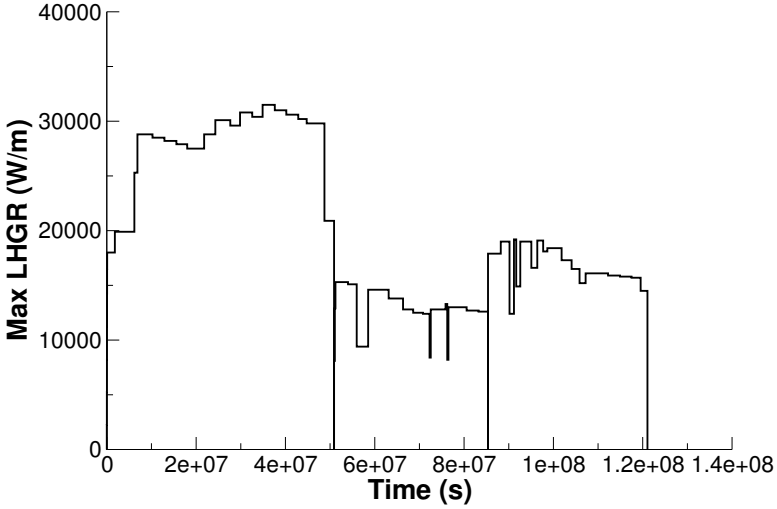

Figure Y.3.: BN3/15 power history

Table Y.3.: Operational input parameters

Base Irradiation		
Coolant inlet temperature	K	529.15
Coolant pressure for BR3 Irradiation	MPa	13.729
Coolant pressure for BR2 Irradiation	MPa	14.0

Y.3. Model Description

Y.3.1. Geometry and Mesh

The rod specifications in Table Y.2 were used to define the geometry for these simulations. The BN1/3, BN1/4 and BN3/15 rods were modeled as a two-dimensional, axi-symmetric linear mesh with quadratic elements. The fuel mesh for all three rods consisted of 11 radial elements and the cladding mesh consisted of four radial elements to form a cladding thickness of 0.63 mm. In order to accurately model the

fuel rod initial free volume, the overall fuel rod length and upper plenum height were adjusted during mesh generation to account for the volume of the plenum spring which is not explicitly modeled. The overall fuel rod lengths for BN1/3, BN1/4, and BN3/15 were reduced from 1135.2 mm, 1136.0 mm, and 1135.8 mm to 1081.01 mm, 1081.46 mm and 1081.34 mm, respectively. The plenum heights for BN1/3, BN1/4, and BN3/15 were reduced from 88.3 mm, 93.4 mm, and 95.2 mm to 67.5 mm, 71.3 mm, and 73.1 mm, respectively. The TRIBULATION BN1/3, BN1/4 and BN3/15 meshes are shown in Figures Y.4, Y.5 and Y.6 respectively.

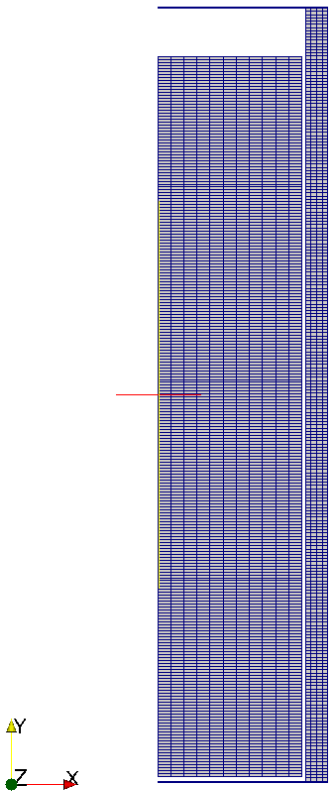

Figure Y.4.: BN1/3 mesh

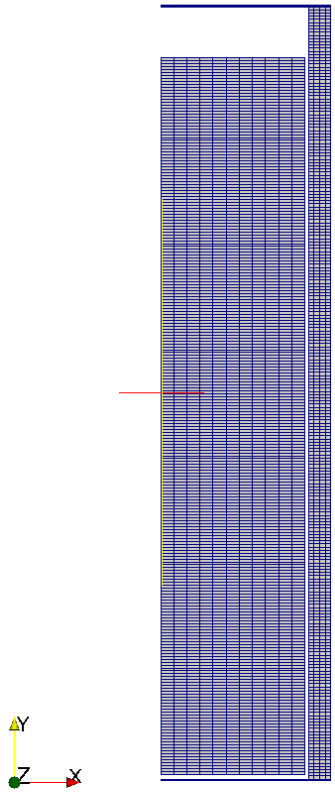

Figure Y.5.: BN1/4 mesh

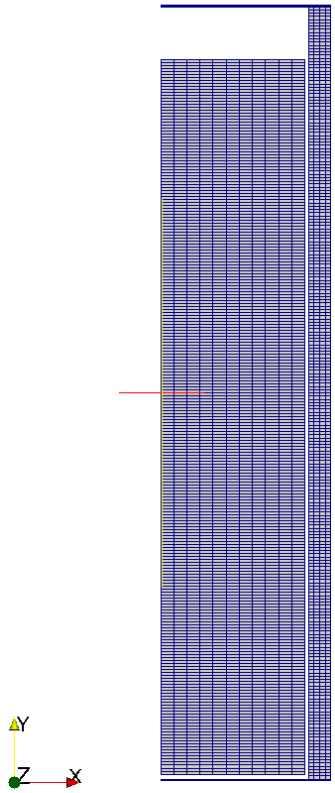

Figure Y.6.: BN3/15 mesh

Y.3.2. Material and Behavioral Models

The following material and behavioral models were used for the UO_2 fuel:

- ThermalFuel - NFIR: temperature and burnup dependent thermal properties.
- RelocationUO2: relocation strains, relocation activation threshold power set to 5 kW/m.
- Sifgrs: fission gas release model with the combined gaseous swelling model.
- MechZry: model irradiation growth for Zircaloy-4.

For the cladding material, a constant thermal conductivity of 16 W/m-K was used and both thermal and irradiation creep were considered using the Limback model [26].

Y.3.3. Input files

The BISON input and all supporting files (power histories, axial power profiles, etc.) for BN1/3, BN1/4 and BN3/15 are provided with the code distribution at bison/assessment/Tribulation/analysis/BN1X3, bison/assessment/Tribulation/ analysis/BN1X4, and bison/assessment/Tribulation/analysis/BN3X15, respectively.

Y.3.4. Execution Summary

Table Y.4.: Execution summary.

Machine	Operating System	Code Version
FALCON	LINUX	1.2

Y.4. Results Comparison

Data from the TRIBULATION irradiation program was used to assess the code's capability to capture the integral fuel rod fission gas release, cladding creep down strain, fuel column changes, fuel rod growth, and rod internal void volume. A comparison of the predicted values from BISON calculations versus measured values from experimental data are shown in Tables Y.5, Y.6, and Y.7 for BN1/3, BN1/4, and BN3/15 rods, respectively.

Table Y.5.: Bison prediction versus measured data for BN1/3.

	BISON prediction	Measured Data
Burnup (MWd/kgU)	50.65	51.6
Fission Gas Release (%)	7.083	5.4
Fuel column changes (mm)	9.048	4.5 (Length Increase)
Final void volume (cc)	4.36	6.46
Fuel rod growth (mm)	2.877	6.03

Table Y.6.: Bison prediction versus measured data for BN1/4.

	BISON prediction	Measured Data
Burnup (MWd/kgU)	50.59	51.2
Fission Gas Release %	8.335	5.5
Fuel column changes (mm)	8.915	3.9 (Length Increase)
Final void volume (cc)	4.56	6.12
Fuel rod growth (mm)	2.997	4.86

Table Y.7.: Bison prediction versus measured data for BN3/15.

	BISON prediction	Measured Data
Burnup (MWd/kgU)	50.66	51.1
Fission Gas Release %	16.47	5.6
Fuel column changes (mm)	10.295	7.4 (Length Increase)
Final void volume (cc)	4.43	6.02
Fuel rod growth (mm)	2.858	1.62

Y.4.1. Fission Gas Release

The only fission gas release data available for this experiment is from destructive PIE puncture tests. Figures Y.7, Y.8, and Y.9 show BISON's comparisons with end-of-life measurement for the BN1/3, BN1/4, and BN3/15, respectively. BISON computes a reasonable FGR value that over predicts the measured results for BN1/3 and BN1/4 by a small margin. However, BISON over predicts the measured result for BN3/15 by a fairly large margin.

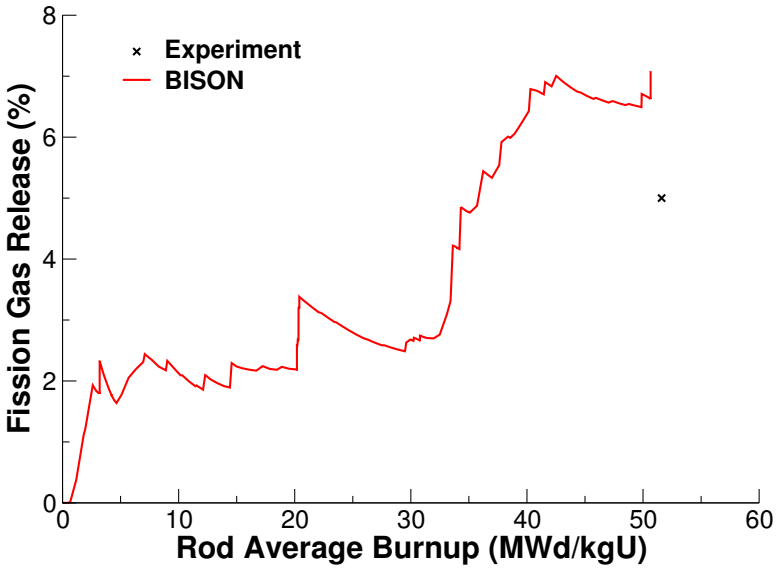

Figure Y.7.: Fission gas release comparisons for BN1/3

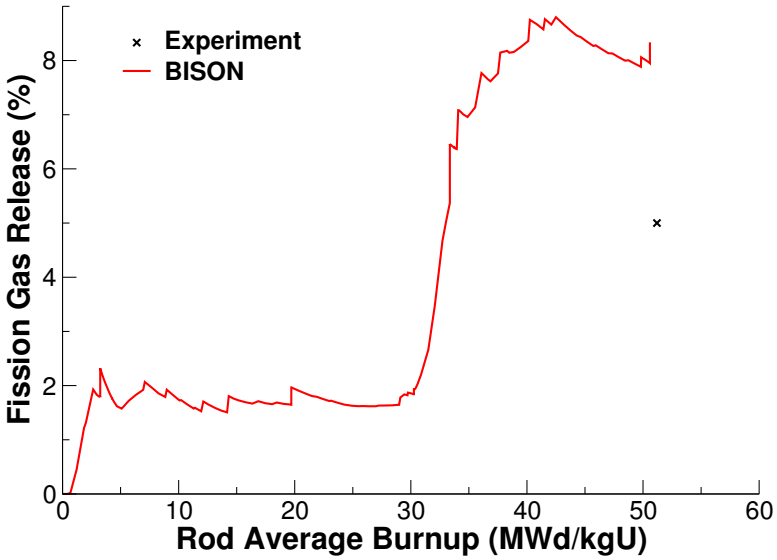

Figure Y.8.: Fission gas release comparisons for BN1/4

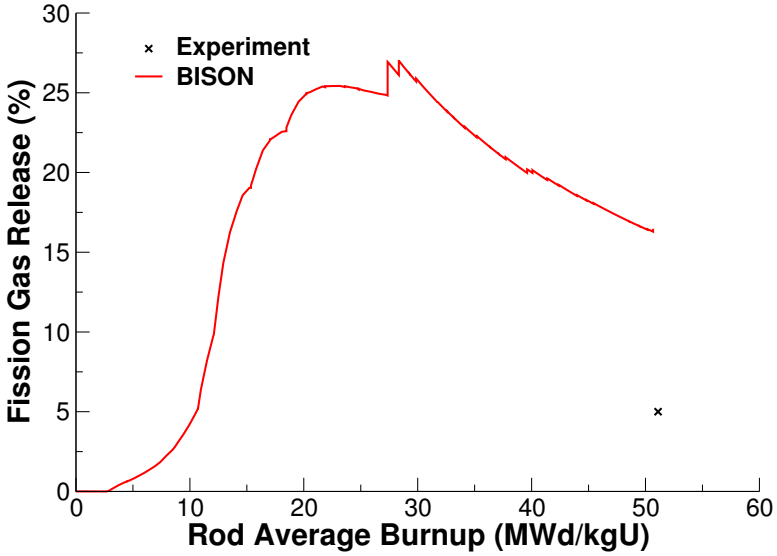

Figure Y.9.: Fission gas release comparisons for BN3/15

Y.4.2. Cladding Creep Down Strain

The calculated cladding creep down strain as a function of axial position is compared to measured data. The cladding creep down strain is calculated from the computed cladding diamter. Figure Y.10 shows comparisons of BISON computed results for BN1/3 to the measured cladding creep down strain data at the end of the first BR3 irradiation, after the BR2 transient, and at the end of the second BR3 irradiation. Reasonable cladding creep down strain values are computed at the end of the first BR3 irradiation and after the BR2 transient, but not at the end of the second BR3 irradiation. BISON strongly over predicts the cladding creep down strain toward the center of the fuel stack at the end of the second BR3 irradiation. Figure Y.11 shows comparisons of BISON computed results to measured cladding creep down strain data at the end of the first and second BR3 irradiation for BN1/4. Similar to the BN1/3 results, reasonable cladding creep down values at the end of the first BR3 irradiation are computed for BN1/4, but not at the end of the second BR3 irradiation. Figure Y.12 shows comparisons of BISON computed results to measured cladding creep down strain data at the end of the second BR3 irradiation for BN3/15. For BN3/15, BISON strongly over predicts the cladding creep down strain toward the center of the fuel stack at the end of the second BR3 irradiation.

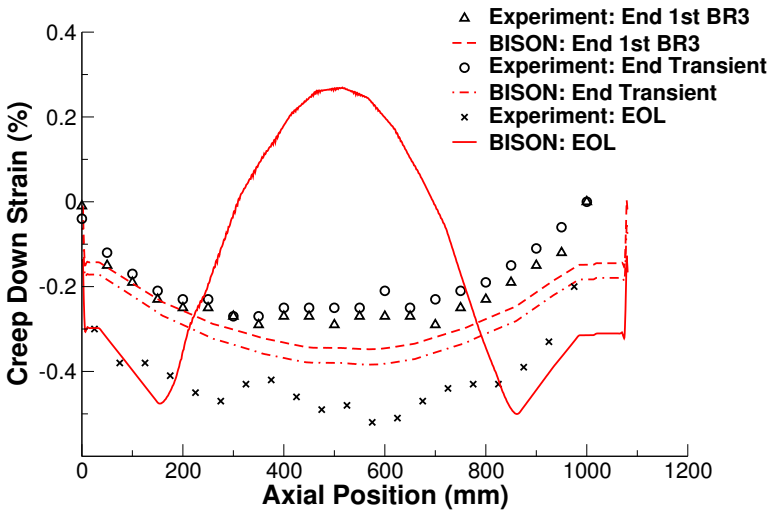

Figure Y.10.: Cladding creep down strain comparisons for BN1/3

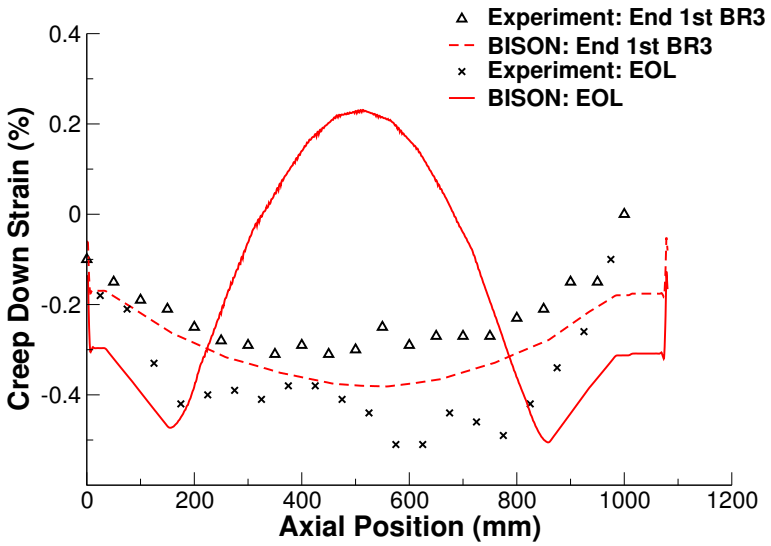

Figure Y.11.: Cladding creep down strain comparisons for BN1/4

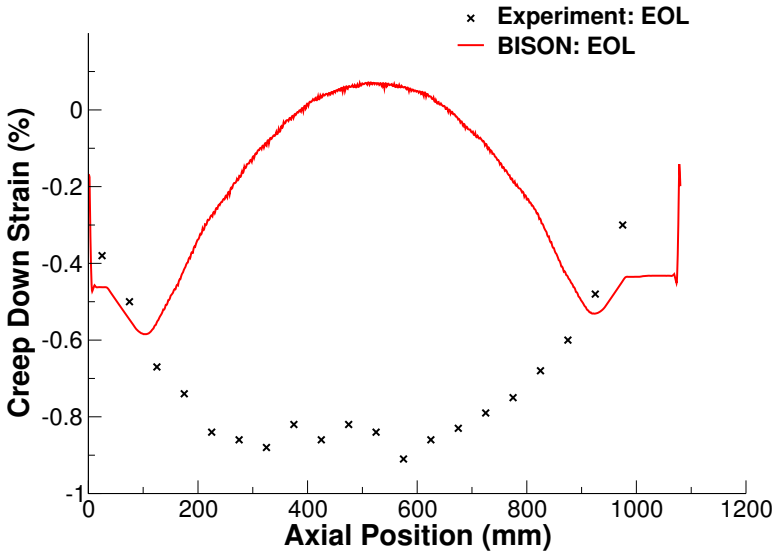

Figure Y.12.: Cladding creep down strain comparisons for BN3/15

Y.4.3. Discussion

Based on the data presented above, several observations can be made regarding the code execution and the results obtained from BISON analyses of the BN1/3, BN1/4, and BN3/15 test fuel rods.

- Due to the low initial fill gas pressure for the BN3/15 rod, BISON experienced difficulty converging. The convergence issue appears to be related to fission gas release, rod internal pressure prediction and fuel/cladding contact behavior. Therefore, the PETSc option and time stepping controls were updated in the Executioner block to obtain convergence. The PETSc options selected for -pc_type and -pc_factor_mat_solver_package input is 'lu' and 'superlu_dist'. The timestep_limiting_function, max_function_change, and force_step_every_function_point options were not used. These updates resolve the convergence issues for the simulation of BN3/15 rod. However, this issue warrants further review for the analysis of rods with low initial fill gas pressure.

- BISON over predicts the EOL FGR by a large margin for BN3/15 rod.
  - From Figures Y.7, Y.8 and Y.9, sharp increases in FGR can be seen that correspond to large power drops. This rapid release of fission gas during power drop appears to be characteristic of the SIFGRs model implemented in BISON. This response may not be representative of FGR kinetics and warrants further review.
- BISON over predicts the EOL cladding creep down strain for all three rods by a very large margin.
  - Based on evaluation of these and other assessment cases, this behavior appears to be related to fuel swelling, especially affecting cladding creep down after fuel/cladding contact. Additionally, other effects on fuel deformation including relocation, densification, fuel creep, etc. The combined effect of these mechanisms could also influence the behavioral response seen in these analyses.

Z. Calvert Cliffs-1 Prototype

Z.1. Overview

To demonstrate safe and reliable methods to implement improved uranium utilization in light water reactors, the high burnup demonstration program called PROTOTYPE was jointly initiated by Baltimore Gas and Electric Co. and Combustion Engineering, Inc. [54] in 1978. The objectives of this program were to 1) extend the operating cycle length of Calvert Cliffs Units-1 and -2 from 12 to 18 months and 2) to demonstrate acceptable performance of fuel rods to peak-rod, discharge burnups of approximately 50 GWd/MTU [54]. The PROTOTYPE program included the irradiation of four Batch G assemblies and a Batch H assembly. The PROTOTYPE fuel rods in Batch G assemblies which have variations in the fuel pellet geometry underwent 4 cycles of irradiation that was extended to include a 5th cycle of irradiation while fuel rods in Batch H assembly which has higher initial enrichment than Batch G rods underwent 4 cycles of irradiation in Calvert Cliffs-1. Batch G assemblies average and peak rod burnup after five cycles is 54.4 and 63.5 GWd/MTU, respectively. Batch H assembly average and peak rod burnup after four cycles of irradiation is 50.6 and 56.0 GWd/MTU, respectively. For the purpose of this fuel analysis problem, 11 fuel rods from Batch G assemblies and two fuel rods from Batch H assembly were evaluated with BISON. All 13 fuel rods were fabricated by Combustion Engineering (CE) and are referred to as test rods BFM034, BFG092, BFL009, BFM156, BFM043, BEN013, BFL031, BFM073, BFM070, BFJ027, and BFM071 from Batch G, and UFE067 and UFE019 from Batch H in this document. These fuel rods used standard Zircaloy-4 cladding but have variations in the pellet design characteristics. Poolside examinations were performed visually after each cycle of irradiation. Destructive examination was performed in hot cell at AECL's Chalk River Laboratories for seven fuel rods from Batch G Assembly C1G003, four fuel rods from Batch G Assembly C1G006, and two fuel rods from Batch H Assembly C1H038. Destructive Post Irradiation Examination (PIE) was performed at the end-of-life (EOL) for evaluation of fission gas release, internal void volume, and oxide thickness. This experiment was chosen for analysis because they represent full size, commercial fuel rods designs, and a large inventory of measured data. The measured data from the hot cell examination are provided in the TR-103302-V2 [55] and NPSD-493-NP [56] reports to EPRI.

Z.2. Test Description

Z.2.1. Fuel Rod Design Specifications

An overview of the 13 Calvert Cliffs-1 fuel rods that were destructively examined in hot cell and chosen for BISON simulation are shown below in Table Z.1 [54]. These commercial fuel rods have variations in the pellet design characteristics which include standard length, reduced length and annular pellet. The two test rods with annular pellets are BFL031 and BFL009. The five test rods with reduced length pellets are BFM034, BFM043, BFM073, BFM070 and BFM071. The rest of the test rods have standard pellet length. Zircaloy-4 cladding material was used for all the test rods and was supplied by Sandvik Special Metals. The fuel rod characterization parameters are summarized in Tables Z.2 and Z.3 [54]. All 13 test rods have cladding outer diameter of 11.176 mm, cladding inner diameter of 9.7536 mm, and pellet outer diameter of 9.5631 mm. The nominal fuel stack height is 3.472 m. The pellet mean density varies based on the fuel design characteristics. This simulation assumed the pellet theoretical density of 10972.65 kg/m^3. Since the average grain sizes were not characterized for rods UFE067 and UFE019, they were assumed to be 8.4 microns in this simulation based on grain sizes noted for the other standard

fuel pellets in the experiment. Batch G test rods have initial enrichment of 3.67% except for rod BFJ027 which has an initial enrichment of 3.66%. Batch H test rods have initial enrichment of 3.98%.

Table Z.1.: Overview of Calvert Cliffs-1 Fuel Rods Destructively Examined in Hot Cell

Assembly Serial No. and Fuel Batch	Rod Serial Number	Rod Type (pellet)	Rod Average Burnup (GWd/MTU)	Cladding Material	Number of Cycles
C1G003(Batch G)	BFM034	Reduced Length	63.451	Zircaloy-4	5
C1G003(Batch G)	BFG092	Standard	57.945	Zircaloy-4	5
C1G003(Batch G)	BFL009	Annular	58.106	Zircaloy-4	5
C1G003(Batch G)	BFM156	Standard	56.854	Zircaloy-4	5
C1G003(Batch G)	BFM043	Reduced Length	60.506	Zircaloy-4	5
C1G003(Batch G)	BEN013	Standard	59.835	Zircaloy-4	5
C1G003(Batch G)	BFL031	Annular	58.268	Zircaloy-4	5
C1G006(Batch G)	BFM073	Reduced Length	60.319	Zircaloy-4	5
C1G006(Batch G)	BFM070	Reduced Length	60.761	Zircaloy-4	5
C1G006(Batch G)	BFJ027	Standard	58.726	Zircaloy-4	5
C1G006(Batch G)	BFM071	Reduced Length	57.143	Zircaloy-4	5
C1H038(Batch H)	UFE067	Standard	54.841	Zircaloy-4	4
C1H038(Batch H)	UFE019	Standard	46.791	Zircaloy-4	4

Table Z.2.: Fuel Rod Characterization Data

Rod Serial Number	Rod Length (m)	Enrich. wt % U235	Pellet Length (mm)	Open Porosity (%)	Avg. Initial Density %TD	Avg. Grain Size (micron)
BFM034	3.733	3.67	7.62	0.482	94.662	7.7
BFG092	3.733	3.67	11.43	0.142	94.882	8.4
BFL009	3.733	3.67	11.43	0.398	95.332	7.7
BFM156	3.733	3.67	11.43	0.142	94.882	8.4
BFM043	3.733	3.67	7.62	0.482	94.662	7.7
BEN013	3.733	3.67	11.43	0.142	94.882	8.4
BFL031	3.733	3.67	11.43	0.398	95.332	7.7
BFM073	3.733	3.67	7.62	0.482	94.662	7.7
BFM070	3.733	3.67	7.62	0.482	94.662	7.7
BFJ027	3.733	3.66	11.43	0.142	94.882	8.4
BFM071	3.733	3.67	7.62	0.482	94.662	7.7
UFE067	3.728	3.98	11.43	not meas.	94.750	not meas.
UFE019	3.728	3.98	11.43	not meas.	94.750	not meas.

Table Z.3.: Additional Fuel Rod Characterization Data

Rod Serial Number	Nominal Fuel Stack Height (m)	Cladding OD (mm)	Cladding ID (mm)	Clad Thickness (mm)	Pellet OD (mm)	Pellet ID (mm)
BFM034	3.472	11.176	9.7536	0.7112	9.5631	0
BFG092	3.472	11.176	9.7536	0.7112	9.5631	0
BFL009	3.472	11.176	9.7536	0.7112	9.5631	2.7178
BFM156	3.472	11.176	9.7536	0.7112	9.5631	0
BFM043	3.472	11.176	9.7536	0.7112	9.5631	0
BEN013	3.472	11.176	9.7536	0.7112	9.5631	0
BFL031	3.472	11.176	9.7536	0.7112	9.5631	2.7178
BFM073	3.472	11.176	9.7536	0.7112	9.5631	0
BFM070	3.472	11.176	9.7536	0.7112	9.5631	0
BFJ027	3.472	11.176	9.7536	0.7112	9.5631	0
BFM071	3.472	11.176	9.7536	0.7112	9.5631	0
UFE067	3.472	11.176	9.7536	0.7112	9.5631	0
UFE019	3.472	11.176	9.7536	0.7112	9.5631	0

Z.2.2. Operating Conditions and Irradiation History

The irradiation of the fuel rods in Batch G assemblies chosen for the PROTOTYPE Program and fuel rods in the Batch H assembly was carried out in the Calvert Cliffs Unit 1 reactor. The test rods in the Batch G assemblies were irradiated for five cycles (Cycle 5 to 9) and were discharged with an assembly average burnup of 57.4 GWd/MTU while the test rods in the Batch H assembly were irradiated for four cycles (Cycle 6 to 9) and were discharged with an assembly average burnup of 50.6 GWd/MTU [54]. Following each irradiation cycle, the fuel assemblies underwent poolside examinations to monitor the overall assembly condition and test rod performance. For selected rods from Batch G and Batch H assemblies, the poolside examinations after the last cycle included detailed visual examinations, eddy current testing, rod length measurements, oxide film thickness measurements, and profilometry. The selected fuel rods were then shipped to AECL's Chalk River Laboratories for destructive examination.
The power mode selected in the BISON input deck for these simulations was PiecewiseConstant. The power histories for seven selected test rods in Batch G Assembly C1G003 and four selected test rods in Batch G Assembly C1G006 are shown in Figures Z.1 and Z.2, respectively. The power histories for two selected test rods in Batch H Assembly C1H038 are shown in Figure Z.3. These power histories assumed a 24 hour startup time that was broken into 24 timesteps of one hour increments. Because only cycle burnup data for each power step and rod average burnup data at the end of each cycle were available, the equations below were used to convert the power history data from a function of burnup to a function of time. These equations were derived by ANATECH to calculate time-based power histories from burnup-based power history data.

The linear mass density of Uranium is calculated as follows

$$wt = \frac{\pi}{4} \cdot f_{uo2} \cdot f_d \cdot t_d \cdot d_p^2 \tag{Z.1}$$

The time difference between each burnup increment is calculated by

$$\Delta t_i = ucf \left[\frac{\Delta bu \cdot wt}{LP} \right] \tag{Z.2}$$

where,

t_d is the fuel theoretical density (10972.65 kg/m^3),
f_{uo2} is the fractional uranium mass (0.881),
ucf is the units conversion factor (24000 kW-hr/MWd),
f_d is the fuel fractional density (unitless),
d_p is the pellet diameter (m),
Δbu is the difference in burnup increment (MWd/kgU), and
LP is the linear power (kW/m)

Because the rod average burnup data at the end of each cycle of irradiation is available in addition to the cycle burnup data, the difference in burnup increment, Δbu, is calculated as follows

$$\Delta bu = \frac{(bu_i - bu_{i-1})}{\Delta bu_{eoc}} \cdot \Delta bu_{rodavg} \tag{Z.3}$$

where,

bu_i - bu_{i-1} is the difference in cycle burnup increment (MWd/kgU),
Δbu_{eoc} is the difference in cycle burnup at the end of the cycle

and beginning of the cycle (MWd/kgU), and
Δbu_{rodavg} is the difference in rod average burnup at the
end-of-cycle and beginning of cycle (MWd/kgU)

Because the power histories are input as functions of cumulative time, the time during burnup increments must be summed to obtain cumulative time.

$$t_{ci} = t_{ci-1} + \Delta t_i \tag{Z.4}$$

Table Z.4 below provides the input and calculated linear mass density, wt, values for the 13 selected test rods. Because rods BFL009 and BFL031 have annular pellets, the pellet diameter was recalculated to be 0.0091688 m based on the area of the solid pellet. The annular pellet diameter was recalculated because the input pellet diameter, d_p, requires a solid pellet diameter in order to correctly calculate the linear mass density.

Table Z.4.: Fuel Rod Parameters and Calculated Linear Mass Density

Rod Serial Number	Fractional Uranium Mass f_{uo2}	Fractional Density f_d	Pellet Diameter d_p (m)	Calculated wt
BFM034	0.881	0.94662	0.0095631	0.6573
BFG092	0.881	0.94882	0.0095631	0.6588
BFL009	0.881	0.95332	0.0091688	0.6085
BFM156	0.881	0.94882	0.0095631	0.6588
BFM043	0.881	0.94662	0.0095631	0.6573
BEN013	0.881	0.94882	0.0095631	0.6588
BFL031	0.881	0.95332	0.0091688	0.6085
BFM073	0.881	0.94662	0.0095631	0.6573
BFM070	0.881	0.94662	0.0095631	0.6573
BFJ027	0.881	0.94882	0.0095631	0.6588
BFM071	0.881	0.94662	0.0095631	0.6573
UFE067	0.881	0.94750	0.0095631	0.6579
UFE019	0.881	0.94750	0.0095631	0.6579

Because the axial power shapes and boundary conditions are modeled as PieceswiseBilinear, a ramp time of 360 seconds (0.1 hours) was assumed at each power step for the axial power shape and boundary condition input. The startup time of 24 hours, the equations for unit conversion of burnup to time, and the ramp time of 360 seconds (0.1 hours) are based on ANATECH's experience with fuel rod modelling for steady state operation and the development of Falcon Verification and Validation cases. They are intended to minimize the introduction of computational artifacts from unrealistic power changes and ramp rates into the analyses. The normalized axial power profile as a function of time was calculated from the data package. The coolant system pressure was 15.51 MPa and the initial fill-gas (Helium) pressure was 2.723 MPa. Operational and fast neutron flux input parameters are summarized in Table Z.5 and Table Z.6, respectively.

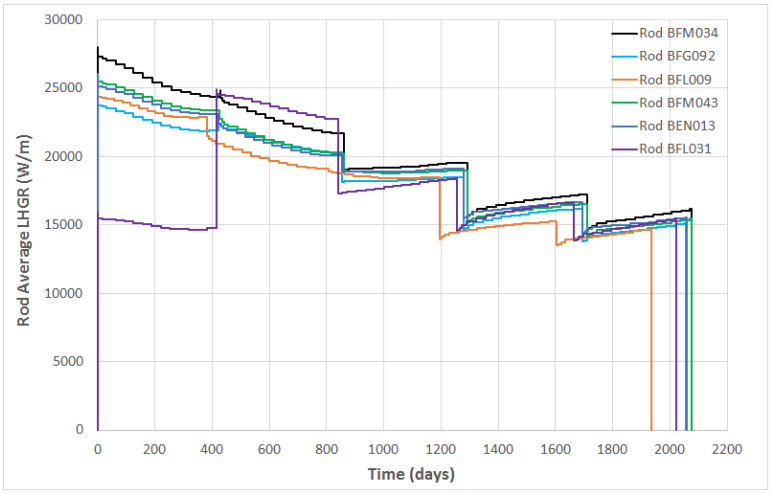

Figure Z.1.: Assembly C1G003 Rods BFM034, BFG092, BFL009, BFM156, BFM043, BEN013, and BFL031 power histories

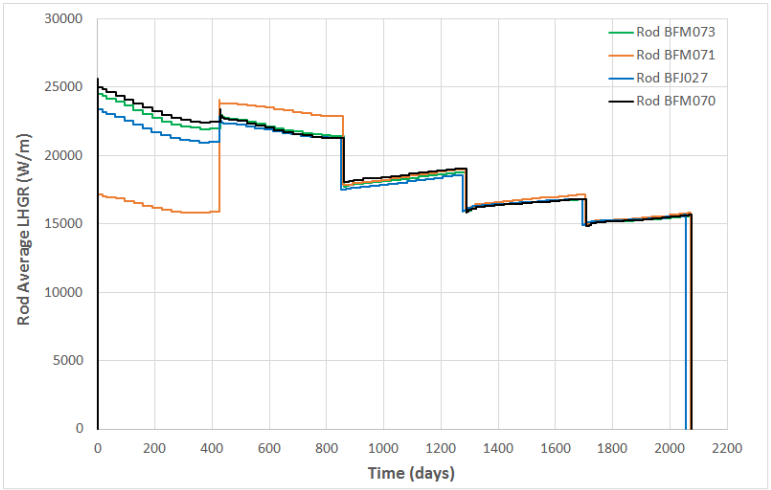

Figure Z.2.: Assembly C1G006 Rods BFM073, BFM070, BFJ027, and BFM071 power histories

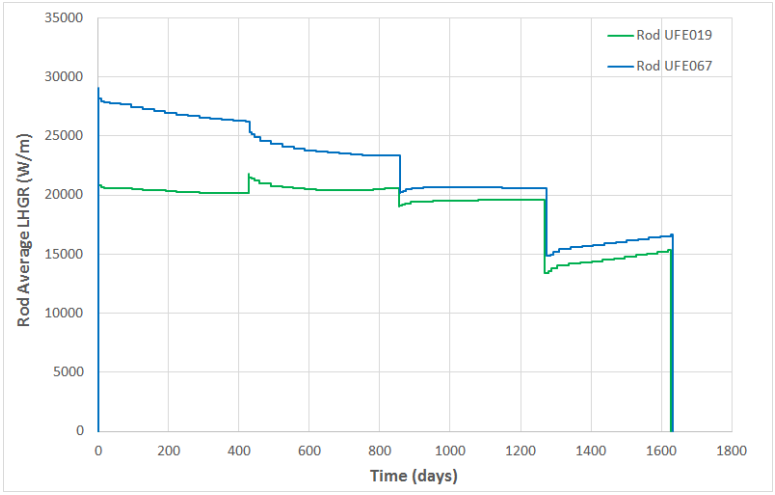

Figure Z.3.: Assembly C1H038 Rods UFE067 and UFE019 power histories

Table Z.5.: Operational Input Parameters

Parameter	Unit	Value
Coolant inlet temperature	K	557.15
Coolant system pressure	MPa	15.513
Coolant mass velocity	$kg/m^2 - s$	3682.14

Table Z.6.: Core Average Fast Neutron Flux Input Parameters

	BOC $n/m^2 - s$ $(\times 10^{17})$	EOC $n/m^2 - s$ $(\times 10^{17})$
Cycle 5	6.288	6.776
Cycle 6	7.663	6.736
Cycle 7	6.567	6.749
Cycle 8	6.541	6.797
Cycle 9	6.411	6.622

Z.3. Model Description

Z.3.1. Geometry and Mesh

The rod specifications in Table Z.2 were used to define the geometry for these simulations. The 13 selected rods were modeled as a two-dimensional, axi-symmetric linear mesh with quadratic elements. The fuel mesh for all 13 test rods consisted of 12 radial elements and the cladding mesh consisted of four radial elements to form a cladding thickness of 0.7112 mm. In order to accurately model the fuel rod initial free volume, the overall fuel rod length and upper plenum height were adjusted during mesh generation to account for the volume of the plenum spring which is not explicitly modeled. The adjusted fuel rod lengths and plenum heights for the 13 test cases are shown in Table Z.7. The mesh for 11 out of the 13 selected test rods that have standard or reduced length pellet types is shown in Figure Z.4. The mesh for the two fuel rods (BFL031 and BFL009) which have annular pellet types is shown in Figure Z.5.

Table Z.7.: Adjusted Fuel Rod Length and Plenum Height

Rod Serial Number	Adjusted Rod Length(m)	Adjusted Plenum Height (m)
BFM034	3.79312	0.31392
BFG092	3.76274	0.28354
BFL009	3.70247	0.22327
BFM156	3.81935	0.34015
BFM043	3.79754	0.31834
BEN013	3.76501	0.28581
BFL031	3.69979	0.22059
BFM073	3.79834	0.31914
BFM070	3.80088	0.32168
BFJ027	3.76863	0.28943
BFM071	3.79647	0.31727
UFE067	3.77933	0.30013
UFE019	3.77693	0.29773

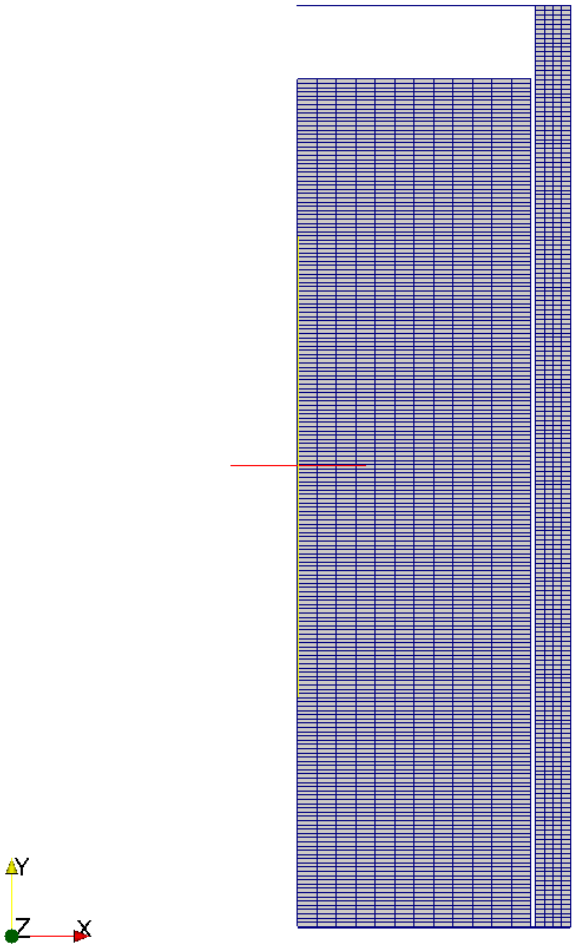

Figure Z.4.: Fuel rod with standard or reduced length pellet mesh (not to scale)

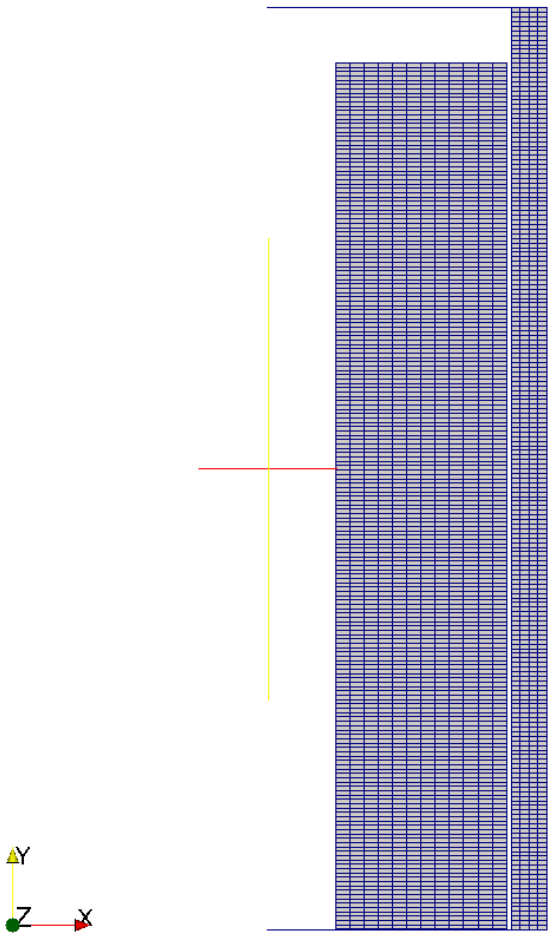

Figure Z.5.: Fuel rod with annular pellet type mesh (not to scale)

Z.3.2. Material and Behavioral Models

The following material and behavioral models were used for the UO_2 fuel:

- ThermalFuel - NFIR: temperature and burnup dependent thermal properties.
- RelocationUO2: relocation strains, relocation activation threshold power set to 5 kW/m.
- Sifgrs: fission gas release model with the combined gaseous swelling model.
- MechZry: model mechanical deformation for Zircaloy-4.

For the cladding material, a constant thermal conductivity of 16 W/m-K was used and both thermal and irradiation creep were considered using the Limback model [26].

Z.3.3. Input files

The BISON input and all supporting files (power histories, axial power profiles, etc.) for all 13 selected Calvert Cliffs-1 test rods are provided with the code distribution at bison/assessment/Calvert_Cliffs-1_Prototype/analysis.

Z.3.4. Execution Summary

Table Z.8.: Execution summary.

Machine	Operating System	Code Version
INL HPC FALCON	LINUX	BISON 1.2

Z.4. Results Comparison

Data from the PROTOTYPE irradiation program was used to assess the code's capability to capture the integral fuel rod fission gas release, cladding creep down strain, oxide thickness, fuel rod growth, rod internal pressure, and void volume. The predicted values for all 13 selected test rods from BISON calculations are shown in Table Z.9. The measured values from experimental data are shown in Table Z.10 for comparisons. The rod axial growth measured data is not available for rod BFL031. BISON computes reasonable burnup, end-of-life (EOL) void volume, fission gas release, and EOL rod internal pressure for all 13 test rods when compared to measured data. BISON consistently under predicts fuel rod axial growth by a significant margin for all 13 test rods.

Table Z.9.: Bison prediction for Calvert Cliffs-1 test rods

Rod Serial Number	Burnup (GWd/ MTU)	FGR (%)	Initial Void Vol. (cc)	Final Void Vol. (cc)	Rod Axial Growth (mm)	Axial Growth Strain (m/m)	Rod Int. Pressure (MPa)
BFM034	64.211	1.749	33.680	22.976	11.239	0.00296	4.371
BFG092	58.635	0.863	31.410	21.273	14.466	0.00384	4.212
BFL009	58.605	0.183	47.050	37.465	12.442	0.00336	3.454
BFM156	57.541	0.738	35.640	25.397	13.820	0.00362	3.959
BFM043	61.227	1.215	34.010	23.524	12.716	0.00335	4.186
BEN013	60.548	1.166	31.580	21.301	13.642	0.00362	4.299
BFL031	58.870	0.210	46.850	37.261	11.912	0.00322	3.462
BFM073	61.015	1.250	34.070	23.607	12.626	0.00332	4.185
BFM070	61.469	1.310	34.260	23.753	12.432	0.00327	4.194
BFJ027	59.429	1.043	31.850	21.646	13.849	0.00367	4.234
BFM071	57.904	1.200	33.930	23.675	13.348	0.00352	4.135
UFE067	55.357	2.672	32.650	22.479	10.910	0.00289	4.462
UFE019	47.246	0.817	32.470	23.036	15.295	0.00405	3.976

Table Z.10.: Measured data for Calvert Cliffs-1 test rods

Rod Serial Number	Burnup (GWd/ MTU)	FGR (%)	Initial Void Vol. (cc)	Final Void Vol. (cc)	Rod Axial Growth (mm)	Axial Growth Strain (m/m)	Rod Int. Pressure (MPa)
BFM034	63.451	3.8	33.68	26.3	34.366	0.00921	4.302
BFG092	57.945	1.7	31.41	24.65	39.116	0.01048	3.634
BFL009	58.106	1.6	47.05	38.91	33.655	0.00902	3.392
BFM156	56.854	1.4	35.64	28.2	31.826	0.00853	3.558
BFM043	60.506	3.0	34.01	27.35	35.052	0.00939	4.061
BEN013	59.835	2.3	31.58	24.71	29.616	0.00793	3.806
BFL031	58.268	1.6	46.85	39.51			3.323
BFM073	60.319	2.9	34.07	27.73	35.966	0.00963	3.992
BFM070	60.761	3.1	34.26	27.14	33.579	0.00900	4.089
BFJ027	58.726	2.0	31.85	24.95	39.853	0.01068	3.689
BFM071	57.143	2.3	33.93	27.7	32.791	0.00878	3.868
UFE067	54.841	2.6	32.65	24.66	28.346	0.00760	4.020
UFE019	46.791	0.9	32.47	26.24	28.346	0.00760	3.544

Z.4.1. Fission Gas Release

The only fission gas release data available for this experiment is from destructive PIE puncture tests. Figures Z.6 to Z.18 show BISON's comparisons with EOL measurement for the 13 selected test rods in the current evaluation. BISON consistently under predicts the measured results by up to 2.1% for 12 out of the 13 selected test rods. Only rod UFE067 slightly over predicts the measured value. Both rods UFE019 and UFE067 predicts the fission gas release reasonably well compared to the measured result. Some adjustment may be needed to improve the FGR prediction since it is systemic and consistently under predicting. Currently, there's no specific model for gas release at high burnup. The next step is to investigate the high burnup gas release model.

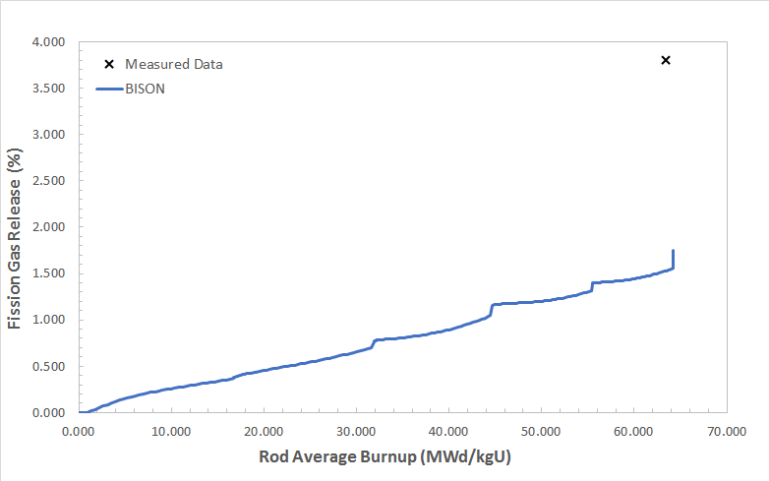

Figure Z.6.: Fission gas release comparisons for BFM034

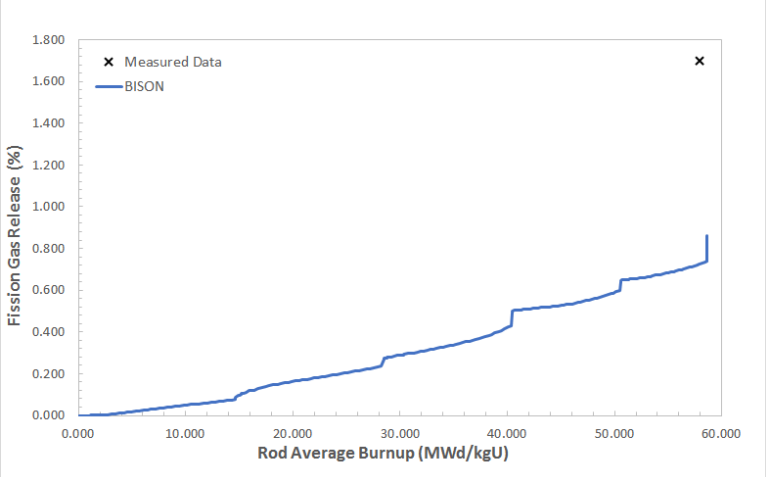

Figure Z.7.: Fission gas release comparisons for BFG092

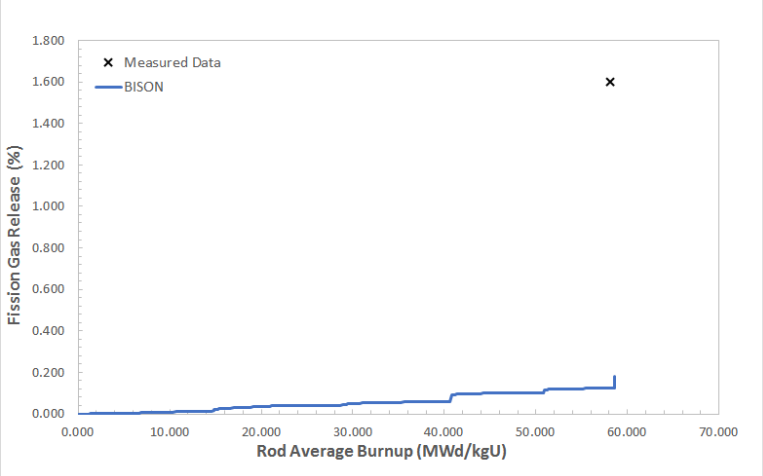

Figure Z.8.: Fission gas release comparisons for BFL009

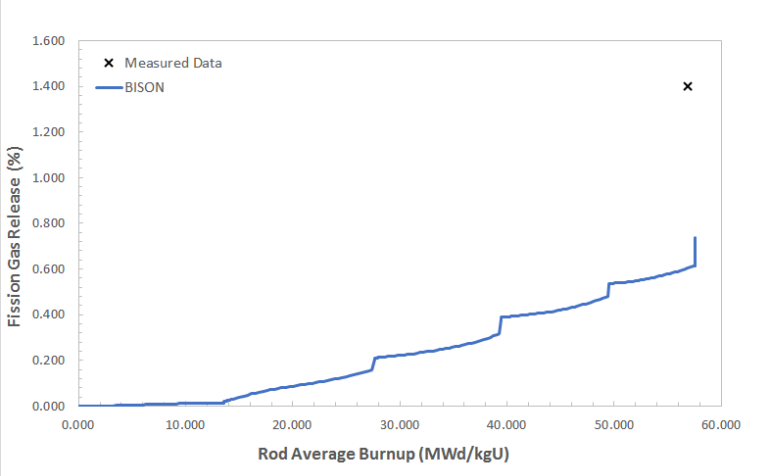

Figure Z.9.: Fission gas release comparisons for BFM156

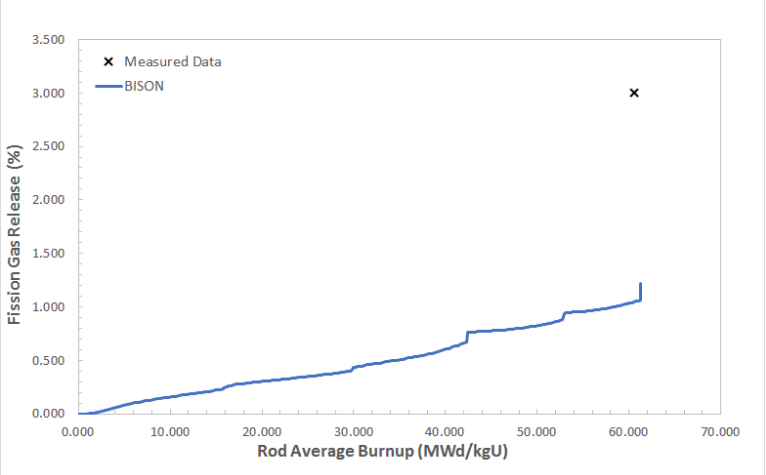

Figure Z.10.: Fission gas release comparisons for BFM043

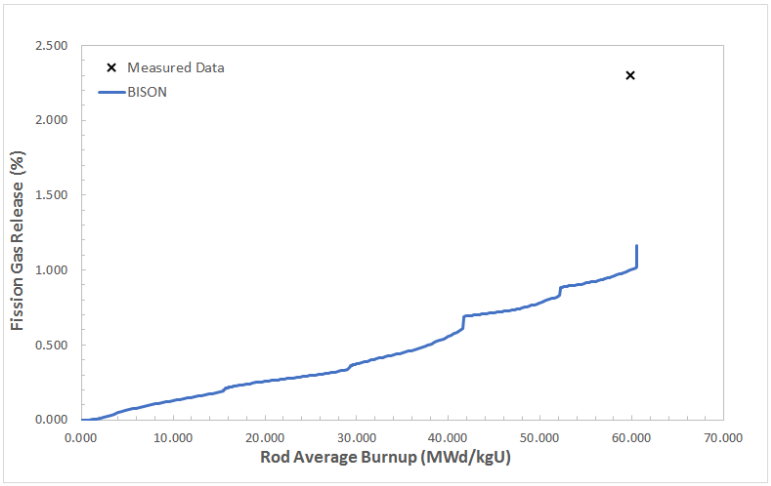

Figure Z.11.: Fission gas release comparisons for BEN013

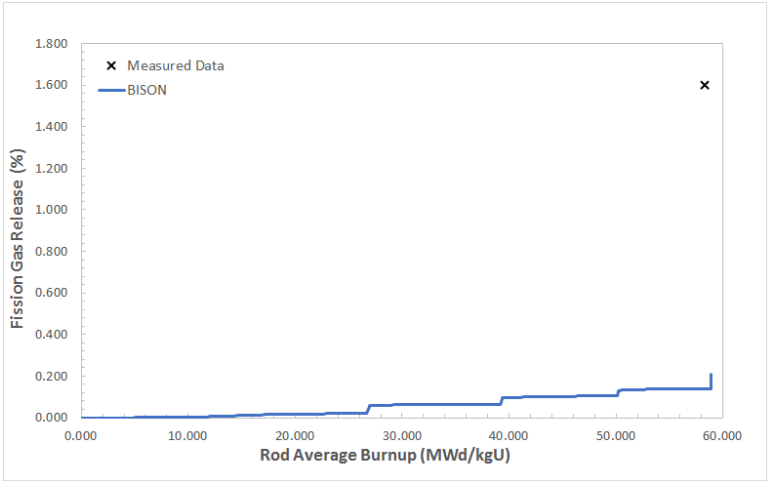

Figure Z.12.: Fission gas release comparisons for BFL031

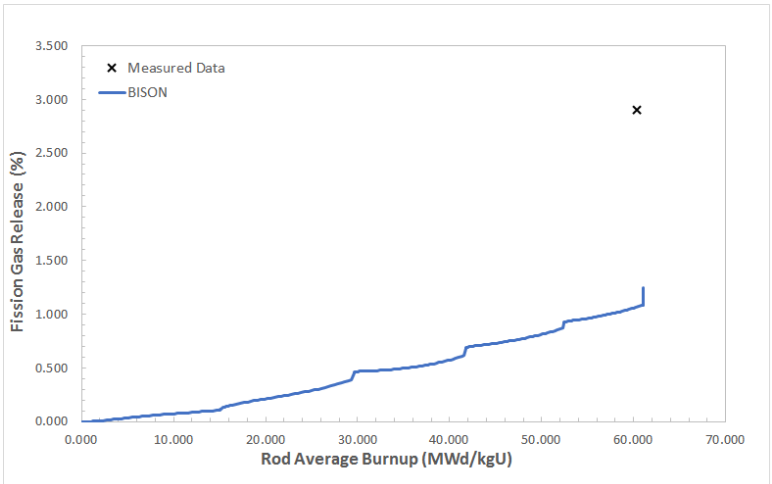

Figure Z.13.: Fission gas release comparisons for BFM073

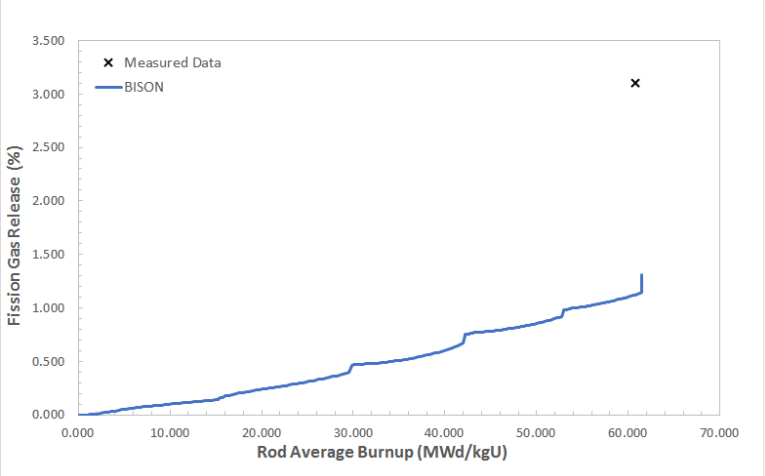

Figure Z.14.: Fission gas release comparisons for BFM070

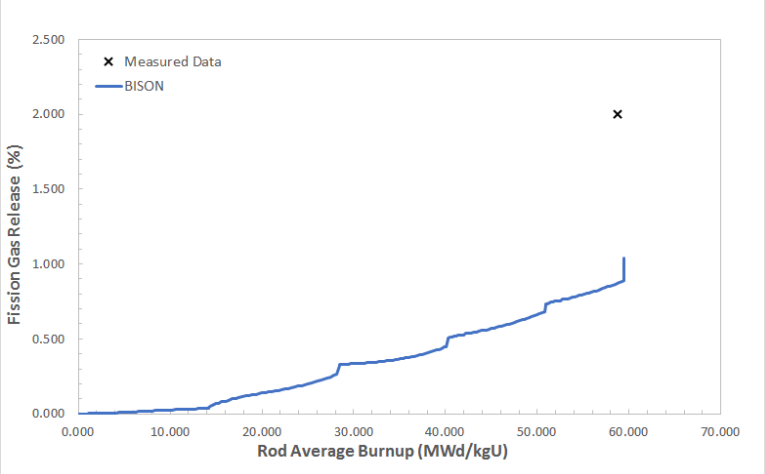

Figure Z.15.: Fission gas release comparisons for BFJ027

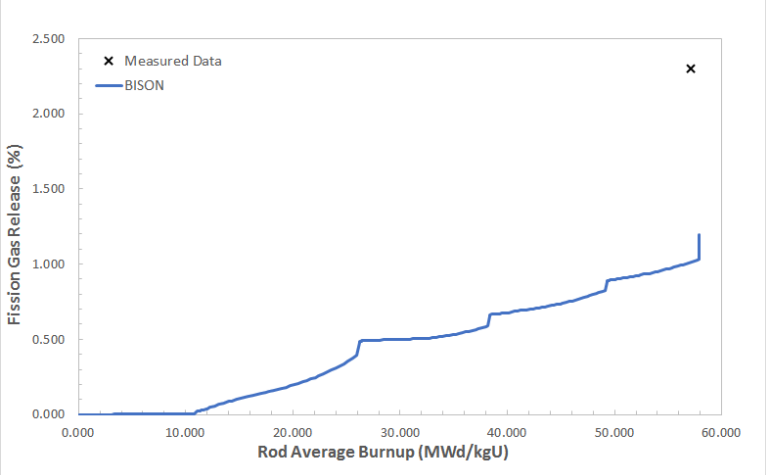

Figure Z.16.: Fission gas release comparisons for BFM071

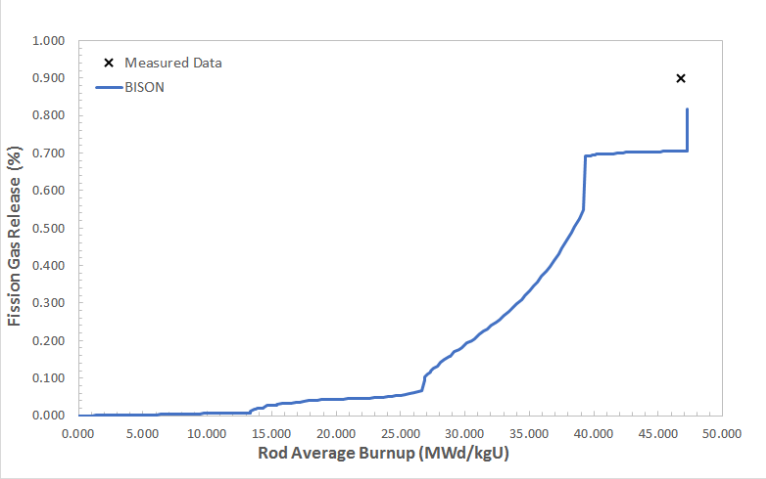

Figure Z.17.: Fission gas release comparisons for UFE019

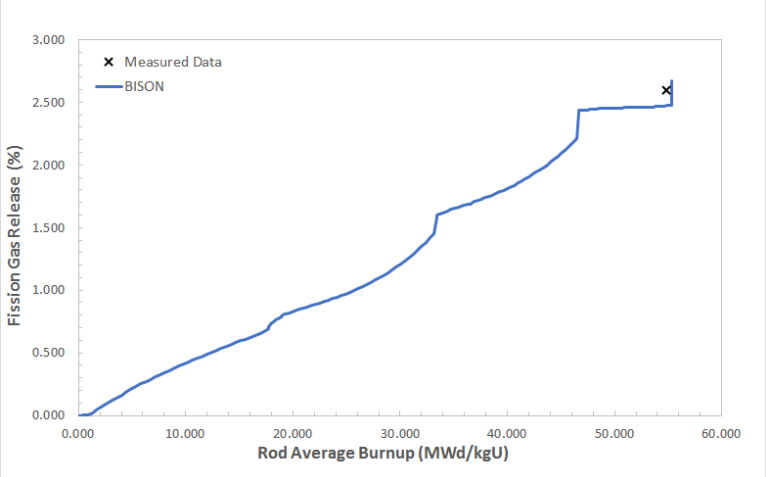

Figure Z.18.: Fission gas release comparisons for UFE067

Z.4.2. Rod Internal Pressure

The only rod internal pressure data available for this experiment is from destructive PIE puncture tests. Figures Z.19 to Z.31 show BISON's comparisons with EOL measurement for the 13 selected test rods. BISON predicts the rod internal pressure reasonably well compared to the measured result for all 13 test rods.

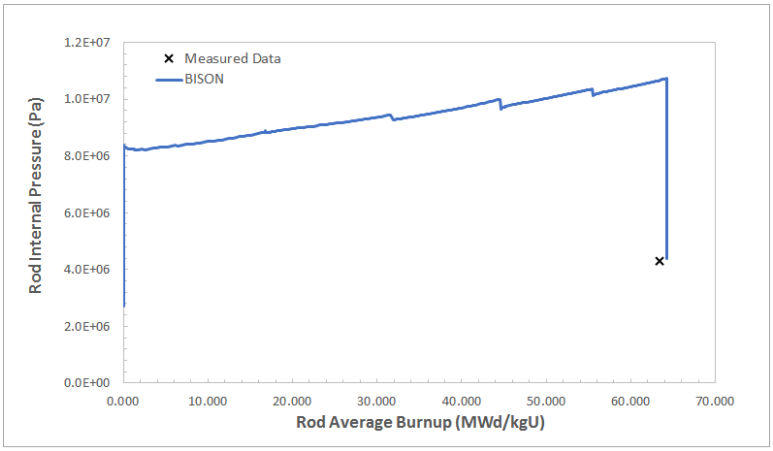

Figure Z.19.: Rod internal pressure comparisons for BFM034

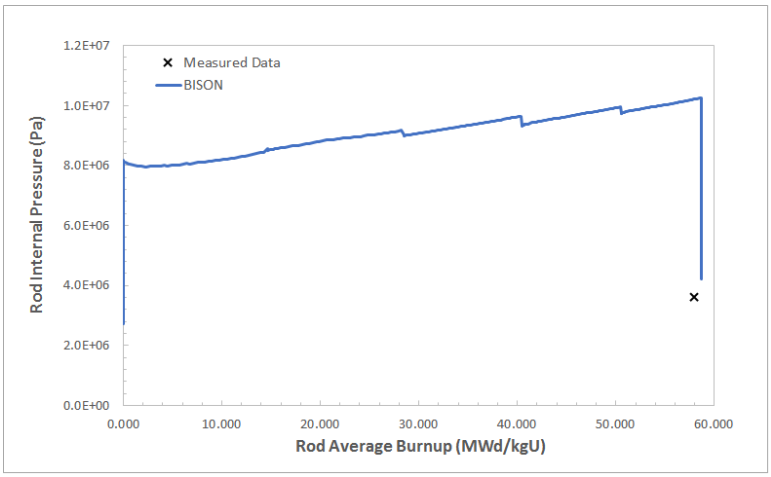

Figure Z.20.: Rod internal pressure comparisons for BFG092

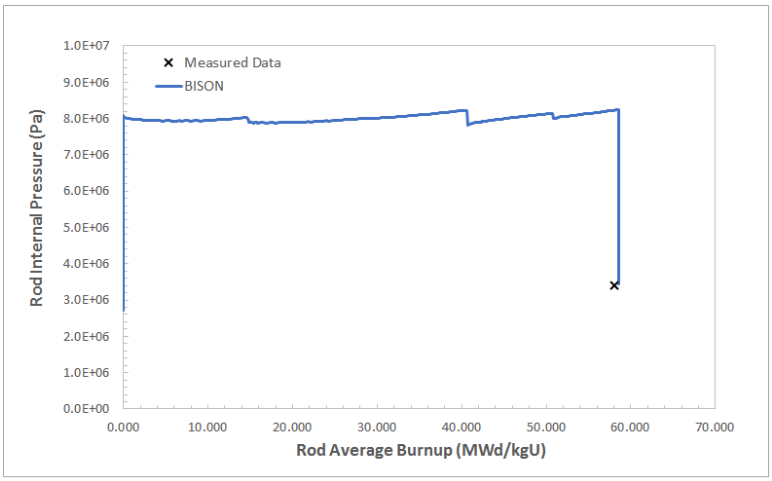

Figure Z.21.: Rod internal pressure comparisons for BFL009

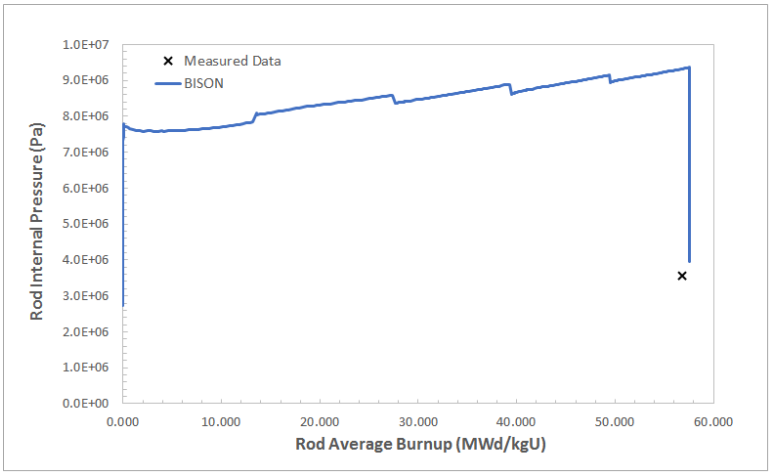

Figure Z.22.: Rod internal pressure comparisons for BFM156

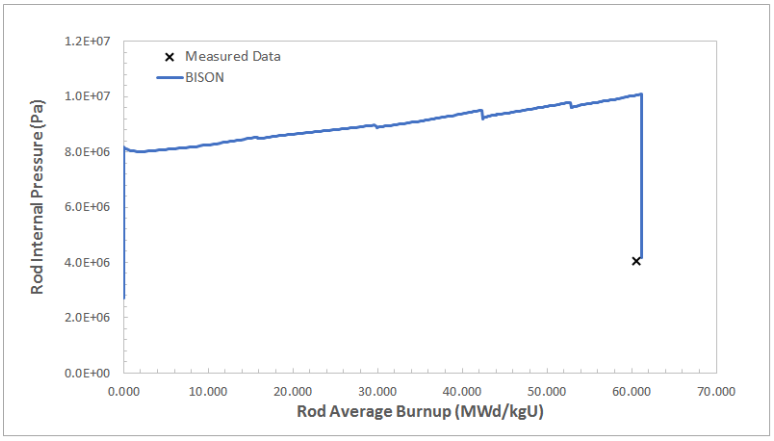

Figure Z.23.: Rod internal pressure comparisons for BFM043

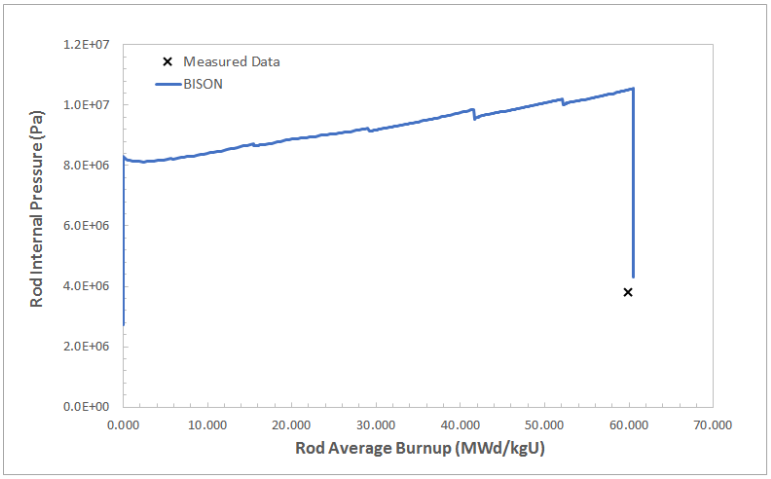

Figure Z.24.: Rod internal pressure comparisons for BEN013

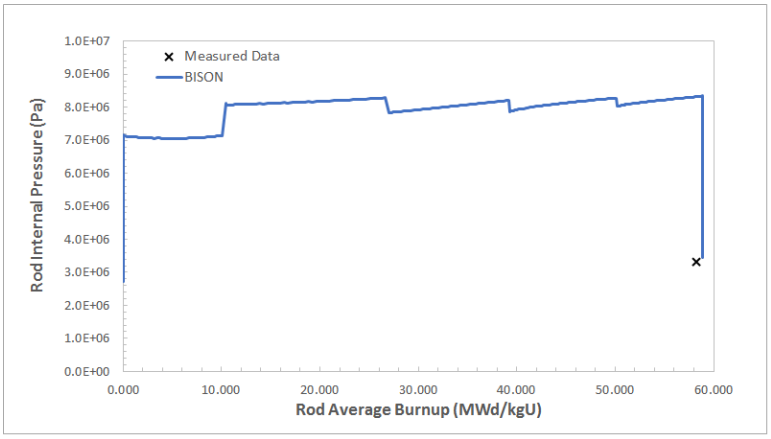

Figure Z.25.: Rod internal pressure comparisons for BFL031

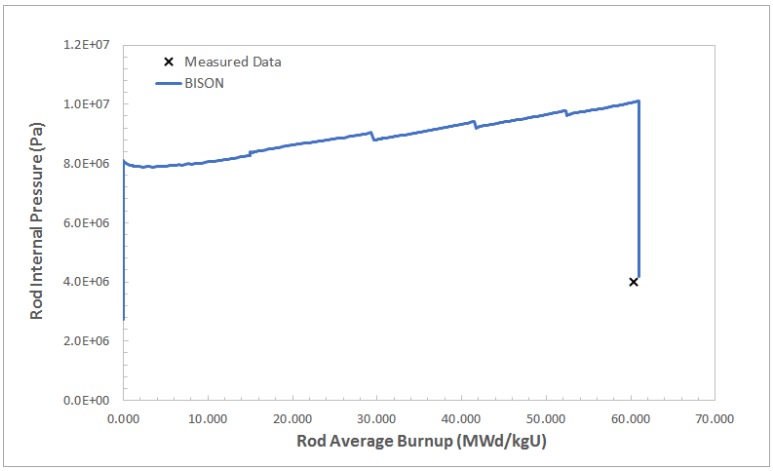

Figure Z.26.: Rod internal pressure comparisons for BFM073

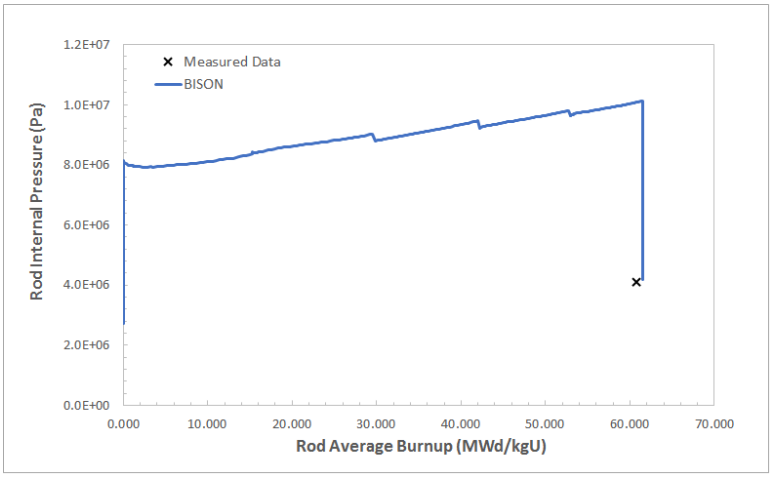

Figure Z.27.: Rod internal pressure comparisons for BFM070

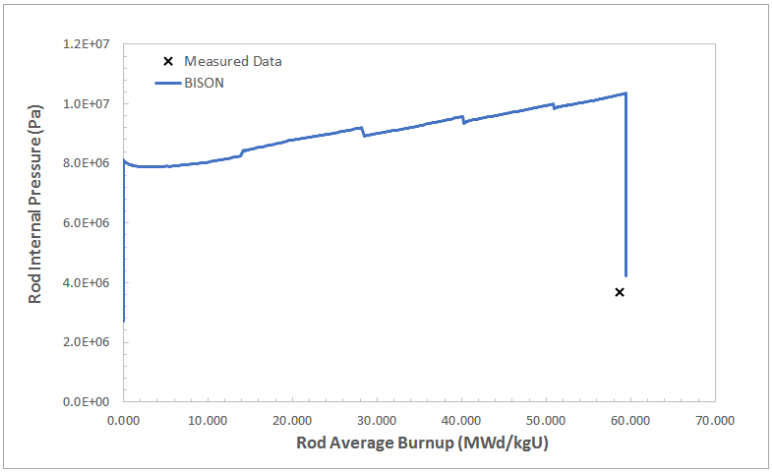

Figure Z.28.: Rod internal pressure comparisons for BFJ027

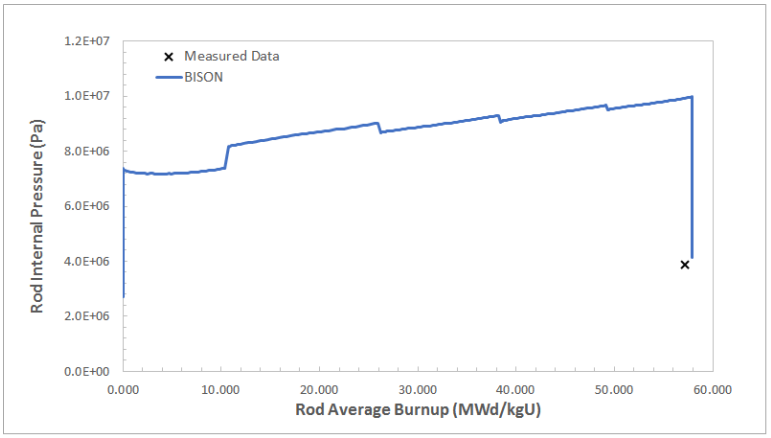

Figure Z.29.: Rod internal pressure comparisons for BFM071

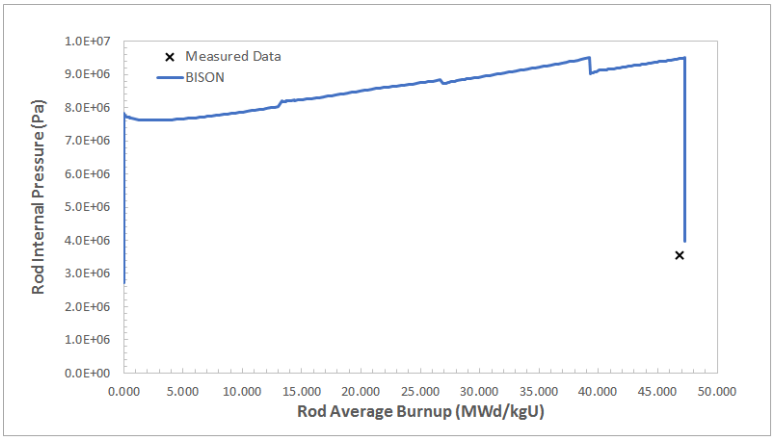

Figure Z.30.: Rod internal pressure comparisons for UFE019

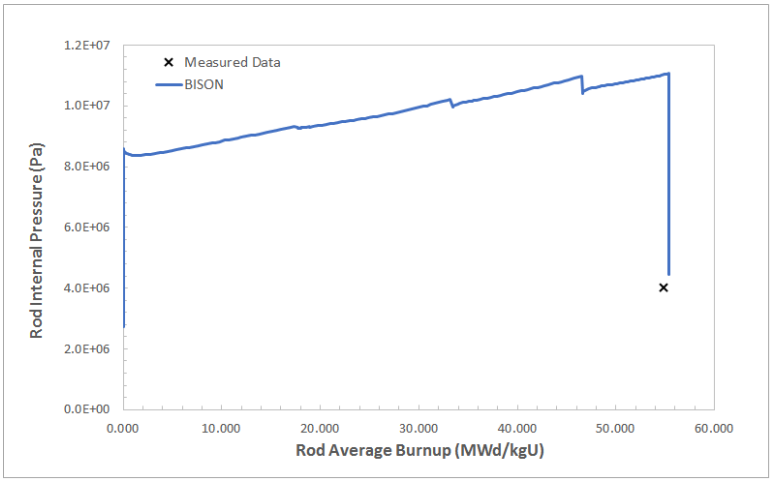

Figure Z.31.: Rod internal pressure comparisons for UFE067

Z.4.3. Cladding Creep Down Strain

The calculated cladding creep down strain as a function of axial position is compared to measured data. The cladding creep down strain is calculated from the computed cladding diameter. Figures Z.32 to Z.43 show comparisons of BISON computed results to the measured cladding creep down strain data for 12 out of the 13 selected test rods. Cladding strain data were not available for rod BFL031. The results show BISON over predicts the cladding outer diameter at the EOL for all 12 test rods.

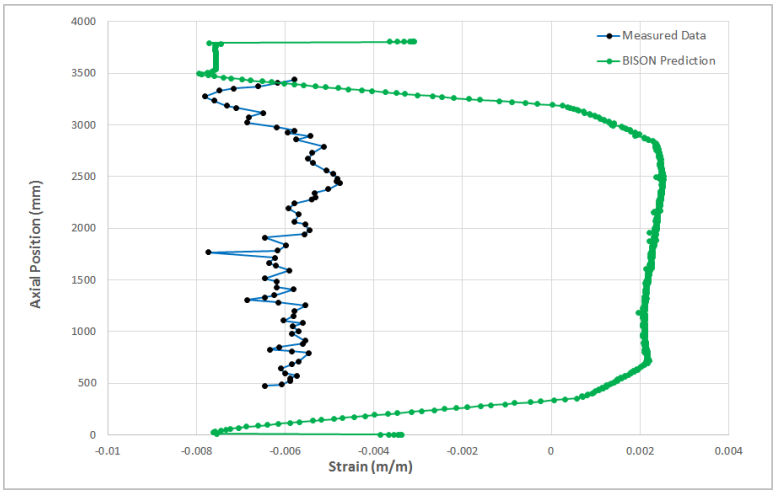

Figure Z.32.: Cladding creep down strain comparisons for BFM034

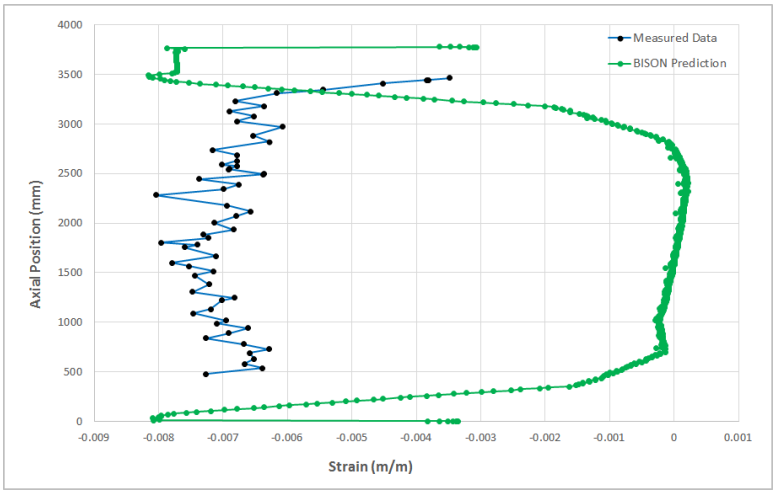

Figure Z.33.: Cladding creep down strain comparisons for BFG092

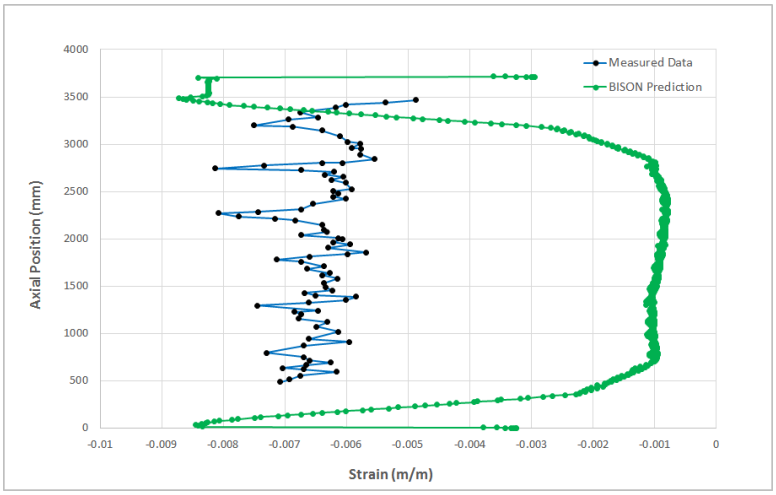

Figure Z.34.: Cladding creep down strain comparisons for BFL009

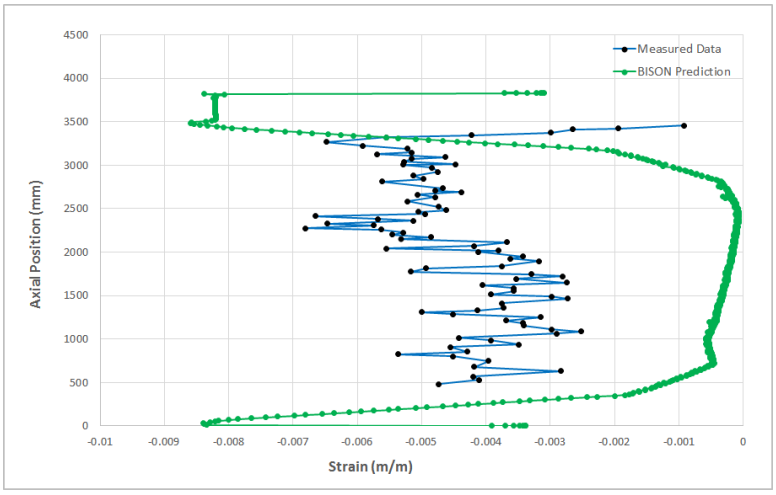

Figure Z.35.: Cladding creep down strain comparisons for BFM156

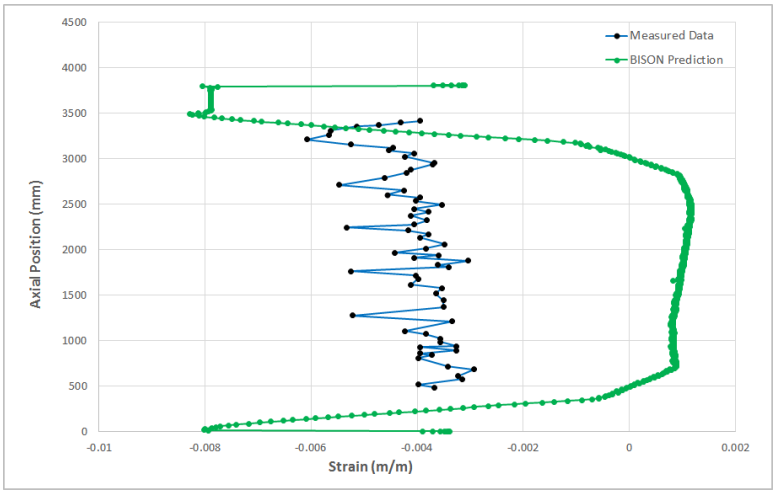

Figure Z.36.: Cladding creep down strain comparisons for BFM043

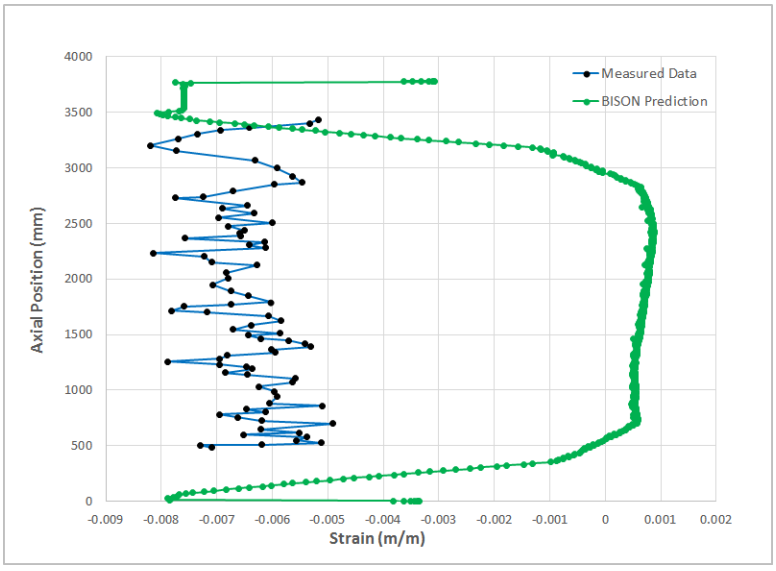

Figure Z.37.: Cladding creep down strain comparisons for BEN013

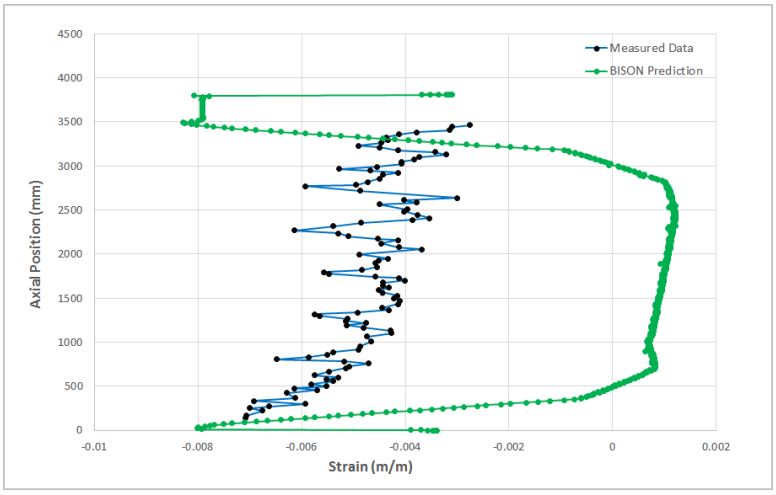

Figure Z.38.: Cladding creep down strain comparisons for BFM073

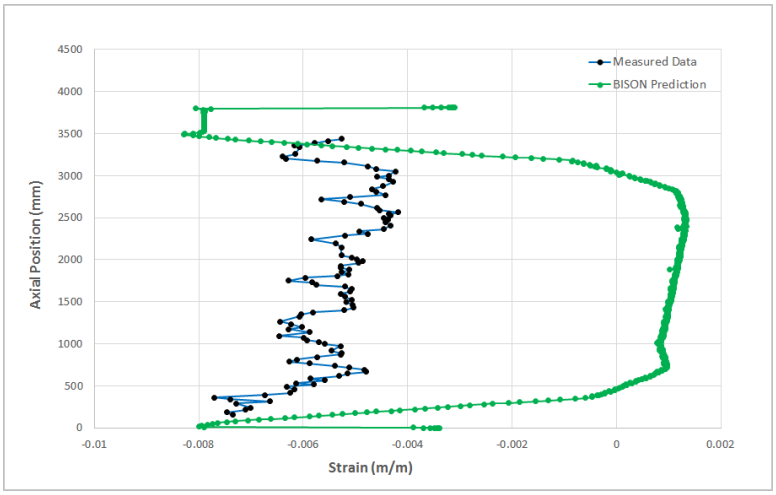

Figure Z.39.: Cladding creep down strain comparisons for BFM070

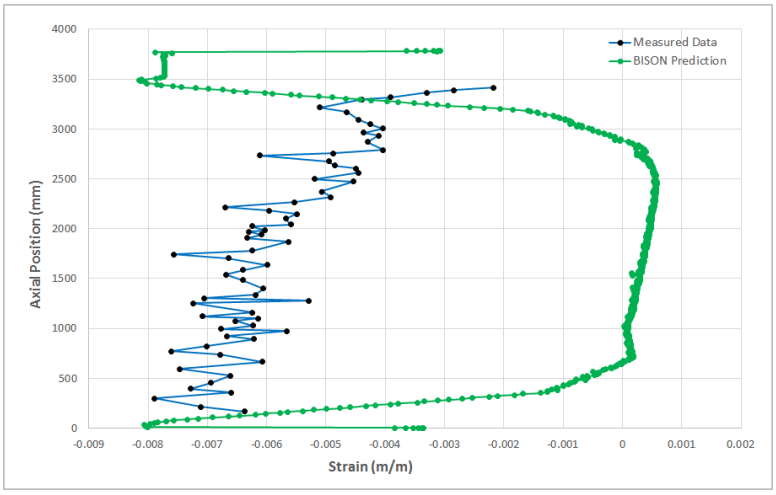

Figure Z.40.: Cladding creep down strain comparisons for BFJ027

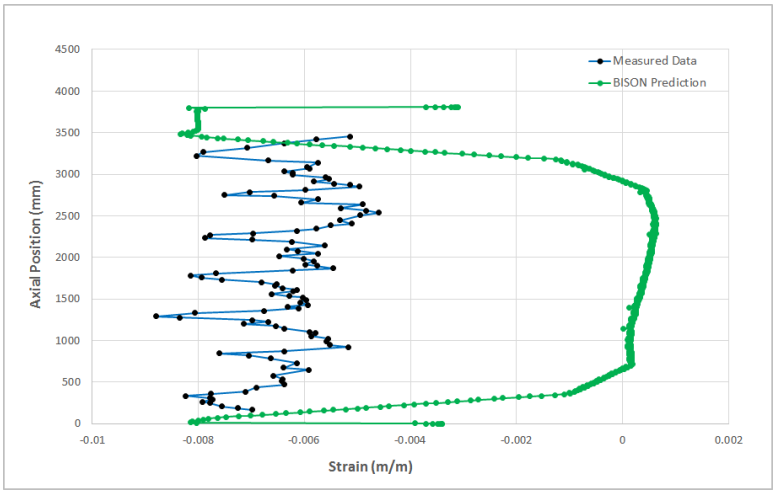

Figure Z.41.: Cladding creep down strain comparisons for BFM071

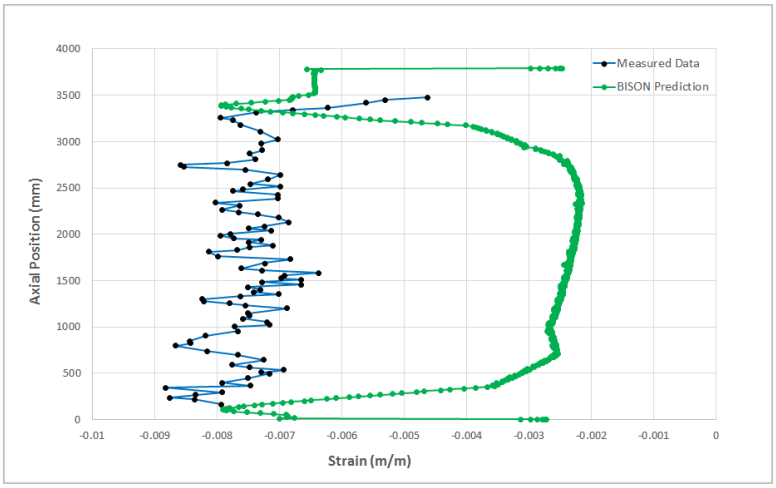

Figure Z.42.: Cladding creep down strain comparisons for UFE019

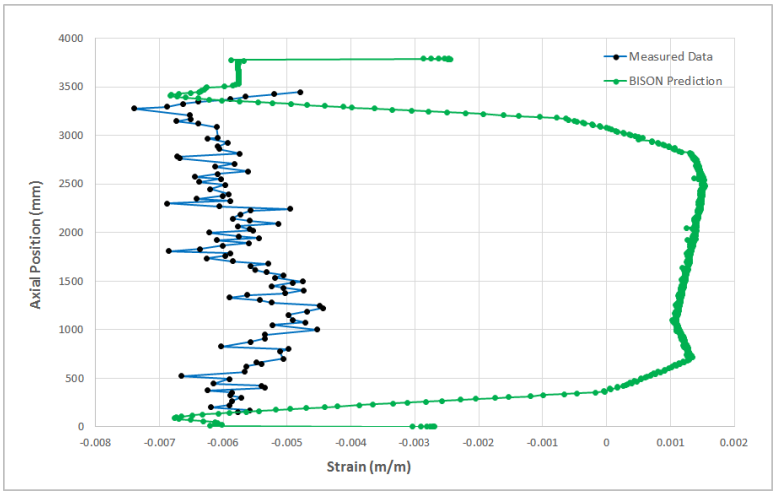

Figure Z.43.: Cladding creep down strain comparisons for UFE067

Z.4.4. Cladding Oxide Thickness

The calculated cladding oxide thickness as a function of axial position is compared to measured data. Figures Z.44 to Z.54 show comparisons of BISON computed results to the measured cladding oxide thickness data for 11 out of the 13 selected test rods. Cladding oxide thickness data were not available for rods BFM070 and BFL031. The OxidationCladding model under the Materials block was used for the oxide thickness calculation. The results show BISON under predicts the peak oxide thickness for rods BFL009, BFM043, BEN013, BFM073, BFJ027, and BFM071, and over predicts the peak oxide thickness for rods BFM034, UFE019, and UFE067 by a significant margin compared to the measured results at the EOL. Only rods BFG092 and BFM156 were predicted with reasonable peak oxide thickness values compared to the measured result.

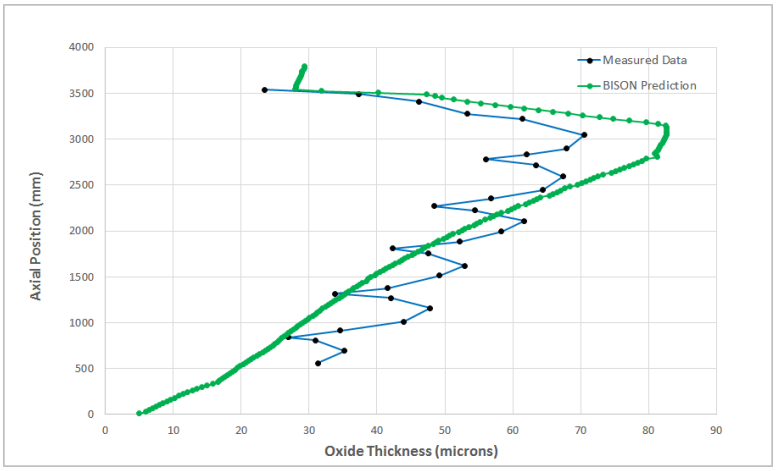

Figure Z.44.: Cladding oxide thickness comparisons for BFM034

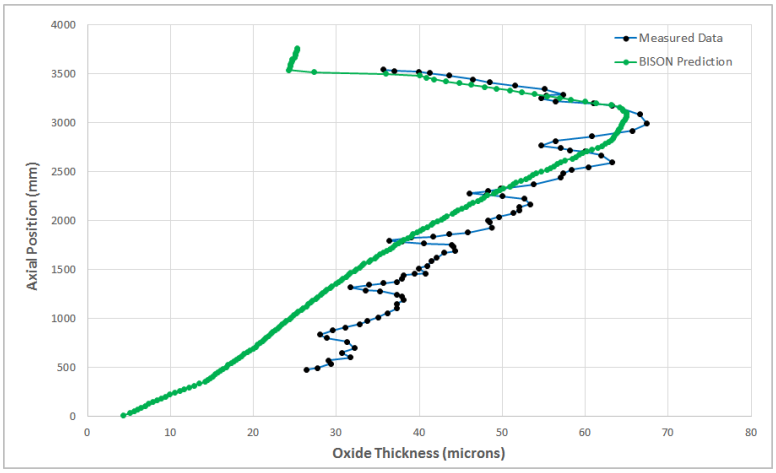

Figure Z.45.: Cladding oxide thickness comparisons for BFG092

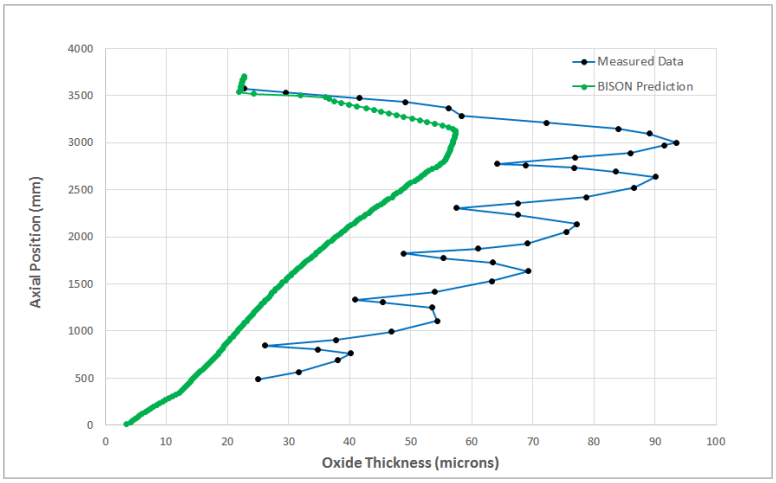

Figure Z.46.: Cladding oxide thickness comparisons for BFL009

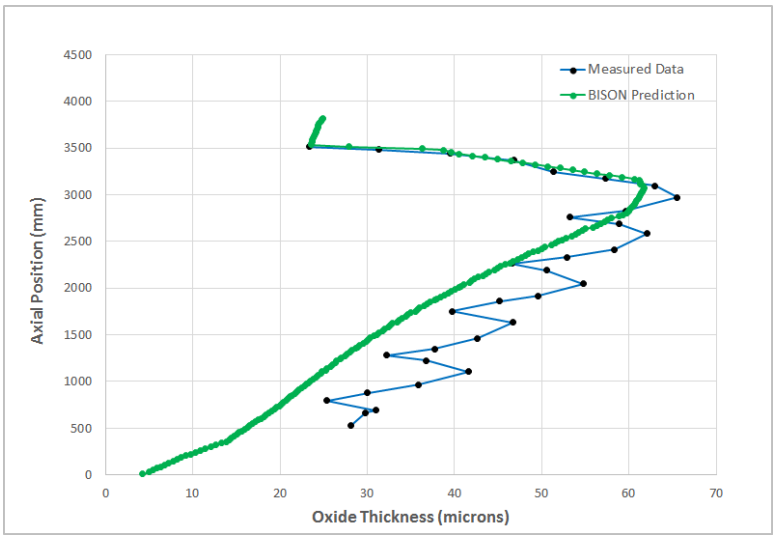

Figure Z.47.: Cladding oxide thickness comparisons for BFM156

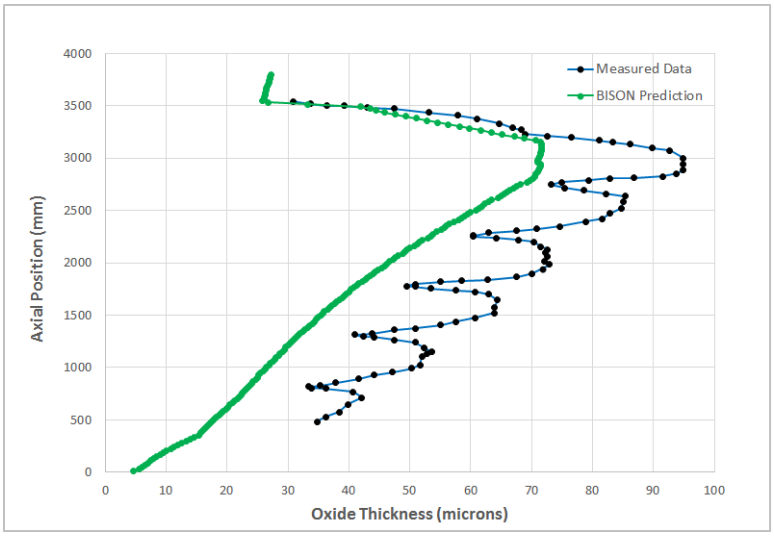

Figure Z.48.: Cladding oxide thickness comparisons for BFM043

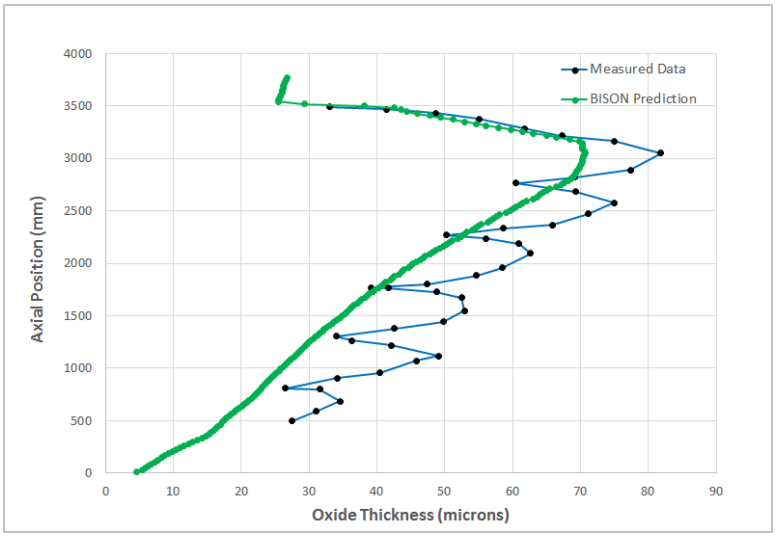

Figure Z.49.: Cladding oxide thickness comparisons for BEN013

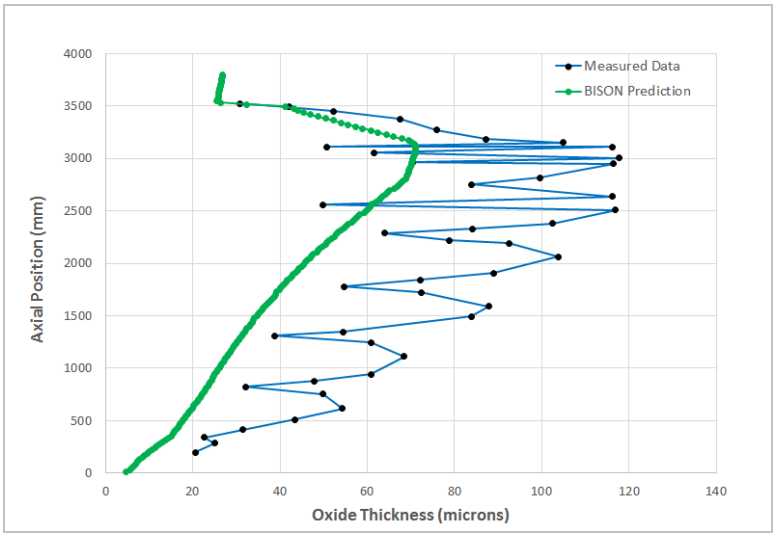

Figure Z.50.: Cladding oxide thickness comparisons for BFM073

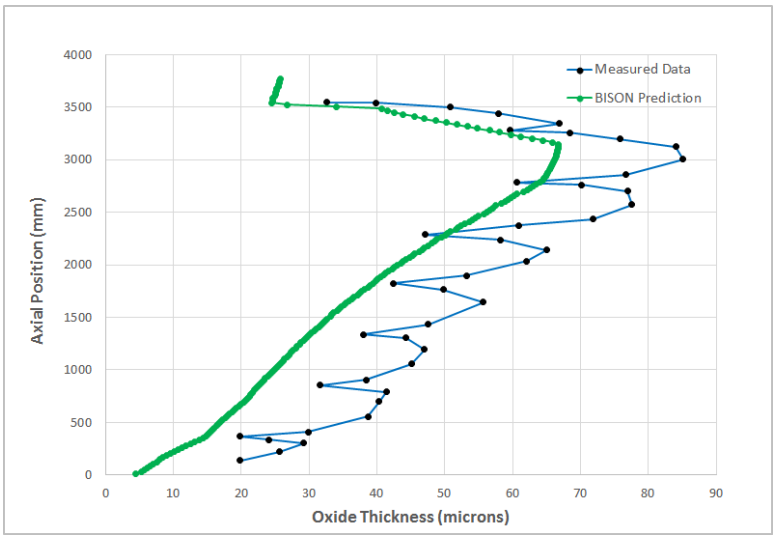

Figure Z.51.: Cladding oxide thickness comparisons for BFJ027

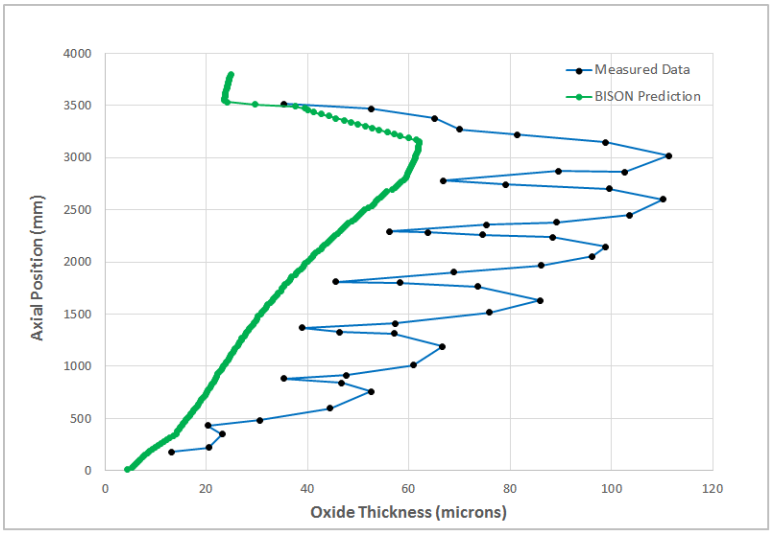

Figure Z.52.: Cladding oxide thickness comparisons for BFM071

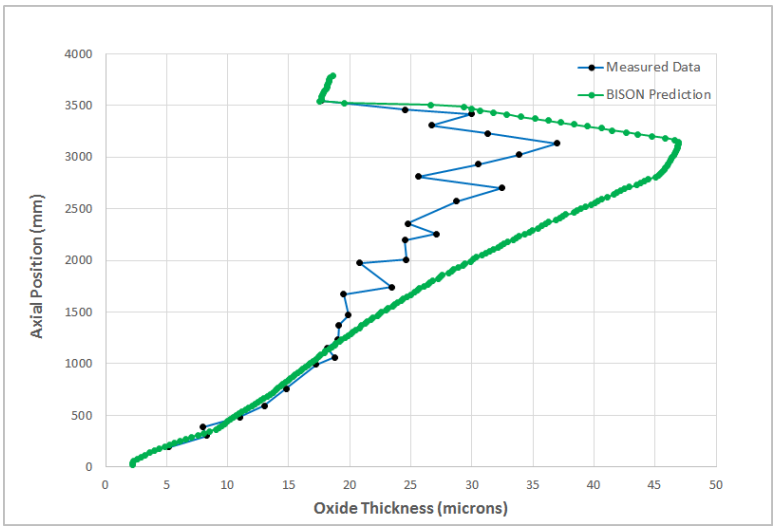

Figure Z.53.: Cladding oxide thickness comparisons for UFE019

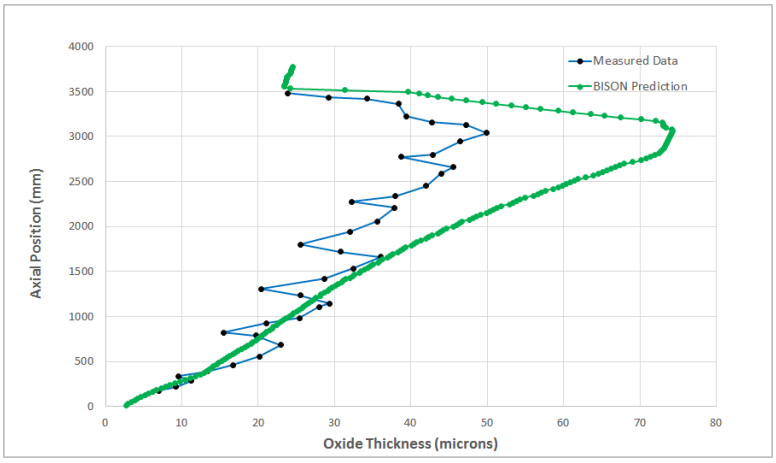

Figure Z.54.: Cladding oxide thickness comparisons for UFE067

Z.4.5. Discussion

Based on the data presented above, several observations can be made regarding the results obtained from BISON analyses of the 13 selected Calvert Cliffs-1 test fuel rods.

- BISON consistently under predicts the EOL FGR by up to 2.1% for 12 out of the 13 selected test rods. The next step is to investigate inclusion of a high burnup gas release model in BISON.
- BISON consistently under predicts the EOL rod axial growth for all 13 selected test rods by a large margin. This may be related to fuel/cladding interaction driven by friction (which is currently not modeled) as well as application of axial creep strain and the axial growth model. Further review is recommended to determine the root cause of the large under prediction of rod axial growth.
- BISON consistently over predicts the EOL cladding outer diameter for the 12 test rods with available data by a significant margin. This is likely related to fuel pellet behavior rather than cladding creep. More specifically, fuel pellet relocation and relocation recovery. Further review is recommended to determine the root cause of this behavior.
- Using the OxidationCladding model under the Materials block, BISON under predicts the EOL cladding oxide thickness for 6 out of the 11 test rods with available data by a significant margin. BISON also over predicts 3 out of the 11 test rods by a large margin. Further review of the cladding corrosion model, its input and implementation is warranted.

Based on the evaluation of these assessment cases, further evaluations of the fission gas release, cladding creep down strain, fuel relocation, rod axial growth and cladding oxide thickness characteristics in commercial rods are needed to extend the code's validation.

Bibliography

[1] R. L. Williamson, J. D. Hales, S. R. Novascone, M. R. Tonks, D. R. Gaston, C. J. Permann, D. Andrs, and R. C. Martineau. Multidimensional multiphysics simulation of nuclear fuel behavior. *J. Nucl. Mater.*, 423:149–163, 2012.

[2] J. D. Hales, R. L. Williamson, S. R. Novascone, D. M. Perez, B. W. Spencer, and G. Pastore. Multidimensional multiphysics simulation of TRISO particle fuel. *J. Nucl. Mater.*, 443:531–543, November 2013.

[3] Pavel Medvedev. Fuel performance modeling results for representative FCRD irradiation experiments: Projected deformation in the annular AFC-3A U-10Zr fuel pins and comparison to alternative designs. Technical Report INL/EXT-12-27183 Revision 1, Idaho National Laboratory, 2012.

[4] J. Killeen, E. Sartori, and T. Tverberg. FUMEX-III: A new IAEA coordinated research project on fuel modeling at extended burnup, paper 2176. In *Proceedings of Top Fuel 2009*, Paris, France, Sept 6-10, 2009.

[5] J. C. Killeen, J. A. Turnbull, and E. Sartori. Fuel modelling at extended burnup: IAEA coordinated research project FUMEX-II. In *Proceedings of the 2007 International LWR Fuel Performance Meeting*, San Francisco, California, Paper 1102, September 30–October 3 2007.

[6] IAEA. Advances in high temperature gas cooled reactor fuel technology. Technical Report IAEA-TECDOC-1674, International Atomic Energy Agency, 2012.

[7] J. D. Hales, S. R. Novascone, G. Pastore, D. M. Perez, B. W. Spencer, and R. L. Williamson. BISON theory manual: The equations behind nuclear fuel analysis. Technical report, Idaho National Laboratory, September 2014.

[8] J. D. Hales, S. R. Novascone, G. Pastore, D. M. Perez, B. W. Spencer, and R. L. Williamson. BISON users manual. Technical report, Idaho National Laboratory, September 2014.

[9] K. Lassmann, C. O'Carroll, J. van de Laar, and C. T. Walker. The radial distribution of plutonium in high burnup UO_2 fuels. *J. Nucl. Materials*, 208:223–231, 1994.

[10] J.B. Ainscough, B.W. Oldfield, and J.O. Ware. Isothermal grain growth kinetics in sintered UO_2 pellets. *J. Nucl. Mater.*, 49:117–128, 1973.

[11] A. M. Ross and R. L. Stoute. Heat transfer coefficient between UO_2 and Zircaloy-2. Technical Report AECL-1552, Atomic Energy of Canada Limited, 1962.

[12] C. M. Allison, G. A. Berna, R. Chambers, E. W. Coryell, K. L. Davis, D. L. Hagrman, D. T. Hagrman, N. L. Hampton, J. K. Hohorst, R. E. Mason, M. L. McComas, K. A. McNeil, R. L. Miller, C. S. Olsen, G. A. Reymann, and L. J. Siefken. SCDAP/RELAP5/MOD3.1 code manual, volume IV: MATPRO–A library of materials properties for light-water-reactor accident analysis. Technical Report NUREG/CR-6150, EGG-2720, Idaho National Engineering Laboratory, 1993.

[13] D. D. Lanning and C. R. Hann. Review of methods applicable to the calculation of gap conductance in zircaloy-clad uo2 fuel rods. Technical Report BWNL-1894, UC-78B, 1975.

[14] A. Marion (NEI) letter dated June 13, 2006 to H. N. Berkow (USNRC/NRR). Safety Evaluation by the Office of Nuclear Reactor Regulation of Electric Power Research Institute (EPRI) Topical Report TR-1002865, Topical Report on Reactivity Initiated Accidents: Bases for RIA Fuel rod Failures and Core Coolability Criteria. http://pbadupws.nrc.gov/docs/ML0616/ML061650107.pdf, 2006.

[15] T. Tverberg, M. Amaya. Study of thermal behavious of UO_2 and (U,Gd)O_2 to high burnup (IFA-515). Technical Report HWR-671, Halden, February 2001.

[16] P. Lösönen. Early-in-life irradiation of IFA-562.2 (The Ultra High Burn-up Experiment). Technical Report HWR-247, Halden, December 1989.

[17] Giovanni Pastore, L.P. Swiler, J.D. Hales, S.R. Novascone, D.M. Perez, B.W. Spencer, L. Luzzi, P. Van Uffelen, and R.L. Williamson. Uncertainty and sensitivity analysis of fission gas behavior in engineering-scale fuel modeling. *Journal of Nuclear Materials*, 456:398–408, 2015.

[18] IAEA. Fuel Modelling at Extened Burnup (FUMEX-II): Report of a Coordinated Research Project 2002-2007. Technical Report IAEA-TECDOC-1687, International Atomic Energy Agency, 2002-2007.

[19] G. K. Miller, D. A. Petti, J. T. Maki, and D. L. Knudsen. PARFUME theory and model basis report. Technical Report INL/EXT-08-14497, Idaho National Laboratory, 2009.

[20] M. Phelip, F. Michel, M. Pelletier, G. Degeneve, and P. Guillermier. The ATLAS HTR fuel simulation code objectives, description and first results. In *2nd International Topical Meeting on High Temperature Reactor Technology*, pages 1–10, Beijing, China, September 2004.

[21] D. G. Martin. Considerations pertaining to the achievement of high burn-ups in htr fuel. *Nuclear Engineering and Design*, 213:241–258, 2002.

[22] E. Proksch, A. Strigl, and H Nabielek. Production of carbon monoxide during burn-up of UO_2 kerneled HTR fuel particles. *Journal of Nuclear Material*, 107:280–285, 1982.

[23] E. R. Bradley, M. E. Cunningham, and D. D. Lanning. Final data report for the instrumented fuel assembly (IFA)-432. Technical Report NUREG/CR-2567, PNNL-4240, 1982.

[24] C. R. Hann, D. D. Lanning, E. R. Bradley, R. K. Marshall, M. E. Cunningham, and R. E. Williford. Data Report for the NRC/PNL Halden Assembly IFA-432. Technical Report NUREG/CR-0560, PNL-2673, 1978.

[25] Wolfgang Wiesenack, September 2012. IFA-431 Rods 1, 2, and 3 Halden data.

[26] M. Limbäck and T. Andersson. A model for analysis of the effect of final annealing on the in- and out-of-reactor creep behavior of zircaloy cladding. In *Zirconium in the Nuclear Industry: Eleventh International Symposium*, ASTM STP 1295, pages 448–468, 1996.

[27] Y. Rashid, R. Dunham, and R. Montgomery. Fuel analysis and licensing code: FALCON MOD01. Technical Report EPRI 1011308, Electric Power Research Institute, December 2004.

[28] L. P. Swiler, R. L. Williamson, and D. M. Perez. Calibration of a fuel relocation model in BISON. In *Proceedings of the International Conference on Mathematics and Computational Methods Applied to Nuclear Science and Engineering*, Sun Valley, Idaho, May 5-9, 2013.

[29] Wolfgang Wiesenack, November 2012. IFA-432 Rods 1, 2, and 3 Halden data.

[30] J. A. Turnbull. Concluding Report on Three PWR Rods Irradiated to 90 MWd/kgUO2 in IFa-519.9: Analysis of Measurements Obtained In-Pile and By PIE. Technical Report HWR-668, Halden, January 2001.

[31] I. Matsson. The Effects of Grain Size on FGR and PCMI in High Burnup Fuel (IFA-534.14). Technical Report HWR-558, Halden, February 1999.

[32] Wolfgang Wiesenack, 2014. IFA-534 Rods 18 and 19 Halden data.

[33] Halden, May 2003. QA Report for Halden IFA-534.14 Revision 1.

[34] Glyn Rossiter. Iaea fumex-iii co-ordinated research programme: Nnl final report. Technical Report NNL (12) 12172, National Nuclear Laboratory, 2012.

[35] IAEA. Improvement of Computer Codes Used for Fuel Behaviour Simulation (FUMEX-III): Report of a Coordinated Research Project 2008-2012. Technical Report IAEA-TECDOC-1697, International Atomic Energy Agency, 2008-2012.

[36] M. Vankeerbergen. The Integral Fuel Rod Behaviour Test IFA-597.2: Pre-characterization and Analysis of measurements. Technical Report HWR-442, Halden, March 1996.

[37] I. Matsson and J. A. Turnbull. The Integral fuel rod behaviour test IFA-597.3: Analysis of the Measurements. Technical Report HWR-543, Halden, January 1998.

[38] D. R. Packard. Preirradiation characterization of ginna/eseerco lead fuel assemblies containing barrier cladding and annular pellets. Technical Report XN-NF-85-79(P) Revision 1, Exxon Nuclear Company Inc., June 1986.

[39] Siemens Power Corporation. Annular-pellet barrier-clad fuel assemblies at the r. e. ginna pwr: Hot-cell examinations. Technical Report EP 80-17 volume 1, Empire State Electric Energy Research Corporation, April 1997.

[40] OECD Nuclear Engergy Data Bank. Ifpe/spc-re-ginna database. Technical report, May 2002.

[41] Qa report for spc irradiation in r e ginna reactor. Technical report.

[42] The Third Risø Fission Gas Project: Bump Test AN2 (CB6). Technical Report Risø-FGP3-AN2, Risø, September 1990.

[43] "MATPRO-9 A Handbook of Materials Properties for Use in the Analysis of Light Water Reactor Fuel Behaviour". Technical Report TREE-NUREG-1005, 1976.

[44] The Third Risø Fission Gas Project: Bump Test AN3 (CB8-2R). Technical Report Risø-FGP3-AN3, Risø, September 1990.

[45] The Third Risø Fission Gas Project: Bump Test AN4 (CB7-2R). Technical Report Risø-FGP3-AN4, Risø, September 1990.

[46] HBEP. Summary of the High Burn-up Effects Programme as abstracted from the Programme Final Report. Technical report, High Burn-up Effects Programme, December 2002.

[47] C. Vitanza, E. Kolstad, and U. Graziani. Fission gas release from UO_2 pellet fuel at high burnup. In *Proceedings of the American Nuclear Society Meeting on Light Water Reactor Fuel Performance*, page 361, Portland, Oregon, Apr 29 to May 3, 1979.

[48] The Third Risø Fission Gas Project: Bump Test GEM (STR013). Technical Report Risø-FGP3-GEM, Risø, September 1990.

[49] The Third Risø Fission Gas Project: Bump Test II3 (STR014-3R). Technical Report Risø-FGP3-II3, Risø, September 1990.

[50] The Third Risø Fission Gas Project: Bump Test GE7 (ZX115). Technical Report Risø-FGP3-GE7, Risø, September 1990.

[51] OECD Nuclear Energy Data Bank. Ifpe/osiris r3 database. Technical report, May 2002.

[52] M. Lippens and D. Boulanger. Tribulation international programme: Final report. Technical Report 89/79, BelgoNucleaire, September 1989.

[53] IFPE/Tribulation Database. Oecd nuclear energy data bank. Technical report, May 2002.

[54] Jr G. P. Smith, E.J. Ruzauskas, R. C. Pirek, and M. Griffiths. Hot cell examination of extended burnup fuel from calvert cliffs-1 volume 1. Technical Report TR-103302-V1, November 1993.

[55] G. P. Smith Jr, R. C. Pirek, and M. Griffiths. Hot cell examination of extended burnup fuel from calvert cliffs-1 volume 2. Technical Report TR-103302-V2, July 1994.

[56] ABB Combustion Engineering-Nuclear Fuel. Examination of the prototype and 1h038 assemblies after reactor cycle 9 in calvert cliffs unit 1. Technical Report CE NPSD-493-NP, November 1992.